NASA Contractor Report 145331

(NASA-CR-145331) REXOR 2 ROTORCRAFT SIMULATION MODEL. VOLUME 1: ENGINEERING DOCUMENTATION Final Technical Report (Lockheed-California Co., Burbank.) 272 p HC A12/MF A01 CSCL 01A G3/02

N78-30042

Unclas 28587

REXOR II ROTORCRAFT SIMULATION MODEL

VOLUME I - ENGINEERING DOCUMENTATION

J. S. Reaser,
P. H. Kretsinger

LOCKHEED-CALIFORNIA CO.
P.O. BOX 551
BURBANK, CALIF. 91520

CONTRACT NAS1-14570
JUNE 1978

National Aeronautics and Space Administration

Langley Research Center
Hampton, Virginia 23665

FOREWORD

This report describes a nonlinear rotorcraft model and associated computer software which has been developed and documented for NASA, Langley Research Center, Hampton, Virginia under contract NAS1-14570 (July 1976). This work has been performed by the Lockheed-California Company, Burbank, California.

P. H. Kretsinger (Lockheed) performed the software implementation. W. D. Anderson and Fox Conner (both of Lockheed) assisted in preparation of the program.

TABLE OF CONTENTS

TABLE OF CONTENTS (Continued)

TABLE OF CONTENTS (Continued)

TABLE OF CONTENTS (Continued)

TABLE OF CONTENTS (Continued)

LIST OF ILLUSTRATIONS

LIST OF ILLUSTRATIONS (Continued)

LIST OF TABLES

REXOR II ROTORCRAFT SIMULATION MODEL*

Volume I – Engineering Documentation

J. S. Reaser and P. H. Kretsinger

Lockheed-California Company

SUMMARY

This report describes a generalized format rotorcraft nonlinear simulation called REXOR II. The program models single main rotor vehicles with up to seven main rotor blades. Wings, two horizontal tail planes, and auxiliary thrustors may be included to model a variety of compound helicopter configurations.

Program output is primarily in the form of machine plotted time histories specified from a signal list. This list is, in turn, user selected from a set of computation variables used by the program.

LIST OF SYMBOLS

The symbols used in the REXOR II equations are quite numerous. In order to keep the catalog of symbols to manageable proportions the following list is divided according to the discussion in Section 3. Namely, a list of basic symbols is given, followed by subscripts, superscripts, and postscripts. Nonconforming cases of usage together with complicated or obscure subscripting are fully annotated in the basic list.

SYMBOLS

a	arbitrary vector
a_s	speed of sound, m/s
$\ddot{a}_0$	acceleration vector, m/s (ft/s^2)
a_1	longitudinal component of blade first harmonic flapping, rad
$[A]$	generalized mass element matrix
$A_{1,2,3}$	modal variables
A_{1n}	generalized displacement of nth blade, first mode

*The contract research effort which has lead to the results in this report was financially supported by USARTL (AVRADCOM) Structures Laboratory.

A_{2n}	generalized displacement of nth blade, second mode
A_{3n}	generalized displacement of nth blade, third mode
A_{1S}	cosine component of blade first harmonic cyclic, rad
b	number of main rotor blades; arbitrary vector
B	dissipation function
B_{1S}	sine component of blade first harmonic cyclic, rad
c	blade segment chord, m (ft)
[C]	damping matrix
C_D	aerodynamic drag coefficient
C_L	aerodynamic lift coefficient
C_M	aerodynamic pitching moment coefficient
C_P	power coefficient
C_T	thrust coefficient
$C_{X,Y,Z}$	linear damping, N/m/s (lb/ft/s)
$C_{\phi,\theta,\psi}$	rotary damping, N-m/rad/s (ft-lb/rad/s)
$C_{1,2,3}$	blade bending to feathering couplings
C(k)	lift deficiency function
d	infinitesimal increment
dr	increment in rotor, radius, m (ft)
dt	increment in time
d/dt	derivative with respect to time
$(d/e)_0$	swashplate to feather gear ratio, zero collective
$(d/e)_1$	swashplate to feather gear ratio slope with collective
e	pitch horn effective crank arm, m (ft)
EI	blade bending stiffness distribution, $N\text{-}m^2$ ($lb\text{-}ft^2$)
f_{iMR}	ground effect factor for main rotor

F	factor; force, N (lb)
$F_{X,Y,Z}$	force components along X,Y,Z directions, N (lb)
$F_{\phi,\theta,\psi}$	generalized force about ϕ, θ, ψ axis
$F_{\beta PH}$	feathering mode generalized force
g	gravity, m/s^2 (ft/s^2)
$g_{X,Y,Z}$	gravity components along X,Y,Z directions
G	gear ratio
$\{G\}$	generalized force vector
$\ddot{G}$	gyro angular acceleration partial product
GJ	blade torsional stiffness, $N\text{-}m^2$ ($lb - ft^2$)
I_X	$= \Sigma m_i X_i^2$, $kg\text{-}m^2$ ($slug\text{-}ft^2$)
I_Y	$= \Sigma m_i Y_i^2$, $kg\text{-}m^2$ ($slug\text{-}ft^2$)
I_Z	$= \Sigma m_i Z_i^2$, $kg\text{-}m^2$ ($slug\text{-}ft^2$)
I_{XX}	$= \Sigma m_i (Y_i^2 + Z_i^2)$, $kg\text{-}m^2$ ($slug\text{-}ft^2$)
I_{YY}	$= \Sigma m_i (X_i^2 + Z_i^2)$, $kg\text{-}m^2$ ($slug\text{-}ft^2$)
I_{ZZ}	$= \Sigma m_i (X_i^2 + Y_i^2)$, $kg\text{-}m^2$ ($slug\text{-}ft^2$)
I_{XY}	$= \Sigma m_i X_i Y_i$, $kg\text{-}m^2$ ($slug\text{-}ft^2$)
I_{XZ}	$= \Sigma m_i X_i Z_i$, $kg\text{-}m^2$ ($slug\text{-}ft^2$)
I_{YZ}	$= \Sigma m_i Y_i Z_i$, $kg\text{-}m^2$ ($slug\text{-}ft^2$)
i	unit vector
j	unit vector
J	advance ratio
k	number of blade radial stations; reduced frequency, rad/s; unit vector
$[K]$	spring matrix
K_{mj}	blade spring matrix element

$K_{X,Y,Z}$	spring constants along X,Y,Z direction, N/m (lb/ft)
$K_{\phi,\theta,\psi}$	spring rates about ϕ, θ, ψ axis, N-m/rad (ft-lb/rad)
l_{IB}	location inboard feather bearing, m (ft)
l_{OB}	location outboard feather bearing, m (ft)
l_p	radial location of intersection of precone and feather axis, m (ft)
L	rolling moment, N-m (ft-lb)
m	mass of element, kg (slugs)
m_F	summed fuselage coordinate mass, kg (slugs)
m_H	summed hub axis mass, kg (slugs)
m_i	mass of ith particle or blade segment, kg (slugs)
m_{SP}	swashplate summed mass, kg (slugs)
M	pitching moment, N-m (ft-lb); = Σm_i, kg (slugs); mach number
[M]	generalized mass matrix
M_{rk}	generalized mass matrix element
$M_{\overline{X}}$	= $\Sigma m_i X_i$, kg-m (slug-ft)
$M_{\overline{Y}}$	= $\Sigma m_i Y_i$, kg-m (slug-ft)
$M_{\overline{Z}}$	= $\Sigma m_i Z_i$, kg-m (slug-ft)
$M_{X,Y,Z}$	moments about X,Y,Z axis, N-m (ft-lb)
M_ϕ	blade torsional moment, N-m/m (ft-lb/ft)
N	number of system particles
p	angular velocity about X axis, rad/s; particle
p_{iMR}	main rotor pitch moment inflow, m/s (ft/s)
q	generalized coordinate; angular velocity about Y axis, rad/s

q_{iMR}	main rotor roll moment inflow, m/s (ft/s)
Q	generalized forcing function
Q_A	aerodynamic pressure times reference wing area, kg (lb)
QLOADS	total nonmain rotor aerodynamic loads matrix
Q_{TR}	tail rotor torque, N-m (ft-lb)
r	general vector; radius of curvature, ft; angular velocity about r axis, rad/sec; notation for (X,Y,Z)
r_S	static blade shape
R	vector displacement of particle p in X,Y,Z axis system
R_C	vector displacement of x,y,z origin in X,Y,Z system
$R_{Z\phi,Z}$	gyro damper coupling ratios
S	Laplace variable, path of motion of particle p
S_{NA}	blade spline length along neutral axis locii, m (ft)
t	time
T	kinetic energy, N-m (ft-lb)
[T]	transformation of coordinates matrix
u	velocity in X direction, m/s (ft/s)
U	potential energy function, N-m (ft-lb); strain energy, N-m (ft-lb)
$U_{C,P,S,T}$	air velocity on blade element, m/s (ft/sec)
v	velocity in Y direction, m/s (ft/sec)
V_T	trajectory velocity
w	velocity in Z direction, m/s (ft/sec)
w_{iMR}	main rotor collective inflow, m/s (ft/sec)
w_{iTR}	tail rotor collective inflow, m/s (ft/sec)
x	motion in X direction, m (ft); blade span location

X	coordinate direction; axis; deflection, m (ft); location, m (ft); cross product
X_{SW}	blade radial station of sweep and jog, m (ft)
X_T	trajectory path, m (ft)
X_{TR}	tail rotor longitudinal force, m (lb)
y	motion in Y direction, m (ft)
Y	coordinate direction; axis; deflection, m (ft); location, m (ft)
$Y_{TTO_{1,2,3}}$	tension torsion pack outboard end modal coefficients
Y_{ONA}	difference between Y direction locations of cg and neutral axis points of blade element, m (ft)
z	motion in Z direction
Z	coordinate direction; axis; deflection, m (ft); location, m (ft)
Z_{SP}	relative swashplate vertical displacement with respect to the hub, m (ft)
$Z_{TTO_{1,2,3}}$	tension-torsion pack outboard end modal coefficients
Z_{OBL}	teetering rotor undersling, m (ft)
Z_{OF}	hub set distance above fuselage set, m (ft)
Z_{OSP}	hub set distance above swashplate set, m (ft)
α	angle of attack, rad
α_2	angle of attack with hub set, rad
β	sideslip angle, rad
β_{FA}	blade feathering angle, rad
β_{PHn}	feathering/pitch-horn bending or dynamic torsion generalized coordinate displacement
β_0	blade droop relative to precone angle, rad

γ	blade sweep angle, rad; dynamic stall delay, s
γ_T	trajectory path angle with E set, rad
δ	limit deflection, rad; freeplay, rad; small increment
δ_{3TR}	tail rotor pitch - flap coupling
$\partial\epsilon/\partial\alpha$	downwash factor of wing on horizontal tail
ζ	vector notation of ϕ, θ, ψ
θ	rotation about Y axis, rad
θ_0	collective blade angle, rad
Λ	sideslip at blade element, rad
ρ	air density, kg/m^3, $(slugs/ft^3)$
τ	time constant, s; natural period, s
τ_0	feathering axis precone, rad
ϕ	rotation about X axis, rad
ϕ_F	feathering angle, rad
ϕ_{Fn}	feathering angle of blade element of nth blade, rad
ϕ_{REF}	blade root reference feather angle, rad
ϕ_T	blade torsion, rad
Φ_T	sum of blade twist and torsion, rad
χ_{iMR}	wake angle of main rotor, rad, (deg)
ψ	rotation about Z axis, rad; sideslip angle with hub set, rad
ψ_c	control input axis rotation from swashplate, rad
ψ_{PH}	pitch lead angle, rad, (deg)
ψ_T	trajectory path yaw with E set, rad
ψ_W	main rotor apparent airflow angle, rad
ω	rotational speed, rad/s; angular velocity, rad/s; natural frequency, rad/s

∂	partial derivative, derivation

SUBSCRIPTS

a	arbitrary coordinate set a
A	due to aerodynamics
b	arbitrary coordinate set b
BEND	associated with blade elastic bending
BLE	blade element coordinate system
BLn	blade reference axis system for the nth blade
C	associated with pilot control input, chordwise
CG	associated with center of gravity location
CORR	corrective, correction
DW	referring to downwash
DYN	referring to dynamic component
E	earth axis
ENG	associated with powerplant - engine
EST	estimated
F	fuselage axis; associated with blade feathering
FA	referring to blade feather axis
FB	associated with feedback
Fn	associated with feathering of the nth blade
FR	due to friction
G	referring to gyro or gyro coordinate system
GEN	associated with gas generator section of powerplant
GFB	associated with gyro control feedback
GSP	gyro to swashplate connection

GUB	relating to gyro gimbal unbalance
H	referring to hub or principal reference axis system
HT	associated with horizontal tail
i	referring to inflow, particle
IB	referring to inboard feather bearing location
j	spring matrix index
Jog	associated with blade attachment joggle
J	associated with gyro end of feedback rod linkage
Jn	associated with feedback rod coming from the nth blade
k	generalized mass index
LAG	associated with lead-lag damper
LIMIT	signifying limiting value
m	blade mode index, spring matrix index
MR	associated with main rotor
n	blade number index
NA	referring to blade segment neutral axis
NEW	newly determined value
NO	normal (to airflow) component
NR	pertaining to nonrotating value
OB	referring to outboard feather bearing location
OLD	value from previous time step
P	associated with propeller; perpendicular blade component
PH	referring to pitch horn
r	generalized mass index
R	referring to rotor axis system

REF	associated with blade feather reference value
RM	referring to control gyro feedback lever moment
S	referring to blade spanwise velocity; general mode; static; structural; shaft
SC	referring to blade segment shear center
SP	referring to swashplate
SP_c	command to swashplate
S, SP	referring to swashplate limit stop
STEADY	steady component
SW	referring to blade sweep angle location
T	associated with trajectory path relating to E axis; tangential blade component; blade torsion; blade twist
TR	associated with the tail rotor
TRIM	initial or trim value
TW	associated with blade twist (built in)
UB	relating to control gyro unbalance
UNSTEADY	associated with unsteady component
VT	associated with vertical tail
WING	associated with the wing
X	relating to component in X direction
Y	relating to component in Y direction
YA	relating to aerodynamic component in Y direction
Z	relating to component in Z direction
ZA	relating to aerodynamic component in Y direction

0	(nought) associated with collective value, coordinate axis value, with respect to principal reference axis, blade root summation
1,2,3	with respect to blade modes 1, 2, or 3
1S	first harmonic component shaft axis feathering
1/4 c	with respect to blade 1/4 chord
3/4 c	with respect to blade 3/4 chord
β_{PHn}	associated with the feathering mode of the nth blade
ϕ	relating to component in the ϕ direction
θ	relating to component in the θ direction
ψ	relating to component in the ψ direction

SUPERSCRIPTS

I	referring to inertial reference
T	matrix transpose
(-)	(bar) average quantity
(')	(prime) slope with respect to blade span
($\cdot$)	(dot) time derivative of basic quantity
($\cdot\cdot$)	(double dot) second time derivative
(-1)	matrix inverse
($\rightarrow$)	vector quantity

POSTSCRIPTS

(i)	blade radial station index
(n)	blade number index

1. INTRODUCTION

1.1 Scope of the REXOR II Program

REXOR II is a rotorcraft analysis tool which has resulted from applying an interdisciplinary math modeling philosophy. The REXOR II math model is written for a single rotor helicopter with capability for analysis of hingeless or hinged rotor systems with conventional controls. This helicopter may be conventional in design, winged, or compounded. The main rotor may have a maximum of seven blades. The model is broken down into the three major categories shown in Figure 1. These categories are the control system, the rotor, and the body.

Figure 1 indicates the manner in which these components are related to one another as utilized in the analysis. The analysis is the simulation of an entire aircraft, which includes detailed dynamic description of the rotor and control system as well as conventional six-degree-of-freedom body dynamic description which operates in two modes identified as TRIM and FLY. In the TRIM mode, the aircraft is constrained to a prescribed static flight condition while the controls are activated and the rotor is allowed to respond to obtain a force and moment equilibrium of the aircraft at that static condition. In the FLY mode the entire aircraft is free to respond dynamically to control inputs or to any other arbitrary inputs such as gusts. Pilot inputs can be any single or multiple control manipulation in the form of simple steps or pulses, doublets, stick stirs, or other transient input within the capabilities of the control system simulated. As a result, transient loads and resulting aircraft and rotor dynamic response can be obtained. For correlation purposes, actual flight test control motions can be used as input to provide comparative response data. Additionally, gust inputs and other types of external excitations can be applied directly to the rotor and/or airframe.

1.2 REXOR II Capabilities

REXOR II is a detailed rotorcraft math model simulation with particular emphasis on the main rotor mechanics. The program is particularly valuable in a detailed exploration of rotor characteristics of proposed designs, in identifying problem areas and verifying fixes in flight test development programs. A case history is given in Reference 1.

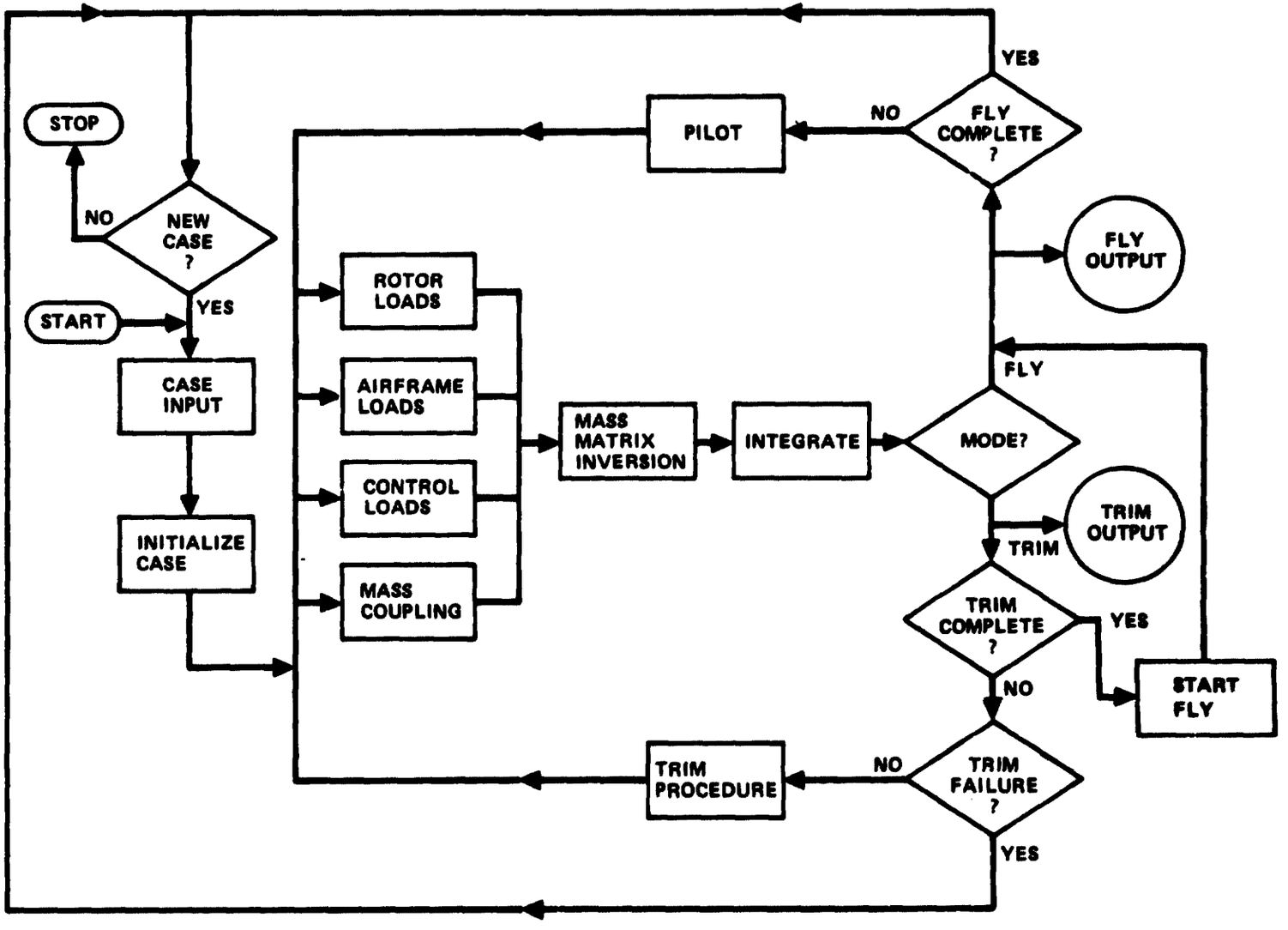

Figure 1. - Block diagram model description.

Typical REXOR II applications are listed below.

Dynamics:

- Rotor stability as a function of flight speed, maneuvers, rotor rpm, nonlinear blade aerodynamics
- Rotor/body sensitivity and dissipation capacity as a function of gusts and pilot control inputs
- Effects of design parameters (mechanical and elastic couplings, controls, etc.) on rotor stability and load sensitivity
- Correlation and check of specialized dynamic models.

Handling Qualities:

- Vehicle response to pilot control inputs for vehicle flight conditions, speed, altitude, rotor rpm, design parameter variations
- Vehicle stability as function of speed, rotor rpm, flight conditions, design parameters
- Effect of design parameter variations on handling qualities
- Development and checking of handling qualities models.

Failure Analysis:

- Effect of loss of one inplane damper on subsequent flight time history
- Blade projectile hit and ensuing events
- Blade strike and resulting rotor track.

Performance:

- Correlation and independent check of performance models, particularly in regions of highly nonlinear blade aerodynamic operation (retreating blade stall and compressibility effects)
- Develop data for performance models for use in nonlinear areas

Loads:

- Steady-state rotor loads as a function of rotor rpm, flight velocity, control trim settings
- Dynamic rotor loads as a function of rotor rpm, flight velocity, vehicle maneuvers, pilot control inputs
- Rotor/fuselage clearances as a function of speed, vehicle maneuvers, rotor rpm, pilot control inputs, flight configuration
- Rotor/fuselage/wing design characteristics requirements as functions of maneuver load factor, control commands (see Reference 2).

1.3 Improper Application REXOR II

While REXOR II is capable of performing a number of analysis tasks, the program range of use is certainly not all inclusive. Examples of types of use where REXOR II either wouldn't work well or would be impractical are given below.

REXOR II is an extensive math model and, as such, may consume a considerable amount of computer time to execute a case. Therefore, the program is not intended as a parametric design analysis tool, but rather as a device to verify the correctness of a parametric selection process.

REXOR II does not treat blade-to-blade vortex interaction. This condition limits the validity of the vibration solution in the transition flight regime.

REXOR II typically uses twenty or less blade radial stations. The computer blade deflections show good correlation to measured data with this modeling. However, since shear is a first derivative, and moment is a second derivative of deflection data, care needs to be exercised in their use (Reference 3).

1.4 The REXOR II Report and Its Use

This report is presented in three volumes.

- Volume I

  A development of rotorcraft mechanics and aerodynamics including a derivation of the equations of motion from first principles.

- Volume II

  The development and explanation of the computer code required to implement the equations of motion.

- Volume III

  A user's manual containing a description of code input/output and instructions to operate the program.

Volume I is intended to be a self-sufficient guide to the math development of the equations of motion and is the reference background as such. Volume II gives the location of computation elements, and serves to locate elements for inspection or modification. Volume III presents normal program operation plus troubleshooting guide material required for day-to-day program use.

2. BASIC COMPUTATIONAL IDEA

2.1 Modal Solution - Overview

The aircraft is described dynamically by an array of fully-coupled degrees of freedom. In addition to the six degrees of freedom of the fuselage principal reference axes, six degrees of freedom describe rotor hub to fuselage deflection due to shaft bending and transmission mount motion. Rotor/engine speed is a degree of freedom. The control swashplate has three degrees of freedom. Motion of each of the main rotor blades is described by three coupled flapwise and inplane modes and a pitch horn bending degree of freedom which couples blade feathering to the swashplate. The total number of degrees of freedom possible is $16 + 4b$, where b is the number of blades.

The blade modes are primitive modes in that they are determined from a lumped parameter analysis at a selected rotor speed and collective blade angle, hereafter referred to as the reference feather angle. The generalized stiffness matrix is computed using these rotating modes and contains only the structural stiffness of the blades and hub. This formulation ensures proper internal and external force and moment balance. The model deflections outboard of the feather hinge are rotated through the actual feather angle less the reference feather angle. Thus, blade element deflections outboard of the feathering hinge due to modal displacements are defined to remain aligned with a coordinate axis system which is orthogonal to a plane containing the instaneous deformed feather axis and rotated through the instantaneous feather angle less the reference feather angle. As a result, the internal strain energy in the blade due to unit model displacements is invariant with variation in blade angle. This technique permits the highest resolution of motion and forces for the blade with an assumed mode solution for a given number of modes.

2.2 Energy Methods Development

The equations of motion for REXOR II are developed from Lagrange's equations, which is an energy approach. If one can express the kinetic, potential, and dissipative energies of a system in addition to the work done by external forces, then Lagrange's equations provide a powerful method for developing the equations of motion.

The dynamic equations of motion are written in matrix form as

$$-[A]\ \{\ddot{q}\} + \{G\} = 0 \qquad (1)$$

where $[A]$ is a square matrix of generalized mass elements, $\{\ddot{q}\}$ is a column vector of accelerations of the generalized coordinates and $\{G\}$ is a column vector derived from the Lagrangian energy functions, dissipation function and generalized forces, which take the form:

$$\{\ddot{q}\} = -[B]\{\dot{q}\} - [C]\{q\} + [Q]\{f(t)\} \qquad (2)$$

The equations of motion are solved using a time history solution with rotor azimuth angle increments required to provide a stable solution at the highest frequency mode present.

2.3 Calculation of Rotor Mode Displacements, Velocities, and Accelerations

In a rotor simulation of this type, it is difficult to compute the proper displacement velocities and accelerations and associated inertia and aerodynamic forces and moments which are required for high resolution of the blade feathering moments. This requires exacting aerodynamic data as well as a precise statement of the inertial loadings. To establish the feathering moments due to these loads, the relationship between the feather axis and the point of application of the loads must be precisely determined. This is accomplished by a very accurate analytic construction of the undeformed blade and a superposition of the blade elastic bending on this shape. In order to achieve the highest resolution of the predicted blade shape and feather axis position, the blade modes are defined at approximately the trim collective blade angle. The blade static position is also constructed at this blade angle. Blade element displacements, velocities, and accelerations are then computed from the combined static shape, the elastic blade motion, and blade feathering with respect to the reference feather angle.

The aerodynamic description used in the analysis is composed of a rotor inflow model, nonlinear steady and unsteady blade element aerodynamics, nonlinear fuselage aerodynamic characteristics, rotor/body aerodynamic interference, and auxiliary airloads from the tail rotor and tail surfaces. The main rotor downwash effect on the wing and horizontal tail angles of attack is an empirical function of rotor thrust and forward velocity. The nonlinear fuselage aerodynamics may be inputted as tables of actual wind tunnel test data.

The aircraft primary control systems are simulated from the pilot control levers operating through a boost system in all control axes. Gearing and gains in the control path are inputs to the analysis and may be easily changed for studying the effects of design changes in the control system.

Control servos are simulated by first-order lags with rate limits and with soft and hard physical stops. Control stiffnesses in collective and cyclic pitch axes of the main rotor are included in the dynamic equations of motion.

2 4 Output

The analysis is a time history solution of the equations of motion. REXOR II does not directly process the results of the solution process for output, it creates an output file of user selected parameters which are correlated by the computation time step. From this data bank the recorded signals can be selected for tabular or plotted output. Assuming a good selection of parameters is chosen to be recorded, the user in an interactive mode may select as little or as much of the information for viewing as is needed. Thus a configuration can be examined thoroughly without having to rerun the case to select additional output.

3. SYMBOLS

The notation used in REXOR II generally follows what could be termed NASA notation. In general:

- Axis systems use a right-hand triad X, Y, Z
- Rotations about these axes are also a right-hand triad θ, ϕ, ψ
- Rotation rates, again a right-hand triad, are p, q, r
- Velocity components of X, Y, Z are u, v, w.

3.1 Subscripting Notation

Subscripting is used as a rule in REXOR II to further identify a variable. Superscripts except in a few column vectors are reserved to denote raising to a power. The subscripting can mean:

- Type of element; F for fuselage, SP for swashplate, TR for tail rotor, R for rotor, etc.
- Coordinate system reference; BLn for blade axis, H for hub axis, R for rotor axis, etc.
- Modal identifiers.

3.1.1 Blade number. - The blade modal identifier typically is of the form A_{mn}. Where n is the blade number.

3.1.2 Mode number. - Also from A_{mn}, m is the mode number, and is keyed to the symbol A. A represents blade bending modes (3). Therefore m can be 1 to 3.

3.1.3 Mode type. - Other than blade bending the remaining blade mode is torsion, and is separately identified as β_{PHn}. Nonblade modes are identified by the direction and subscripted axis of motion. Examples are ψ_R for rotation of the rotor and θ_S for shaft pitching.

3.1.4 Generalized mass, damper, spring, forces. - The generalized masses are denoted as M doubly subscripted by the two modes active for that mass. Examples are $M_{\phi_S \phi_S}$ and $M_{A_{mn}\,\theta_H}$. This scheme is also used for other elements of the equations of motion, dampers (C), springs (K), forces (F). Note the forces are a column vector and singly subscripted.

3.1.5 Forces and moments. - In the process of forming the equations of motion many subelements of forces and moments are formed, translated and combined. Several levels of subscripting may exist in performing this process. The guidelines to the layering are:

- First level denotes the direction or axis system that the quantity is formed in. Examples are X and BLE.
- Second is the axis system involved or axis system being translated to, depending on the specification of the first level. The second level may also be specified as 0 or nought, to indicate the value is at the coordinate system origin. This notation is used to show an inertial reference and blade root summation quantities.
- The third level, usually outside a series of bracketed quantities, shows the blade number being computed, or the overall coordinate system in use for the computation at hand.

4. COORDINATE SYSTEMS AND TRANSFORMATIONS

4.1 Introduction

Prior to developing the equations of motion, a system of coordinate sets with a description of the elements of the system in these sets and the interrelationship of the sets is required.

4.2 Coordinate Sets

4.2.1 Fuselage coordinates (X_F, Y_F, Z_F). - The fuselage X and Z axes lie in the fuselage plane of symmetry. The location of the origin is arbitrary. See Figure 2. The coordinates form a right-hand triad X_F, Y_F, Z_F. Notations for velocities with respect to earth of these coordinates are either $\dot{X}_F$, $\dot{Y}_F$, $\dot{Z}_F$ or u_F, v_F, w_F. A conventional double dot notation is used for acceleration. Euler rotations of the set follow conventional practice of roll right ϕ_F, pitch up θ_F, and yaw right ψ_F. Rates of rotation are either denoted by dot notation or p_F, q_F, r_F. Angular acceleration is double dot notation of the rotation or dot notation of the rates, $\ddot{\phi}_F$, $\ddot{\theta}_F$, $\ddot{\psi}_F$ or $\dot{p}_F$, $\dot{q}_F$, $\dot{r}_F$.

Numerous aerodynamic terms are referenced to the fuselage set. Figure 3 shows the relationship of airflow to this set. The components of airflow, also noted as u_F, v_F, w_F, are defined with respect to the fuselage set by an angle of attack α, and a sideslip angle β. The angle of attack is the arcsin of the ratio of the vertical component and the vector sum of the X and Z components. The sideslip is the Y component of airflow in relation to the total vector airflow sum. The angle of attack is positive (pitch up) of the fuselage set with respect to the airflow. The sideslip is positive (yaw left) for the airflow relative to the set. The airflow is the vector sum of the fuselage set inertial motion and flow fields from other parts of the vehicle, such as main rotor downwash.

4.2.2 Hub coordinates (X_H, Y_H, Z_H). - The hub set origin is at the top of the main rotor mast, but does not rotate with the mast.

Airflow information is referenced to the hub set for use in the main rotor aerodynamic calculations. The reference scheme is shown on Figure 4. For components of airflow u_H, v_H, w_H with respect to the hub set, an angle of

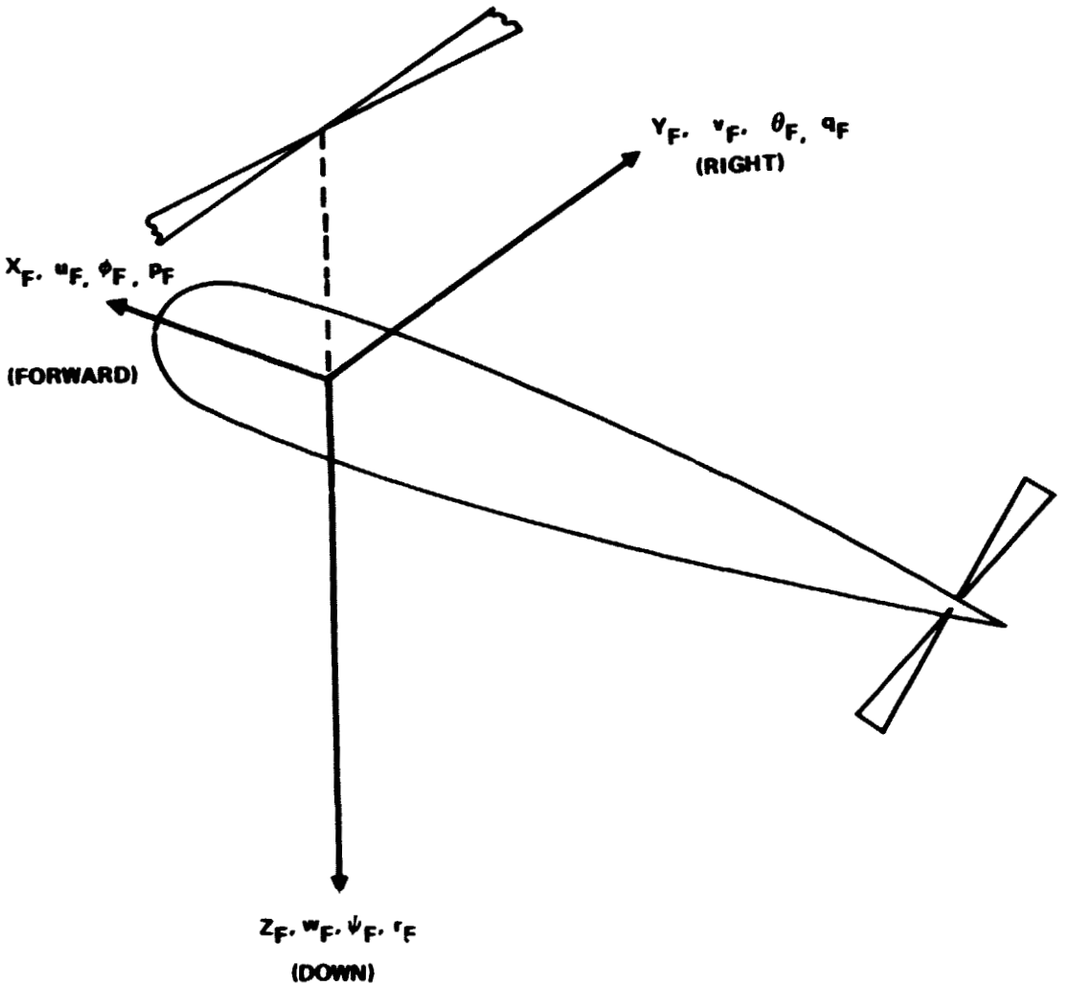

Figure 2. - Coordinate systems-fuselage set.

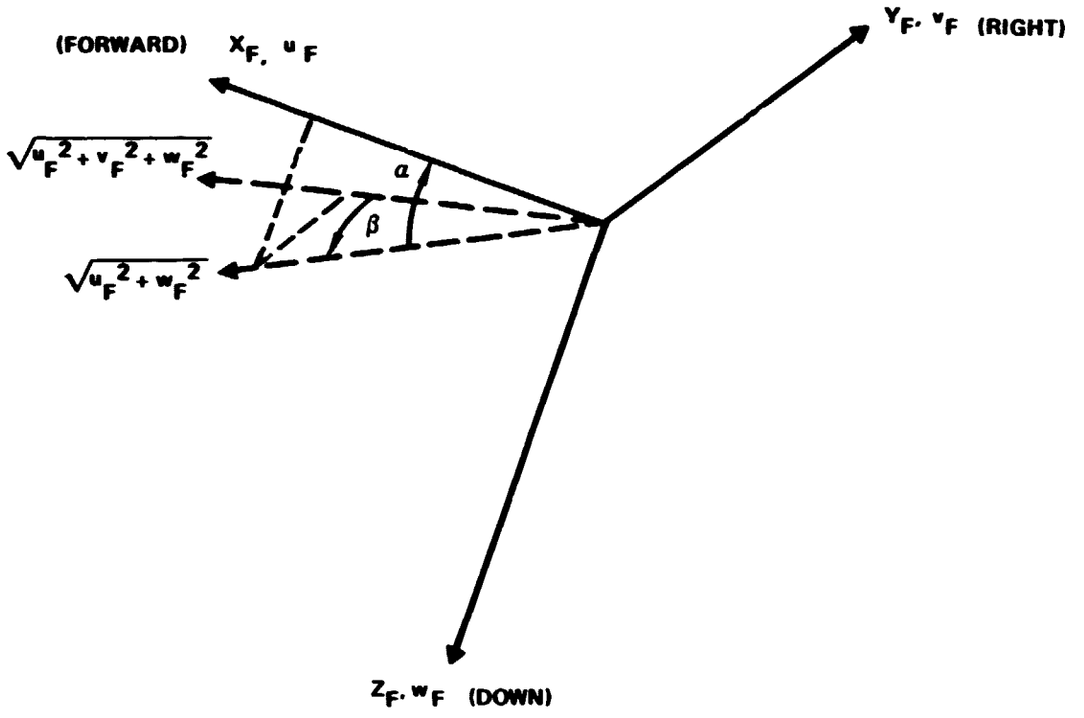

$$\alpha = \sin^{-1} \frac{w_F}{\sqrt{u_F^2 + w_F^2}} \quad ; \quad \beta = \sin^{-1} \frac{v_F}{\sqrt{u_F^2 + v_F^2 + w_F^2}}$$

Figure 3. - Coordinate systems fuselage axis to airmass.

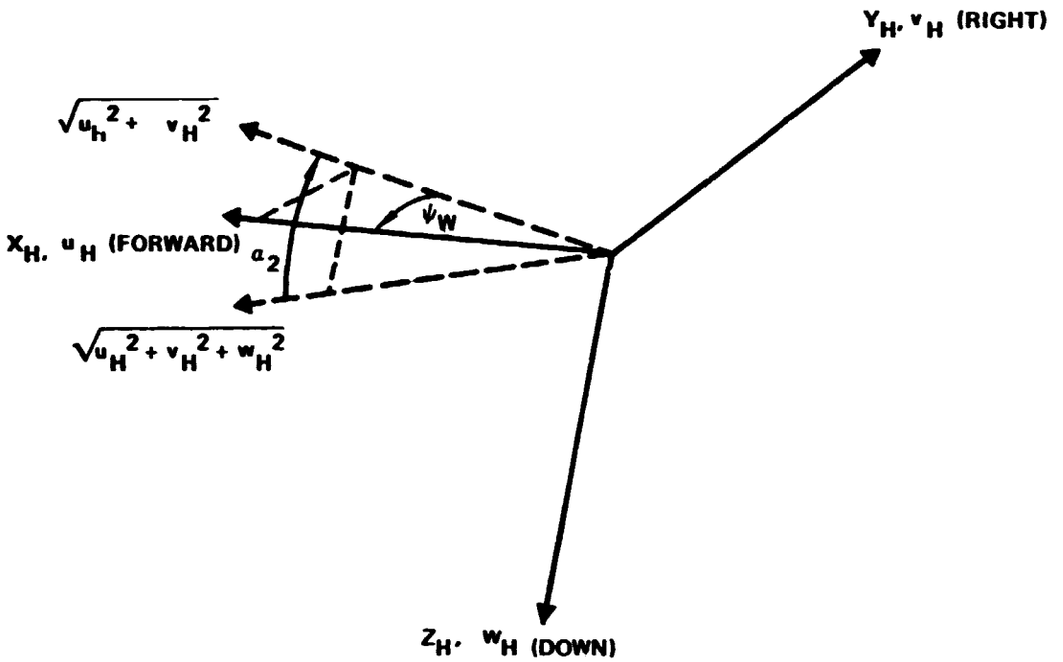

$$a_2 = \sin^{-1} \frac{w_H}{\sqrt{u_H^2 + v_H^2 + w_H^2}} \quad ; \quad \psi_W = \sin^{-1} \frac{v_H}{\sqrt{u_H^2 + v_H^2}}$$

Figure 4. - Coordinate systems - hub axis to airmass.

attack α_2, and sideslip ψ are defined. The generation conventions are different from the fuselage airflow reference in order to clearly separate the inplane and outplane airflow components.

4.2.3 Shaft coordinates (X_s, Y_s, Z_s). - The shaft axes are an intermediate set between the hub and fuselage sets, see Figure 5. The geometry is determined by the distances $(X_o, Y_o, Z_o)_{F-H}$ and $(X_o, Y_o, Z_o)_{S-H}$ that the hub origin is located from the fuselage and shaft axes and by the rotation $(\phi_o, \theta_o, \psi_o)_{S-H}$ of the shaft axes from the fuselage axes. The hub axes are parallel to the shaft axes.

The elastic deflections due to motions of the shaft and transmission suspension are given by the set of coordinates $(X_s, Y_s, Z_s, \phi_s, \theta_s, \psi_s)$. The hub is assumed to move as a rigid body with respect to the shaft axis origin.

4.2.4 Rotor coordinates (X_R, Y_R, Z_R). - The undeflected rotor set has the same origin as the hub set. See Figure 6. The X_R and Y_R axes rotate with the blade number 1 reference axis system. At $\psi_R = 0$, the X_R and Z_R axes are aligned but point in a direction opposite to the X_H and Z_H axes. The rotation of the rotor set is measured counterclockwise (CCW) from the $-X_H$ axis by the angle ψ_R.

4.2.5 Blade coordinates $(X_{BLn}, Y_{BLn}, Z_{BLn})$. - To bookkeep the deflections properly for all the main rotor blades, sets equivalent to the rotor set are created for each blade. These are the BLn sets, where n is the blade number (counted clockwise from blade number one). All BLn sets are identical except for an azimuthal rotation $(n - 1)\,\Delta\psi$, where $\Delta\psi$ is the interblade angular spacing. The rotation is about the Z_R axis. Note that BLn sets are rotating coordinates and have a common Z axis.

4.2.6 Blade element coordinates $(X_{BLE}, Y_{BLE}, Z_{BLE})$. - The blade element set origin is located at the center of gravity of an element of a particular blade. See Figure 7. Reference to a column vector subscripted by BLE is used to denote the blade element located by the blade element set origin. The right-hand coordinate triad of this set has the X axis parallel to the local quarter chord line, the Y axis along the chord line toward the leading edge. The Z axis is mutually perpendicular and pointed up. The BLE set is used to track the local feather angle, to develop aerodynamic and dynamic loading terms.

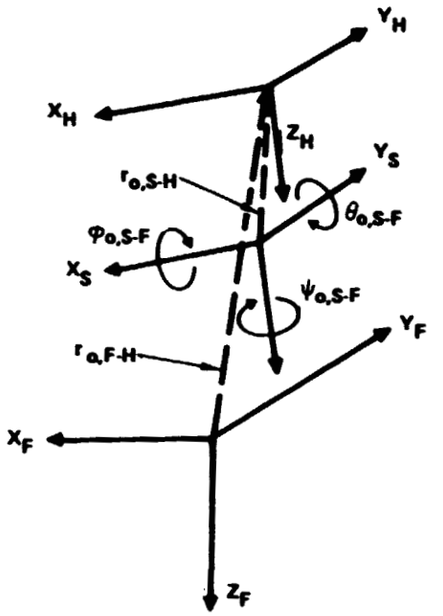

(a) GEOMETRY

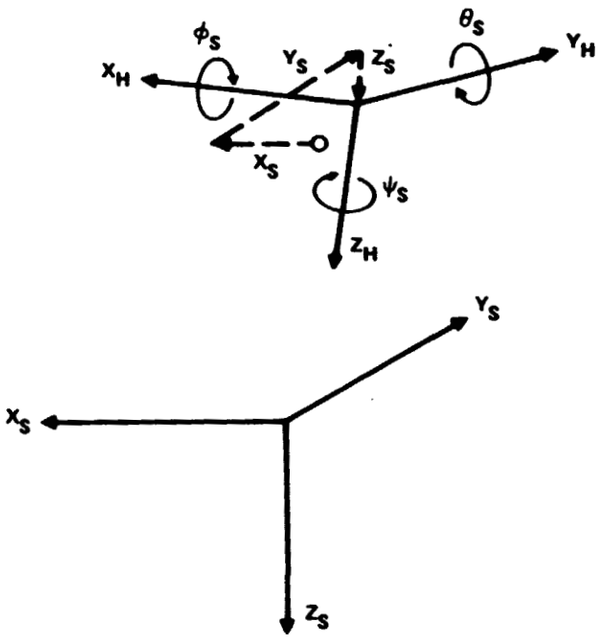

(b) SHAFT AND TRANSMISSION DEFLECTIONS

Figure 5. - Coordinate systems - hub, shaft, and fuselage sets.

a. ROTOR AND HUB AXIS SETS

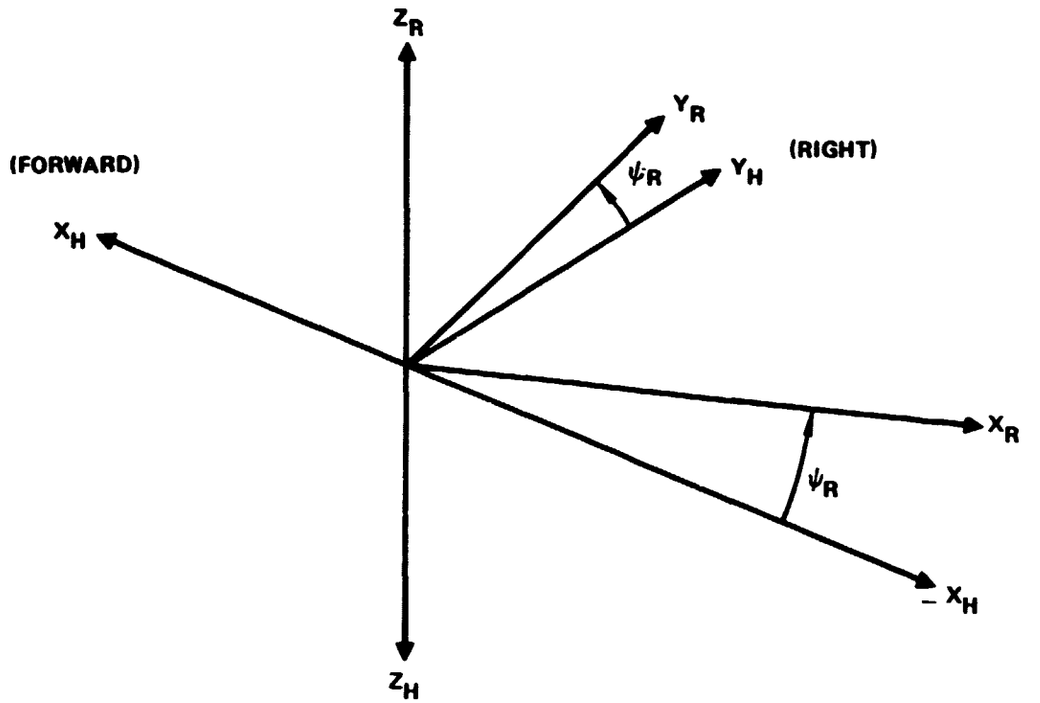

b. ROTOR AND BLADE AXIS SETS

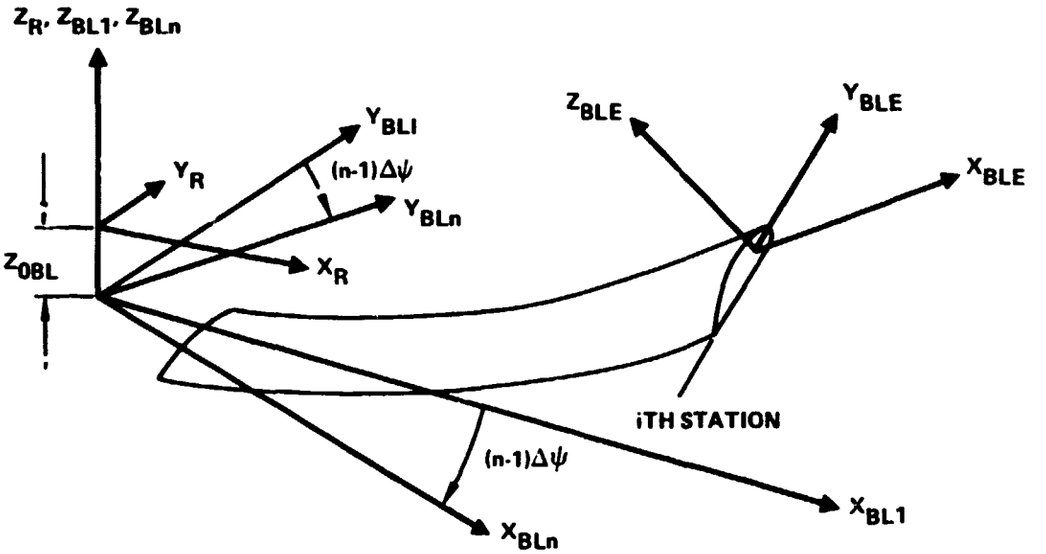

Figure 6. - Coordinate systems - rotor, blade, and blade element sets.

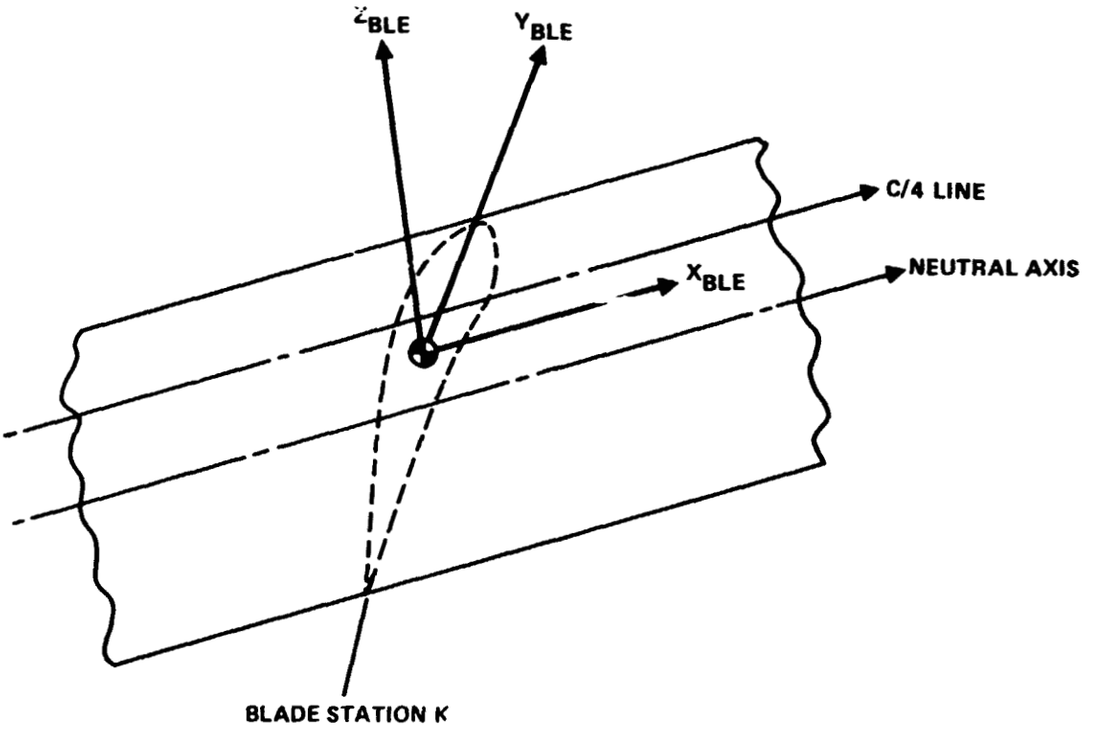

Figure 7. - Coordinate systems - blade element set.

The BLE set origin for each blade element specifies the element c.g. with respect to the quarter chord, and in terms of the BLE directions, i.e., for the Kth element the position coordinates are SY(K) and SX(K) where SX(K) is the blade radial station. Transformations to the neutral, no-stretch axis are made for X deflections. Note: The quarter chord is merely a convenient reference datum, and does not convey any model limitations or assumptions.

4.2.7 Freestream (earth) set (X_E, Y_E, Z_E). - The freestream set is essentially the earth or inertial set inasmuch as the axis alignments are the same. However, the freestream set can assume any origin. Thus the use of the set is to reference the local gravity vector and/or an absolute angular displacement or linear velocity acceleration of another set. As shown on Figure 8, the Z_E axis points down toward local gravity. Other sets reference to the E set, as the F set shown here, may assume any starting value of roll and pitch such as the trim initial conditions. The relative orientation changes with progressing time of flight.

With the freestream set origin located coincident with the fuselage set, the components of fuselage set velocity in E set are u_E, v_E, w_E. These components combine into a trajectory velocity u_T and path X_T. The trajectory path is yawed right ψ_T and pitched up γ_T from the E set. See Figure 9.

4.2.8 Swashplate coordinates (X_{SP}, Y_{SP}, Z_{SP}). - As shown on Figure 10, the SP set origin is located in line with the Z_H axis and above the hub set a distance Z_{OSP}. The SP set does not rotate with the rotor shaft. For no deflection of the SP set, the X and Y axes have the same alignment as the X and Y of the hub set.

4.3 Degrees of Freedom

The degrees of freedom of the REXOR II equations are defined as the generalized coordinate variables of the set of equations of motion to be developed in Section 5. These degrees of freedom fully describe the motion of the physical elements of the modeled helicopter, but each direction of motion of the helicopter may not have a degree of freedom directly associated with it. The physical motions may be described by a series of modal variables (Section 5.4) or through a set of transformations and combinations of the degrees of freedom as developed in Sections 4.4 and 4.5.

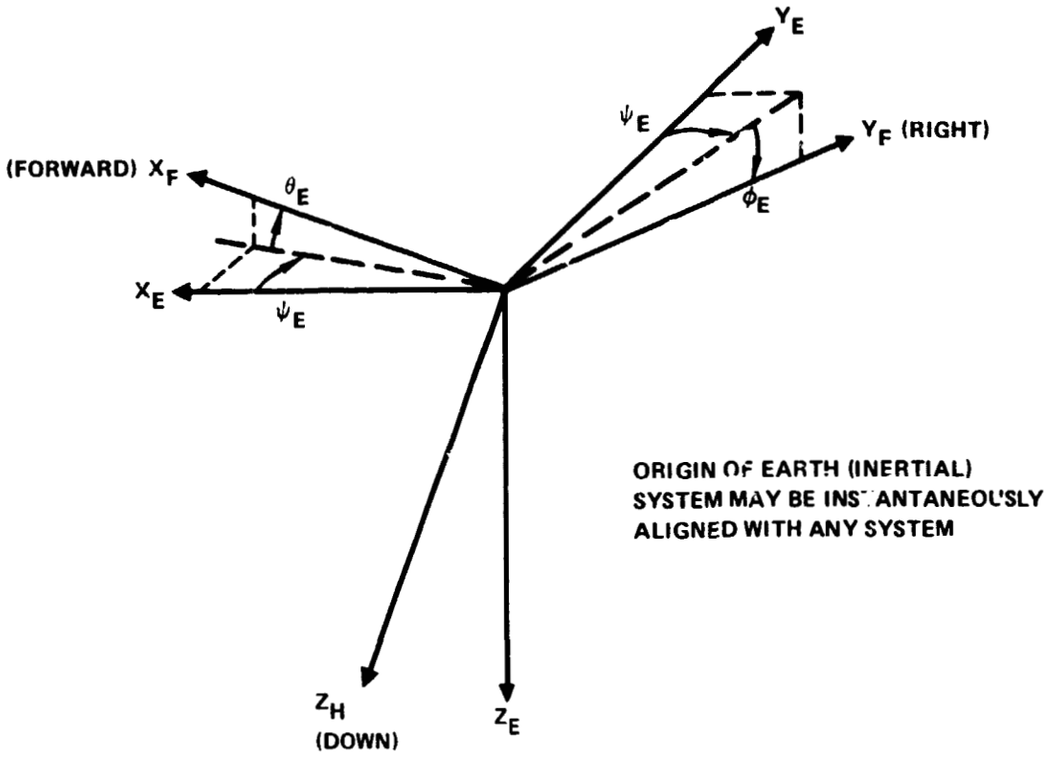

Figure 8. - Coordinate systems - freestream (earth) to principal reference axis.

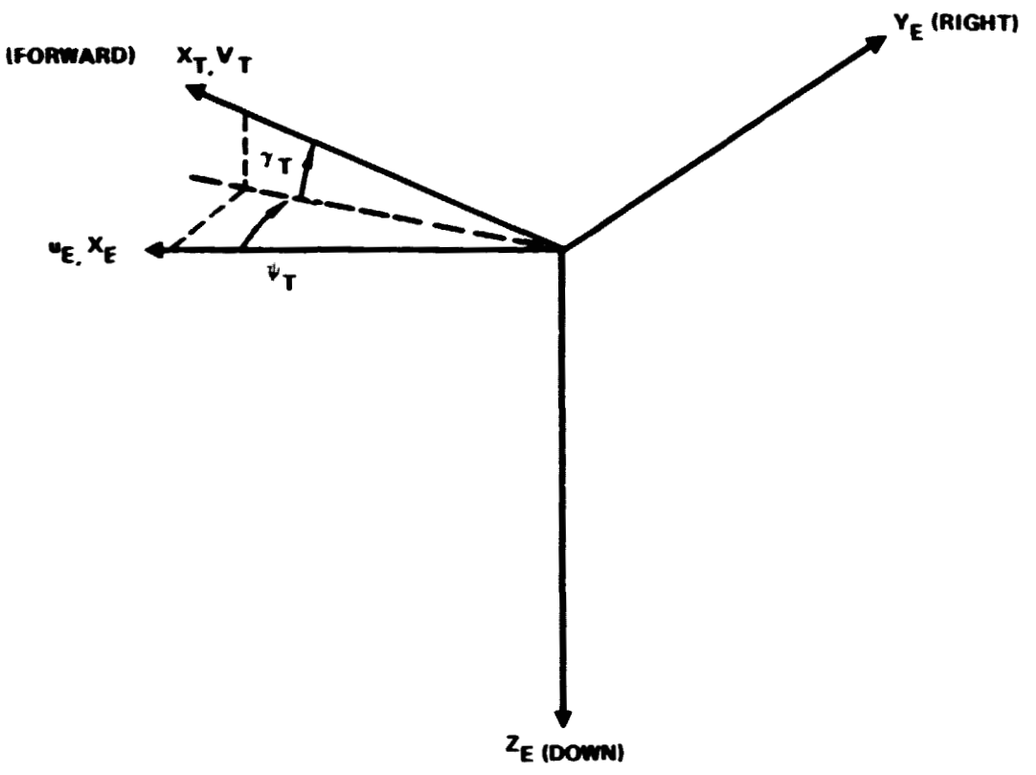

$$V_T = \sqrt{u_E^2 + v_E^2 + w_E^2}$$

$$\psi_T = \sin^{-1} \frac{v_E}{\sqrt{u_E^2 + v_E^2}} \qquad \gamma_T = \sin^{-1} \frac{w_E}{\sqrt{u_E^2 + v_E^2 + w_E^2}}$$

BY DEFINITION: $v_T, w_T \equiv 0$

Figure 9. - Coordinate systems - trajectory path to freestream axis.

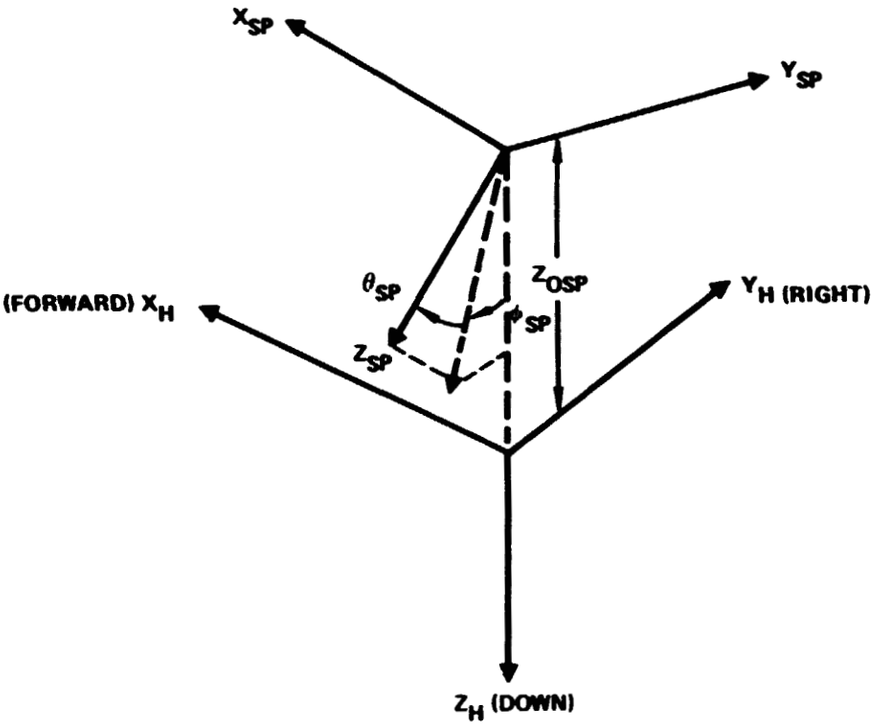

Figure 10. - Swashplate coordinate system.

The REXOR II rotorcraft simulation analysis can be applied to describe the vehicle-rotor-control system dynamic response for up to 16+ 4b (where b is the number of blades) fully-coupled degrees of freedom. These include the normal six rigid body or vehicle degrees of freedom; rotor speed; provisions for up to twenty-eight degrees of freedom defining rotor blade motion (four mode degrees of freedom for seven blade maximum). Three swashplate degrees-of-freedom and six for describing shaft/transmission deflection. The equations of motion are written in a general form so that additional degrees-of-freedom can be added if desired. The current degrees-of-freedom are listed in Figure 11. The discussion following describes them in detail.

4.3.1 Vehicle or rigid body. - The six rigid body degrees-of-freedom; three translations, and three rotations, are defined as motions of the fuselage or principal reference axis system, Section 4.2.2, relative to freestream (inertial) reference datum. Translational displacements $(X, Y, Z)_{OF}$ of the origin of the fuselage coordinate, and rotational displacements $(\phi, \theta, \psi)_F$ about the fuselage axes describe these degrees of freedom. See Figure 8. As mentioned in Section 4.2.7, the freestream set may instantaneously assume any reference point; therefore, only the time derivatives of $(X, Y, Z)_{OH}$ and $(\phi, \theta, \psi)_H$ have significance. In order to locate the direction of the gravity vector relative to the hub, a running calculation of the Euler angles ϕ_E, θ_E, ψ_E must be made. Since these are not degrees of freedom and therefore not calculated in the equations of motion, they must be calculated outside the dynamic equations as the time history proceeds. When the initial orientation of the hub is defined, ϕ_E, θ_E, and ψ_E are known and their changing values may be calculated by integrating the hub rotation rates in the earth or freestream axes.

4.3.2 Rotor. - The rotation for the rotor degree of freedom $\dot{\psi}_R$ is defined as motion of the rotor coordinate system relative to the hub axis system. This is shown in Figure 6. This figure also indicates the change from Z down to Z up axis, which is equivalent to a 180-degree positive rotation about the Y axis. Note: Rotor rotation also includes blade feathering from swashplate rotation in addition to blade root rotation.

4.3.3 Shaft or transmission deflections. - Shaft or transmission degrees-of-freedom are defined as motions of the hub coordinates relative to the shaft axis system. Hence, as shown in Figure 4, hub motions are dependent variables which are functions of the shaft deflections.

ITEM	SYMBOL	TYPE OF MOTION
FUSELAGE PRINCIPAL AXIS	X_{0F}, Y_{0F}, Z_{0F} ϕ_F, θ_F, ψ_F	TRANSLATION AND ROTATION WITH RESPECT TO INERTIAL REFERENCE
ROTOR	ψ_R	ROTATION OF ROTOR SET WITH RESPECT TO HUB AXES
SHAFT OR TRANSMISSION DEFLECTION	$X_S, Y_S, Z_S,$ ϕ_S, θ_S, ψ_S	DEFLECTION OF HUB SET WITH RESPECT TO SHAFT AXES
BLADES	A_{1n}, A_{2n}, A_{3n}	BLADE BENDING MODES AND FEATHER/PITCH HORN
(n = 7 MAXIMUM)	β_{PHn}	BENDING OR TORSION WITH RESPECT TO BLADE ROOT AXES
SWASHPLATE	ϕ_{SP}, θ_{SP} Z_{SP}	SWASHPLATE AXES MOTIONS WITH RESPECT TO HUB AXES

Figure 11. - Degrees of freedom.

4.3.4 Blades. - Each blade's motion relative to the rotor coordinate system is defined in terms of four generalized coordinates. These consist of three blade bending modes and a combined feathering, pitch arm bending mode, or a torsion mode.

4.3.4.1 Blade bending. - Blade motion due to blade bending is defined by the generalized modal coordinates A_{mn} which typically represent a coupled first inplane bending mode, a coupled first flapwise bending mode, and a coupled second flapwise bending mode. Ordinarily in a modal analysis, the effects of centrifugal and structural stiffness are lumped together into a generalized stiffness which is simply the modal natural frequency squared times the generalized mass. In contrast to this, the REXOR II analysis separately treats the strain energy or structural stiffness in each mode and the stiffening due to the centrifugal force field. This provides the capability of being able to account for the periodic variation of stiffness in the modes due to the reorientation of the centrifugal force field with respect to the blade principal axis due to variations in blade angle. This feature can be important in the study of subharmonic stability where the periodic variation of coefficients may be important, but it also permits being able to make rather large changes in rotor speed and collective blade angle without having to change blade modal data.

Mode shapes and natural frequencies are initially determined for a twisted blade at or near the collective blade angle and rotor speed to be analyzed. Such effects as precone, blade sweep, blade droop, and blade angle variation are included in the REXOR II analysis and couple the initially orthogonal modes. The elastic bending contribution due to the modal deflections is calculated relative to the blade's static shape.

As previously noted, the blade modes are initially defined at some reference feathering angle, ϕ_{REF}. As time progresses in the analysis, the blade feather angle varies about this reference position. The mode shapes are correspondingly transformed to account for the difference between the instantaneous feathering angle and the reference feathering angle, at the same time accounting for other effects such as the static and instantaneous shape of the blades. This yields the modal coefficients (partial derivatives) that relate blade element motion to the blade bending generalized coordinates as a function of time.

The vertical and inplane blade element variational motions, δY_i and δZ_i, can be written as follows:

$$\delta Y_{in} = \frac{\partial Y_i}{\partial A_{1n}}(q_r,t)\delta A_{1n} + \frac{\partial Y_i}{\partial A_{2n}}(q_r,t)\delta A_{2n} + \frac{\partial Y_i}{\partial A_{3n}}(q_r,t)\delta A_{3n} \qquad (3)$$

and

$$\delta Z_{in} = \frac{\partial Z_i}{\partial A_{1n}}(q_r,t)\delta A_{1n} + \frac{\partial Z_i}{\partial A_{2n}}(q_r,t)\delta A_{2n} + \frac{\partial Z_i}{\partial A_{3n}}(q_r,t)\delta A_{3n} \qquad (4)$$

where the given or input partial derivatives are the true modal coefficients of the orthogonal modes for the blade in an undeformed shape, with no static geometry accounted for, and at the rotor speed and collective angle for which the blade modes were initially calculated.

The orthogonal bending modes used in the analysis are illustrated in Figures 12, 13, and 14. Observe that the root boundary conditions for the modes may be cantilevered or articulated.

Note that in addition to the normal bending responses, Y_i and Z_i, the spanwise motion of each blade element is also determined, and blade feathering due to pitch-lag and pitch-flap kinematic coupling effects are also accounted for in each blade bending mode. This feathering is added to that due to swashplate motion as is blade feathering due to flexibility.

This modal data is developed to the form used in the blade equations in Section 4.5.5. The discussion of modes is carried on from a math viewpoint in Section 5.4.

4.3.4.2 Pitch horn bending - dynamic torsion. - The remaining mode per blade, pitch horn bending, is comprised of either a blade feathering drive flexibility with a torsionally rigid blade or an uncoupled torsion mode. Examining the first alternative, the swashplate position determines the primary blade feathering motion. In addition, the linkage between the swashplate and the blade (see Figure 15) has flexibility in the pitch link, pitch horn, and cuff. The feathering or pitch horn bending degree-of-freedom therefore can be rigid blade feathering motion outboard of the blade cuff coupled with a net inboard stiffness. Inboard of the blade cuff, feathering flexibility results from the pitch link, pitch link bearings, pitch horn, and cuff. The relationship between blade feathering, ϕ_{Fn}, and motion of this degree-of-freedom, β_{PHn}, is defined as the partial derivative, $\left(\frac{\partial \phi_F}{\partial \beta_{PH}}\right)_n$.

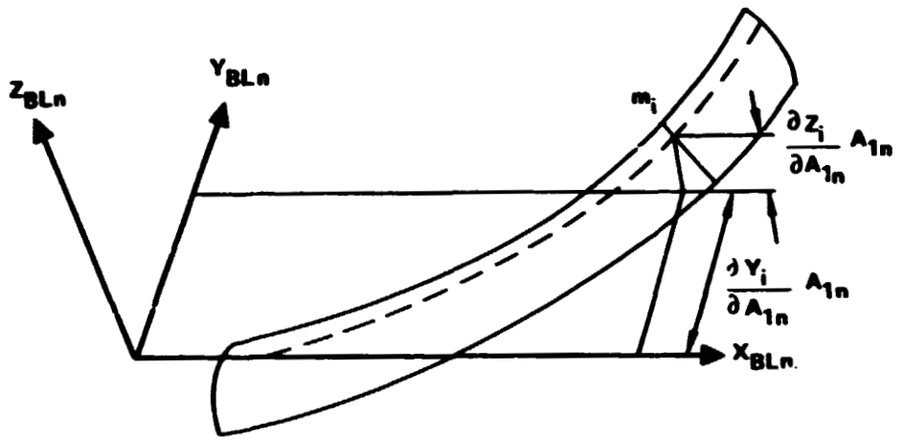

Figure 12. - First inplane mode.

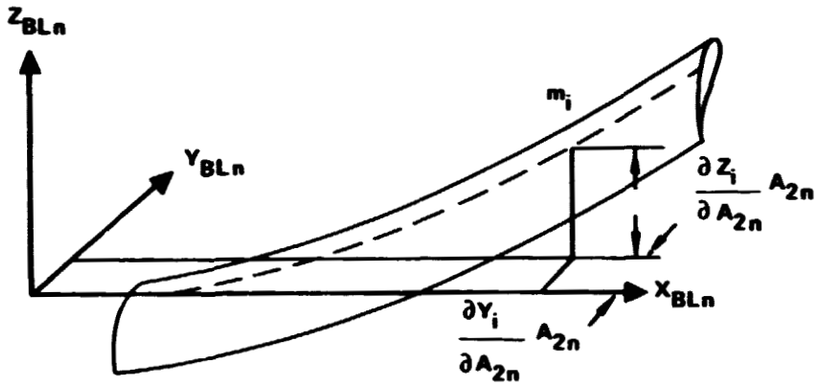

Figure 13. - First flap mode.

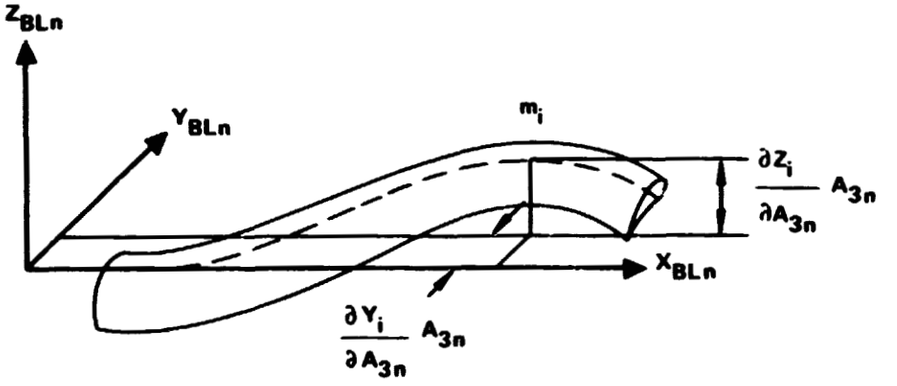

Figure 14. - Second flap mode.

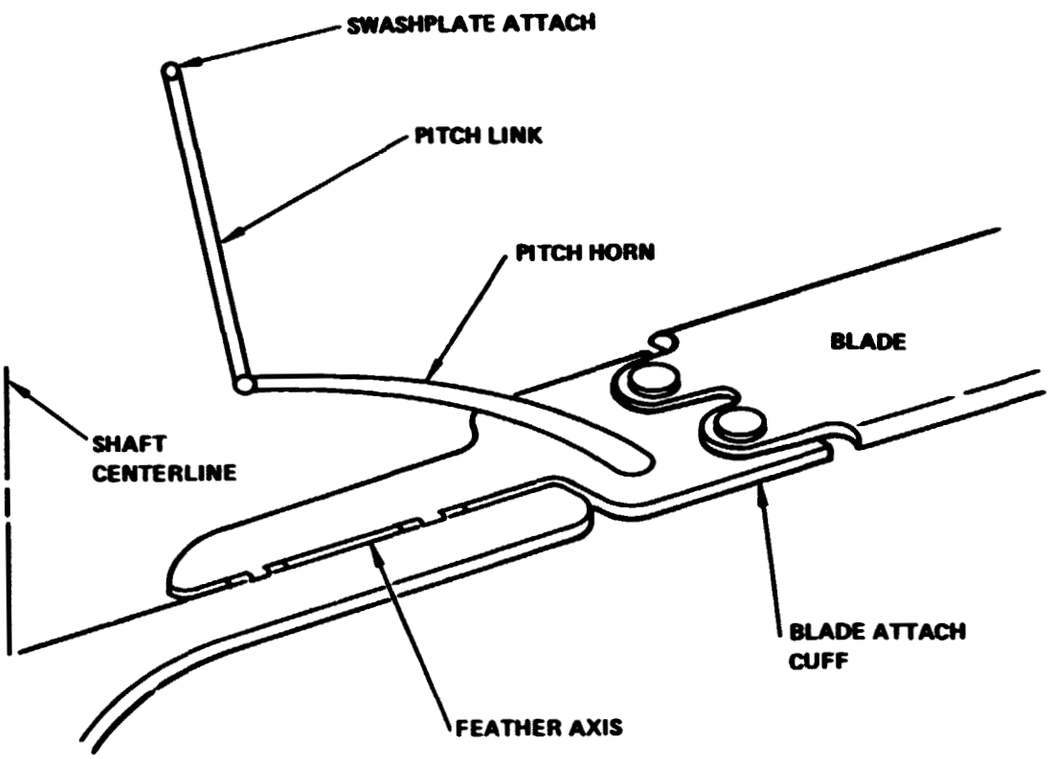

Figure 15. - Blade, pitch horn, and feather hinge geometry.

Alternatively, this degree of freedom, β_{PHn}, can be a distributed torsional response of the blade based upon defining an uncoupled dynamic torsion mode. The selection of the degree-of-freedom representation is made on the basis of the type of analysis being performed. The mode defined is uncoupled in the sense that it is not a function of the flapping or lead-lag modes.

An optional quasi-steady torsional response of the blade may be used in conjunction with pitch horn bending. This is superimposed on the rigid blade feathering and permits a distributed torsional response alternative of the blade reacting the spanwise variation of applied torsional momen s from aerodynamics, coriolis, and centrifugal force terms. The blade torsional response at the ith blade station is computed from the following equation:

$$\phi_{Ti} = \frac{1}{\tau_T S+1} \int_{root}^{x_i} \frac{dx}{GJ(x)} \int_{x_i}^{tip} M_\phi(x)dx \qquad (5)$$

where S is the Laplace operator, and τ_T is the time constant associated with blade torsional response. This equation is implemented numerically in the REXOR II program.

To aid in program trouble shooting the pitch horn bending representation (with or without quasi-static torsion) may also be operated as a quasi-static degree of freedom without second-order response.

4.3.5 Swashplate. - The swashplate has three degrees of freedom: ϕ_{SP}, θ_{SP}, and Z_{SP}. Rotations ϕ_{SP} and θ_{SP} are Euler angles defining the orientation of swashplate coordinates relative to the hub. Likewise, the translation Z_{SP} defines vertical displacement of the swashplate relative to the hub axis. These are shown schematically in Figure 10.

4.4 General Motion and Coordinate Transformations

In development of the equations of motion, it is convenient to write the forces, moments, velocities, and accelerations in coordinate systems related to separate elements of the system. Consider the concept of general space motion of a particle.

4.4.1 General case of space motion. - For the general case of space motion, a particle, p, moves with respect to a reference axis system which is, in turn, in motion with respect to a fixed coordinate system. This is illustrated in Figure 16 where the fixed or inertial coordinate system is designated by capital letters X, Y, Z, and the moving coordinate system is designated by lower case letters x, y, z. The moving coordinate system is rotating at an angular velocity, $\vec{\omega}$. The vector $\vec{\omega}$ may, in general, vary in magnitude and direction, both of which can be referenced with respect to the fixed X, Y, Z axes.

Thus, the absolute motion of the particle p, referred to the inertial X, Y, Z axes, is equal to the motion of the particle relative to the moving coordinate axes x, y, z plus the motion of the moving axis system with respect to inertial space.

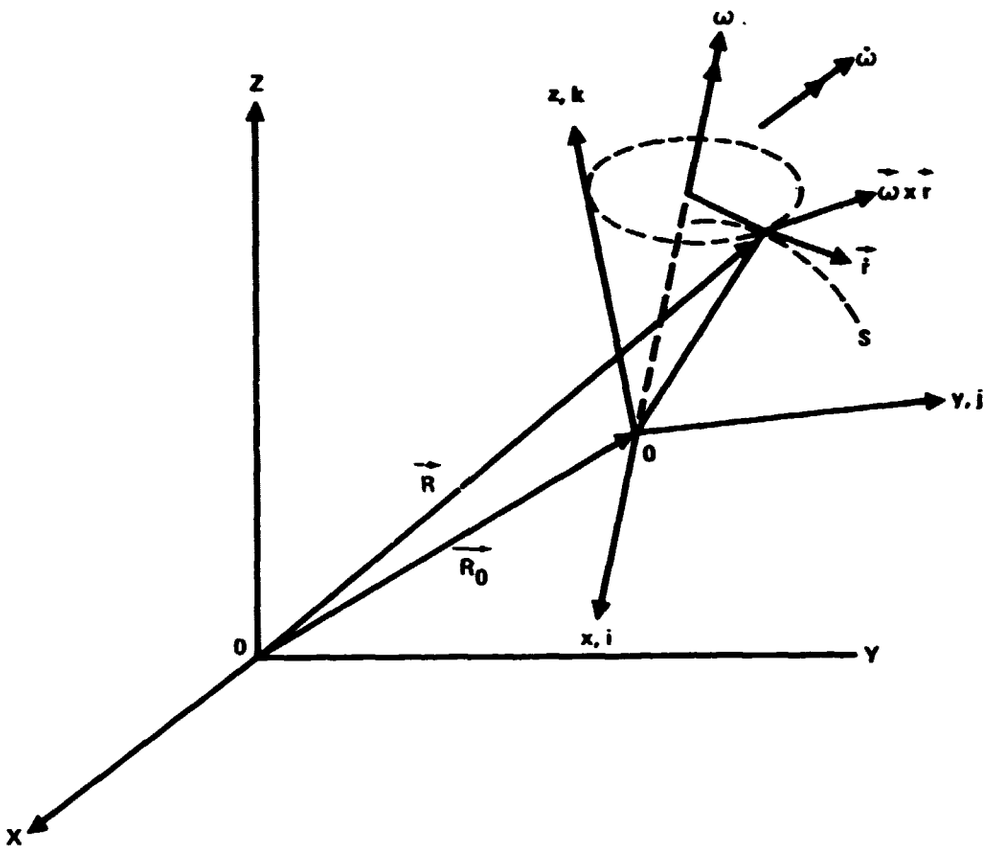

Figure 16. - General case of space motion in terms of moving coordinate axes x, y, z and inertial axes X, Y, Z.

To visualize the motion of the particle p, let its motion with respect to the moving axis system be indicated along a curve s fixed in the moving axis system, x, y, z. An observer sitting on the moving axis system would therefore see only the motion of p along the curve s.

From Figure 16, the position of p relative to the x, y, z axes is represented by the vector

$$\vec{r}_R = x\vec{i} + y\vec{j} + z\vec{k} \tag{6}$$

where i, j, and k are unit vectors along x, y, z, and therefore must be treated as variables due to their changing direction. Differentiating $\vec{r}_R$ results in

$$\dot{\vec{r}} = \dot{x}\vec{i} + \dot{y}\vec{j} + \dot{z}\vec{k} + x\frac{d\vec{i}}{dt} + y\frac{d\vec{j}}{dt} + z\frac{d\vec{k}}{dt} \tag{7}$$

Since $\frac{d\vec{i}}{dt} = \vec{\omega} \times \vec{i}$, $\frac{d\vec{j}}{dt} = \vec{\omega} \times \vec{j}$ and $\frac{d\vec{k}}{dt} = \vec{\omega} \times \vec{k}$, this expression can be written as

$$\dot{\vec{r}} = \dot{x}\vec{i} + \dot{y}\vec{j} + \dot{z}\vec{k} + \vec{\omega} \times (x\vec{i} + y\vec{j} + z\vec{k}) \tag{8}$$

or

$$\dot{\vec{r}} = \dot{\vec{r}} + \vec{\omega} \times \vec{r} \tag{9}$$

In this equation, the first term, $\dot{\vec{r}}$ represents the velocity p relative to the rotating axis, x, y, z. The second term, $\vec{\omega} \times \vec{r}$, is the velocity of the point in the moving coordinate system due to the rotation ω. The absolute or inertial velocity $\dot{\vec{R}}$ of the point p is obtained by adding the velocity of the origin $\dot{\vec{R}}_0$ of the moving axis system to $\dot{\vec{r}}$, or:

$$\dot{\vec{R}} = \dot{\vec{R}}_0 + \dot{\vec{r}} + \vec{\omega} \times r \tag{10}$$

where $\vec{\omega} = p\vec{i} + q\vec{j} + r\vec{k}$

and $\dot{\omega} = \dot{p}\vec{i} + \dot{q}\vec{j} + \dot{r}\vec{k}$

The inertial accelerations of the point p can now be determined by simply differentiating this expression with respect to time. Performing this differentiation yields

$$\ddot{\vec{R}} = \ddot{\vec{R}}_0 + \ddot{\vec{r}} + \vec{\omega} \times \vec{\omega} \times \vec{r} + \dot{\vec{\omega}} \times \vec{r} + 2\vec{\omega} \times \dot{\vec{r}} \tag{11}$$

where the terms $\vec{\omega} \times \vec{\omega} \times \vec{r}$ and $\dot{\vec{\omega}} \times r$ represent accelerations of the coincident point in the moving axis system, $\ddot{\vec{r}}$ is the acceleration of p relative to the moving axes, x, y, z, and $2\vec{\omega} \times \vec{r}$ is the coriolis acceleration which is directed normal to the plane containing the vectors $\vec{\omega}$ and the relative velocity $\dot{\vec{r}}$, as given by the right-hand rule.

The vectors expressed in the preceding equations are in the most general form for defining the motion of a particle moving in a moving coordinate system. All special cases can be deduced from these equations.

For convenience, the time derivative equations can be expanded in matrix form. The inertial or absolute velocity and accelerations of the particle p, written in expanded matrix form, are given by:

$$\begin{Bmatrix} \dot{X} \\ \dot{Y} \\ \dot{Z} \end{Bmatrix}^I = \begin{Bmatrix} \dot{X}_0 \\ \dot{Y}_0 \\ \dot{Z}_0 \end{Bmatrix}^I + \begin{Bmatrix} \dot{x} \\ \dot{y} \\ \dot{z} \end{Bmatrix} + \begin{bmatrix} 0 & -r & q \\ r & 0 & -p \\ -q & p & 0 \end{bmatrix} \begin{Bmatrix} x \\ y \\ z \end{Bmatrix} \tag{12}$$

and

$$\begin{Bmatrix} \ddot{X} \\ \ddot{Y} \\ \ddot{Z} \end{Bmatrix}^I = \begin{Bmatrix} \ddot{X}_0 \\ \ddot{Y}_0 \\ \ddot{Z}_0 \end{Bmatrix}^I + \begin{Bmatrix} \ddot{x} \\ \ddot{y} \\ \ddot{z} \end{Bmatrix} + \begin{bmatrix} 0 & -r & q \\ r & 0 & -p \\ -q & p & 0 \end{bmatrix} \begin{bmatrix} 0 & -r & q \\ r & 0 & -p \\ -q & p & 0 \end{bmatrix} \begin{Bmatrix} x \\ y \\ z \end{Bmatrix}$$

$$+ \begin{bmatrix} 0 & -\dot{r} & \dot{q} \\ \dot{r} & 0 & -\dot{p} \\ -\dot{q} & \dot{p} & 0 \end{bmatrix} \begin{Bmatrix} x \\ y \\ z \end{Bmatrix} + 2 \begin{bmatrix} 0 & -r & q \\ r & 0 & -p \\ -q & p & 0 \end{bmatrix} \begin{Bmatrix} \dot{x} \\ \dot{y} \\ \dot{z} \end{Bmatrix} \tag{13}$$

Performing the indicated matrix multiplication gives:

$$\begin{Bmatrix} \dot{X} \\ \dot{Y} \\ \dot{Z} \end{Bmatrix}^I = \begin{Bmatrix} \dot{X}_0 \\ \dot{Y}_0 \\ \dot{Z}_0 \end{Bmatrix}^I + \begin{Bmatrix} \dot{x} \\ \dot{y} \\ \dot{z} \end{Bmatrix} + \begin{Bmatrix} zq - yr \\ xr - zp \\ yp - xq \end{Bmatrix} \tag{14}$$

and

$$\begin{Bmatrix} \ddot{X} \\ \ddot{Y} \\ \ddot{Z} \end{Bmatrix}^I = \begin{Bmatrix} \ddot{X}_0 \\ \ddot{Y}_0 \\ \ddot{Z}_0 \end{Bmatrix}^I + \begin{Bmatrix} \dot{x} \\ \dot{y} \\ \dot{z} \end{Bmatrix}$$

$$+ \begin{Bmatrix} x(-r^2-q^2) + y(pq-\dot{r}) + z(pr+\dot{q}) + 2\dot{z}q - 2\dot{y}r \\ x(pq+\dot{r}) + y(-r^2-p^2) + z(qr-\dot{p}) + 2\dot{x}r - 2\dot{z}p \\ x(pr-\dot{q}) + y(qr+\dot{p}) + z(-p^2-q^2) + 2\dot{y}p - 2\dot{x}q \end{Bmatrix} \tag{15}$$

4.4.2 Coordinate transformations - Euler angles. - To describe motions in one coordinate system in terms of motions in another coordinate system, Euler angles ϕ, θ, and ψ with the appropriate subscripts are introduced. These angles can be applied to define the rotation of one coordinate system, x, y, z, relative to another coordinate reference frame, X, Y, Z. Since the development contained in this report utilizes these angles in relating coordinate systems, a brief explanation is given here.

Rotational displacement of a coordinate system can be represented by the three rotational displacements ϕ, θ, and ψ, as shown in Figure 17. The order of rotation is not important as long as the sequence selected remains consistent and the reverse order is used when rotating back to the

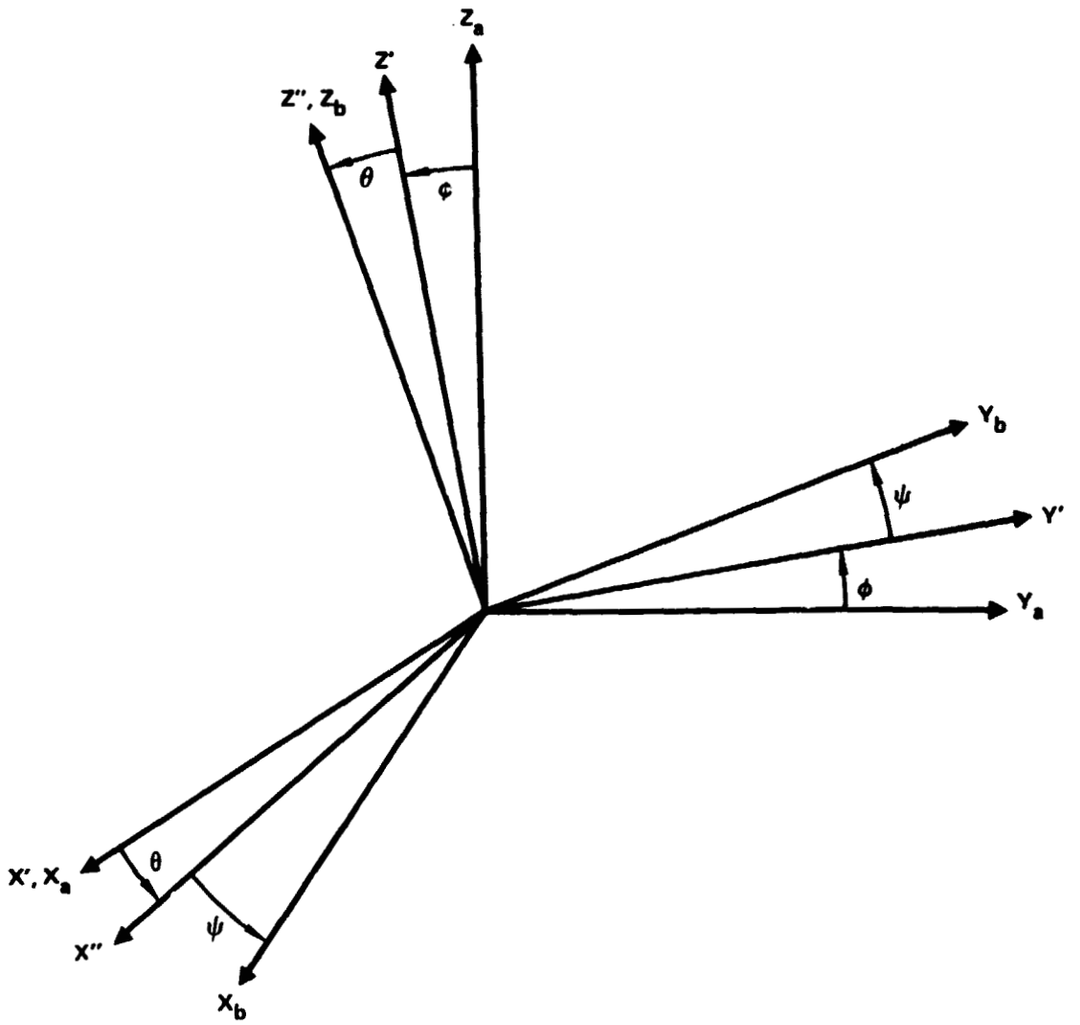

AXES $(X, Y, Z)_b$ DEFINED RELATIVE TO REFERENCE
AXES $(X, Y, Z)_a$ BY EULER ANGLES ϕ, θ, ψ

Figure 17. - Rotational displacement of a coordinate system.

original position. In this analysis, the rotations start with displacement ϕ about the x axis, then a rotation θ about the new y axis, followed by a rotation ψ about the new or final z axis unless geometry or physical considerations of the modeled part dictates another order.

This means the $(X, Y, Z)_a$ coordinates can be rotated into the $(X, Y, Z)_b$ axis system as follows:

$$\begin{Bmatrix} X \\ Y \\ Z \end{Bmatrix}_b = \begin{bmatrix} \cos\psi & \sin\psi & 0 \\ -\sin\psi & \cos\psi & 0 \\ 0 & 0 & 1 \end{bmatrix} \begin{bmatrix} \cos\theta & 0 & -\sin\theta \\ 0 & 1 & 0 \\ \sin\theta & 0 & \cos\theta \end{bmatrix} \begin{bmatrix} 1 & 0 & 0 \\ 0 & \cos\phi & \sin\phi \\ 0 & -\sin\phi & \cos\phi \end{bmatrix} \begin{Bmatrix} X \\ Y \\ Z \end{Bmatrix}_a \tag{16}$$

or:

$$\begin{Bmatrix} X \\ Y \\ Z \end{Bmatrix}_b = \left[T_{a-b}\right] \begin{Bmatrix} X \\ Y \\ Z \end{Bmatrix}_a \tag{17}$$

and the inverse transformation can be written as

$$\begin{Bmatrix} X \\ Y \\ Z \end{Bmatrix}_a = \left[T_{a-b}\right]^{-1} \begin{Bmatrix} X \\ Y \\ Z \end{Bmatrix}_b = \left[T_{b-a}\right] \begin{Bmatrix} X \\ Y \\ Z \end{Bmatrix}_b \tag{18}$$

where

$$\left[T_{a-b}\right] = \begin{bmatrix} \cos\psi & \sin\psi & 0 \\ -\sin\psi & \cos\psi & 0 \\ 0 & 0 & 1 \end{bmatrix} \begin{bmatrix} \cos\theta & 0 & -\sin\theta \\ 0 & 1 & 0 \\ \sin\theta & 0 & \cos\theta \end{bmatrix} \begin{bmatrix} 1 & 0 & 0 \\ 0 & \cos\phi & \sin\phi \\ 0 & -\sin\phi & \cos\phi \end{bmatrix} \tag{19}$$

and

$$\left[T_{a-b}\right]^{-1} = \begin{bmatrix} 1 & 0 & 0 \\ 0 & \cos\phi & -\sin\phi \\ 0 & \sin\phi & \cos\phi \end{bmatrix} \begin{bmatrix} \cos\theta & 0 & \sin\theta \\ 0 & 1 & 0 \\ -\sin\theta & 0 & \cos\theta \end{bmatrix} \begin{bmatrix} \cos\psi & -\sin\psi & 0 \\ \sin\psi & \cos\psi & 0 \\ 0 & 0 & 1 \end{bmatrix} \quad (20)$$

By inspection, then, it can be seen that

$$\text{inverse of } [T] = \text{transpose of } [T]$$

or

$$\left[T_{a-b}\right]^{-1} = \left[T_{a-b}\right]^{T} = \left[T_{b-a}\right] \quad (21)$$

Carrying out the indicated matrix multiplication yields the transformation matrix $[T]$:

$$\left[T_{a-b}\right] = \begin{bmatrix} (\cos\psi\cos\theta) & (\sin\phi\sin\theta\cos\psi+\cos\phi\sin\psi) & (-\sin\theta\cos\phi\cos\psi+\sin\phi\sin\psi) \\ (-\sin\psi\cos\theta) & (-\sin\psi\sin\phi\sin\theta+\cos\psi\cos\phi) & (\sin\psi\sin\theta\cos\phi+\cos\psi\sin\phi) \\ (\sin\theta) & (-\cos\theta\sin\phi) & (\cos\phi\cos\theta) \end{bmatrix} \quad (22)$$

Using this transformation, the inertial velocities and accelerations of a point or particle be written in one coordinate system in terms of those in the other coordinate system as follows:

$$\begin{Bmatrix} \dot{X} \\ \dot{Y} \\ \dot{Z} \end{Bmatrix}_b^I = \left[T_{a-b}\right] \begin{Bmatrix} \dot{X} \\ \dot{Y} \\ \dot{Z} \end{Bmatrix}_a^I \quad (23)$$

and:

$$\begin{Bmatrix} \ddot{X} \\ \ddot{Y} \\ \ddot{Z} \end{Bmatrix}_b^I = \left[T_{a-b}\right] \begin{Bmatrix} \ddot{X} \\ \ddot{Y} \\ \ddot{Z} \end{Bmatrix}_a^I \tag{24}$$

and inversely,

$$\begin{Bmatrix} \dot{X} \\ \dot{Y} \\ \dot{Z} \end{Bmatrix}_a^I = \left[T_{b-a}\right] \begin{Bmatrix} \dot{X} \\ \dot{Y} \\ \dot{Z} \end{Bmatrix}_b^I \tag{25}$$

and

$$\begin{Bmatrix} \ddot{X} \\ \ddot{Y} \\ \ddot{Z} \end{Bmatrix}_a^I = \left[T_{b-a}\right] \begin{Bmatrix} \ddot{X} \\ \ddot{Y} \\ \ddot{Z} \end{Bmatrix}_b^I \tag{26}$$

4.4.3 Angular velocities and accelerations - general. - For the general case, consider the coordinates in the previous section, and let $(p, q, r)_a$ and $(p, q, r)_b$ be the respective angular velocities of and about the $(x, y, z)_a$ and $(s, y, a)_b$ axis systems. Also, assume that the Euler angles are varying with time ($\dot{\phi}$, $\dot{\theta}$, and $\dot{\psi}$), and let $(x, y, z)_a$ be the reference coordinate set with $(x, y, z)_b$ coordinate set moving relative to it. This is illustrated in Figure 18.

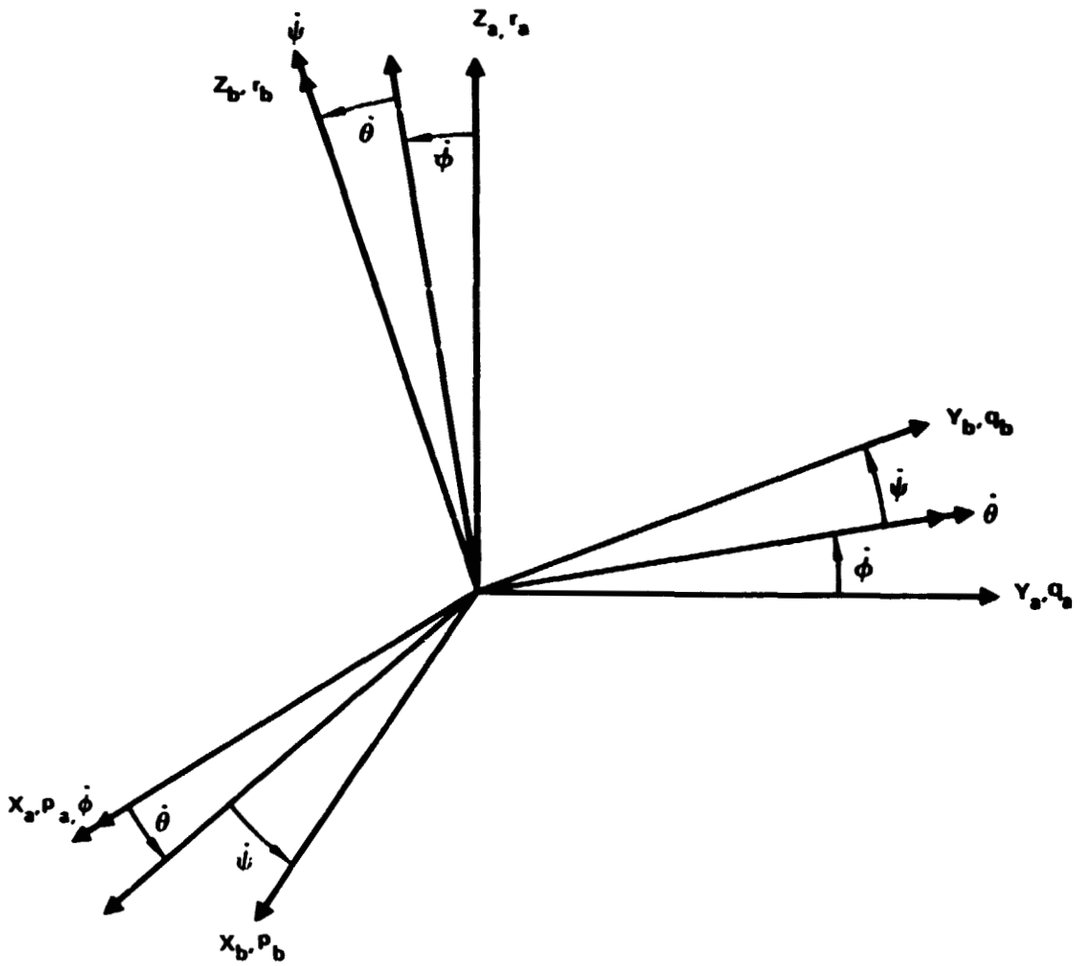

Figure 18. - Relationship of Euler angle and coordinate system angular rates.

From this figure, the following can be written.

$$\begin{Bmatrix} p \\ q \\ r \end{Bmatrix}_b = \begin{Bmatrix} 0 \\ 0 \\ \dot{\psi} \end{Bmatrix} + \begin{bmatrix} \cos\psi & \sin\psi & 0 \\ -\sin\psi & \cos\psi & 0 \\ 0 & 0 & 1 \end{bmatrix} \left\{ \begin{Bmatrix} 0 \\ \dot{\theta} \\ 0 \end{Bmatrix} + \begin{bmatrix} \cos\theta & 0 & -\sin\theta \\ 0 & 1 & 0 \\ \sin\theta & 0 & \cos\theta \end{bmatrix} \left\{ \begin{Bmatrix} \dot{\phi} \\ 0 \\ 0 \end{Bmatrix} + \begin{bmatrix} 1 & 0 & 0 \\ 0 & \cos\phi & \sin\phi \\ 0 & -\sin\phi & \cos\phi \end{bmatrix} \begin{Bmatrix} p \\ q \\ r \end{Bmatrix}_a \right\} \right\} \tag{27}$$

Differentiating this expression with respect to time results in angular accelerations $(\dot{p}, \dot{q}, \dot{r})_b$ in terms of the reference coordinate system angular velocities and accelerations. This results in the following:

$$\begin{Bmatrix} \dot{p} \\ \dot{q} \\ \dot{r} \end{Bmatrix}_b = \begin{Bmatrix} 0 \\ 0 \\ \ddot{\psi} \end{Bmatrix} + \dot{\psi} \begin{bmatrix} -\sin\psi & \cos\psi & 0 \\ -\cos\psi & -\sin\psi & 0 \\ 0 & 0 & 0 \end{bmatrix} \left\{ \begin{Bmatrix} 0 \\ \dot{\theta} \\ 0 \end{Bmatrix} + \begin{bmatrix} \cos\theta & 0 & -\sin\theta \\ 0 & 1 & 0 \\ \sin\theta & 0 & \cos\theta \end{bmatrix} \left\{ \begin{Bmatrix} \dot{\phi} \\ 0 \\ 0 \end{Bmatrix} + \begin{bmatrix} 1 & 0 & 0 \\ 0 & \cos\phi & \sin\phi \\ 0 & -\sin\phi & \cos\phi \end{bmatrix} \begin{Bmatrix} p \\ q \\ r \end{Bmatrix}_a \right\} \right\} + \begin{bmatrix} \cos\psi & \sin\psi & 0 \\ -\sin\psi & \cos\psi & 0 \\ 0 & 0 & 1 \end{bmatrix} \left\{ \begin{Bmatrix} 0 \\ \ddot{\theta} \\ 0 \end{Bmatrix} + \dot{\theta} \begin{bmatrix} -\sin\theta & 0 & -\cos\theta \\ 0 & 0 & 0 \\ \cos\theta & 0 & -\sin\theta \end{bmatrix} \left\{ \begin{Bmatrix} \dot{\phi} \\ 0 \\ 0 \end{Bmatrix} + \begin{bmatrix} 1 & 0 & 0 \\ 0 & \cos\phi & \sin\phi \\ 0 & -\sin\phi & \cos\phi \end{bmatrix} \begin{Bmatrix} p \\ q \\ r \end{Bmatrix}_a \right\} + \begin{bmatrix} \cos\theta & 0 & -\sin\theta \\ 0 & 1 & 0 \\ \sin\theta & 0 & \cos\theta \end{bmatrix} \left\{ \begin{Bmatrix} \ddot{\phi} \\ 0 \\ 0 \end{Bmatrix} + \dot{\phi} \begin{bmatrix} 0 & 0 & 0 \\ 0 & -\sin\phi & \cos\phi \\ 0 & -\cos\phi & -\sin\phi \end{bmatrix} \begin{Bmatrix} p \\ q \\ r \end{Bmatrix} + \begin{bmatrix} 1 & 0 & 0 \\ 0 & \cos\phi & \sin\phi \\ 0 & -\sin\phi & \cos\phi \end{bmatrix} \begin{Bmatrix} \dot{p} \\ \dot{q} \\ \dot{r} \end{Bmatrix}_a \right\} \right\} \tag{28}$$

These equations represent a general form for defining angular velocities and accelerations of one axis system rotating relative to another axis system, which in turn is in motion.

A special case is the angular velocities of system b with zero Euler angles.

$$\begin{Bmatrix} \dot{p} \\ \dot{q} \\ \dot{r} \end{Bmatrix}_b = \begin{Bmatrix} \dot{p} \\ \dot{q} \\ \dot{r} \end{Bmatrix}_a + \begin{Bmatrix} \ddot{\phi} \\ \ddot{\theta} \\ \ddot{\psi} \end{Bmatrix}_a + \begin{Bmatrix} \dot{\psi}\dot{\theta} + \dot{\psi} q - \dot{\theta} r \\ -\dot{\psi}\dot{\phi} + \dot{\phi} r - \dot{\psi} p \\ \dot{\theta}\dot{\phi} + \dot{\theta} p - \dot{\phi} q \end{Bmatrix}_a$$

4.5 Relative Motions and Transformations Used in the Equations of Motion

In this section the inertial linear and angular velocities and accelerations of major components of the vehicle, are presented. Also included is the development of coordinate transformations that relate motion in one axis system to another. Motion of the principal reference axis system in relation to the earth is described. Motion of each component or reference axis system is then defined in terms of the degrees of freedom.

4.5.1 Fuselage motion in inertial space. - At each instant in time the fuselage axis (Section 4.2.1) is related to an inertial coordinate axis system. Inertial accelerations of the fuselage axis system are defined by the vector

$$\begin{Bmatrix} \ddot{X}_0 \\ \ddot{Y}_0 \\ \ddot{Z}_0 \\ \ddot{\phi}_0 \\ \ddot{\theta}_0 \\ \ddot{\psi}_0 \end{Bmatrix}_F \tag{29}$$

where the quantities represent the total inertial acceleration of the generalized coordinates of the vehicle as defined by motion of the principal coordinate axis system.

Orientation of this system relative to the earth is specified by Euler angles ϕ_E, θ_E, and ψ_E as seen in Figure 8. The sequence and definition of these angles is ψ_E (yaw), θ_E (pitch), ϕ_E (roll). Note that the sequence of rotations is opposite to that given by Figure 17. The angular rates, p_F, q_F, r_F, of the fuselage or principal reference axis system with respect to the inertial coordinate system can be written as

$$\begin{Bmatrix} p \\ q \\ r \end{Bmatrix}_F = \begin{Bmatrix} \dot{\phi}_E \\ 0 \\ 0 \end{Bmatrix} + \begin{bmatrix} 1 & 0 & 0 \\ 0 & \cos\phi_E & \sin\phi_E \\ 0 & -\sin\phi_E & \cos\phi_E \end{bmatrix} \left\{ \begin{Bmatrix} 0 \\ \dot{\theta}_E \\ 0 \end{Bmatrix} + \begin{bmatrix} \cos\theta_E & 0 & -\sin\theta_E \\ 0 & 1 & 0 \\ \sin\theta_E & 0 & \cos\theta_E \end{bmatrix} \begin{Bmatrix} 0 \\ 0 \\ \dot{\psi}_E \end{Bmatrix} \right\} \tag{30}$$

This equation can be rewritten to solve for ϕ_E, θ_E, and ψ_E as

$$\begin{Bmatrix} \dot{\phi}_E \\ \dot{\theta}_E \\ \dot{\psi}_E \end{Bmatrix} = \begin{bmatrix} 1 & \sin\phi_E \tan\theta_E & \cos\phi_E \tan\theta_E \\ 0 & \cos\phi_E & -\sin\phi_E \\ 0 & \sin\phi_E \sec\theta_E & \cos\phi_E \sec\theta_E \end{bmatrix} \begin{Bmatrix} p \\ q \\ r \end{Bmatrix}_F \tag{31}$$

The Euler angles defining orientation of the principal reference axis system with respect to the earth is next obtained by integrating the rates with respect to time, or

$$\phi_E = \int_0^t \dot{\phi}_E \, dt + \phi_{t=0,E} \tag{32}$$

$$\theta_E = \int_0^t \dot{\theta}_E \, dt + \theta_{t=0,E} \tag{33}$$

$$\psi_E = \int_0^t \dot{\psi}_E \, dt + \psi_{t=0,E} \tag{34}$$

Angular velocities of the fuselage, with respect to the inertial axes reference system, p_F, q_F, r_F, are defined in terms of the degrees of freedom as

$$\begin{Bmatrix} p \\ q \\ r \end{Bmatrix}_F = \begin{Bmatrix} \dot{\phi}_0 \\ \dot{\theta}_0 \\ \dot{\psi}_0 \end{Bmatrix}_F^I = \int_0^t \begin{Bmatrix} \dot{p} \\ \dot{q} \\ \dot{r} \end{Bmatrix}_F dt + \begin{Bmatrix} p \\ q \\ r \end{Bmatrix}_{t = 0,F} \tag{35}$$

where

$$\begin{Bmatrix} \dot{p} \\ \dot{q} \\ \dot{r} \end{Bmatrix}_F = \begin{Bmatrix} \ddot{\phi}_0 \\ \ddot{\theta}_0 \\ \ddot{\psi}_0 \end{Bmatrix}_F^I \tag{36}$$

Linear velocities of the fuselage or principal axis system are now determined. The first three quantities of the fuselage axis acceleration vector represent the linear interial acceleration of the fuselage. For a system in motion, the inertial acceleration, $\ddot{a}_0^I$, at the origin of the system is defined, based on the vector algebra of Section 4.4.1, as

$$\vec{\ddot{a}}_0^I = \vec{\ddot{a}}_0 + \vec{\omega} \times \vec{V}_0 \tag{37}$$

where $\vec{\ddot{a}}_0$ is $\frac{d\vec{V}_0}{dt}$ is the rate of change of velocity, V_0, of the origin of the moving coordinate system and ω is the rotational velocity of the moving coordinate system, both relative to the earth. Now defining:

$$\begin{Bmatrix} V_0 \end{Bmatrix}_F^I = \begin{Bmatrix} u \\ v \\ w \end{Bmatrix}_F \tag{38}$$

gives

$$\begin{Bmatrix} \ddot{X}_0 \\ \ddot{Y}_0 \\ \ddot{Z}_0 \end{Bmatrix}^I = \begin{Bmatrix} \dot{u} \\ \dot{v} \\ \dot{w} \end{Bmatrix}_F + \begin{bmatrix} 0 & -r & q \\ r & 0 & -p \\ -q & p & 0 \end{bmatrix}_F \begin{Bmatrix} u \\ v \\ w \end{Bmatrix}_F \tag{39}$$

From this equation, then, the rate of change of velocity of the moving coordinate reference system becomes

$$\begin{Bmatrix} \dot{u} \\ \dot{v} \\ \dot{w} \end{Bmatrix}_F = \begin{Bmatrix} \ddot{X}_0^I - qw + rv \\ \ddot{Y}_0^I - ru + pw \\ \ddot{Z}_0^I - pv + qu \end{Bmatrix}_F \tag{40}$$

This set of accelerations and the time integral represent airflow acceleration and velocity incident on the helicopter.

A separate set of accelerations is carried through the analysis which contain the acceleration due to gravity. Ordinarily, gravity is treated as a force of mg on the right-hand side of the equations. However, the gravitational term can be accounted for by defining

$$\begin{Bmatrix} \ddot{X}_0 \\ \ddot{Y}_0 \\ \ddot{Z}_0 \end{Bmatrix}_{EI} = \begin{Bmatrix} \ddot{X}_0 \\ \ddot{Y}_0 \\ \ddot{Z}_0 \end{Bmatrix}^I - \begin{Bmatrix} g_X \\ g_Y \\ g_Z \end{Bmatrix}_F \tag{41}$$

where g_{XF}, g_{YF}, g_{ZF} are the three components of the gravity vector to be defined. The acceleration on the left may be defined as being in earth-inertial, EI, axes.

The logic behind this substitution is as follows. For a rigid body in motion, the equilibrium equations can be written as

$$\begin{aligned} m\ddot{X} &= m(\dot{u} + qw - rv) = F_x \\ m\ddot{Y} &= m(\dot{v} + ru - pw) = F_Y \\ m\ddot{Z} &= m(\dot{w} + pv - qu) = F_Z \end{aligned} \tag{42}$$

where

$$\begin{Bmatrix} F_X \\ F_Y \\ F_Z \end{Bmatrix} = \begin{Bmatrix} \bar{F}_X \\ \bar{F}_Y \\ \bar{F}_Z \end{Bmatrix} + \begin{Bmatrix} g_X \\ g_Y \\ g_Z \end{Bmatrix} m \tag{43}$$

$\bar{F}_X$, $\bar{F}_Y$, and $\bar{F}_Z$ represent the external forces acting on the body, exclusive of gravitational forces.

Subtracting the gravitational vector from each side of the previous equations yields:

$$m(\ddot{X} - g_X) = m(\dot{u} + qw - rv - g_X) = \bar{F}_X \tag{44}$$

$$m(\ddot{Y} - g_Y) = m(\dot{v} + ru - pw - g_Y) = \bar{F}_Y \tag{45}$$

$$m(\ddot{Z} - g_Z) = m(\dot{w} + pv - qu - g_Z) = \bar{F}_Z \tag{46}$$

which by inspection gives

$$\ddot{X} - g_X = \dot{u} + qw - rv - g_X \tag{47}$$

$$\ddot{Y} - g_Y = \dot{v} + ru - pw - g_Y \tag{48}$$

$$\ddot{Z} - g_Z = \dot{w} + pv - qu - q_Z \tag{49}$$

Rearranging these equations yields:

$$\dot{u} = (\ddot{X} - g_X) - qw + rv + g_X \tag{50}$$

$$\dot{v} = (\ddot{Y} - g_Y) - ru + pw + g_Y \tag{51}$$

$$\dot{w} = (\ddot{Z} - g_Z) - pv + qu + g_Z \tag{52}$$

The first terms on the right side of the equation are identified with the proposed gravitational acceleration definition of Equation 41.

Making the substitution:

$$\begin{Bmatrix} \dot{u} \\ \dot{v} \\ \dot{w} \end{Bmatrix}_F = \begin{Bmatrix} \ddot{X}_O^{EI} - qw + rv + g_X \\ \ddot{Y}_O^{EI} - ru + pw + g_Y \\ \ddot{Z}_O^{EI} - pv + qu + g_Z \end{Bmatrix}_F \tag{53}$$

In this equation, the accelerations $\ddot{X}_{OF}^{EI}$, $\ddot{Y}_{OF}^{EI}$, and $\ddot{Z}_{OF}^{EI}$ are the degree-of-freedom accelerations of the principal reference axis system used in the REXOR II analysis. These accelerations represent the inertial accelerations plus the equivalent accelerations of the reaction force to gravity. Thus, gravity is an equivalent acceleration applied to the reference coordinate axis system. Via coordinate system referencing, every mass element on the vehicle is therefore acted upon by this acceleration. This avoids including gravitational force as an external force individually applied to each mass element.

The gravitational vector at the fuselage is simply the gravity vector in earth axis transformed to the fuselage axis system through the Euler angle rotations ϕ_E, θ_E, and ψ_E. Or

$$\begin{Bmatrix} g_X \\ g_Y \\ g_Z \end{Bmatrix}_F = \left[T_{E-F}\right] \begin{Bmatrix} 0 \\ 0 \\ g \end{Bmatrix} \tag{54}$$

where

$$\left[T_{E-F}\right] = \begin{bmatrix} 1 & 0 & 0 \\ 0 & \cos\phi_E & \sin\phi_E \\ 0 & -\sin\phi_E & \cos\phi_E \end{bmatrix} \begin{bmatrix} \cos\theta_E & 0 & -\sin\theta_E \\ 0 & 1 & 0 \\ \sin\theta_E & 0 & \cos\theta_E \end{bmatrix} \begin{bmatrix} \cos\psi_E & \sin\psi_E & 0 \\ -\sin\psi_E & \cos\psi_E & 0 \\ 0 & 0 & 1 \end{bmatrix} \tag{55}$$

The velocities of the principal axis system are obtained by integrating the rates of change of velocity with time, or

$$\begin{Bmatrix} \dot{X}_0 \\ \dot{Y}_0 \\ \dot{Z}_0 \end{Bmatrix}_F^I = \begin{Bmatrix} u \\ v \\ w \end{Bmatrix}_F^I = \int_0^t \begin{Bmatrix} \dot{u} \\ \dot{v} \\ \dot{w} \end{Bmatrix}_F dt + \begin{Bmatrix} u \\ v \\ w \end{Bmatrix}_{t = 0,F} \tag{56}$$

These velocities in earth coordinates can be written as

$$\begin{Bmatrix} \dot{X}_0 \\ \dot{Y}_0 \\ \dot{Z}_0 \end{Bmatrix}_E^I = \left[T_{F-E}\right] \begin{Bmatrix} \dot{X}_0 \\ \dot{Y}_0 \\ \dot{Z}_0 \end{Bmatrix}_F^I = \left[T_{E-F}\right]^T \begin{Bmatrix} \dot{X}_0 \\ \dot{Y}_0 \\ \dot{Z}_0 \end{Bmatrix}_F^I \tag{57}$$

which can be integrated to give the position of the system relative to the earth. Doing this yields

$$\begin{Bmatrix} X_0 \\ Y_0 \\ Z_0 \end{Bmatrix}_E = \int_0^t \begin{Bmatrix} \dot{X}_0 \\ \dot{Y}_0 \\ \dot{Z}_0 \end{Bmatrix}_E^I dt + \begin{Bmatrix} X_0 \\ Y_0 \\ Z_0 \end{Bmatrix}_{t = 0,E} \tag{58}$$

4.5.2 Hub motions in inertial space. - The geometry of the hub, shaft and fuselage is described in Sections 4.2.1 through 4.2.3. Forming the motions of the hub first requires knowledge of the shaft set motions and shaft generalized coordinates. The transform from fuselage to shaft set, $\left[T_{F-S}\right]$, involves rotor tilt alignment data ϕ_{o_s} and θ_{o_s}. Elastic motions of the transmission suspension, and consequently the hub, are described by the generalized coordinates $(X, Y, Z, \phi, \theta, \psi)_S$ which are measured with respect to the shaft (S) set. The transform from shaft to hub, $\left[T_{S-H}\right]$ is a function of the generalized coordinate angles $(\phi, \theta, \psi)_S$.

The development starts with fuselage to shaft set relations:

$$\begin{Bmatrix} \dot{X}_0 \\ \dot{Y}_0 \\ \dot{Z}_0 \end{Bmatrix}_S^I = \left[T_{F-S}\right] \left\{ \begin{Bmatrix} \dot{X}_0 \\ \dot{Y}_0 \\ \dot{Z}_0 \end{Bmatrix}_F^I + \begin{bmatrix} 0 & -r & q \\ r & 0 & -p \\ -q & p & o \end{bmatrix}_F \begin{Bmatrix} X_{O_S} \\ Y_{O_S} \\ Z_{O_S} \end{Bmatrix}_F \right\} \tag{59}$$

$$\begin{Bmatrix} \ddot{X}_0 \\ \ddot{Y}_0 \\ \ddot{Z}_0 \end{Bmatrix}_S^{EI} = \left[T_{F-S}\right] \left\{ \begin{Bmatrix} \ddot{X}_0 \\ \ddot{Y}_0 \\ \ddot{Z}_0 \end{Bmatrix}_F^{EI} + \left[\begin{bmatrix} 0 & -r & q \\ r & 0 & -p \\ -q & p & 0 \end{bmatrix}_F \begin{bmatrix} 0 & -r & q \\ r & 0 & -p \\ -q & p & 0 \end{bmatrix}_F + \begin{bmatrix} 0 & -\dot{r} & \dot{q} \\ \dot{r} & 0 & -\dot{p} \\ -\dot{q} & \dot{p} & 0 \end{bmatrix}_F \right] \begin{Bmatrix} X_{O_S} \\ Y_{O_S} \\ Z_{O_S} \end{Bmatrix}_F \right\} \tag{60}$$

Noting the following transformations:

$$\begin{Bmatrix} p_F \\ q_F \\ r_F \end{Bmatrix}_S = \left[T_{F-S}\right] \begin{Bmatrix} p \\ q \\ r \end{Bmatrix}_F \tag{61}$$

$$\begin{Bmatrix} \dot{p}_F \\ \dot{q}_F \\ \dot{r}_F \end{Bmatrix}_S = \begin{bmatrix} T_{F-S} \end{bmatrix} \begin{Bmatrix} \dot{p} \\ \dot{q} \\ \dot{r} \end{Bmatrix}_F \tag{62}$$

Applied to hub set equations:

$$\begin{Bmatrix} \dot{X}_O \\ \dot{Y}_O \\ \dot{Z}_O \end{Bmatrix}_H^I = \begin{bmatrix} T_{S-H} \end{bmatrix} \left\{ \begin{Bmatrix} \dot{X}_O \\ \dot{Y}_O \\ \dot{Z}_O \end{Bmatrix}^I + \begin{Bmatrix} \dot{X}_H \\ \dot{Y}_H \\ \dot{Z}_H \end{Bmatrix}_S + \begin{bmatrix} 0 & -r_F & q_F \\ r_F & 0 & -p_F \\ -q_F & p_F & 0 \end{bmatrix}_S \begin{Bmatrix} X_H \\ Y_H \\ Z_H \end{Bmatrix}_S \right\}$$

$$= \begin{Bmatrix} u \\ v \\ w \end{Bmatrix}_H$$

and

$$\begin{Bmatrix} \ddot{X}_O \\ \ddot{Y}_O \\ \ddot{Z}_O \end{Bmatrix}_H^{EI} = \begin{bmatrix} T_{S-H} \end{bmatrix} \left\{ \begin{Bmatrix} \ddot{X}_O \\ \ddot{Y}_O \\ \ddot{Z}_O \end{Bmatrix}_S^{EI} + \begin{Bmatrix} \ddot{X}_H \\ \ddot{Y}_H \\ \ddot{Z}_H \end{Bmatrix}_S + 2 \begin{bmatrix} 0 & -r_F & q_F \\ r_F & 0 & -p_F \\ -q_F & p_F & 0 \end{bmatrix}_S \begin{Bmatrix} \dot{X}_H \\ \dot{Y}_H \\ \dot{Z}_H \end{Bmatrix}_S \right.$$

$$\left. + \left[\begin{bmatrix} 0 & -r_F & q_F \\ r_F & 0 & -p_F \\ -q_F & p_F & 0 \end{bmatrix}_S \begin{bmatrix} 0 & -r_F & q_F \\ r_F & 0 & -p_F \\ -q_F & p_F & 0 \end{bmatrix}_S + \begin{bmatrix} 0 & -\dot{r}_F & \dot{q}_F \\ \dot{r}_F & 0 & -\dot{p}_F \\ -\dot{q}_F & \dot{p}_F & 0 \end{bmatrix}_S \right] \begin{Bmatrix} X_H \\ Y_H \\ Z_H \end{Bmatrix}_S \right\} \tag{64}$$

where

$$\begin{Bmatrix} X_H \\ Y_H \\ Z_H \end{Bmatrix}_S = \begin{Bmatrix} X \\ Y \\ Z \end{Bmatrix}_S + \begin{bmatrix} 0 & -\psi_S & \vartheta_S \\ \psi_S & 0 & -\phi_S \\ -\vartheta_S & \phi_S & 0 \end{bmatrix} \begin{Bmatrix} X_{O_H} \\ Y_{O_H} \\ Z_{O_H} \end{Bmatrix}_S \tag{65}$$

$$\begin{Bmatrix} \dot{X}_H \\ \dot{Y}_H \\ \dot{Z}_H \end{Bmatrix}_S = \begin{Bmatrix} \dot{X} \\ \dot{Y} \\ \dot{Z} \end{Bmatrix}_S - \begin{bmatrix} 0 & -\dot{\psi}_S & \dot{\vartheta}_S \\ \dot{\psi}_S & 0 & -\dot{\phi}_S \\ -\dot{\vartheta}_S & \dot{\phi}_S & 0 \end{bmatrix} \begin{Bmatrix} X_{O_H} \\ Y_{O_H} \\ Z_{O_H} \end{Bmatrix}_S \tag{66}$$

$$\begin{Bmatrix} \ddot{X}_H \\ \ddot{Y}_H \\ \ddot{Z}_H \end{Bmatrix}_S = \begin{Bmatrix} \ddot{X} \\ \ddot{Y} \\ \ddot{Z} \end{Bmatrix}_S \begin{bmatrix} 0 & -\ddot{\psi}_S & \ddot{\vartheta}_S \\ \ddot{\psi}_S & 0 & -\ddot{\phi}_S \\ -\ddot{\vartheta}_S & \ddot{\phi}_S & 0 \end{bmatrix} \begin{Bmatrix} X_{O_H} \\ Y_{O_H} \\ Z_{O_H} \end{Bmatrix}_S \tag{67}$$

Forming the relative location of the hub in fuselage coordinates:

$$\begin{Bmatrix} X_H \\ Y_H \\ Z_H \end{Bmatrix}_F \quad \begin{Bmatrix} X_{O_S} \\ Y_{O_S} \\ Z_{O_S} \end{Bmatrix}_F + \left[T_{F-S}\right]^T \begin{Bmatrix} X_H \\ Y_H \\ Z_H \end{Bmatrix}_S \tag{68}$$

Looking at angular information in the hub set:

$$\begin{Bmatrix} p \\ q \\ r \end{Bmatrix}_H = \begin{Bmatrix} 0 \\ 0 \\ \dot{\psi}_S \end{Bmatrix} + \begin{bmatrix} \cos\psi & \sin\psi & 0 \\ -\sin\psi & \cos\psi & 0 \\ 0 & 0 & 1 \end{bmatrix}_S \left\{ \begin{Bmatrix} 0 \\ \dot{\theta} \\ 0 \end{Bmatrix}_S \right.$$

$$+\begin{bmatrix}\cos\theta & 0 & -\sin\theta\\ 0 & 1 & 0\\ \sin\theta & 0 & \cos\theta\end{bmatrix}_S\left\{\begin{Bmatrix}\dot\phi\\0\\0\end{Bmatrix}_S+\begin{bmatrix}1 & 0 & 0\\ 0 & \cos\phi & \sin\phi\\ 0 & -\sin\phi & \cos\phi\end{bmatrix}\begin{Bmatrix}p_F\\q_F\\r_F\end{Bmatrix}_S\right\}\Bigg\} \tag{69}$$

$$\begin{Bmatrix}\dot p\\ \dot q\\ \dot r\end{Bmatrix}_H=\begin{Bmatrix}0\\0\\\ddot\psi\end{Bmatrix}_S+\dot\psi\begin{bmatrix}-\sin\psi & \cos\psi & 0\\ -\cos\psi & -\sin\psi & 0\\ 0 & 0 & 0\end{bmatrix}_S\Bigg\{\begin{Bmatrix}0\\\dot\theta\\0\end{Bmatrix}_S+\begin{bmatrix}\cos\theta & 0 & -\sin\theta\\ 0 & 1 & 0\\ \sin\theta & 0 & \cos\theta\end{bmatrix}_S\Bigg\{\begin{Bmatrix}\dot\phi\\0\\0\end{Bmatrix}_S$$

$$+\begin{bmatrix}1 & 0 & 0\\ 0 & \cos\phi & \sin\phi\\ 0 & -\sin\phi & \cos\phi\end{bmatrix}\begin{Bmatrix}p_F\\q_F\\r_F\end{Bmatrix}_S\Bigg\}\Bigg\}+\begin{bmatrix}\cos\psi & \sin\psi & 0\\ -\sin\psi & \cos\psi & 0\\ 0 & 0 & 1\end{bmatrix}_S\Bigg\{\begin{Bmatrix}0\\\dot\theta\\0\end{Bmatrix}_S$$

$$+\dot\theta_S\begin{bmatrix}-\sin\theta & 0 & -\cos\theta\\ 0 & 0 & 0\\ \cos\theta & 0 & -\sin\theta\end{bmatrix}_S\Bigg\{\begin{Bmatrix}\dot\phi\\0\\0\end{Bmatrix}_S+\begin{bmatrix}1 & 0 & 0\\ 0 & \cos\phi & \sin\phi\\ 0 & -\sin\phi & \cos\phi\end{bmatrix}\begin{Bmatrix}p_F\\q_F\\r_F\end{Bmatrix}_S\Bigg\}$$

$$+\begin{bmatrix}\cos\theta & 0 & -\sin\theta\\ 0 & 1 & 0\\ \sin\theta & 0 & \cos\theta\end{bmatrix}_S\Bigg\{\begin{Bmatrix}\ddot\phi\\0\\0\end{Bmatrix}_S+\dot\phi_S\begin{bmatrix}0 & 0 & 0\\ 0 & -\sin\phi & \cos\phi\\ 0 & -\cos\phi & -\sin\phi\end{bmatrix}\begin{Bmatrix}p_F\\q_f\\r_F\end{Bmatrix}_S$$

$$+\begin{bmatrix}1 & 0 & 0\\ 0 & \cos\phi & \sin\phi\\ 0 & -\sin\phi & \cos\phi\end{bmatrix}\begin{Bmatrix}\dot p_F\\ \dot q_F\\ \dot r_F\end{Bmatrix}_S\Bigg\}\Bigg\} \tag{7C}$$

4.5.3 Motion of rotor coordinate axis. - The rotor coordinate axis system is shown in Figure 6. Note that the rotor coordinate axis system is rotated 180 degrees about the Y axis relative to the hub axis system at the time when the rotor is at azimuth position zero. That is, X and Z change directions. The rotor coordinate system then rotates through the angle ψ_R from this position.

The sequence of rotation in going from hub to rotor coordinates consists of first a 180-degree θ rotation, followed by the ψ_R rotation. Following the convention established in Section 4.4.2 for Euler angles:

$$\left[T_{H-R}\right] = \begin{bmatrix} \cos\psi_R & \sin\psi_R & 0 \\ -\sin\psi_R & \cos\psi_R & 0 \\ 0 & 0 & 1 \end{bmatrix} \begin{bmatrix} \cos\pi & 0 & \sin\pi \\ 0 & 1 & 0 \\ -\sin\pi & 0 & \cos\pi \end{bmatrix}$$

$$= \begin{bmatrix} \cos\psi_R & \sin\psi_R & 0 \\ -\sin\psi_R & \cos\psi_R & 0 \\ 0 & 0 & 1 \end{bmatrix} \begin{bmatrix} -1 & 0 & 0 \\ 0 & 1 & 0 \\ 0 & 0 & -1 \end{bmatrix} \tag{71}$$

where the last matrix represents the 180-degree θ rotation. The next matrix is the rotor rotation, $\psi_R = \int_0^t \Omega_R \, dt$.

Since the origins of the rotor coordinate system and the principal reference axis system are coincident, the linear velocities and accelerations of the origin of the rotor coordinate system can be directly written as:

$$\begin{Bmatrix} X_0 \\ Y_0 \\ Z_0 \end{Bmatrix}_R^I = \left[T_{H-R}\right] \begin{Bmatrix} \dot{X}_0 \\ \dot{Y}_0 \\ \dot{Z}_0 \end{Bmatrix}_H^I \tag{72}$$

and

$$\begin{Bmatrix} \ddot{X}_0 \\ \ddot{Y}_0 \\ \ddot{Z}_0 \end{Bmatrix}_R^{EI} = \left[T_{H-R}\right] \begin{Bmatrix} \ddot{X}_0 \\ \ddot{Y}_0 \\ \ddot{Z}_0 \end{Bmatrix}_H^{EI} \tag{73}$$

Noting gravity has been treated as an equivalent acceleration in the hub generalized coordinate accelerations. This same equivalent acceleration is included in $(\ddot{X}_0, \ddot{Y}_0, \ddot{Z}_0)_R^{EI}$, the rotor coordinate accelerations.

The angular velocities, p_R, q_R, r_R, and accelerations, $\dot{p}_R$, $\dot{q}_R$, $\dot{r}_R$ of the rotor coordinate system are determined; again noting the rotation order. The rotor coordinate system angular velocities are:

$$\begin{Bmatrix} p \\ q \\ r \end{Bmatrix}_R = \left\{ \begin{Bmatrix} 0 \\ 0 \\ \dot{\psi}_R \end{Bmatrix}_H + \begin{bmatrix} \cos\psi_R & \sin\psi_R & 0 \\ -\sin\psi_R & \cos\psi_R & 0 \\ 0 & 0 & 1 \end{bmatrix} \begin{Bmatrix} -p \\ q \\ -r \end{Bmatrix}_H \right\} \tag{74}$$

Likewise, accelerations of the rotor coordinate system are:

$$\begin{Bmatrix} \dot{p} \\ \dot{q} \\ \dot{r} \end{Bmatrix}_R = \left\{ \begin{Bmatrix} 0 \\ 0 \\ \ddot{\psi}_R \end{Bmatrix}_H + \dot{\psi}_R \begin{bmatrix} -\sin\psi_R & \cos\psi_R & 0 \\ -\cos\psi_R & -\sin\psi_R & 0 \\ 0 & 0 & 0 \end{bmatrix} \begin{Bmatrix} -p \\ q \\ -r \end{Bmatrix}_H \right.$$

$$\left. + \begin{bmatrix} \cos\psi_R & \sin\psi_R & 0 \\ -\sin\psi_R & \cos\psi_R & 0 \\ 0 & 0 & 1 \end{bmatrix} \begin{Bmatrix} -\dot{p} \\ \dot{q} \\ -\dot{r} \end{Bmatrix}_H \right\} \tag{75}$$

The above equations then define the coordinate transformation from hub to rotor coordinates; and rotor axis system linear and angular velocities and accelerations in terms of velocities and accelerations of hub and the rotor degrees of freedom ψ_R.

4.5.4 Blade coordinate relative to rotor coordinates. - Since each blade has its own blade reference system, as shown in Figure 6, the X_{BLn} and Y_{BLn} axes are rotated with respect to the X_R and Y_R axes azimuthally by an angle ψ_{BLn} defined by the equation

$$\psi_{BLn} = \frac{-2\pi(n-1)}{b} \tag{76}$$

where b is the number of blades and n is the blade number. This equation states that the X_{BL1} and X_R, and the Y_{BL1} and the Y_R axes are coincident.

The transformations between the rotor coordinate axis system and the blade coordinate axis systems are defined by the equation

$$\left[T_{R-BLn}\right] = \begin{bmatrix} \cos\psi_{BLn} & \sin\psi_{BLn} & 0 \\ -\sin\psi_{BLn} & \cos\psi_{BLn} & 0 \\ 0 & 0 & 1 \end{bmatrix} \tag{77}$$

Note that these equations define blade one as being straight aft at time zero.

In the blade reference axes, the velocities and accelerations of the origin of the blade reference axis system become:

$$\begin{Bmatrix} \dot{X}_{OBLn} \\ \dot{Y}_{OBLn} \\ \dot{Z}_{OBLn} \end{Bmatrix}_{BLn}^{I} = \left[T_{R-BLn}\right] \begin{Bmatrix} \dot{X}_{O} \\ \dot{Y}_{O} \\ \dot{Z}_{O} \end{Bmatrix}_{R}^{I} \tag{78}$$

and

$$\begin{Bmatrix} \ddot{X}_{OBLn} \\ \ddot{Y}_{OBLn} \\ \ddot{Z}_{OBLn} \end{Bmatrix}_{BLn}^{EI} = \left[T_{R-BLn}\right] \begin{Bmatrix} \ddot{X}_{O} \\ \ddot{Y}_{O} \\ \ddot{Z}_{O} \end{Bmatrix}_{R}^{EI} \tag{79}$$

Likewise, the angular velocities and accelerations of the blade reference axis systems become:

$$\begin{Bmatrix} p \\ q \\ r \end{Bmatrix}_{BLn} = \left[T_{R-BLn}\right] \begin{Bmatrix} p \\ q \\ r \end{Bmatrix}_{R} \tag{80}$$

and

$$\begin{Bmatrix} \dot{p} \\ \dot{q} \\ \dot{r} \end{Bmatrix}_{BLn} = \left[T_{R-BLn}\right] \begin{Bmatrix} \dot{p} \\ \dot{q} \\ \dot{r} \end{Bmatrix}_{R} \tag{81}$$

4.5.5 Blade element motion. - The following blade motion description, due to the involved nature of the geometry, is rather lengthy. First, in this development, the motion of the blade with respect to the relative blade coordinates is given. This motion is the sum of static and modal deflections. Then the relation to freestream coordinates is computed. Partial derivatives are extracted from the transformations for use in the equations of motion of the blade in Section 5.6.

The blade element motions for the nth blade are defined relative to the blade (BLn) coordinate reference axes (Figure 6). The blade element relative motions are functions of the static shape, of blade feathering and torsional deflection, and of blade bending of the coupled inplane and flapping modes.

The static shape includes such items as blade twist, ϕ_{TW}, hub precone angle, β_0, blade droop angle relative to the precone angle, γ, blade sweep angle, τ_0, feathering axis precone, β_{FA}, the blade feathering angle, and the blade element center of gravity location.

The blade motions about this static shape include the effects of the three blade bending modes, A_{1n}, A_{2n} and A_{3n}, blade feathering, ϕ_F, and blade torsional deflection, ϕ_t.

The blade element motions are now defined. The blade static position in the blade reference axis system is first developed. The blade bending and feathering deflections are then introduced. Both deflections and slopes are developed and then these equations are differentiated with respect to time to obtain the blade element linear and angular velocities and accelerations.

The blade element linear motions are developed in blade (BLn) coordinates and the blade element angular velocities and accelerations are developed in blade element (BLE) coordinates. The coordinate transformation matrix $\left[T_{BLn-BLE}\right]$ is also defined to permit the transformation of the inertial velocities and accelerations from one axis system to the other. The development of the blade relative motion equations now starts with the description of the shape of the blade.

4.5.5.1 Blade static shape. - Blade elemental motion is defined as motion of the blade element reference axis system which has its origin at the blade element center of gravity. The blade aerodynamic reference axis is selected as the 1/4 chord. Likewise, the geometry and dynamics are referenced to the 1/4 chord, though any reference line could have been used. Starting with the straight untwisted blade with the blade 1/4 chord lying along the X_{BLn} axis as in Figure 19, the blade element cg and blade element coordinate axis system origin are defined by the coincident point defined by the vector

$$\begin{Bmatrix} X_{CG}(i) \\ Y_{CG}(i) \\ Z_{CG}(i) \end{Bmatrix}_{BLn} \tag{82}$$

in blade coordinates. Thd dimension $X_{CG}(i)_{BLn}$ is the undeformed spanwise location of the cg/blade element origin. The dimension $Y_{CG}(i)_{BLn}$ is the chordwise location of the c.g./blade element axis system origin forward of the blade 1/4 chord and $Z_{CG}(i)_{BLn}$ is any vertical offset of the c.g./blade element origin with respect to the reference chord plane of the blade.

Now, introducing blade twist by rotating about the X_{BLn} axis through the local blade twist angles, Figure 20, results in:

$$\begin{Bmatrix} X(i)_{BLE} \\ Y(i)_{BLE} \\ Z(i)_{BLE} \end{Bmatrix}_{I} = \begin{Bmatrix} X(i)_{BLE} \\ Y(i)_{BLE} \\ Z(i)_{BLE} \end{Bmatrix}_{BLn} = \begin{bmatrix} 1 & 0 & 0 \\ 0 & \cos\phi_{TW} & -\sin\phi_{TW} \\ 0 & \sin\phi_{TW} & \cos\phi_{TW} \end{bmatrix} \begin{Bmatrix} X_{CG} \\ Y_{CG} \\ Z_{CG} \end{Bmatrix}_{BLn} \tag{83}$$

The Roman numeral subscript I denotes the first of a sequence of static line transformations.

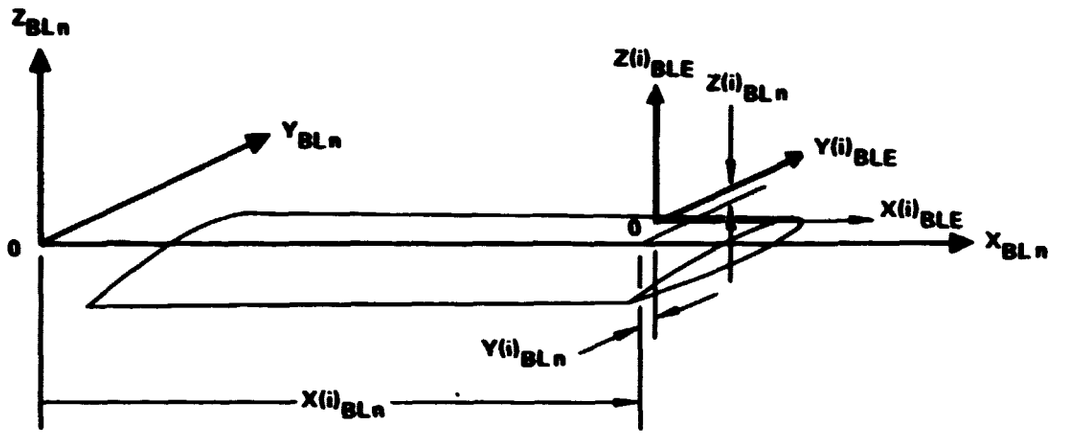

Figure 19. - Blade element c.g./origin location in blade coordinates.

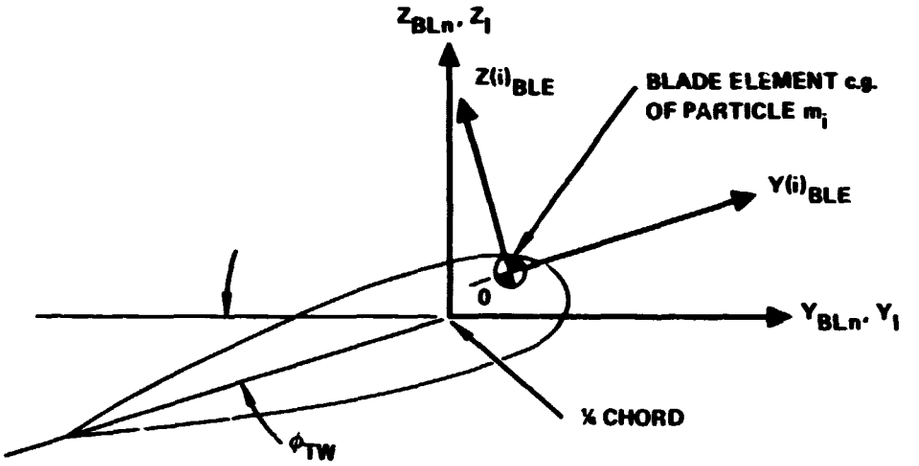

Figure 20. - Effect of blade twist on location of blade element c.g./axis system origin.

At this point the subscripting, BLE will be dropped to simplify the development. Rewriting the above equation, we have:

$$\begin{Bmatrix} X(i) \\ Y(i) \\ Z(i) \end{Bmatrix}_I = \begin{bmatrix} 1 & 0 & 0 \\ 0 & \cos\phi_{TW} & -\sin\phi_{TW} \\ 0 & \sin\phi_{TW} & \cos\phi_{TW} \end{bmatrix} \begin{Bmatrix} X_{CG} \\ Y_{CG} \\ Z_{CG} \end{Bmatrix} \tag{84}$$

Introducing blade coning, β_0, results in the location of the blade as shown in Figure 21. This results in:

$$\begin{Bmatrix} X(i) \\ Y(i) \\ Z(i) \end{Bmatrix}_{II} = \begin{bmatrix} \cos\beta_0 & 0 & -\sin\beta_0 \\ 0 & 1 & 0 \\ \sin\beta_0 & 0 & \cos\beta_0 \end{bmatrix} \begin{Bmatrix} X(i) \\ Y(i) \\ Z(i) \end{Bmatrix}_I \tag{85}$$

The next item of static geometry that is considered is blade droop, γ, and then blade sweep, τ_0. These rotations are shown in Figure 22. Note that since the blade sweep and droop angles are introduced at a distance X_{SW} out on the blade, it is first necessary to transfer axes to this location before making the rotations. Therefore, the blade displacements outboard of Station X_{SW} become:

$$\begin{Bmatrix} X(i) \\ Y(i) \\ Z(i) \end{Bmatrix}_{III} = \begin{bmatrix} \cos\tau_0 & -\sin\tau_0 & 0 \\ \sin\tau_0 & \cos\tau_0 & 0 \\ 0 & 0 & 1 \end{bmatrix} \begin{bmatrix} \cos\gamma & 0 & \sin\gamma \\ 0 & 1 & 0 \\ -\sin\gamma & 0 & \cos\gamma \end{bmatrix} \left\{ \begin{Bmatrix} X(i) \\ Y(i) \\ Z(i) \end{Bmatrix}_{II} - \begin{Bmatrix} X_{SW}\cos\beta_0 \\ 0 \\ X_{SW}\sin\beta_0 \end{Bmatrix} \right\} \tag{86}$$

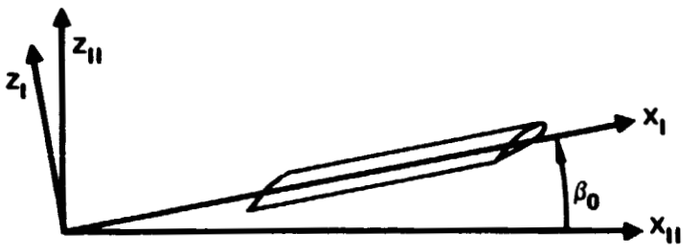

Figure 21. - Blade precone angle, β_0.

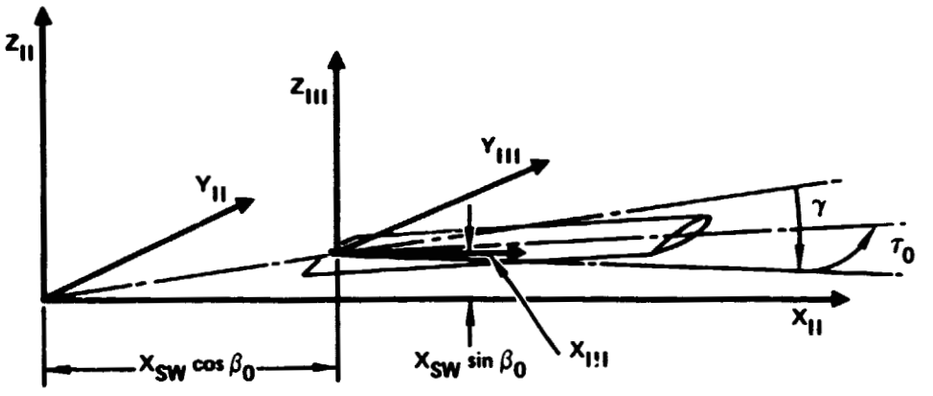

Figure 22. - Blade sweep, τ_0, and blade droop, γ.

At this same station, provisions are introduced to allow for offsets of the blade in both the vertical and horizontal directions by Z_{jog} and Y_{jog}, respectively. These offsets are shown in Figure 23. These offsets represent displacement of the blade 1/4 chord with respect to the blade precone line at blade station X_{SW}.

Introduction these offsets, then, and transferring back to the center of rotation through X_{SW} results in the description of the blade displacements outboard of station X_{SW}, including the effects of precone, sweep, droop, and offset of the blade from the precone line.

$$\begin{Bmatrix} X(i) \\ Y(i) \\ Z(i) \end{Bmatrix}_{IV} = \begin{Bmatrix} X(i) \\ Y(i) \\ Z(i) \end{Bmatrix}_{III} + \begin{Bmatrix} 0 \\ Y_{jog} \\ Z_{jog} \end{Bmatrix} + \begin{Bmatrix} X_{SW}\cos\beta_0 \\ 0 \\ X_{SW}\sin\beta_0 \end{Bmatrix} \tag{87}$$

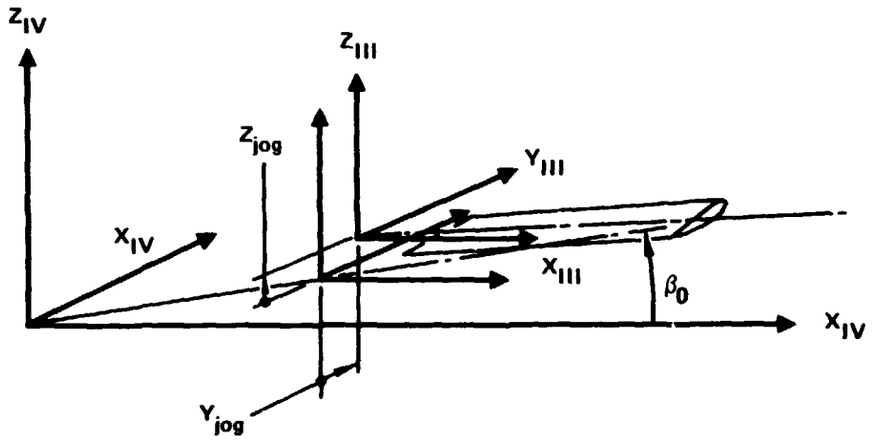

Figure 23. - Introduction of blade 1/r chord offset, Y_{jog} and Z_{jog} with respect to precone line.

At this point, a reminder that the prior development represents the blade displacement inboard of Station X_{SW} and the above equation outboard of Station X_{SW}. Therefore, inboard of Station X_{SW}:

$$\begin{Bmatrix} X(i) \\ Y(i) \\ Z(i) \end{Bmatrix} = \begin{Bmatrix} X(i) \\ Y(i) \\ Z(i) \end{Bmatrix}_{II} \tag{88}$$

Outboard of Station X_{SW}:

$$\begin{Bmatrix} X(i) \\ Y(i) \\ Z(i) \end{Bmatrix} = \begin{Bmatrix} X(i) \\ Y(i) \\ Z(i) \end{Bmatrix}_{IV} \tag{89}$$

With this in mind, the remaining developing of including the effects of feathering axis static precone and blade reference feather angle in describing the static blade position continues. No distinction will be made in the following developments between inboard of Station X_{SW} and outboard of Station X_{SW}.

Figure 24 shows how blade feathering is introduced. The axis system is translated to a point p which is located at the intersection of the precone line and the feathering axis. The location of this point is a distance ℓ_p along the cone line, as shown in this figure. The blade is first rotated to the feather axis; then rotated about the reference feathering angle, ϕ_{REF}, the feathering angle for which the blade modes are defined. Doing this results in:

$$\begin{Bmatrix} X(i) \\ Y(i) \\ Z(i) \end{Bmatrix}_V = \begin{bmatrix} 1 & 0 & 0 \\ 0 & \cos\phi_{REF} & -\sin\phi_{REF} \\ 0 & \sin\phi_{REF} & \cos\phi_{REF} \end{bmatrix} \begin{bmatrix} \cos\beta_{FA} & 0 & \sin\beta_{FA} \\ 0 & 1 & 0 \\ -\sin\beta_{FA} & 0 & \cos\beta_{FA} \end{bmatrix} \left\{ \begin{Bmatrix} X(i) \\ Y(i) \\ Z(i) \end{Bmatrix} - \begin{Bmatrix} \ell_p\cos\beta_0 \\ 0 \\ \ell_p\sin\beta_0 \end{Bmatrix} \right\} \tag{90}$$

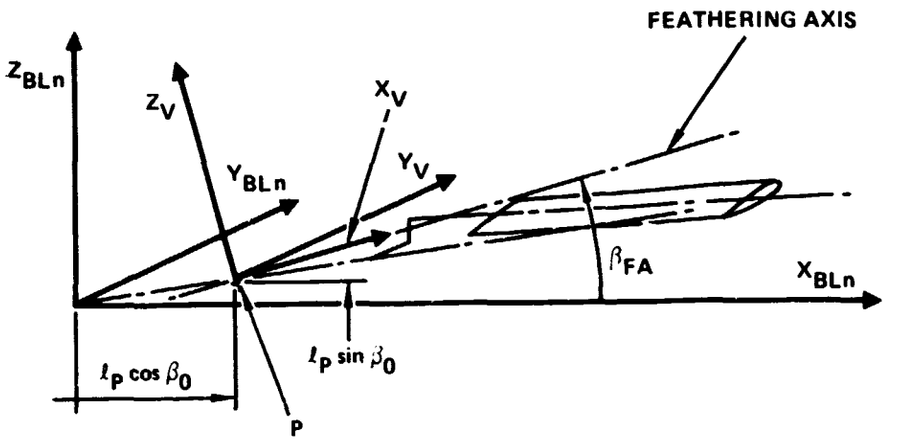

Figure 24. - Point p and feathering axis precone β_{FA}.

This equation defines the location of the static shape of the blade in an axis system with the y-axis horizontal and the x-axis aligned with the blade static feathering axis. Transforming now back through the feathering axis precone angle and translating back to the rotor shaft centerline results in the static shape of the blade defined in blade coordinates, or

$$\begin{Bmatrix} X_S(i) \\ Y_S(i) \\ Z_S(i) \end{Bmatrix}_{ELn} = \begin{bmatrix} \cos\beta_{FA} & 0 & -\sin\beta_{FA} \\ 0 & 1 & 0 \\ \sin\beta_{FA} & 0 & \cos\beta_{FA} \end{bmatrix} \begin{Bmatrix} X(i) \\ Y(i) \\ Z(i) \end{Bmatrix}_V + \begin{Bmatrix} \ell_p \cos\beta_0 \\ 0 \\ \ell_p \sin\beta_0 \end{Bmatrix} \tag{91}$$

where subscript S refers to blade static or undeformed shape. Combining equations developed so far results, then, in the following two equations which represent the static shape of the blade for both inboard and outboard of blade station X_{SW}.

Inboard of Station X_{SW}:

$$\{r_S\}_{BLn} = \begin{Bmatrix} X_S \\ Y_S \\ Z_S \end{Bmatrix}_{BLn} = \begin{bmatrix} \cos\beta_{FA} & 0 & -\sin\beta_{FA} \\ 0 & 1 & 0 \\ \sin\beta_{FA} & 0 & \cos\beta_{FA} \end{bmatrix} \begin{bmatrix} 1 & 0 & 0 \\ 0 & \cos\phi_{REF} & -\sin\phi_{REF} \\ 0 & \sin\phi_{REF} & \cos\phi_{REF} \end{bmatrix}$$

$$\cdot \begin{bmatrix} \cos\beta_{FA} & 0 & \sin\beta_{FA} \\ 0 & 1 & 0 \\ -\sin\beta_{FA} & 0 & \cos\beta_{FA} \end{bmatrix} \left\{ \begin{bmatrix} \cos\beta_0 & 0 & -\sin\beta_0 \\ 0 & 1 & 0 \\ \sin\beta_0 & 0 & \cos\beta_0 \end{bmatrix} \right.$$

$$\cdot \begin{bmatrix} 1 & 0 & 0 \\ 0 & \cos\phi_{TW} & -\sin\phi_{TW} \\ 0 & \sin\phi_{TW} & \cos\phi_{TW} \end{bmatrix} \left\{ \begin{Bmatrix} X_{CG} \\ Y_{CG} \\ Z_{CG} \end{Bmatrix} - \left. \begin{Bmatrix} \ell_p \cos\beta_0 \\ 0 \\ \ell_p \sin\beta_0 \end{Bmatrix} \right\} \right\}$$

$$+ \begin{Bmatrix} \ell_p \cos\beta_0 \\ 0 \\ \ell_p \sin\beta_0 \end{Bmatrix} \qquad (92)$$

Outboard of Station X_{SW}:

$$\{r_S\}_{BLn} = \begin{Bmatrix} X_S \\ Y_S \\ Z_S \end{Bmatrix} = \begin{bmatrix} \cos\beta_{FA} & 0 & -\sin\beta_{FA} \\ 0 & 1 & 0 \\ \sin\beta_{FA} & 0 & \cos\beta_{FA} \end{bmatrix} \begin{bmatrix} 1 & 0 & 0 \\ 0 & \cos\phi_{REF} & -\sin\phi_{REF} \\ 0 & \sin\phi_{REF} & \cos\phi_{REF} \end{bmatrix}$$

$$\cdot \begin{bmatrix} \cos\beta_{FA} & 0 & \sin\beta_{FA} \\ 0 & 1 & 0 \\ -\sin\beta_{FA} & 0 & \cos\beta_{FA} \end{bmatrix} \left\{ \begin{bmatrix} \cos\tau_0 & -\sin\tau_0 & 0 \\ \sin\tau_0 & \cos\tau_0 & 0 \\ 0 & 0 & 1 \end{bmatrix} \begin{bmatrix} \cos\gamma & 0 & \sin\gamma \\ 0 & 1 & 0 \\ -\sin\gamma & 0 & \cos\gamma \end{bmatrix} \right.$$

$$\cdot \left\{ \begin{bmatrix} \cos\beta_0 & 0 & -\sin\beta_0 \\ 0 & 1 & 0 \\ \sin\beta_0 & 0 & \cos\beta_0 \end{bmatrix} \begin{bmatrix} 1 & 0 & 0 \\ 0 & \cos\phi_{TW} & -\sin\phi_{TW} \\ 0 & \sin\phi_{TW} & \cos\phi_{TW} \end{bmatrix} \begin{Bmatrix} X_{CG} \\ Y_{CG} \\ Z_{CG} \end{Bmatrix} \right.$$

$$\left. - \begin{Bmatrix} X_{SW}\cos\beta_0 \\ 0 \\ X_{SW}\sin\beta_0 \end{Bmatrix} \right\} + \begin{Bmatrix} 0 \\ Y_{jog} \\ Z_{jog} \end{Bmatrix} + \begin{Bmatrix} X_{SW}\cos\beta_0 \\ 0 \\ X_{SW}\sin\beta_0 \end{Bmatrix} - \left. \begin{Bmatrix} \ell_p\cos\beta_0 \\ 0 \\ \ell_p\sin\beta_0 \end{Bmatrix} \right\}$$

$$+ \begin{Bmatrix} \ell_p\cos\beta_0 \\ 0 \\ \ell_p\sin\beta_0 \end{Bmatrix} \qquad (93)$$

These two equations then define completely the static shape of the blade. The development will not proceed to include the blade bending or elastic deformation. However, before proceeding with this, the static location of the blade feathering bearing is defined since these will be used in the development that follows.

Referring to Figure 25, it can be seen that the static position of the inboard feather bearing location can be written as:

$$\begin{Bmatrix} X_{S_{IB}} \\ Y_{S_{IB}} \\ Z_{S_{IB}} \end{Bmatrix}_{BLn} = \begin{Bmatrix} \ell_{IB}\cos\beta_0 \\ 0 \\ \ell_{IB}\sin\beta_0 - \left(\ell_p - \ell_{IB}\right)\left(\tan(\beta_{FA} - \beta_0)\right)\cos\beta_0 \end{Bmatrix} \tag{94}$$

The static location of the outboard feather bearing is:

$$\begin{Bmatrix} X_{S_{OB}} \\ Y_{S_{OB}} \\ Z_{S_{OB}} \end{Bmatrix}_{BLn} = \begin{Bmatrix} \ell_{OB}\cos\beta_0 \\ 0 \\ \ell_{OB}\sin\beta_0 + \left(\ell_{OB} - \ell_p\right)\left(\tan(\beta_{FA} - \beta_0)\right)\cos\beta_0 \end{Bmatrix} \tag{95}$$

With these definitions, the analysis will not proceed to include the effects of blade bending, blade feathering, and torsional deflection.

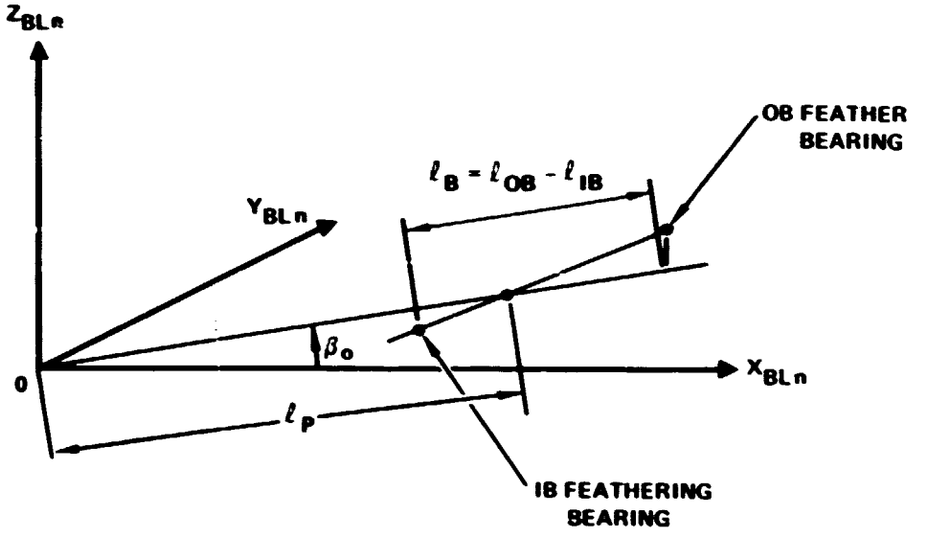

Figure 25. - Static feather bearing geometry.

4.5.5.2 Blade shape - elastic deformation. - In the foregoing development, the analysis has proceeded in a completely rigorous fashion. At this point, though, a departure from a completely rigorous simulation of the elemental blade motions will be made. It will be assumed, as far as blade elastic deformation is concerned, that the cosine of angles, like precone less droop, blade sweep, elastic flapping, and elastic inplane slopes, but not blade feathering is approximately equal to 1, and therefore, the blade elastic deflections, y and z, in blade coordinates, will be assumed to be equal to those in the static blade element coordinates. This assumption is a reasonably valid assumption and is completely consistent with standard practice in the mathematical representation of blade element motions.

Additionally, as far as the effect on structural axis reorientation due to blade ζ rotation, the effect due to blade leastic twist is considered to be small compared to that due to blade cyclic and collective feathering. Also it will be assumed that the contributions to blade Y and Z motion are small due to blade torsional motion, other than that due to local center of gravity offset.

With these assumptions in mind, blade elastic bending will now be introduced. The contribution to elastic blade bending is simply

$$\begin{Bmatrix} 0 \\ Y_{BEND} \\ Z_{BEND} \end{Bmatrix}_{BLn} = \begin{bmatrix} 0 & 0 & 0 \\ Y_1 & Y_2 & Y_3 \\ Z_1 & Z_2 & Z_3 \end{bmatrix} \begin{Bmatrix} A_{1n} \\ A_{2n} \\ A_{3n} \end{Bmatrix} \tag{96}$$

Note that X or spanwise motions are not included in this equation. Blade spanwise motion will be determined separately by utilizing blade slope data to determine the change in the projected blade length upon the blade X axis. With this in mind, the total Y and Z blade motions including blade bending, but not yet including blade feathering or blade elastic twist, is strictly the sum of the previous static line expressions and the modal deflection. Blade torsional deflection is treated as an independent degree of freedom, and therefore is not included as part of these blade modes. Combining the previous static deflection with the modal deflections gives:

$$\begin{Bmatrix} X_{(B+S)} \\ Y_{(B+S)} \\ Z_{(B+S)} \end{Bmatrix}_{BLn} = \begin{Bmatrix} X_S \\ Y_S \\ Z_S \end{Bmatrix}_{BLn} + \begin{Bmatrix} 0 \\ Y_{BEND} \\ Z_{BEND} \end{Bmatrix}_{BLn} \tag{97}$$

4.5.5.3 Blade feathering. - Blade feathering is relative to the reference feathering angle ϕ_{REF}. The feather angle, then, as far as blade motion is concerned, is due to the difference in the total feather angle ϕ_F and the reference feather angle ϕ_{REF}.

The blade feathering motion is introduced similarly to the way the blade reference feathering angle was introduced, except that the feather axis slopes are due to the static position as well as due to elastic deformation in both the flapwise and inplane deflection.

If we let Z'_{FA} and Y'_{FA} represent the instantaneous vertical and inplane slopes of the feathering axis, then transferring to the inboard feathering bearing, making the rotations through Z'_{FA} and Y'_{FA} to the feathering axis, rotating through the delta feather angle $-(\phi_F-\phi_{REF})$ of $-\Delta\phi_F$, rotating back through $-Y'_{FA}$ and $-Z'_{FA}$, and then transferring back to the BLn axis system results in the definition of the displacements in blade axis coordinates.

However, before proceeding with this, the feathering axis slopes Y'_{FA} and Z'_{FA} are defined. The slopes are simply defined as the difference in the total static and elastic deflection of the outboard and inboard feather bearings divided by the spanwise distance between the bearings. Then from Figure 25 and the bearing static location equation:

$$Y'_{FA} \approx \sin^{-1}\left(\frac{Y_{OB} - Y_{IB}}{\ell_B}\right) \tag{98}$$

and

$$Z'_{FA} \approx \sin^{-1}\left(\frac{Z_{OB} - Z_{IB}}{\ell_B}\right) \tag{99}$$

where in terms of the static and modal deflections

$$\begin{Bmatrix} X_{IB} \\ Y_{IB} \\ Z_{IB} \end{Bmatrix} = \begin{Bmatrix} X_{S_{IB}} \\ Y_{S_{IB}} \\ Z_{S_{IB}} \end{Bmatrix} + \begin{bmatrix} 0 & 0 & 0 \\ Y_{IB_1} & Y_{IB_2} & Y_{IB_3} \\ Z_{IB_1} & Z_{IB_2} & Z_{IB_3} \end{bmatrix} \begin{Bmatrix} A_{1n} \\ A_{2n} \\ A_{3n} \end{Bmatrix} \tag{100}$$

and

$$\begin{Bmatrix} X_{OB} \\ Y_{OB} \\ Z_{OB} \end{Bmatrix} = \begin{Bmatrix} X_{S_{OB}} \\ Y_{S_{OB}} \\ Z_{S_{OB}} \end{Bmatrix} + \begin{bmatrix} 0 & 0 & 0 \\ Y_{OB_1} & Y_{OB_2} & Y_{OB_3} \\ Z_{OB_1} & Z_{OB_2} & Z_{OB_3} \end{bmatrix} \begin{Bmatrix} A_{1n} \\ A_{2n} \\ A_{3n} \end{Bmatrix} \tag{101}$$

In the development that follows, the time derivatives of Y'_{FA} and Z'_{FA} are required, so therefore, they are now defined. Taking the first and second time derivatives of the slope equations yields

$$\dot{Y}'_{FA} \approx (\dot{Y}_{OB} - \dot{Y}_{IB}) / \cos(Y'_{FA}) \ell_B \tag{102}$$

$$\dot{Z}'_{FA} \approx (\dot{Z}_{OB} - \dot{Z}_{IB}) / \cos(Z'_{FA}) \ell_B \tag{103}$$

and

$$\ddot{Y}'_{FA} \approx (\ddot{Y}_{OB} - \ddot{Y}_{IB}) / \cos(Y'_{FA}) \ell_B + \sin(Y'_{FA}) \dot{Y}'^{2}_{FA} / \cos(Y'_{FA}) \tag{104}$$

$$\ddot{Z}'_{FA} \approx (\ddot{Z}_{OB} - \ddot{Z}_{IB}) / \cos(Z'_{FA}) \ell_B + \sin(Z'_{FA}) \dot{Z}'^{2}_{FA} / \cos(Z'_{FA}) \tag{105}$$

where

$$\begin{Bmatrix} \dot{Y}_{IB} \\ \dot{Z}_{IB} \end{Bmatrix} = \begin{bmatrix} Y_{IB_1} & Y_{IB_2} & Y_{IB_3} \\ Z_{IB_1} & Z_{IB_2} & Z_{IB_3} \end{bmatrix} \begin{Bmatrix} \dot{A}_{1n} \\ \dot{A}_{2n} \\ \dot{A}_{3n} \end{Bmatrix} \tag{106}$$

$$\begin{Bmatrix} \dot{Y}_{OB} \\ \dot{Z}_{OB} \end{Bmatrix} = \begin{bmatrix} Y_{OB_1} & Y_{OB_2} & Y_{OB_3} \\ Z_{OB_1} & Z_{OB_2} & Z_{OB_3} \end{bmatrix} \begin{Bmatrix} \dot{A}_{1n} \\ \dot{A}_{2n} \\ \dot{A}_{3n} \end{Bmatrix} \tag{107}$$

and where

$$\begin{Bmatrix} \ddot{Y}_{IB} \\ \ddot{Z}_{IB} \end{Bmatrix} = \begin{bmatrix} Y_{IB_1} & Y_{IB_2} & Y_{IB_3} \\ Z_{IB_1} & Z_{IB_2} & Z_{IB_3} \end{bmatrix} \begin{Bmatrix} \ddot{A}_{1n} \\ \ddot{A}_{2n} \\ \ddot{A}_{3n} \end{Bmatrix} \tag{108}$$

$$\begin{Bmatrix} \ddot{Y}_{OB} \\ \ddot{Z}_{OB} \end{Bmatrix} = \begin{bmatrix} Y_{OB_1} & Y_{OB_2} & Y_{OB_3} \\ Z_{OB_1} & Z_{OB_2} & Z_{OB_3} \end{bmatrix} \begin{Bmatrix} \ddot{A}_{1n} \\ \ddot{A}_{2n} \\ \ddot{A}_{3n} \end{Bmatrix} \tag{109}$$

Transferring the blade displacements as indicated above to the inboard feather bearing, transforming to the feathering axis, and performing the feathering rotation as discussed earlier, yields the following equation which defines the blade displacements in blade axis coordinates:

$$
\begin{Bmatrix} X_{(F+B+S)} \\ Y_{(F+B+S)} \\ Z_{(F+B+S)} \end{Bmatrix}_{BLn} = \begin{bmatrix} \cos Z'_{FA} & 0 & -\sin Z'_{FA} \\ 0 & 1 & 0 \\ \sin Z'_{FA} & 0 & \cos Z'_{FA} \end{bmatrix} \begin{bmatrix} \cos Y'_{FA} & -\sin Y'_{FA} & 0 \\ \sin Y'_{FA} & \cos Y'_{FA} & 0 \\ 0 & 0 & 1 \end{bmatrix}
$$

$$
\cdot \begin{bmatrix} 1 & 0 & 0 \\ 0 & \cos\Delta\phi_F & -\sin\Delta\phi_F \\ 0 & \sin\Delta\phi_F & \cos\Delta\phi_F \end{bmatrix} \begin{bmatrix} \cos Y'_{FA} & \sin Y'_{FA} & 0 \\ -\sin Y'_{FA} & \cos Y'_{FA} & 0 \\ 0 & 0 & 1 \end{bmatrix}
$$

$$
\cdot \begin{bmatrix} \cos Z'_{FA} & 0 & \sin Z'_{FA} \\ 0 & 1 & 0 \\ -\sin Z'_{FA} & 0 & \cos Z'_{FA} \end{bmatrix} \cdot \left\{ \begin{Bmatrix} X_{(B+S)} \\ Y_{(B+S)} \\ Z_{(B+S)} \end{Bmatrix} - \begin{Bmatrix} X_{IB} \\ Y_{IB} \\ Z_{IB} \end{Bmatrix} \right\} + \begin{Bmatrix} X_{IB} \\ Y_{IB} \\ Z_{IB} \end{Bmatrix} \tag{110}
$$

This equation then gives the blade displacement in blade coordinates, including the effects of the static shape, blade bending, and blade static twist. The effect of blade elastic twist is now considered.

4.5.5.4 Blade elastic twist. - Blade motion due to blade elastic twist is accounted for by going back to the static twist equation. Blade elastic twist, ϕ_T is assumed to be directly superpositionable with blade static or blade pretwist, ϕ_{TW}, except that the static pretwist takes place about the 1/4 chord, and the blade elastic twist takes place about the blade element shear center. This is shown in Figure 26. From this figure it can be seen that previous static twist equation can be rewritten as:

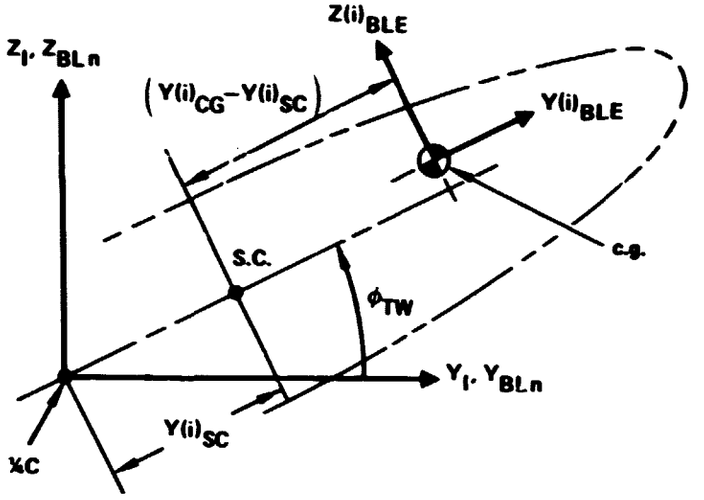

a) BLADE PRETWIST, $\phi(i)_{TW}$, ABOUT BLADE REFERENCE AXIS

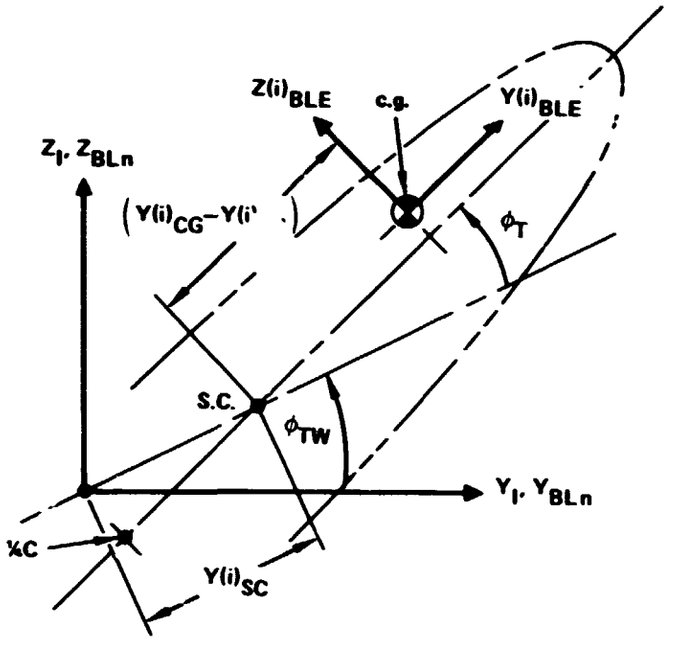

b) BLADE ELASTIC TWIST, $\phi(i)_T$ ABOUT BLADE SHEAR CENTER

Figure 26. - Blade static pretwist, ϕ_{TW} and elastic twist, ϕ_T.

$$\begin{Bmatrix} X_{BLE} \\ Y_{BLE} \\ Z_{BLE} \end{Bmatrix}_I = \begin{bmatrix} 1 & 0 & 0 \\ 0 & \cos\phi_T & -\sin\phi_T \\ 0 & \sin\phi_T & \cos\phi_T \end{bmatrix} \begin{bmatrix} 1 & 0 & 0 \\ 0 & \cos\phi_{TW} & -\sin\phi_{TW} \\ 0 & \sin\phi_{TW} & \cos\phi_{TW} \end{bmatrix} \left\{ \begin{Bmatrix} X_{CG} \\ Y_{CG} \\ Z_{CG} \end{Bmatrix} - \begin{Bmatrix} 0 \\ Y_{SC} \\ 0 \end{Bmatrix} \right\} + \begin{bmatrix} 1 & 0 & 0 \\ 0 & \cos\phi_{TW} & -\sin\phi_{TW} \\ 0 & \sin\phi_{TW} & \cos\phi_{TW} \end{bmatrix} \begin{Bmatrix} 0 \\ Y_{SC} \\ 0 \end{Bmatrix} \tag{111}$$

If we let $\Phi_T = (\phi_T + \phi_{TW})$ then this equation becomes

$$\begin{Bmatrix} X_{BLE} \\ Y_{BLE} \\ Z_{BLE} \end{Bmatrix}_I = \begin{bmatrix} 1 & 0 & 0 \\ 0 & \cos\Phi_T & -\sin\Phi_T \\ 0 & \sin\Phi_T & \cos\Phi_T \end{bmatrix} \left\{ \left\{ \begin{Bmatrix} X_{CG} \\ Y_{CG} \\ Z_{CG} \end{Bmatrix} - \begin{Bmatrix} 0 \\ Y_{SC} \\ 0 \end{Bmatrix} \right\} + \begin{Bmatrix} 0 \\ Y_{SC}\cos\phi_{TW} \\ Y_{SC}\sin\phi_{TW} \end{Bmatrix} \right\}$$

$$= \begin{bmatrix} 1 & 0 & 0 \\ 0 & \cos\Phi_T & -\sin\Phi_T \\ 0 & \sin\Phi_T & \cos\Phi_T \end{bmatrix} \begin{Bmatrix} X_{CG} \\ Y_{CG} \\ Z_{CG} \end{Bmatrix} + Y_{SC} \begin{Bmatrix} 0 \\ \cos\phi_{TW} - \cos\Phi_T \\ \sin\phi_{TW} - \sin\Phi_T \end{Bmatrix} \tag{112}$$

4.5.5.5 Final blade element Y, Z displacement equation. - Suostituting the above equation in the previous development sequence yields the blade displacement equation which includes the effect of the static shape of blade bending, of blade feathering, and of blade elastic twist.

However, before proceeding with these substitutions, the following column vector is defined to simplify the notation.

$$\left\{r_a\right\} = \begin{Bmatrix} X_a \\ Y_a \\ Z_a \end{Bmatrix} \tag{113}$$

The total blade element displacement equation becomes:

$$\begin{aligned}
\left\{r_{BLE}\right\}_{BLn} = &\left[\left[T_{Z'FA}\right]^T \left[T_{Y'FA}\right]^T \left[T_{\Delta\phi_F}\right]^T \left[T_{Y'FA}\right] \left[T_{Z'FA}\right]\right] \left\{\left[\frac{\partial r}{\partial A_n}\right] \left\{A_{jn}\right\}\right\} \\
&+ \left\{\left[\left[T_{\beta_{FA}}\right]^T \left[T_{\phi_{REF}}\right]^T \left[T_{\beta_{FA}}\right]\right] \left\{\left[\left[T_{\iota_0}\right]^T \left[T_\gamma\right]^T\right]\right.\right. \\
&\cdot \left\{\left[T_{\beta_0}\right]^T \left\{\left[T_{\phi_T}\right]^T \left\{r_{CG}\right\} + \left\{\left[T_{\phi_{TW}}\right]^T - \left[T_{\phi_T}\right]^T\right\} \left\{r_{SC}\right\}\right.\right. \\
&- \left.\left[T_{\beta_0}\right]^T \left\{r_{SW}\right\}\right\} + \left\{\left\{r_{jog}\right\} + \left[T_{\beta_0}\right]^T \left\{r_{SW}\right\}\right. \\
&- \left.\left[T_{\beta_0}\right]^T \left\{r_F\right\}\right\}\right\} + \left\{\left[T_{\beta_0}\right]^T \left\{r_p\right\}\right. \\
&- \left.\left.\left.\left\{r_{IB}\right\}\right\}\right\}\right\} + \left\{r_{IB}\right\}
\end{aligned} \tag{114}$$

where:

$$\left[\frac{\partial r}{\partial A_n}\right] \left\{A_{jn}\right\} = \begin{bmatrix} 0 & 0 & 0 \\ Y_{1n} & Y_{2n} & Y_{3n} \\ Z_{1n} & Z_{2n} & Z_{3n} \end{bmatrix} \begin{Bmatrix} A_{1n} \\ A_{2n} \\ A_{3n} \end{Bmatrix} \tag{115}$$

Note that for convenience of using the condensed matrix notation discussed above, the most general vectors for such terms as ℓ_p, X_{SW}, Z_{jog}, and Y_{SC} have been used. As can be seen in this equation, these have all been treated as full vectors. Making the appropriate substitutions of course will result in the expressions previously obtained.

It is noted that the equation is written for the relative displacement of points on the blade outboard of Station X_{SW}. Inboard of that station, the displacements are determined from the previous inboard equation or simply by zeroing out such terms as $\left\{r_{jog}\right\}$ and $\left\{r_{SW}\right\}$ and substituting unit diagonal transformations for $\left[T_{T_0}\right]$ and $\left[T_Y\right]$ in the full equation. Following either approach yields the blade displacement equation for points inboard of Station X_{SW}; or

$$\begin{aligned}\left\{r_{BLE}\right\}_{BLn} = &\left[\left[T_{Z'FA}\right]^T\left[T_{Y'FA}\right]^T\left[T_{\Delta\phi_F}\right]^T\left[T_{Y'FA}\right]\left[T_{Z'FA}\right]\right]\left\{\left\{\left[\frac{\partial r}{\partial A_n}\right]\left\{A_{jn}\right\}\right\}\right. \\ &+\left\{\left[\left[T_{\beta_{FA}}\right]^T\left[T_{\phi_{REF}}\right]^T\left[T_{\beta_{FA}}\right]\right]\left\{\left[T_{\beta_0}\right]^T\left\{\left[T_{\phi_T}\right]^T\left\{r_{CG}\right\}\right.\right.\right. \\ &\left.\left.\left.+\left\{\left[T_{\phi_{TW}}\right]^T-\left[T_{\phi_T}\right]^T\right\}\left\{r_{SC}\right\}\right\}-\left\{r_{IB}\right\}\right\}+\left\{r_{IB}\right\}\right\} \qquad (116)\end{aligned}$$

The ith station blade displacements, Y and Z, in blade coordinates for points on the blade both outboard and inboard of station X_{SW} are then defined.

4.5.5.6 Blade element Y and Z relative velocities and accelerations. - The blade element coordinate axis system linear Y and Z velocities relative to the blade reference axis system can be found by differentiating the position equation with respect to time. Note that no distinction will be made at this point between outboard or inboard of station X_{SW}, but using the equation for displacements outboard of this station and as discussed earlier, zeroing out certain terms, results in the equations for velocities or accelerations of points inboard of that station.

$$
\begin{aligned}
\left\{\dot{r}_{BLE}\right\}_{BLn} = {} & \left[\dot{Z}'_{FA}\left[\left[\dot{T}_{Z'FA}\right]^T\left[T_{Y'FA}\right]^T\left[T_{\Delta\phi_F}\right]^T\left[T_{Y'FA}\right]\left[T_{Z'FA}\right]\right.\right. \\
& + \left[T_{Z'FA}\right]^T\left[\dot{T}_{Y'FA}\right]^T\left[T_{\Delta\phi_F}\right]^T\left[T_{Y'FA}\right]\left[T_{Z'FA}\right] \\
& + \dot{Y}'_{FA}\left[\left[T_{Z'FA}\right]^T\left[T_{Y'FA}\right]^T\left[\dot{T}_{\Delta\phi_F}\right]^T\left[T_{Y'FA}\right]\left[T_{Z'FA}\right]\right. \\
& + \left[T_{Z'FA}\right]^T\left[T_{Y'FA}\right]^T\left[T_{\Delta\phi_F}\right]^T\left[\dot{T}_{Y'FA}\right]\left[T_{Z'FA}\right] \\
& + \dot{\phi}_F\left[\left[T_{Z'FA}\right]^T\left[T_{Y'FA}\right]\left[\dot{T}_{\Delta\phi_F}\right]\left[T_{Y'FA}\right]\left[T_{Z'FA}\right]\right]\Big] \\
& \cdot \left\{\left(\left[\frac{\partial r}{\partial A_n}\right]\left\{A_{jn}\right\}\right) + \left\{\left[\left[T_{\beta_{FA}}\right]^T\left[T_{\phi_{REF}}\right]^T\left[T_{\beta_{FA}}\right]\right]\right.\right. \\
& \cdot \left\{\left[\left[T_{\tau_0}\right]^T\left[T_\gamma\right]^T\right]\left\{\left[T_{\beta_0}\right]^T\left\{\left[T_{\phi_T}\right]^T\left\{r_{CG}\right\}\right.\right.\right. \\
& + \left\{\left[T_{\phi_{TW}}\right]^T - \left[T_{\phi_T}\right]^T\right\}\left\{r_{SC}\right\}\Big\} - \left[T_{\beta_0}\right]^T\left\{r_{SW}\right\}\Big\} + \left\{\left\{r_{jog}\right\}\right. \\
& + \left[T_{\beta_0}\right]^T\left\{r_{SW}\right\} - \left[T_{\beta_0}\right]^T\left\{r_p\right\}\Big\}\Big\} + \left\{\left[T_{\beta_0}\right]^T\left\{r_p\right\}\right. \\
& \left.\left.\left.\left. - \left\{r_{IB}\right\}\right\}\right\}\right\}\Big] + \left[\left[T_{Z'FA}\right]^T\left[T_{Y'FA}\right]^T\left[T_{\Delta\phi_F}\right]^T\left[T_{Y'FA}\right]\left[T_{Z'FA}\right]\right] \\
& \cdot \left\{\left(\left[\frac{\partial r}{\partial A_n}\right]\left\{\dot{A}_{jn}\right\}\right) + \left[\left[T_{\beta_{FA}}\right]^T\left[T_{\phi_{REF}}\right]^T\left[T_{\beta_{FA}}\right]\right]\left[\left[T_{\tau_0}\right]^T\left[T_\gamma\right]^T\right]\right. \\
& \cdot \left[T_{\beta_0}\right]^T\dot{\phi}_T\left[\dot{T}_{\phi_T}\right]^T\left\{\left\{r_{CG}\right\} - \left\{r_{SC}\right\}\right\}\Big\} - \left\{\dot{r}_{IB}\right\}\Big\} + \left\{\dot{r}_{IB}\right\} \qquad (117)
\end{aligned}
$$

Note in the above equation that the $\left[\dot{T}_\zeta\right]$ matrices are not time derivatives of the $\left[T_\zeta\right]$ matrices but are derivatives of the transformation matrices with respect to the transformation angle ζ. This is arrived at by making the substitution that:

$$\frac{d}{dt}\left[T_\zeta\right] = \frac{d\zeta}{dt}\left[\frac{dT_\zeta}{d\zeta}\right] = \dot{\zeta}\left[\dot{T}_\zeta\right] \tag{118}$$

and

$$\frac{d^2}{dt^2}\left[T_\zeta\right] = \ddot{\zeta}\left[\dot{T}_\zeta\right] + \dot{\zeta}^2\left[\ddot{T}_\zeta\right] \tag{119}$$

Taking the time derivative again of Equation 113 yields the blade element Y and Z linear accelerations relative to the blade reference axis system.

$$\begin{aligned}
\left\{\ddot{r}_{BLE}\right\}_{BLn} = {} & \left[\ddot{Z}'_{FA}\left[\left[\dot{T}_{Z'_{FA}}\right]^T\left[T_{Y'_{FA}}\right]^T\left[T_{\Delta\phi_F}\right]^T\left[T_{Y'_{FA}}\right]\left[T_{Z'_{FA}}\right]\right.\right. \\
& + \left[T_{Z'_{FA}}\right]^T\left[T_{Y'_{FA}}\right]^T\left[T_{\Delta\phi_F}\right]^T\left[T_{Y'_{FA}}\right]\left[\dot{T}_{Z'_{FA}}\right]\Big] \\
& + \ddot{Y}'_{FA}\left[\left[T_{Z'_{FA}}\right]^T\left[\dot{T}_{Y'_{FA}}\right]^T\left[T_{\Delta\phi_F}\right]^T\left[T_{Y'_{FA}}\right]\left[T_{Z'_{FA}}\right]\right. \\
& + \left[T_{Z'_{FA}}\right]^T\left[T_{Y'_{FA}}\right]^T\left[T_{\Delta\phi_F}\right]^T\left[\dot{T}_{Y'_{FA}}\right]\left[T_{Z'_{FA}}\right] \\
& + \ddot{\phi}_F\left[\left[T_{Z'_{FA}}\right]^T\left[T_{Y'_{FA}}\right]^T\left[\dot{T}_{\Delta\phi_F}\right]^T\left[T_{Y'_{FA}}\right]\left[T_{Z'_{FA}}\right]\right] \\
& + \left(\dot{Z}'_{FA}\right)^2\left[\left[\ddot{T}_{Z'_{FA}}\right]^T\left[T_{Y'_{FA}}\right]^T\left[T_{\Delta\phi_F}\right]^T\left[T_{Y'_{FA}}\right]\left[T_{Z'_{FA}}\right]\right. \\
& + 2\left[\dot{T}_{Z'_{FA}}\right]^T\left[T_{Y'_{FA}}\right]^T\left[T_{\Delta\phi_F}\right]^T\left[T_{Y'_{FA}}\right]\left[\dot{T}_{Z'_{FA}}\right]
\end{aligned}$$

$$+ \left[T_{Z'_{FA}}\right]^T \left[T_{Y'_{FA}}\right]^T \left[T_{\Delta\phi_F}\right]^T \left[T_{Y'_{FA}}\right] \left[\ddot{T}_{Z'_{FA}}\right]\Big]$$

$$+ \left(\dot{Y}'_{FA}\right)^2 \Big[\Big[T_{Z'_{FA}}\Big]^T \left[\ddot{T}_{Y'_{FA}}\right]^T \left[T_{\Delta\phi_F}\right]^T \left[T_{Y'_{FA}}\right] \left[T_{Z'_{FA}}\right]$$

$$+ 2\left[T_{Z'_{FA}}\right]^T \left[\dot{T}_{Y'_{FA}}\right]^T \left[T_{\Delta\phi_F}\right]^T \left[\dot{T}_{Y'_{FA}}\right] \left[T_{Z'_{FA}}\right]\Big]$$

$$+ \left[T_{Z'_{FA}}\right]^T \left[T_{Y'_{FA}}\right]^T \left[T_{\Delta\phi_F}\right]^T \left[\ddot{T}_{Y'_{FA}}\right] \left[T_{Z'_{FA}}\right]$$

$$+ \left(\dot{\phi}_F\right)^2 \Big[\Big[T_{Z'_{FA}}\Big]^T \left[T_{Y'_{FA}}\right]^T \left[\ddot{T}_{\Delta\phi_F}\right]^T \left[T_{Y'_{FA}}\right] \left[T_{Z'_{FA}}\right]\Big]$$

$$+ 2\left(\dot{Z}'_{FA}\right)\left(Y'_{FA}\right)\Big[\Big[\dot{T}_{Z'_{FA}}\Big]^T \left[\dot{T}_{Y'_{FA}}\right]^T \left[T_{\Delta\phi_F}\right]^T \left[T_{Y'_{FA}}\right] \left[T_{Z'_{FA}}\right]$$

$$+ \left[\dot{T}_{Z'_{FA}}\right]^T \left[T_{Y'_{FA}}\right]^T \left[T_{\Delta\phi_F}\right]^T \left[\dot{T}_{Y'_{FA}}\right] \left[T_{Z'_{FA}}\right]$$

$$+ \left[T_{Z'_{FA}}\right]^T \left[\dot{T}_{Y'_{FA}}\right]^T \left[T_{\Delta\phi_F}\right]^T \left[T_{Y'_{FA}}\right] \left[\dot{T}_{Z'_{FA}}\right]$$

$$+ \left[T_{Z'_{FA}}\right]^T \left[T_{Y'_{FA}}\right]^T \left[T_{\Delta\phi_F}\right]^T \left[\dot{T}_{Y'_{FA}}\right] \left[\dot{T}_{Z'_{FA}}\right]\Big]$$

$$+ 2\left(\dot{Z}'_{FA}\right)\left(\dot{\phi}_F\right)\Big[\Big[\dot{T}_{Z'_{FA}}\Big]^T \left[T_{Y'_{FA}}\right]^T \left[\dot{T}_{\Delta\phi_F}\right]^T \left[T_{Y'_{FA}}\right] \left[T_{Z'_{FA}}\right]$$

$$+ \left[T_{Z'_{FA}}\right]^T \left[T_{Y'_{FA}}\right]^T \left[\dot{T}_{\Delta\phi_F}\right]^T \left[T_{Y'_{FA}}\right] \left[\dot{T}_{Z'_{FA}}\right]$$

$$+ 2\left(\dot{Y}'_{FA}\right)\left(\dot{\phi}_F\right)\Big[\Big[T_{Z'_{FA}}\Big]^T \left[\dot{T}_{Y'_{FA}}\right]^T \left[\dot{T}_{\Delta\phi_F}\right]^T \left[T_{Y'_{FA}}\right] \left[T_{Z'_{FA}}\right]$$

$$+ \left[T_{Z'_{FA}}\right]^T \left[T_{Y'_{FA}}\right]^T \left[\dot{T}_{\Delta\phi_F}\right]^T \left[\dot{T}_{Y'_{FA}}\right] \left[T_{Z'_{FA}}\right]\Big]\Big]\Big\{\Big\{\left[\frac{\partial r}{\partial A_n}\right]\left\{A_{jn}\right\}\Big\}$$

C-2

$$
+ \left\{\left[\left[T_{\beta_{FA}}\right]^T \left[T_{\phi_{REF}}\right]^T \left[T_{\beta_{FA}}\right]\right]\left\{\left[\left[T_{\tau_0}\right]^T \left[T_\gamma\right]^T\right]\left\{\left[T_{\beta_0}\right]^T \left\{\left[T_{\phi_T}\right]^T\right.\right.\right.\right.
$$

$$
\cdot \left\{r_{CG}\right\} + \left\{\left[T_{\phi_{TW}}\right]^T - \left[T_{\phi_T}\right]^T\right\}\left\{r_{SC}\right\} - \left[T_{\beta_0}\right]^T \left\{r_{SW}\right\} + \left\{\left\{r_{jog}\right\}\right.
$$

$$
\left.\left.\left.\left. + \left[T_{\beta_0}\right]^T \left\{r_{SW}\right\} - \left[T_{\beta_0}\right]^T \left\{r_p\right\}\right\}\right\} + \left\{\left[T_{\beta_0}\right]^T \left\{r_p\right\} - \left\{r_{IB}\right\}\right\}\right\}\right\}
$$

$$
+ 2\left[\dot{Z}'_{FA}\left[\left[\dot{T}_{Z'FA}\right]^T \left[T_{Y'FA}\right]^T \left[T_{\Delta\phi_F}\right]^T \left[T_{Y'FA}\right]\left[T_{Z'FA}\right]\right.\right.
$$

$$
\left.\left. + \left[T_{Z'FA}\right]^T \left[T_{Y'FA}\right]^T \left[T_{\Delta\phi_F}\right]^T \left[T_{Y'FA}\right]\left[\dot{T}_{Z'FA}\right]\right]\right.
$$

$$
+ \dot{Y}'_{FA}\left[\left[T_{Z'FA}\right]^T \left[\dot{T}_{Y'FA}\right]^T \left[T_{\Delta\phi_F}\right]^T \left[T_{Y'FA}\right]\left[T_{Z'FA}\right]\right.
$$

$$
\left. + \left[T_{Z'FA}\right]^T \left[T_{Y'FA}\right]^T \left[T_{\Delta\phi_F}\right]^T \left[\dot{T}_{Y'FA}\right]\left[T_{Z'FA}\right]\right]
$$

$$
+ \dot{\phi}_F\left[\left[T_{Z'FA}\right]^T \left[T_{Y'FA}\right]^T \left[\dot{T}_{\Delta\phi_F}\right]^T \left[T_{Y'FA}\right]\left[T_{Z'FA}\right]\right]\Bigg]
$$

$$
\cdot \left\{\left\{\left[\frac{\partial r}{\partial A_n}\right]\left\{\dot{A}_{jn}\right\}\right\} + \left[\left[T_{\beta_{FA}}\right]^T \left[T_{\phi_{REF}}\right]^T \left[T_{\beta_{FA}}\right]\right]\left[\left[T_{\tau_0}\right]^T \left[T_\gamma\right]^T\right]\right.
$$

$$
\left.\cdot \left[T_{\beta_0}\right]^T \left\{\dot{\phi}_T\left[\dot{T}_{\phi_T}\right]^T \left\{\left\{r_{CG}\right\} - \left\{r_{SC}\right\}\right\}\right\} - \left\{\dot{r}_{IB}\right\}\right\}
$$

$$
+ \left[\left[T_{Z'FA}\right]^T \left[T_{Y'FA}\right]^T \left[T_{\Delta\phi_F}\right]^T \left[T_{Y'FA}\right]\left[T_{Z'FA}\right]\right]\left\{\left\{\left[\frac{\partial r}{\partial A_n}\right]\left\{\ddot{A}_{jn}\right\}\right\}\right.
$$

$$
+ \left[\left[T_{\beta_{FA}}\right]^T \left[T_{\phi_{REF}}\right]^T \left[T_{\beta_{FA}}\right]\right]\left[\left[T_{\tau_0}\right]^T \left[T_\gamma\right]^T\right]\left[T_{\beta_0}\right]^T
$$

$$
\left.\cdot \left\{\ddot{\phi}_T\left[\dot{T}_{\phi_T}\right]^T \left\{\left\{r_{CG}\right\} - \left\{r_{SC}\right\}\right\}\right\} - \left\{\ddot{r}_{IB}\right\}\right\} + \left\{\ddot{r}_{IB}\right\} \qquad (120)
$$

These equations define the blade element relative displacement velocities and accelerations, respectively, required by the blade inertial velocity equations developed shortly. Note that in the preceding development these equations are written for the nth blade, and with the exception of the $\left[\frac{\partial r}{\partial A_n}\right]$, $\left[T_{\beta_{FA}}\right]$, $\left[T_{\phi_{REF}}\right]$, $\left[T_{\tau_0}\right]$, $\left[T_\gamma\right]$, $\left[T_{\beta_0}\right]$, $\left[T_{\phi_{TW}}\right]$, $\left\{r_{SC}\right\}$, $\left\{r_{SW}\right\}$, $\left\{r_{jog}\right\}$, $\left\{r_p\right\}$, and $\left\{r_{CG}\right\}$ matrices, the terms are all blade dependent. Remember, also, that inboard of $\left\{r_{SW}\right\}$ the $\left[T_{\tau_0}\right]$ and $\left[T_\gamma\right]$ matrices are unit diagonal.

4.5.5.7 Blade element slopes. - The blade element Y' and Z' slopes are determined by differentiating the deflection equation with respect to the nth blade radial distance, X_{BLn}. These formulations are used for quasi-static torsion formulation and output. Performing the required differentiation for points along the blade reference line:

$$\frac{\partial}{\partial X_{BLn}}\begin{Bmatrix} - \\ Y_{BLE} \\ Z_{BLE} \end{Bmatrix}_{BLn} = \begin{Bmatrix} - \\ Y'_{BLE} \\ Z'_{BLE} \end{Bmatrix}_{BLn} = \left\{r'_{BLE}\right\}_{BLn} \tag{121}$$

$$\left\{r'_{BLE}\right\}_{BLn} = \left[\left[T_{Z'_{FA}}\right]^T \left[T_{Y'_{FA}}\right]^T \left[T_{\Delta\phi_F}\right]^T \left[T_{Y'_{FA}}\right] \left[T_{Z'_{FA}}\right]\right] \left\{\left\{\left[\frac{\partial r'}{\partial A_n}\right]\left\{A_{jn}\right\}\right\}\right.$$
$$+ \left[\left[T_{\beta_{FA}}\right]^T \left[T_{\phi_{REF}}\right]^T \left[T_{\beta_{FA}}\right] \left[T_{\tau_0}\right]^T \left[T_\gamma\right]^T \left[T_{\beta_0}\right]^T\right] \tag{122}$$
$$\left. \cdot \left\{\phi_{T'}\left[\dot{T}_{\phi_T}\right]^T \left\{r_{CG} - r_{SC}\right\} + \left[T_{\phi_T}\right]^T \left\{r'_{CG} - r'_{SC}\right\}\right\}\right.$$

where

$$\left\{\phi_{T'}\left[\dot{T}_{\phi_T}\right]^T \left\{r_{CG} - r_{SC}\right\} + \left[T_{\phi_T}\right]^T \left\{r'_{CG} - r'_{SC}\right\}\right\} \simeq \begin{Bmatrix} 1 \\ 0 \\ 0 \end{Bmatrix} \quad \text{as programmed)} \tag{123}$$

4.5.5.8 Transformation from blade-to-blade element coordinates. - In this section, the transformation matrix for the blade root to the ith blade element motion will be developed. Each blade will have its own transformation matrix for each ith blade station. The transformation matrix will initially be developed as the transform from blade element to blade coordinates, $\left[T_{BLE-BLn}\right]$.

The transformation matrix, $\left[T_{BLE-BLn}\right]$, can be developed by referring to the development of the deflection equations. The first rotation from blade element to blade coordinates is through the combined twist angle, $-\phi_T$; the second rotation is through the negative of the precone, β_0; the third through the negative of thw sweep and droop angles, τ_0, γ; the fourth through the feathering axis angle, β_{FA}; the fifth through the negative of the reference feathering angles ϕ_{REF}; and the sixth back through the negative of the feathering axis precone angle, β_{FA}.

These rotations then define the transformation from blade element to blade coordinates, including the effects of the static shape of the blade, pretwist, precone, sweep, droop, etc. Also included is the effect of blade elastic twist. Again note that for stations inboard of Station X_{SW}, the sweep and droop angles, τ_0 and γ, respectively must be set to zero in the formulation of the transformation matrix as in the definition of the blade displacements and blade slopes. This portion of the transformation matrix which includes the static blade shape and combined twist is defined as follows:

$$\left[T_{BLE-BLn}\right]_S = \left[\left[T_{\beta_{FA}}\right]^T \left[T_{\phi_{REF}}\right]^T \left[T_{\beta_{FA}}\right]\right]\left[\left[T_{\tau_0}\right]^T \left[T_{\gamma}\right]^T \left[T_{\beta_0}\right]^T \left[T_{\phi_T}\right]^T\right] \tag{124}$$

The next two rotations from blade element to blade coordinates are due to the elastic blade bending slopes. Since Y'_{BEND} and Z'_{BEND} are motions of the blade elements with respect to the blade, then to transform from blade element to blade coordinates requires negative rotations of Y'_{BEND} and Z'_{BEND} to be included. Finally, the blade feathering rotation from the reference feather angle must be included. The final transformation then, from blade element to blade coordinates, is defined by the following equation:

$$\left[T_{BLE-BLn}\right] = \left[T_{Z'_{FA}}\right]^T \left[T_{Y'_{FA}}\right]^T \left[T_{\Delta\phi_F}\right]^T \left[T_{Y'_{FA}}\right]\left[T_{Z'_{FA}}\right]\left[T_{Z'_{BEND}}\right]^T \left[T_{Y'_{BEND}}\right]^T$$

$$\cdot \left[T_{\beta_{FA}}\right]^T \left[T_{\phi_{REF}}\right]^T \left[T_{\beta_{FA}}\right] \left[T_{\tau_0}\right]^T \left[T_{\gamma}\right]^T \left[T_{\beta_0}\right]^T \left[T_{\phi_T}\right]^T \tag{125}$$

where

$$\left[T_{Z'_{BEND}}\right] = \begin{bmatrix} \cos(Z'_{BEND}) & 0 & \sin(Z'_{BEND}) \\ 0 & 1 & 0 \\ -\sin(Z'_{BEND}) & 0 & \cos(Z'_{BEND}) \end{bmatrix} \tag{126}$$

and

$$\left[T_{Y'_{BEND}}\right] = \begin{bmatrix} \cos(Y'_{BEND}) & \sin(Y'_{BEND}) & 0 \\ -\sin(Y'_{BEND}) & \cos(Y'_{BEND}) & 0 \\ 0 & 0 & 1 \end{bmatrix} \tag{127}$$

and again where

$$\left[T_{\tau_0}\right]^T \left[T_{\gamma}\right]^T = \left[I\right] \tag{128}$$

inboard of Station X_{SW}.

Also:

$$\begin{Bmatrix} Y'_{BEND} \\ Z'_{BEND} \end{Bmatrix} = \begin{bmatrix} Y_1' & Y_2' & Y_3' \\ Z_1' & Z_2' & Z_3' \end{bmatrix} \begin{Bmatrix} A_{1n} \\ A_{2n} \\ A_{3n} \end{Bmatrix} \tag{129}$$

The inverse or transpose of this equation yields the transformation from blade to blade element coordinates, or:

$$\begin{aligned} \left[T_{BLn-BLE}\right] &= \left[T_{BLE-BLn}\right]^T \\ &= \left[T_{\Phi_T}\right]\left[T_{\beta_0}\right]\left[T_{\gamma}\right]\left[T_{\tau_0}\right]\left[T_{\beta_{FA}}\right]^T \left[T_{\phi_{REF}}\right]\left[T_{\beta_{FA}}\right] \\ &\quad \cdot \left[T_{Y'_{BEND}}\right]\left[T_{Z'_{BEND}}\right]\left[T_{Z'_{FA}}\right]^T \left[T_{Y'_{FA}}\right]^T \left[T_{\Delta\phi_F}\right]\left[T_{Y'_{FA}}\right]\left[T_{Z'_{FA}}\right] \end{aligned} \tag{130}$$

again where

$$\left[T_{\gamma}\right]\left[T_{\tau_0}\right] = \left[I\right] \tag{131}$$

inboard of station X_{SW}.

4.5.5.9 Blade element angular velocities and accelerations. - From the foregoing discussion, the blade element angular velocity vector can be determined. Starting with the angular velocities $(p, q, r)_{BLn}$ of the blade reference axis system and systematically and progressively transforming these velocities through each axis rotation and adding the respective angular velocity associated with each of the indicated angular rotations, results in the following equation for the blade element angular velocities.

$$\begin{Bmatrix} p \\ q \\ r \end{Bmatrix}_{BLE} = \begin{Bmatrix} \dot{\phi}_T \\ 0 \\ 0 \end{Bmatrix} + \left[T_{\phi_T}\right]\left[T_{\beta_0}\right]\left[T_\gamma\right]\left[T_{\tau_0}\right]\left[T_{\beta_{FA}}\right]^T \left[T_{\phi_{REF}}\right]\left[T_{\beta_{FA}}\right] \left\{\left\{\begin{matrix} 0 \\ 0 \\ \dot{Y}'_{BEND} \end{matrix}\right\}\right.$$

$$+ \left[T_{Y'_{BEND}}\right] \left\{\left\{\begin{matrix} 0 \\ -\dot{Z}'_{BEND} \\ 0 \end{matrix}\right\}\right. + \left[T_{Z'_{BEND}}\right] \left\{\left\{\begin{matrix} 0 \\ \dot{Z}'_{FA} \\ 0 \end{matrix}\right\}\right.$$

$$+ \left[T_{Z'_{FA}}\right]^T \left\{\left\{\begin{matrix} 0 \\ 0 \\ -\dot{Y}'_{FA} \end{matrix}\right\}\right. + \left[T_{Y'_{FA}}\right]^T \left\{\left\{\begin{matrix} \dot{\phi}_F \\ 0 \\ 0 \end{matrix}\right\}\right. + \left[T_{\Delta\phi_F}\right] \left\{\left\{\begin{matrix} 0 \\ 0 \\ Y'_{FA} \end{matrix}\right\}\right.$$

$$\left. + \left[T_{Y'_{FA}}\right] \left\{\left\{\begin{matrix} 0 \\ -\dot{Z}'_{FA} \\ 0 \end{matrix}\right\}\right. + \left[T_{Z'_{FA}}\right] \left\{\begin{matrix} p \\ q \\ r \end{matrix}\right\}_{BLn} \right\}\right\}\right\}\right\}\right\}\right\}\right\} \qquad (132)$$

Note that in this equation, starting on the right-hand side with the quantities in the innermost brackets, the blade reference system angular velocities are first transformed through the increment of feathering axis flapping slope due to bending, Z'_{FA}, and then the feathering axis flapping angular velocity, $-Z'_{FA}$, is added. Minus is used since Z' is a negative Θ rotation. Next, the resultant W vector is transformed through Y'_{FA} and Y'_{FA} is added. This is then transformed through the delta feathering angle, $\Delta\phi_F$, and the feathering angular velocity, $\dot{\phi}_F$, is added. This is then transformed back through the increments of feathering axis slopes due to blade bending, giving the vector:

$$\left\{\left\{\begin{matrix}0\\ \dot{Z}'_{FA}\\ 0\end{matrix}\right\} + \left[T_{Z'_{FA}}\right]^T \left\{\left\{\begin{matrix}0\\ 0\\ -\dot{Y}'_{FA}\end{matrix}\right\} + \left[T_{Y'_{FA}}\right]^T \left\{\left\{\begin{matrix}\dot{\phi}_F\\ 0\\ 0\end{matrix}\right\} + \left[T_{\Delta\phi_F}\right] \left\{\left\{\begin{matrix}0\\ 0\\ \dot{Y}'_{FA}\end{matrix}\right\} \right.\right.\right.$$

$$\left. + \left[T_{Y'_{FA}}\right] \left\{\left\{\begin{matrix}0\\ -\dot{Z}'_{FA}\\ 0\end{matrix}\right\} + \left[T_{Z'_{FA}}\right] \left\{\begin{matrix}p\\ q\\ r\end{matrix}\right\}_{BLn} \right\} \cdots \right\} \qquad (133)$$

which represents the blade element angular velocities due to combined blade feathering and blade reference axis system angular velocities.

Next, the effects of blade bending at each blade station are introduced. The above vector is first transformed through the local blade element flapwise bending slope, Z'_{BEND}, and then the angular velocity, $-Z'_{BEND}$, is added. This result is transformed through the blade element inplane bending slope, Y'_{BEND}, and the inplane angular velocity due to blade bending, Y'_{BEND}, is added, resulting in the total vector less the initial transformation string. This vector represents the blade element angular velocities due to the combined effects of the blade reference axis system angular velocities of the blade feathering angle and of the blade angular velocities due to blade elastic bending. The remaining transformations then include the static effects of the blade feathering axis precone, β_{FA}, the blade reference feathering angle, ϕ_{REF}, blade sweep, τ_0, blade droop, γ, and blade or hub precone, β_0, and the combined effect of blade static and elastic twist, represented by ϕ_T. Finally, the blade elastic twist angular velocity, $\dot{\phi}_T$, is added, giving the total blade element angular velocities, $\left\{\begin{matrix}p\\ q\\ r\end{matrix}\right\}_{BLE}$.

Also note, as indicated before, the matrix $\left[T_\gamma\right]\left[T_{\tau_0}\right]$ has the value calculated if X is greater than X_{SW} and has the value of unity if X is inboard of station X_{SW}.

At this point is has been assumed that the contributions of $\dot{Y}'_{FA}$ and $\dot{Z}'_{FA}$ are small compared to the other contributions to $\begin{Bmatrix} p \\ q \\ r \end{Bmatrix}_{BLE}$. This assumption is supported by referring to the final form of the above development. First of all, both of these vectors are small compared to $\begin{Bmatrix} p \\ q \\ r \end{Bmatrix}_{BLn}$, which is fundamentally the rotational speed of the rotor. Also, both of the feathering axis flapping and inplane angular velocities are first added and then transformed through the delta feathering angle and then subtracted, meaning that fundamentally the principal magnitude or component contributions due to $\dot{Y}'_{FA}$ and $\dot{Z}'_{FA}$ are self-cancelling.

With the above assumption:

$$\begin{Bmatrix} p \\ q \\ r \end{Bmatrix}_{BLE} = \begin{Bmatrix} \dot{\phi}_T \\ 0 \\ 0 \end{Bmatrix} + \left[T_{\phi_T}\right]\left[R\right]^T \left\{\begin{Bmatrix} 0 \\ 0 \\ \dot{Y}'_{BEND} \end{Bmatrix} + \left[T_{Y'_{BEND}}\right] \left\{\begin{Bmatrix} 0 \\ -\dot{Z}'_{BEND} \\ 0 \end{Bmatrix}\right.\right.$$

$$+ \left[T_{Z'_{BEND}}\right] \left[T_{Z'_{FA}}\right]^T \left[T_{Y'_{FA}}\right]^T \left\{\begin{Bmatrix} \dot{\phi}_F \\ 0 \\ 0 \end{Bmatrix}\right.$$

$$\left.\left.\left. + \left[T_{\Delta\phi_F}\right] \left[T_{Y'_{FA}}\right] \left[T_{Z'_{FA}}\right] \begin{Bmatrix} p \\ q \\ r \end{Bmatrix}_{BLn} \right\}\right\}\right\} \qquad (134)$$

where:

$$\left[R\right]^T = \left[T_{\beta_0}\right]\left[T_\gamma\right]\left[T_{\tau_0}\right]\left[T_{\beta_{FA}}\right]^T\left[T_{\phi_{REF}}\right]\left[T_{\beta_{FA}}\right] \tag{135}$$

and:

$$\begin{Bmatrix}\dot{Y}'_{BEND}\\ \dot{Z}'_{BEND}\end{Bmatrix} = \begin{bmatrix}Y_1' & Y_2' & Y_3'\\ Z_1' & Z_2' & Z_3'\end{bmatrix}\begin{Bmatrix}\dot{A}_{1n}\\ \dot{A}_{2n}\\ \dot{A}_{3n}\end{Bmatrix} \tag{136}$$

The blade element angular accelerations can now be determined by differentiating this equation with respect to time. Again, as in the case of the angular velocities, the contributions due to time derivatives of the feathering axis flapping and inplane slope changes due to bending are neglected. With this assumption, the time derivative is:

$$\begin{Bmatrix}\dot{p}\\ \dot{q}\\ \dot{r}\end{Bmatrix}_{BLE} = \begin{Bmatrix}\ddot{\phi}_T\\ 0\\ 0\end{Bmatrix} + \dot{\phi}_T\left[\dot{T}_{\phi_T}\right]\left[R\right]^T\left\{\begin{Bmatrix}0\\ 0\\ \dot{Y}'_{BEND}\end{Bmatrix} + \left[T_{Y'_{BEND}}\right]\left\{\begin{Bmatrix}0\\ -\dot{Z}'_{BEND}\\ 0\end{Bmatrix}\right.\right.$$

$$+ \left[T_{Z'_{BEND}}\right]\left[T_{Z'_{FA}}\right]^T\left[T_{Y'_{FA}}\right]^T\left\{\begin{Bmatrix}\dot{\phi}_F\\ 0\\ 0\end{Bmatrix} + \left[T_{\Delta\phi_F}\right]\left[T_{Y'_{FA}}\right]\left[T_{Z'_{FA}}\right]\right.$$

$$\left.\left.\left.\cdot\begin{Bmatrix}p\\ q\\ r\end{Bmatrix}_{BLn}\right\}\right\} + \left[T_{\phi_T}\right]\left[R\right]^T\left\{\begin{Bmatrix}0\\ 0\\ \ddot{Y}'_{BEND}\end{Bmatrix} + \dot{Y}'_{BEND}\left[\dot{T}_{Y'_{BEND}}\right]\right.$$

$$\left.\cdot\left\{\begin{Bmatrix}0\\ -\dot{Z}'_{BEND}\\ 0\end{Bmatrix} + \left[T_{Z'_{BEND}}\right]\left[T_{Z'_{FA}}\right]^T\left[T_{Y'_{FA}}\right]^T\begin{Bmatrix}\dot{\phi}_F\\ 0\\ 0\end{Bmatrix}\right.\right.$$

$$+ \left[T_{\Delta\phi_F}\right] \left[T_{Y'_{FA}}\right] \left[T_{Z'_{FA}}\right] \left\{\begin{matrix} p \\ q \\ r \end{matrix}\right\}_{BLn} \Bigg\} \Bigg\} + \left[T_{Y'_{BEND}}\right] \left\{\left\{\begin{matrix} 0 \\ -\ddot{Z}'_{BEND} \\ 0 \end{matrix}\right\}\right.$$

$$+ \dot{Z}'_{BEND} \left[\dot{T}_{Z'_{BEND}}\right] \left[\dot{T}_{Z'_{FA}}\right]^T \left[T_{Y'_{FA}}\right]^T \left\{\left\{\begin{matrix} \dot{\phi}_F \\ 0 \\ 0 \end{matrix}\right\}\right.$$

$$+ \left[T_{\Delta\phi_F}\right] \left[T_{Y'_{FA}}\right] \left[T_{Z'_{FA}}\right] \left\{\begin{matrix} p \\ q \\ r \end{matrix}\right\}_{BLn} \Bigg\}$$

$$+ \left[T_{Z'_{BEND}}\right] \left[T_{Z'_{FA}}\right]^T \left[T_{Y'_{FA}}\right]^T \left\{\left\{\begin{matrix} \ddot{\phi}_F \\ 0 \\ 0 \end{matrix}\right\}\right.$$

$$+ \dot{\phi}_F \left[\dot{T}_{\Delta\phi_F}\right] \left[T_{Y'_{FA}}\right] \left[T_{Z'_{FA}}\right] \left\{\begin{matrix} p \\ q \\ r \end{matrix}\right\}_{BLn}$$

$$+ \left[T_{\Delta\phi_F}\right] \left[T_{Y'_{FA}}\right] \left[T_{Z'_{FA}}\right] \left\{\begin{matrix} \dot{p} \\ \dot{q} \\ \dot{r} \end{matrix}\right\}_{BLn} \Bigg\} \Bigg\} \Bigg\} \qquad (137)$$

where:

$$\left\{\begin{matrix} \ddot{Y}'_{BEND} \\ \ddot{Z}'_{BEND} \end{matrix}\right\} = \begin{bmatrix} Y_1' & Y_2' & Y_3' \\ Z_1' & Z_2' & Z_3' \end{bmatrix} \left\{\begin{matrix} \ddot{A}_{1n} \\ \ddot{A}_{2n} \\ \ddot{A}_{3n} \end{matrix}\right\} \qquad (138)$$

4.5.5.10 Blade element X motions. - In the previous development, the equations did not account for the blade element displacement, velocity, and acceleration in the spanwise or X-direction. The method used to define these is one of taking the neutral axis as the axis of no stretch and determing the projection of this axis onto the X-axis as the blade bends. This projection, then, is the spanwise or X location of the neutral axis in blade coordinates. The rate of change of this projection is the spanwise relative velocity and the second rate of change is the spanwise relative acceleration of the blade element neutral axis location or point. The motions are then transformed to the center of gravity to obtain the spanwise motion of the origin of the blade element reference axis.

In Figure 27, the deflected neutral axis is shows as a function of blade radius. The (i-1) and ith station are shown. It can be seen from this figure that as $X_{NA}(i-1)$ approaches $X_{NA}(i)$, then the delta length of the blade $(S_{NA}(i) - S_{NA}(i-1))$, can be written as:

$$\left(S_{NA}(i) - S_{NA}(i-1)\right)^2 = \left(X_{NA}(i) - X_{NA}(i-1)\right)^2_{BLn} + \left(Y_{NA}(i) - Y_{NA}(i-1)\right)^2_{BLn} + \left(Z_{NA}(i) - Z_{NA}(i-1)\right)^2_{BLn} \tag{139}$$

Rearranging this equation and summing from the blade root to the kth blade station yields:

$$X_{NA}(k) = \sum_{i=2}^{k}\left(X_{NA}(i) - X_{NA}(i-1)\right)_{BLn} = \sum_{i=2}^{k}\left[\left(S_{NA}(i) - S_{NA}(i-1)\right)^2 - \left(Y_{NA}(i) - Y_{NA}(i-1)\right)^2_{BLn} - \left(Z_{NA}(i) - Z_{NA}(i-1)\right)^2_{BLn}\right]^{1/2} \tag{140}$$

and

$$S_{NA}(1) \simeq X_{BLE}(1) \tag{141}$$

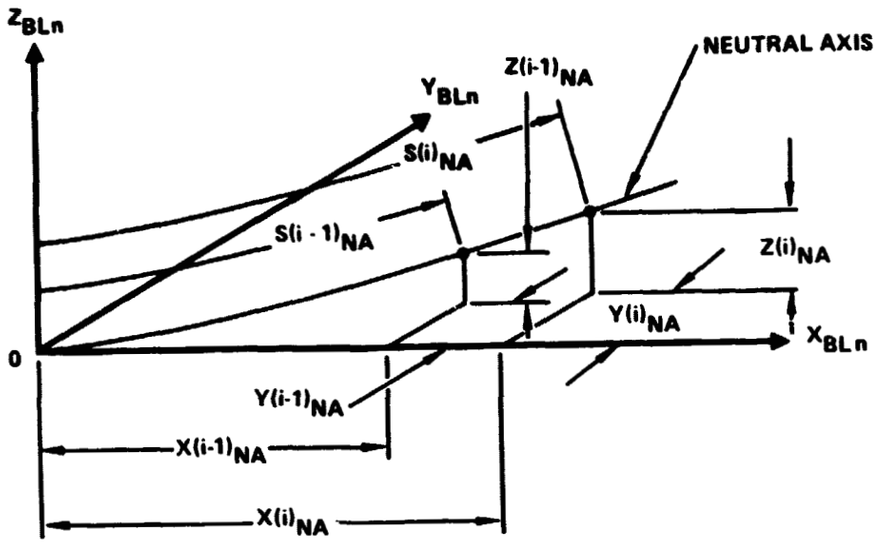

Figure 27. - Neutral axis vs blade radius.

Likewise,

$$\dot{X}_{NA_{BLn}}(1) = \ddot{X}_{NA_{BLn}}(1) = 0 \tag{142}$$

$S_{NA}(i)$ is simply the blade length to the ith station measured along the neutral axis and $Y_{NA_{BLn}}(i)$ and $Z_{NA_{BLn}}(i)$ are the Y and Z locations of the neutral axis in the blade coordinate axis system for the nth blade. These displacements, along with their derivatives, will be defined later. First, however, by taking the first and second time derivative of X equation, the spanwise velocities and accelerations of the blade element neutral axis point are determined and are given by the following two equations.

$$\dot{X}_{NA_{BLn}}(k) = \sum_{i=2}^{k} \left[\frac{-\left(Y_{NA}(i) - Y_{NA}(i-1)\right)_{BLn} \left(\dot{Y}_{NA}(i) - \dot{Y}_{NA}(i-1)\right)_{BLn}}{\left(X_{NA}(i) - X_{NA}(i-1)\right)_{BLn}} \right.$$

$$\left. \frac{-\left(Z_{NA}(i) - Z_{NA}(i-1)\right)_{BLn} \left(\dot{Z}_{NA}(i) - \dot{Z}_{NA}(i-1)\right)_{BLn}}{\left(X_{NA}(i) - X_{NA}(i-1)\right)_{BLn}} \right] \tag{143}$$

$$\ddot{X}_{NA_{BLn}}(k) = \sum_{i=2}^{k} \left[\frac{-\left(\dot{Y}_{NA}(i) - \dot{Y}_{NA}(i-1)\right)^2_{BLn} - \left(\dot{Z}_{NA}(i) - \dot{Z}_{NA}(i-1)\right)^2_{BLn}}{\left(X_{NA}(i) - X_{NA}(i-1)\right)_{BLn}} \right.$$

$$\frac{-\left(Y_{NA}(i) - Y_{NA}(i-1)\right)_{BLn} \left(\ddot{Y}_{NA}(i) - \ddot{Y}_{NA}(i-1)\right)_{BLn}}{\left(X_{NA}(i) - X_{NA}(i-1)\right)_{BLn}}$$

$$\frac{-\left(Z_{NA}(i) - Z_{NA}(i-1)\right)_{BLn} \left(\ddot{Z}_{NA}(i) - \ddot{Z}_{NA}(i-1)\right)_{BLn}}{\left(X_{NA}(i) - X_{NA}(i-1)\right)_{BLn}}$$

$$- \frac{\left[\left(Y_{NA}(i) - Y_{NA}(i-1)\right)_{BLn} \left(\dot{Y}_{NA}(i) - \dot{Y}_{NA}(i-1)\right)_{BLn}\right.}{\left(X_{NA}(i) - X_{NA}(i-1)\right)^3_{BLn}}$$

$$\left. \frac{\left. + \left(Z_{NA}(i) - Z_{NA}(i-1)\right)_{BLn} \left(\dot{Z}_{NA}(i) - \dot{Z}_{NA}(i-1)\right)_{BLn}\right]^2}{\left(X_{NA}(i) - X_{NA}(i-1)\right)^3_{BLn}} \right] \quad (144)$$

If $Y_{ONA}(i)$ is the distance along the ith blade element chord line from the blade element reference axis origin or center of gravity to the blade element neutral axis, then the blade element neutral axis motions can be written in terms of the blade element motions as:

$$\begin{Bmatrix} \Delta X_{NA}(i) \\ Y_{NA}(i) \\ Z_{NA}(i) \end{Bmatrix}_{BLn} = \begin{Bmatrix} 0 \\ Y_{BLE}(i) \\ Z_{BLE}(i) \end{Bmatrix}_{BLn} + \left[T_{BLE-BLn}\right] \begin{Bmatrix} 0 \\ Y_{ONA}(i) \\ 0 \end{Bmatrix}_{BLE} \quad (145)$$

Referring to Section 4.5, the time derivative of the above equation is:

$$\begin{Bmatrix} \Delta\dot{X}_{NA}(i) \\ \dot{Y}_{NA}(i) \\ \dot{Z}_{NA}(i) \end{Bmatrix}_{BLn} = \begin{Bmatrix} 0 \\ \dot{Y}_{BLE}(i) \\ \dot{Z}_{BLE}(i) \end{Bmatrix}_{BLn} + \left[T_{BLE-BLn}\right] \begin{Bmatrix} -r_{BLE}Y_{ONA} \\ 0 \\ p_{BLE}Y_{ONA} \end{Bmatrix}_{BLE_{(i)}} \tag{146}$$

and likewise, the second time derivative is:

$$\begin{Bmatrix} \Delta\ddot{X}_{NA}(i) \\ \ddot{Y}_{NA}(i) \\ \ddot{Z}_{NA}(i) \end{Bmatrix}_{BLn} = \begin{Bmatrix} 0 \\ \ddot{Y}_{NA}(i) \\ \ddot{Z}_{NA}(i) \end{Bmatrix}_{BLn} + \left[T_{BLE-BLn}\right] \begin{Bmatrix} (p_{BLE}q_{BLE}-\dot{r}_{BLE})Y_{ONA} \\ (-r^2_{BLE}-p^2_{BLE})Y_{ONA} \\ (q_{BLE}r_{BLE}+\dot{p}_{BLE})Y_{ONA} \end{Bmatrix}_{BLE_{(i)}} \tag{147}$$

These three equations, then, define the Y and Z displacements, velocities, and accelerations of the neutral axis point used in the X equations and time derivatives. Also, the increments of spanwise motions due to the offset between the center of gravity and neutral axis are defined by these same three equations. This increment represents the motion of the neutral axis relative to the blade reference axis origin, therefore, the span motion at the center of gravity is determined by subtracting $\Delta X_{NA}(i)_{BLn}$ from the spanwise motion of the neutral axis, or:

$$X_{BLE}(i)_{BLn} = X_{NA}(i)_{BLn} - \Delta X_{NA}(i)_{BLn} \tag{148}$$

$$\dot{X}_{BLE}(i)_{BLn} = \dot{X}_{NA}(i)_{BLn} - \dot{\Delta X}_{NA}(i)_{BLn} \tag{149}$$

$$\ddot{X}_{BLE}(i)_{BLn} = \ddot{X}_{NA}(i)_{BLn} - \ddot{\Delta X}_{NA}(i)_{BLn} \tag{150}$$

These equations, then, along with the previous expressions for X and Z, define the blade element relative displacement, velocity, and acceleration vectors required for the total inertial vectors which follow.

4.5.5.11 Blade motion in absolute coordinates. - To this point the blade element motion has been defined in terms of the blade axis or relative coordinates. The elements defined are:

$$\text{blade element relative displacements} \quad \begin{Bmatrix} X_{BLE}(i) \\ Y_{BLE}(i) \\ Z_{BLE}(i) \end{Bmatrix}_{BLn} \tag{151}$$

$$\text{blade element relative velocities} \quad \begin{Bmatrix} \dot{X}_{BLE}(i) \\ \dot{Y}_{BLE}(i) \\ \dot{Z}_{BLE}(i) \end{Bmatrix}_{BLn} \tag{152}$$

$$\text{and blade element relative accelerations} \quad \begin{Bmatrix} \ddot{X}_{BLE}(i) \\ \ddot{Y}_{BLE}(i) \\ \ddot{Z}_{BLE}(i) \end{Bmatrix}_{BLn} \tag{153}$$

Using the method of Section 4.4.1, expressions in freestream (absolute) coordinates can be written for use in the equations of motion. The blade element velocity becomes:

$$\begin{Bmatrix} \dot{X}_{BLE}(i) \\ \dot{Y}_{BLE}(i) \\ \dot{Z}_{BLE}(i) \end{Bmatrix}_{BLn}^{I} = \begin{Bmatrix} \dot{X}_{OBLn} \\ \dot{Y}_{OBLn} \\ \dot{Z}_{OBLn} \end{Bmatrix}_{BLn}^{I} + \begin{Bmatrix} \dot{X}_{BLE}(i) \\ \dot{Y}_{BLE}(i) \\ \dot{Z}_{BLE}(i) \end{Bmatrix}_{BLn} + \begin{bmatrix} 0 & -r & q \\ r & 0 & -p \\ -q & p & 0 \end{bmatrix}_{BLn} \begin{Bmatrix} X_{BLE}(i) \\ Y_{BLE}(i) \\ Z_{BLE}(i) \end{Bmatrix}_{BLn} \tag{154}$$

The blade element accelerations are:

$$\begin{Bmatrix} \ddot{X}_{BLE}(i) \\ \ddot{Y}_{BLE}(i) \\ \ddot{Z}_{BLE}(i) \end{Bmatrix}^{I}_{BLn} = \begin{Bmatrix} \ddot{X}_{OBLn} \\ \ddot{Y}_{OBLn} \\ \ddot{Z}_{OBLn} \end{Bmatrix}^{I}_{BLn} + \begin{Bmatrix} \ddot{X}_{BLE}(i) \\ \ddot{Y}_{BLE}(i) \\ \ddot{Z}_{BLE}(i) \end{Bmatrix}_{BLn}$$

$$+ \begin{bmatrix} 0 & -\dot{r} & \dot{q} \\ \dot{r} & 0 & -\dot{p} \\ -\dot{q} & \dot{p} & 0 \end{bmatrix}_{BLn} \begin{Bmatrix} X_{BLE}(i) \\ Y_{BLE}(i) \\ Z_{BLE}(i) \end{Bmatrix}_{BLn}$$

$$+ \begin{bmatrix} 0 & -r & q \\ r & 0 & -p \\ -q & p & 0 \end{bmatrix}_{BLn} \begin{bmatrix} 0 & -r & q \\ r & 0 & -p \\ -q & p & 0 \end{bmatrix}_{BLn} \begin{Bmatrix} X_{BLE}(i) \\ Y_{BLE}(i) \\ Z_{BLE}(i) \end{Bmatrix}_{BLn}$$

$$+ 2 \begin{bmatrix} 0 & -r & q \\ r & 0 & -p \\ -q & p & 0 \end{bmatrix}_{BLn} \begin{Bmatrix} \dot{X}_{BLE} \\ \dot{Y}_{BLE} \\ \dot{Z}_{BLE} \end{Bmatrix}_{BLn} \tag{155}$$

where

$$\begin{Bmatrix} \ddot{X}_0 \\ \ddot{Y}_0 \\ \ddot{Z}_0 \end{Bmatrix}_{BLn} , \quad \begin{Bmatrix} \dot{X}_0 \\ \dot{Y}_0 \\ \dot{Z}_0 \end{Bmatrix}_{BLn} , \tag{156}$$

and matching rotation terms are defined in Section 4.5.4 in terms of rotor axis terms which are in turn related to the principal (hub) reference axis.

4.5.6 Swashplate motion. - As shown in Figure 10, the swashplate reference axis system is defined with the Z-axis down. The motion of the swashplate reference system is defined by three generalized coordinate displacements, Z_{SP}, ϕ_{SP}, and θ_{SP}, which move relative to the hub axis system.

The rotations ϕ_{SP} and θ_{SP} are taken in the same order as shown in Figure 18 and therefore, from Section 4.4.3 the angular velocities are:

$$\begin{Bmatrix} p \\ q \\ r \end{Bmatrix}_{SP_R} = \begin{Bmatrix} 0 \\ 0 \\ \dot{\psi}_{SP} \end{Bmatrix} + \begin{bmatrix} \cos\psi & \sin\psi & 0 \\ -\sin\psi & \cos\psi & 0 \\ 0 & 0 & 1 \end{bmatrix} \left\{ \begin{Bmatrix} 0 \\ \dot{\theta}_{SP} \\ 0 \end{Bmatrix} + \begin{bmatrix} \cos\theta_{SP} & 0 & -\sin\theta_{SP} \\ 0 & 1 & 0 \\ \sin\theta_{SP} & 0 & \cos\theta_{SP} \end{bmatrix} \left\{ \begin{Bmatrix} \dot{\phi}_{SP} \\ 0 \\ 0 \end{Bmatrix} + \begin{bmatrix} 1 & 0 & 0 \\ 0 & \cos\phi_{SP} & \sin\phi_{SP} \\ 0 & -\sin\phi_{SP} & \cos\phi_{SP} \end{bmatrix} \begin{Bmatrix} p \\ q \\ r \end{Bmatrix}_H \right\} \right\} \tag{157}$$

where $\dot{\psi}_{SP}$ is the rotational speed of the swashplate, and

$$\dot{\psi}_{SP} = -\dot{\psi}_R \tag{158}$$

where $\dot{\psi}_R$ is the rotational speed of the rotor. Note no coupling is provided for shaft motion, the assumption being that swashplate motions relative to the hub due to shaft motions have been designed out of the system.

As indicated before, the chosen swashplate axes do not rotate at the rotational speed $\dot{\psi}_{SP}$. However, the total angular velocities reflect the rotational

rate $\dot{\psi}_{SP}$. Therefore, the total angular rates of the swashplate in swashplate axes are obtained with $\psi = 0$. This gives

$$\begin{Bmatrix} p \\ q \\ r \end{Bmatrix}_{SP} = \begin{Bmatrix} 0 \\ 0 \\ \dot{\psi}_{SP} \end{Bmatrix} + \begin{Bmatrix} 0 \\ \dot{\theta}_{SP} \\ 0 \end{Bmatrix} + \begin{bmatrix} \cos\theta_{SP} & 0 & -\sin\theta_{SP} \\ 0 & 1 & 0 \\ \sin\theta_{SP} & 0 & \cos\theta_{SP} \end{bmatrix} \left\{ \begin{Bmatrix} \dot{\phi}_{SP} \\ 0 \\ 0 \end{Bmatrix} + \begin{bmatrix} 1 & 0 & 0 \\ 0 & \cos\phi_{SP} & \sin\phi_{SP} \\ 0 & -\sin\phi_{SP} & \cos\phi_{SP} \end{bmatrix} \begin{Bmatrix} p \\ q \\ r \end{Bmatrix}_H \right\} \tag{159}$$

Nonrotating swashplate angular velocities, subscripted SP, are obtained by deleting $\dot{\psi}_{SP}$ above.

The swashplate angular accelerations can be similarly determined by evaluating the general expression at $\psi = \psi_{SP} = 0$. This yields:

$$\begin{Bmatrix} \dot{p} \\ \dot{q} \\ \dot{r} \end{Bmatrix}_{SP} = \begin{Bmatrix} 0 \\ \ddot{\theta}_{SP} \\ 0 \end{Bmatrix} + \begin{Bmatrix} \dot{\psi}_{SP} q_{SP} \\ -\dot{\psi}_{SP} p_{SP} \\ \ddot{\psi}_{SP} \end{Bmatrix} + \dot{\theta}_{SP} \begin{bmatrix} -\sin\theta_{SP} & 0 & -\cos\theta_{SP} \\ 0 & 0 & 0 \\ \cos\theta_{SP} & 0 & -\sin\theta_{SP} \end{bmatrix} \left\{ \begin{Bmatrix} \dot{\phi}_{SP} \\ 0 \\ 0 \end{Bmatrix} + \begin{bmatrix} 1 & 0 & 0 \\ 0 & \cos\phi_{SP} & \sin\phi_{SP} \\ 0 & -\sin\phi_{SP} & \cos\phi_{SP} \end{bmatrix} \begin{Bmatrix} p \\ q \\ r \end{Bmatrix}_H \right\}$$

$$+ \begin{bmatrix} \cos\theta_{SP} & 0 & -\sin\theta_{SP} \\ 0 & 1 & 0 \\ \sin\theta_{SP} & 0 & \cos\theta_{SP} \end{bmatrix} \left\{ \begin{Bmatrix} \ddot{\phi}_{SP} \\ 0 \\ 0 \end{Bmatrix} + \dot{\phi}_{SP} \begin{bmatrix} 0 & 0 & 0 \\ 0 & -\sin\phi_{SP} & \cos\phi_{SP} \\ 0 & -\cos\phi_{SP} & -\sin\phi_{SP} \end{bmatrix} \begin{Bmatrix} p \\ q \\ r \end{Bmatrix}_H + \begin{bmatrix} 1 & 0 & 0 \\ 0 & \cos\phi_{SP} & \sin\phi_{SP} \\ 0 & -\sin\phi_{SP} & \cos\phi_{SP} \end{bmatrix} \begin{Bmatrix} \dot{p} \\ \dot{q} \\ \dot{r} \end{Bmatrix}_H \right\} \tag{160}$$

The vertical velocities and accelerations of the swashplate are simply defined as:

$$\dot{Z}_{OSP}{}^{I} = \dot{Z}_{SP} + \dot{Z}_{OH}{}^{I} \tag{161}$$

and

$$\ddot{Z}_{OSP}{}^{I} = \ddot{Z}_{SP} + \ddot{Z}_{OH}{}^{I} \tag{162}$$

It is noted in these equations that the Z-axis motion is assumed to remain parallel to the hub Z axis.

The swashplate angular displacements are obtained by integrating the angular velocities, or:

$$\phi_{SP} = \int_0^t \dot{\phi}_{SP} dt + \phi_{t=0,\ SP} \tag{163}$$

and

$$\theta_{SP} = \int_0^t \dot{\theta}_{SP} dt + \theta_{t=0,\ SP} \tag{164}$$

Likewise, the vertical displacement of the swashplate relative to the hub is:

$$Z_{SP} = \int_0^t \dot{Z}_{SP} dt + Z_{t=0,\ SP} \tag{165}$$

4.5.7 Blade feathering motion. - The feathering occurring at the feather bearings, Figure 15, is taken to be the sum of the motions of the following dynamic and kinematic elements:

- Swashplate - collective command
- Swashplate - cyclic command
- Blade bending to feathering couplings
- Elastic pitch horn and associated components

The total feathering response is:

$$\phi_{Fn} = \theta_0 - A_{1S} \cos(\psi_{BLn} + \psi_R) - B_{1S} \sin(\psi_{BLn} + \psi_R) + \frac{\partial \phi_{Fn}}{\partial A_1} A_{1n}$$

$$+ \frac{\partial \phi_{Fn}}{\partial A_2} A_{2n} + \frac{\partial \phi_{Fn}}{\partial A_3} A_{3n} + \frac{\partial \phi_F}{\partial \beta_{PH}} \beta_{PHn} \qquad (166)$$

Velocities and accelerations are formed by differentiation. The desired relations are:

$$\dot{\phi}_{Fn} = \dot{\theta}_0 - \dot{A}_{1S} \cos(\psi_{BLn} + \psi_R) - \dot{B}_{1S} \sin(\psi_{BLn} + \psi_R)$$

$$+ \left[A_{1S} \sin(\psi_{BLn} + \psi_R) - B_{1S} \cos(\psi_{BLn} + \psi_R) \right] \dot{\psi}_R$$

$$+ \frac{\partial \phi_{Fn}}{\partial A_1} \dot{A}_{1n} + \frac{\partial \phi_{Fn}}{\partial A_2} \dot{A}_{2n} + \frac{\partial \phi_{Fn}}{\partial A_3} \dot{A}_{3n} + \frac{\partial \phi_F}{\partial \beta_{PH}} \dot{\beta}_{PHn} \qquad (167)$$

and for accelerations:

$$\ddot{\phi}_{Fn} = \ddot{\theta}_0 - \ddot{A}_{1S}\cos(\psi_{BLn} + \psi_R) - \ddot{B}_{1S}\sin(\psi_{BLn} + \psi_R)$$
$$+ 2\left[\dot{A}_{1S}\sin(\psi_{BLn} + \psi_R) - \dot{B}_{1S}\cos(\psi_{BLn} + \psi_R)\right]\dot{\psi}_R$$
$$+ \left[A_{1S}\cos(\psi_{BLn} + \psi_R) + B_{1S}\sin(\psi_{BLn} + \psi_R)\right]\dot{\psi}_R^2$$
$$+ \left[A_{1S}\cos(\psi_{BLn} + \psi_R) - B_{1S}\sin(\psi_{BLn} + \psi_R)\right]\ddot{\psi} + \frac{\partial\phi_{Fn}}{\partial A_1}\ddot{A}_{1n}$$
$$+ \frac{\partial\phi_{Fn}}{\partial A_2}\ddot{A}_{2n} + \frac{\partial\phi_{Fn}}{\partial A_3}\ddot{A}_{3n} + \frac{\partial\phi_F}{\partial\beta_{PH}}\ddot{\beta}_{PHn} \qquad (168)$$

The commanded cyclic blade angles are:

$$\begin{Bmatrix} A_{1S} \\ B_{1S} \end{Bmatrix} = \left(\frac{d}{e}\right)\begin{bmatrix} \sin\psi_{PH} & \cos\psi_{PH} \\ \cos\psi_{PH} & -\sin\psi_{PH} \end{bmatrix}\begin{Bmatrix} \phi_{SP} \\ \theta_{SP} \end{Bmatrix} \qquad (169)$$

where the angle ψ_{PH} is the pitch horn-swashplate connection lead to feather axis. See Figure 28. This angle is computed as a static value. It should be noted that some hub configurations carry the pitch horn toward the blade trailing edge. These configurations are entered in REXOR II by forming the supplement of ψ_{PH}.

$$\psi_{PH} = 180 - \psi_{PH} \text{ (degrees)} \qquad (170)$$

This angle gives the correct modeling of the sense of rotation reversal with the trailing pitch horn geometry.

The velocities and accelerations of the command cyclic are obtained by differentiation.

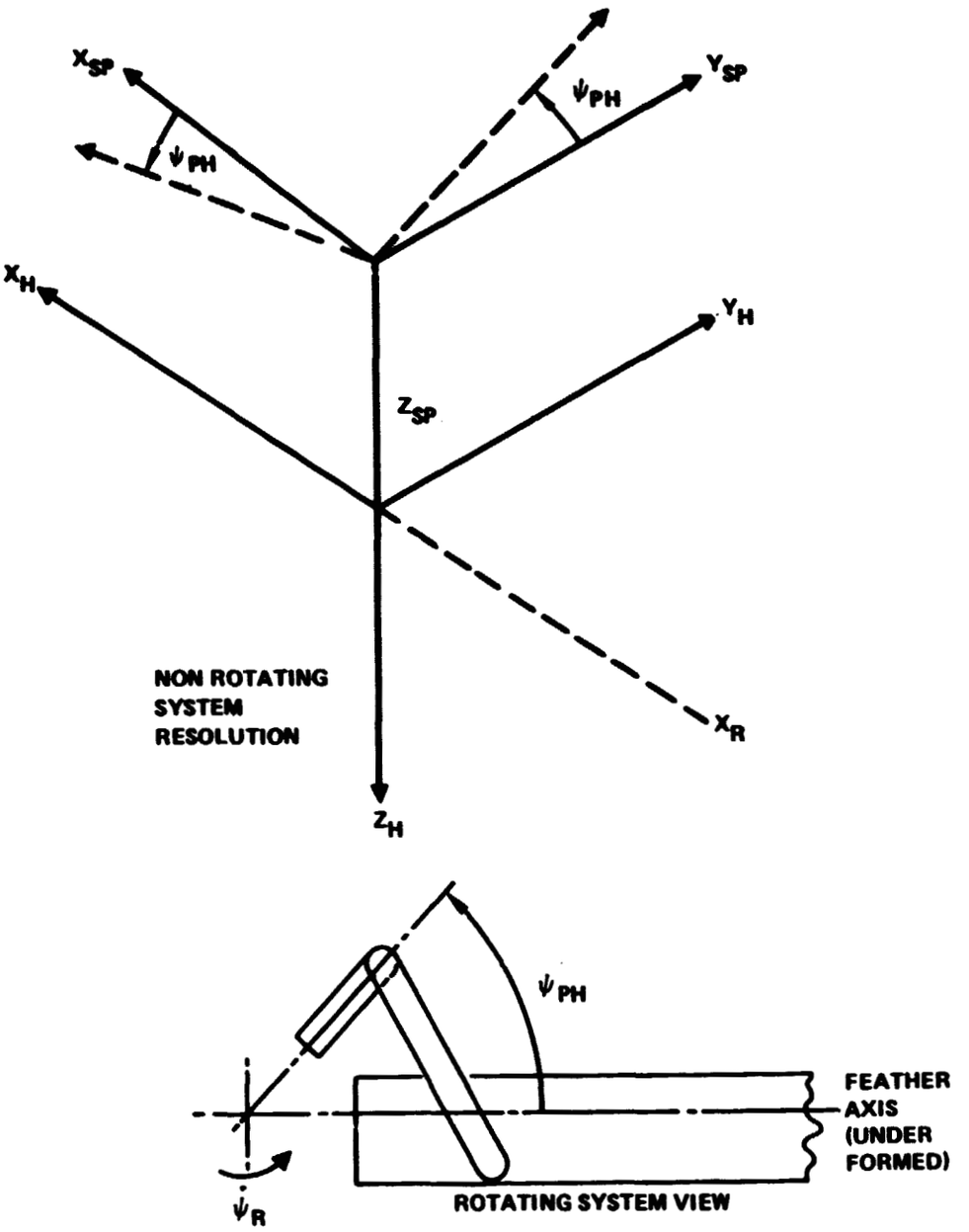

Figure 28. - Pitch horn blade feathering phase angle.

$$\begin{Bmatrix} \dot{A}_{1S} \\ \dot{B}_{1S} \end{Bmatrix} = \left(\frac{d}{e}\right) \begin{bmatrix} \sin\psi_{PH} & \cos\psi_{PH} \\ \cos\psi_{PH} & -\sin\psi_{PH} \end{bmatrix} \begin{Bmatrix} \dot{\phi}_{SP} \\ \dot{\theta}_{SP} \end{Bmatrix}$$

$$+ \left(\frac{d}{e}\right)_1 \dot{\theta}_0 \begin{bmatrix} \sin\psi_{PH} & \cos\psi_{PH} \\ \cos\psi_{PH} & -\sin\psi_{PH} \end{bmatrix} \begin{Bmatrix} \phi_{SP} \\ \theta_{SP} \end{Bmatrix} \tag{171}$$

and

$$\begin{Bmatrix} \ddot{A}_{1S} \\ \ddot{B}_{1S} \end{Bmatrix} = \left(\frac{d}{e}\right) \begin{bmatrix} \sin\psi_{PH} & \cos\psi_{PH} \\ \cos\psi_{PH} & -\sin\psi_{PH} \end{bmatrix} \begin{Bmatrix} \ddot{\phi}_{SP} \\ \ddot{\theta}_{SP} \end{Bmatrix}$$

$$+ 2\left(\frac{d}{e}\right)_1 \dot{\theta}_0 \begin{bmatrix} \sin\psi_{PH} & \cos\psi_{PH} \\ \cos\psi_{PH} & -\sin\psi_{PH} \end{bmatrix} \begin{Bmatrix} \dot{\phi}_{SP} \\ \dot{\theta}_{SP} \end{Bmatrix}$$

$$+ \left(\frac{d}{e}\right)_1 \ddot{\theta}_0 \begin{bmatrix} \sin\psi_{PH} & \cos\psi_{PH} \\ \cos\psi_{PH} & -\sin\psi_{PH} \end{bmatrix} \begin{Bmatrix} \phi_{SP} \\ \theta_{SP} \end{Bmatrix} \tag{172}$$

The overall coupling (swashplate to feathering) gear ratio, d/e, is expressed as a static term plus a first-order collective correction.

$$\left(\frac{d}{e}\right) = \left(\frac{d}{e}\right)_0 + \left(\frac{d}{e}\right)_1 \theta_0 \tag{173}$$

The collective is:

$$\theta_0 = -Z_{SP}/e \tag{174}$$

The swashplate vertical motion, Z_{SP}, is developed in Section 4.5.6. The value e is the static effective crank (pitch horn) arm about the blade feather axis. This crank length is entered as a negative number for a trailing pitch horn geometry to give the proper sense of collective for swashplate vertical translation.

Taking time derivatives:

$$\dot{\theta}_0 = -\dot{Z}_{SP}/e \tag{175}$$

and

$$\ddot{\theta}_0 = -\ddot{Z}_{SP}/e \tag{176}$$

The blade bending to feathering coupling factors are $\frac{\partial \phi_{Fn}}{\partial A_1}$, $\frac{\partial \phi_{Fn}}{\partial A_2}$, and $\frac{\partial \phi_{Fn}}{\partial A_3}$ for the first, second, and third blade modes. The blade bending modes are described without a torsion component; this allows freedom in varying the blade sweep, droop, jog, or other geometric parameters without new input data for the blade mode shape. The torsion either is calculated separately along the blade proper or as a blade root component by pitch horn bending. The coupling factors are intended to add a feathering component to the blade mode which would exist even with no torsion or feathering moments. As such, they are in effect the δ_3, α_2, etc., coupling usually described in the literature. These couplings are usually determined as a function of the distance from the flap or inplane mechanical or vertical hinge to a pitch horn projection.

5. EQUATIONS OF MOTION

5.1 Introduction

With the coordinate systems and transformation between systems well in hand, the development can proceed to the equations of motion. The development yields a set of second-order differential equations with time varying coefficients. These equations are formulated using the energy approach in a form credited to Lagrange. The solution to the system of equations is in the time domain by numerical integration. The result is a time history of the displacements, velocities, accelerations, and loads of the components of the helicopter modeled in detail, and the program treats each blade separately.

In the following development a Lagrangian approach to system modeling is applied to a set of point masses and then extended to discrete masses and inertias. The result is a set of generalized mass and force expressions. In REXOR (Reference 4) these expressions are programmed directly, element by element. In REXOR II extensive use is made of matrix notation both in description and programming. The transition to matrix notation is given at the end of section 5.3.

5.2 Energy Approach to Development of Equations of Motion

There are two basic approaches to developing the equations of motion for a physical system. These are:

- Vector summation of forces
- Energy approach

Given an equal set of conditions, limitations, and assumptions, both procedures should result in equivalent sets of equations. The difference is in the ease of arriving at a complete set of equations. Note that force is a vector, whereas energy is a scalar quantity. Therefore, in dealing in terms of energy, less information regarding direction needs to be handled. Also the systematic nature of the energy approach reduces the risk of error. As stated by Lagrange (Mecanique Analytique, 1788), "The methods which I present here do not require either constructions or reasonings of geometrical or mechanical nature, but only algebraic operations proceeding after a regular and uniform plan".

The starting point of this development is Lagrange's equation. It may be derived by postulating Newton's second law, or from Hamilton's principle. Lagrange's equation may be written in the following form:

$$\frac{d}{dt}\left(\frac{\partial T}{\partial \dot{q}_r}\right) - \frac{\partial T}{\partial q_r} + \frac{\partial B}{\partial \dot{q}_r} + \frac{\partial U}{\partial q_r} = Q_r \qquad (177)$$

where

T is kinetic energy

q is a generalized coordinate

B is dissipation function

U is potential energy function

Q_r is the generalized force, derived from the virtual work, δW, and is defined by the equation

$$Q_r = \frac{\partial \delta W}{\partial q_r} \tag{178}$$

Equation 177 will now be developed into the form as applied in REXOR II. This form bears a close resemblance to a force balance equation, but is derived from energy considerations. For clarity, the development is first shown for a set of discrete mass particles, then, in the section that follows, is extended to the distributed elemental masses of the REXOR II modeling and to the iterative solution scheme used.

In a conventional manner the equation is formulated in terms of generalized coordinates. These coordinates are a function of time, and completely define the system. They are generally not directly identifiable as a physical quantity.

The physical parameters or elemental coordinates are defined to be functions of the generalized coordinates and in turn a function of time. Consider a system to be composed of particles whose physical coordinates are a function of n generalized coordinates. For the ith particle:

$$x_i = x_i(q_1, q_2, \cdots, q_n; t) \tag{179}$$

$$y_i = y_i(q_1, q_2, \cdots, q_n; t) \tag{180}$$

$$z_i = z_i(q_1, q_2, \cdots, q_n; t) \tag{181}$$

Note: a Cartesian coordinate set is selected, and used in REXOR II. However, the argument is true for an arbitrary coordinate set.

The functional relationship of the physical or constrained coordinates and generalized coordinates yields:

$$\delta x_i = \frac{\partial x_i}{\partial q_1} \delta q_1 + \frac{\partial x_i}{\partial q_2} \delta q_2 + \cdots + \frac{\partial x_i}{\partial q_n} \delta q_n \tag{182}$$

$$\delta y_i = \frac{\partial y_i}{\partial q_1} \delta q_1 + \frac{\partial y_i}{\partial q_2} \delta q_2 + \cdots + \frac{\partial y_i}{\partial q_n} \delta q_n \tag{183}$$

$$\delta z_i = \frac{\partial z_i}{\partial q_1} \delta q_1 + \frac{\partial z_i}{\partial q_2} \delta q_2 + \cdots + \frac{\partial z_i}{\partial q_n} \delta q_n \tag{184}$$

The time dependence is implicit in the increments of the generalized coordinates. The equation is strictly true for infinitesimal increments. In REXOR II the generalized coordinates are distinct from physical coordinates in the main rotor blade descriptions. Here the generalized coordinates are blade modal variables. The modal variables represent tangible deflections of the blade from a reference position, and as such are small but not infinitesimal variables.

As the variables are a function of time:

$$\dot{x}_i = \frac{\partial x_i}{\partial q_1} \dot{q}_1 + \frac{\partial x_i}{\partial q_2} \dot{q}_2 + \cdots + \frac{\partial x_i}{\partial q_n} \dot{q}_n \tag{185}$$

$$\dot{y}_i = \frac{\partial y_i}{\partial q_1} \dot{q}_1 + \frac{\partial y_i}{\partial q_2} \dot{q}_2 + \cdots + \frac{\partial y_i}{\partial q_n} \dot{q}_n \tag{186}$$

$$\dot{z}_i = \frac{\partial z_i}{\partial q_1} \dot{q}_1 + \frac{\partial z_i}{\partial q_2} \dot{q}_2 + \cdots + \frac{\partial z_i}{\partial q_n} \dot{q}_n \tag{187}$$

In terms of the ith particle the kinetic energy for the system may be identified as:

$$T = \sum_{i=1}^{N} \frac{1}{2} m_i \left(\dot{x}_i^2 + \dot{y}_i^2 + \dot{z}_i^2 \right) \tag{188}$$

Toward the particular formulation of Lagrange's equation used in REXOR II, the first two terms of the previously stated form, Equation 177, are developed:

$$\frac{d}{dt}\left(\frac{\partial T}{\partial \dot{q}_r}\right) - \frac{\partial T}{\partial q_r} \tag{189}$$

Performing these operations for the ith particle case and the rth generalized coordinate and summing over the system yields:

$$\frac{d}{dt}\left(\frac{\partial T}{\partial \dot{q}_r}\right) - \frac{\partial T}{\partial q_r} = \sum_{i=1}^{N}\left(\frac{1}{2} m_i \frac{d}{dt} \frac{\partial}{\partial \dot{q}_r}\left(\left(\dot{x}_i^2 + \dot{y}_i^2 + \dot{z}_i^2\right)\right)\right.$$

$$\left. - \frac{1}{2} m_i \frac{\partial}{\partial q_r}\left(\dot{x}_i^2 + \dot{y}_i^2 + \dot{z}_i^2\right)\right) \tag{190}$$

A useful math operation of cancellation of the dots is developed prior to proceeding. Recall:

$$\delta x_i = \frac{\partial x_i}{\partial q_1}\delta q_1 + \frac{\partial x_i}{\partial q_2}\delta q_2 + \cdots + \frac{\partial x_i}{\partial q_n}\delta q_n \tag{191}$$

Then also

$$\dot{x}_i = \frac{\partial x_i}{\partial q_1}\dot{q}_1 + \frac{\partial x_i}{\partial q_2}\dot{q}_2 + \cdots + \frac{\partial x_i}{\partial q_n}\dot{q}_n \tag{192}$$

or

$$\frac{\partial \dot{x}_i}{\partial \dot{q}_r} = \frac{\partial x_i}{\partial q_r} \tag{193}$$

This is also true for y and z and for the double dot terms in x, y and z.

An operation to reverse the order of spacial and temporal differentiation is required. To show this the time derivative of a partial is taken as

$$\frac{d}{dt}\left(\frac{\partial x_i}{\partial q_r}\right) = \frac{\partial}{\partial q_1}\left(\frac{\partial x_i}{\partial q_r}\right)\dot{q}_1 + \frac{\partial}{\partial q_2}\left(\frac{\partial x_i}{\partial q_r}\right)\dot{q}_2 + \cdots + \frac{\partial}{\partial q_n}\left(\frac{\partial x_i}{\partial q_r}\right)\dot{q}_n \tag{194}$$

Next the spacial derivative of $\dot{x}_i$ is given as

$$\frac{\partial \dot{x}_i}{\partial q_r} = \frac{\partial}{\partial q_r}\left(\frac{\partial x_i}{\partial q_1}\dot{q}_1 + \frac{\partial x_i}{\partial q_2}\dot{q}_2 + \cdots + \frac{\partial x_i}{\partial q_n}\dot{q}_n\right) \tag{195}$$

Now since

$$x_i = x_i(q_1, q_2, \cdots, q_n) \tag{196}$$

the order of spacial differentiation is reversible

$$\frac{\partial^2 x_i}{\partial q_r \partial q_s} = \frac{\partial^2 x_i}{\partial q_s \partial q_r} \tag{197}$$

and hence

$$\frac{d}{dt}\left(\frac{\partial x_i}{\partial q_r}\right) = \frac{\partial \dot{x}_i}{\partial q_r} \tag{198}$$

Similar relations exist for y_i and z_i.

Proceeding on with the kinetic energy terms:

$$\frac{d}{dt}\left(\frac{\partial T}{\partial \dot{q}_r}\right) - \frac{\partial T}{\partial q_r} = \sum_{i=1}^{N} m_i\left[\ddot{x}_i \frac{\partial \dot{x}_i}{\partial \dot{q}_r} + \ddot{y}_i \frac{\partial \dot{y}_i}{\partial \dot{q}_r} + \ddot{z}_i \frac{\partial \dot{z}_i}{\partial \dot{q}_r} + \dot{x}_i \frac{d}{dt}\left(\frac{\partial \dot{x}_i}{\partial \dot{q}_r}\right) + y_i \frac{d}{dt}\left(\frac{\partial \dot{y}_i}{\partial \dot{q}_r}\right)\right.$$
$$\left. + \dot{z}_i \frac{d}{dt}\left(\frac{\partial \dot{z}_i}{\partial \dot{q}_r}\right) - \dot{x}_i \frac{\partial \dot{x}_i}{\partial q_r} - \dot{y}_i \frac{\partial \dot{y}_i}{\partial q_r} - \dot{z}_i \frac{\partial \dot{z}_i}{\partial q_r}\right] \tag{199}$$

Using the relationship for cancelling dots in partials, reversing the order of differentiation and cancelling terms gives

$$\frac{d}{dt}\left(\frac{\partial T}{\partial \dot{q}_r}\right) - \frac{\partial T}{\partial q_r} = \sum_{i=1}^{N} m_i\left[\ddot{x}_i \frac{\partial x_i}{\partial q_r} + \ddot{y}_i \frac{\partial y_i}{\partial q_r} + \ddot{z}_i \frac{\partial z_i}{\partial q_r}\right] \tag{200}$$

Then from Equation 177, Lagrange's Equation in constrained coordinates with point masses becomes

$$\sum_{i=1}^{N} m_i \left[\ddot{x}_i \frac{\partial x_i}{\partial q_r} + \ddot{y}_i \frac{\partial y_i}{\partial q_r} + \ddot{z}_i \frac{\partial z_i}{\partial q_r} \right] + \frac{\partial B}{\partial \dot{q}_r} + \frac{\partial U}{\partial q_r} = Q_r \tag{201}$$

Also, in the same vein of defining the generalized coordinates, the relationship between the elemental and generalized forces can be developed. This relationship is developed from the definition of virtual work on a particle as the scalar product of the applied force and an infinitesimal displacement. Therefore for the total system of N elements,

$$\delta W = \sum_{i=1}^{N} \left[F_{x_i} \delta x_i + F_{y_i} \delta y_i + F_{z_i} \delta z_i \right] \tag{202}$$

Using the definition of Q_r from Equation 178 gives:

$$Q_r = \sum_{i=1}^{F} \left(F_{x_i} \frac{\partial x_i}{\partial q_r} + F_{y_i} \frac{\partial y_i}{\partial q_r} + F_{z_i} \frac{\partial z_i}{\partial q_r} \right) \tag{203}$$

Substituting Equation 203 into Equation 201 yields the final form of the Lagrange energy equation in constrained coordinates for point masses, which is in the form from which the REXCR II Equations of motion are developed. Making this substitution and rearranging the equation yields

$$\sum_{i=1}^{N} \left[\left(m_i \ddot{x}_i - F_{x_i} \right) \frac{\partial x_i}{\partial q_r} + \left(m_i \ddot{y}_i - F_{y_i} \right) \frac{\partial y_i}{\partial q_r} + \left(m_i \ddot{z}_i - F_{z_i} \right) \frac{\partial z_i}{\partial q_r} \right]$$

$$+ \frac{\partial B}{\partial \dot{q}_r} + \frac{\partial U}{\partial q_r} = 0 \tag{204}$$

The above equation is the basis for the entire derivation of the equations of motion of REXOR II. Note that this equation is written for discrete element masses and discrete forces. Also, at any instant in time all of the ingredients required to define the elemental accelerations, $\ddot{x}_i$, $\ddot{y}_i$, $\ddot{z}_i$, are not known. Specifically, the generalized coordinate displacements and velocities, q_r and $\dot{q}_r$, are known at any instant in time but the generalized coordinate accelerations, $\ddot{q}_r$, remain to be determined at the time the elemental accelerations are computed.

The following section presents the manner in which the foregoing equation set is adapted to the REXOR II numerical solution to solve the equilibrium equations or equations of motions for the generalized coordinate accelerations. This development is first presented in the simpler form, for clarity, for discrete mass elements and forces and then in expanded form to include elemental distributed masses and applied moments.

5.3 Iterative Concept and Equation Set Solution Method

Given a set of equations as developed in the previous section, the next step is to establish a method of solution. The solution process is defined as solving the equation set for the accelerations, integrating the accelerations for updated velocity, and position; then substituting the integrands back into the equations to determine new values of accelerations.

The first step of the process is to define explicitly the accelerations from the equation set. In the process of implementing the REXOR II equations, it is desirable to handle the accelerations as an estimated plus a corrective term. In generalized coordinates then we can write

$$\begin{Bmatrix} \ddot{q}_1 \\ \cdot \\ \cdot \\ \cdot \\ \ddot{q}_n \end{Bmatrix}_{NEW} = \begin{Bmatrix} \ddot{q}_1 \\ \cdot \\ \cdot \\ \cdot \\ \ddot{q}_n \end{Bmatrix}_{CORR.} + \begin{Bmatrix} \ddot{q}_1 \\ \cdot \\ \cdot \\ \cdot \\ \ddot{q}_n \end{Bmatrix}_{OLD} \tag{205}$$

This operation proceeds on a sequential time basis. For each increment advance in time, the previous 'NEW' becomes the 'OLD'. In REXOR II, the time increment corresponds with a step azimuthal advance of the main rotor

blades. However, this need not be the case. The 'NEW' accelerations must be used in the numerical integration process to define the generalized coordinate velocities and displacements. But if some form of a predictor on accelerations is used then the 'OLD' would be this predicted value and in this case it would be an estimated, 'EST', value.

Using the notation 'OLD' and 'EST' interchangeably the linear elemental accelerations can be written at time t as

$$\begin{Bmatrix} \ddot{x}_i \\ \ddot{y}_i \\ \ddot{z}_i \end{Bmatrix}^I_t = \begin{Bmatrix} \ddot{x}_i \\ \ddot{y}_i \\ \ddot{z}_i \end{Bmatrix}_{CORR} + \begin{Bmatrix} \ddot{x}_i \\ \ddot{y}_i \\ \ddot{z}_i \end{Bmatrix}^I_{EST} \tag{206}$$

where the estimated accelerations are determined using the generalized displacements and velocities, q_r and $\dot{q}_r$, at time t, and the generalized coordinate accelerations $\ddot{q}_r$, either estimated or from one previous time step in the numerical integration process.

Then, at any given instant in time where the 'EST' elemental accelerations are thusly determined, the corrective elemental accelerations, $(\ddot{x}, \ddot{y}, \ddot{z})_{i\ CORR}$ can be written as a function of the generalized coordinate corrective accelerations.

Or

$$\begin{Bmatrix} \ddot{x}_i \\ \ddot{y}_i \\ \ddot{z}_i \end{Bmatrix}_{CORR} = \begin{Bmatrix} \frac{\partial x_i}{\partial q_1} \ddot{q}_{1_{CORR}} + \cdots + \frac{\partial x_i}{\partial q_n} \ddot{q}_{n_{CORR}} \\ \frac{\partial y_i}{\partial q_1} \ddot{q}_{1_{CORR}} + \cdots + \frac{\partial y_i}{\partial q_n} \ddot{q}_{n_{CORR}} \\ \frac{\partial z_i}{\partial q_1} \ddot{q}_{1_{CORR}} + \cdots + \frac{\partial z_i}{\partial q_n} \ddot{q}_{n_{CORR}} \end{Bmatrix} . \tag{207}$$

or

$$\begin{Bmatrix} \ddot{x}_i \\ \ddot{y}_i \\ \ddot{z}_i \end{Bmatrix}_{CORR} = \sum_{k=1}^{n} \begin{Bmatrix} \frac{\partial x_i}{\partial q_k} \ddot{q}_{k_{CORR}} \\ \frac{\partial y_i}{\partial q_k} \ddot{q}_{k_{CORR}} \\ \frac{\partial z_i}{\partial q_k} \ddot{q}_{k_{CORR}} \end{Bmatrix} \tag{208}$$

Now making the substitution of Equations 203 and 207 into Equation 201 from the previous section and rearranging terms yields the Lagrange equation for the q_r coordinate in terms of the estimated elemental accelerations and the corrective generalized coordinate accelerations.

$$\sum_{i=1}^{N} \left[\left(m_i \ddot{x}_{i_{EST}} - F_{x_i} \right) \frac{\partial x_i}{\partial q_r} + \left(m_i \ddot{y}_{i_{EST}} - F_{y_i} \right) \frac{\partial y_i}{\partial q_r} + \left(m_i \ddot{z}_{i_{EST}} - F_{z_i} \right) \frac{\partial z_i}{\partial q_r} \right]$$

$$+ \sum_{i=1}^{N} m_i \left[\frac{\partial x_i}{\partial q_r} \sum_{k=1}^{n} \frac{\partial x_i}{\partial q_k} \ddot{q}_{k_{CORR.}} + \frac{\partial y_i}{\partial q_r} \sum_{k=1}^{n} \frac{\partial y_i}{\partial q_k} \ddot{q}_{k_{CORR.}} + \frac{\partial z_i}{\partial q_r} \sum_{k=1}^{n} \frac{\partial z_i}{\partial q_k} \ddot{q}_{k_{CORR.}} \right]$$

$$+ \frac{\partial B}{\partial \dot{q}_r} + \frac{\partial U}{\partial q_r} = 0 \tag{209}$$

The equations of motion for the system can now be combined and presented in matrix form.

$$\left[\begin{array}{c} M_{rk} \\ \text{MASS} \\ \text{MATRIX} \end{array}\right]\left\{\begin{array}{c} \ddot{q}_1 \\ \cdot \\ \cdot \\ \cdot \\ \ddot{q}_n \end{array}\right\}_{CORR} + \left\{\begin{array}{l} \displaystyle\sum_{i=1}^{N}\left[\left(m_i\ddot{x}_{i_{EST}} - F_{x_i}\right)\frac{\partial x_i}{\partial q_1} + \left(\quad\right)\frac{\partial y_i}{\partial q_1} + \left(\quad\right)\frac{\partial z_i}{\partial q_1}\right] \\ \qquad\qquad \vdots \\ \displaystyle\sum_{i=1}^{N}\left[\left(m_i\ddot{x}_{i_{EST}} - F_{x_i}\right)\frac{\partial x_i}{\partial q_n} + \left(\quad\right)\frac{\partial y_i}{\partial q_n} + \left(\quad\right)\frac{\partial z_i}{\partial q_n}\right] \end{array}\right\} +$$

$$\left[\begin{array}{c} + C_{rk} \\ \text{DAMPINC} \\ \text{MATRIX} \end{array}\right]\left\{\begin{array}{c} \dot{q}_1 \\ \cdot \\ \cdot \\ \cdot \\ \dot{q}_n \end{array}\right\} + \left[\begin{array}{c} K_{rk} \\ \text{STIFFNESS} \\ \text{MATRIX} \end{array}\right]\left\{\begin{array}{c} q_1 \\ \cdot \\ \cdot \\ \cdot \\ q_n \end{array}\right\} = 0 \qquad (210)$$

where the matrices, M_{rk}, C_{rk} and K_{rk} will be defined in the following discussion. However before proceeding with this, Equation 210 is now rearranged into the form actually used in the numerical process in REXOR II. The equation is solved in terms of the corrective accelerations.

The correction terms come from an inversion (or simultaneous equation, Cholesky method) operation on the model equation set.

$$\begin{Bmatrix} \ddot{q}_1 \\ \cdot \\ \cdot \\ \cdot \\ \dot{q}_n \end{Bmatrix}_{CORR.} = -\begin{bmatrix} \\ M_{rk} \\ \text{MASS} \\ \text{MATRIX} \\ \\ \end{bmatrix}^{-1} \left\{ \begin{Bmatrix} \sum_{i=1}^{N} \left[\left(m_i \ddot{x}_{i_{EST}} - F_{x_i} \right) \frac{\partial x_i}{\partial q_1} + \cdots \right] \\ \cdot \\ \cdot \\ \cdot \\ \sum_{i=1}^{N} \left[\left(m_i \ddot{x}_{i_{EST}} - F_{x_i} \right) \frac{\partial x_i}{\partial q_n} + \cdots \right] \end{Bmatrix} \right.$$

$$\left. + \begin{bmatrix} \\ C_{rk} \\ \text{DAMPING} \\ \text{MATRIX} \\ \\ \end{bmatrix} \begin{Bmatrix} \dot{q}_1 \\ \cdot \\ \cdot \\ \cdot \\ \dot{q}_n \end{Bmatrix} + \begin{bmatrix} \\ K_{rk} \\ \text{STIFFNESS} \\ \text{MATRIX} \\ \\ \end{bmatrix} \begin{Bmatrix} q_1 \\ \cdot \\ \cdot \\ \cdot \\ q_n \end{Bmatrix} \right\} \tag{211}$$

As indicated before estimated accelerations in physical coordinates come from the 'EST' or 'OLD' generalized coordinate accelerations and the current generalized coordinate velocities and displacements. The integration part of the solution operation supplies the $(\dot{q})$ and (q) data.

$$\dot{q} = \int \ddot{q}_{NEW}\, dt \quad ; \quad q = \int \dot{q}\, dt \tag{212}$$

The whole package operates in a cyclical fashion, as shown in Figure 29. Arranging the solution sequence as such gives it some important attributes and advantages.

First, to determine the corrective acceleration, the inverted mass matrix premultiplies the difference of applied and estimated reactive forces represented by the quantity in the large brackets on the right-hand side

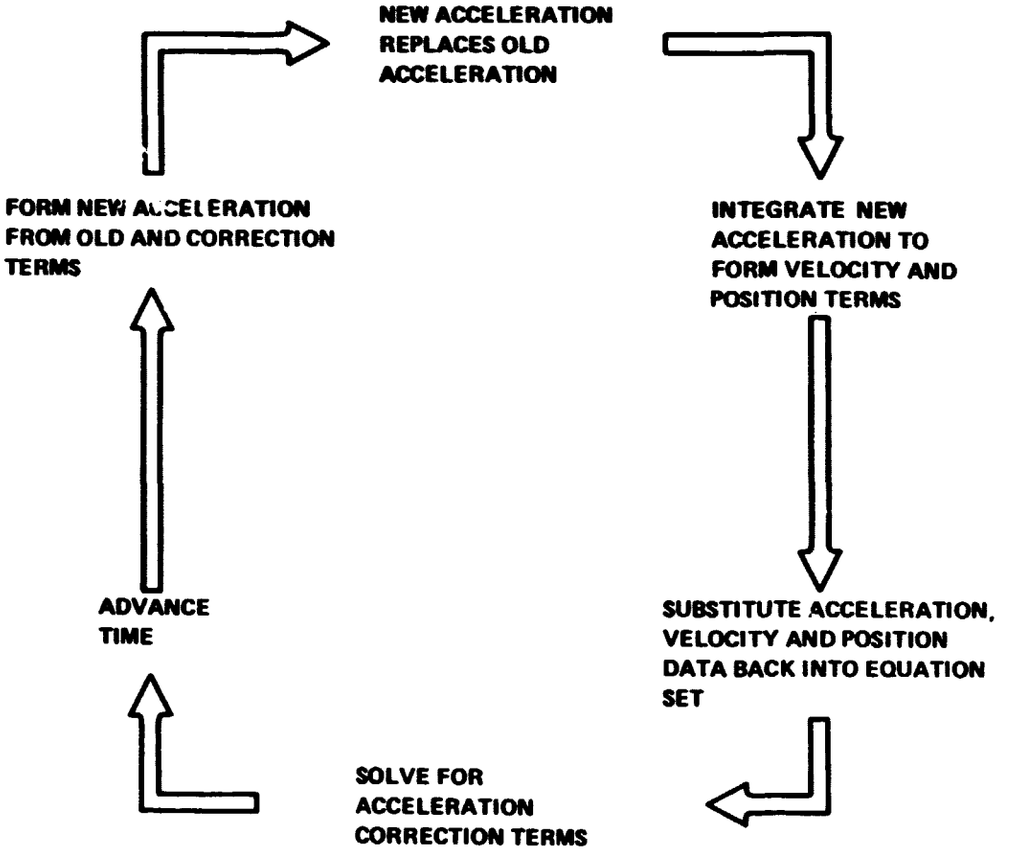

Figure 29. - Equation solution loop.

of Equation 211. With the usual, small, integration steps these differences will be relatively small. Therefore, inaccuracies in the mass matrix or its inversion process only slightly affect the total acceleration determination. This means approximations and simplifications to the mass matrix are acceptable. In some instances, a diagonal mass matrix will give convergence to the required solution.

Second, as will be shown in the Section 5.4, (blade equations section), carrying the running acceleration in elemental coordinates allows for the simple separation of the centrifugal and structural stiffness of the rotor blades which has important advantages which have been discussed. Also, the aerodynamic loading terms, already by nature in physical coordinates, are easily accounted for.

In the actual application of Equation 211 to REXOR II, distributed elemental rigid body masses are associated with each coordinate point and applied moments in addition to forces at each coordinate point are accounted for.

Referring back to Equation 203 the generalized force, Q_r, from virtual work can be simply written in the following form to account for applied moments at each of the ith grid points as

$$Q_r = \sum_{i=1}^{N}\left[F_{x_i}\frac{\partial x_i}{\partial q_r} + F_{y_i}\frac{\partial y_i}{\partial q_r} + F_{z_i}\frac{\partial z_i}{\partial q_r} + M_{x_i}\frac{\partial \phi_i}{\partial q_r} + M_{y_i}\frac{\partial \theta_i}{\partial q_r} + M_{z_i}\frac{\partial \psi_i}{\partial q_r}\right] \quad (213)$$

The terms of Equation 200 in Equation 204 can be developed for the distributed masses by going back to the elemental acceleration equation, Equation 13 of Section 4.4.1 which is repeated here, in a rearranged form, for clarity of this development.

$$\begin{Bmatrix}\ddot{x}\\ \ddot{y}\\ \ddot{z}\end{Bmatrix}^I = \begin{Bmatrix}\ddot{x}_0\\ \ddot{y}_0\\ \ddot{z}_0\end{Bmatrix}^I + \begin{Bmatrix}\ddot{x}\\ \ddot{y}\\ \dot{z}\end{Bmatrix} + \begin{bmatrix}(-r^2-q^2) & pq & pr\\ pq & (-r^2-p^2) & qr\\ pr & qr & (-p^2-q^2)\end{bmatrix}\begin{Bmatrix}x\\ y\\ z\end{Bmatrix}$$

$$+ 2\begin{bmatrix}0 & -r & q\\ r & 0 & -p\\ -q & p & 0\end{bmatrix}\begin{Bmatrix}x\\ y\\ z\end{Bmatrix} + \begin{bmatrix}0 & z & -y\\ -z & 0 & x\\ y & -x & 0\end{bmatrix}\begin{Bmatrix}\dot{p}\\ \dot{q}\\ \dot{r}\end{Bmatrix} \quad (214)$$

For distributed masses of a rigid body with coordinate point and system embedded in the body:

$$\dot{x} = \dot{y} = \dot{z} = 0 \tag{215}$$

and Equation 214 becomes:

$$\begin{Bmatrix} \ddot{x} \\ \ddot{y} \\ \ddot{z} \end{Bmatrix}^I = \begin{Bmatrix} \ddot{x}_0 \\ \ddot{y}_0 \\ \ddot{z}_0 \end{Bmatrix}^I + \begin{Bmatrix} -x(r^2+q^2) + ypq + zpr \\ xpq - y(r^2+p^2) + zqr \\ xpr + yqr - z(p^2+q^2) \end{Bmatrix} + \begin{Bmatrix} z\dot{q} - yr \\ -z\dot{p} + x\dot{r} \\ y\dot{p} - x\dot{q} \end{Bmatrix} \tag{216}$$

Now, remembering that for a point mass,

$$\frac{\partial x}{\partial q_r} = \frac{\partial \ddot{x}}{\partial \ddot{q}_r} \tag{217}$$

$$\frac{\partial y}{\partial q_r} = \frac{\partial \ddot{y}}{\partial \ddot{q}_r} \tag{218}$$

$$\frac{\partial z}{\partial q_r} = \frac{\partial \ddot{z}}{\partial \ddot{q}_r} \tag{219}$$

$$\frac{\partial \phi}{\partial q_r} = \frac{\partial \dot{p}}{\partial \ddot{q}_r} \tag{220}$$

$$\frac{\partial \theta}{\partial q_r} = \frac{\partial \dot{q}}{\partial \ddot{q}_r} \tag{221}$$

and

$$\frac{\partial \psi}{\partial q_r} = \frac{\partial \dot{r}}{\partial \ddot{q}_r} \tag{222}$$

The total partial derivatives relating the motion of the coordinate point and set imbedded within each elemental body and the motion of the generalized coordinate becomes

$$\frac{\partial x}{\partial q_r} = \frac{\partial x_0}{\partial q_r} - y \frac{\partial \psi}{\partial q_r} + z \frac{\partial \theta}{\partial q_r} \tag{223}$$

$$\frac{\partial y}{\partial q_r} = \frac{\partial y_0}{\partial q_r} + x \frac{\partial \psi}{\partial q_r} - z \frac{\partial \phi}{\partial q_r} \tag{224}$$

$$\frac{\partial z}{\partial q_r} = \frac{\partial z_0}{\partial q_r} - x \frac{\partial \theta}{\partial q_r} + y \frac{\partial \phi}{\partial q_r} \tag{225}$$

where on the right side of these equations, x, y, and z represent the location of the distributed masses within the rigid body elemental mass, and x_0, y_0 and z_0 represent the motion of the mass element reference point.

For each jth coordinate of the system, the elements of Equation 200 can be written by substitution of Equations 216, 223, 224 and 225. This gives

$$\left[\sum_{i=1}^{N} m_i \begin{Bmatrix} \ddot{x}_i \\ \ddot{y}_i \\ \ddot{z}_i \end{Bmatrix}_{EST} \cdot \frac{\partial}{\partial q_r} \begin{Bmatrix} x_i \\ y_i \\ z_i \end{Bmatrix}\right]_j$$

$$= \left[\sum_{i=1}^{N} m_i \left[\begin{array}{l} \dot{x}_0 \dfrac{\partial x_0}{\partial q_r} - \ddot{x}_0 y_i \dfrac{\partial \psi}{\partial q_r} + \ddot{x}_0 z_i \dfrac{\partial \theta}{\partial q_r} - x_i(r^2+q^2) \dfrac{\partial x_0}{\partial q_r} + x_i y_i (r^2+q^2) \dfrac{\partial \psi}{\partial q_r} \\ \ddot{y}_0 \dfrac{\partial y_0}{\partial q_r} + \ddot{y}_0 x_i \dfrac{\partial \psi}{\partial q_r} - \ddot{y}_0 z_i \dfrac{\partial \phi}{\partial q_r} + x_i pq \dfrac{\partial y_0}{\partial q_r} + x_i^2 pq \dfrac{\partial \psi}{\partial q_r} - x_i y_i pq \dfrac{\partial \phi}{\partial q_r} \\ \ddot{z}_0 \dfrac{\partial z_0}{\partial q_r} - \ddot{z}_0 x_i \dfrac{\partial \theta}{\partial q_r} + \ddot{z}_0 y_i \dfrac{\partial \phi}{\partial q_r} + x_i pr \dfrac{\partial z_0}{\partial q_r} - x_i^2 pr \dfrac{\partial \theta}{\partial q_r} + x_i y_i pr \dfrac{\partial \phi}{\partial q_r} \end{array}\right]\right.$$

$$+ \left[\begin{array}{l} - x_i z_i (r^2+q^2) \dfrac{\partial \theta}{\partial q_r} + y_i pq \dfrac{\partial x_0}{\partial q_r} - y_i^2 pq \dfrac{\partial \psi}{\partial q_r} + y_i z_i pq \dfrac{\partial \theta}{\partial q_r} + z_i pr \dfrac{\partial x_0}{\partial q_r} \\ - y_i (r^2+p^2) \dfrac{\partial y_0}{\partial q_r} - x_i y_i (r^2+p^2) \dfrac{\partial \psi}{\partial q_r} + y_i z_i (r^2+p^2) \dfrac{\partial \phi}{\partial q_r} + z_i q_r \dfrac{\partial y_0}{\partial q_r} \\ + y_i q_r \dfrac{\partial z_0}{\partial q_r} - x_i y_i q_r \dfrac{\partial \theta}{\partial q_r} + y_i^2 q_r \dfrac{\partial \phi}{\partial q_r} - z_i (p^2+q^2) \dfrac{\partial z_0}{\partial q_r} \end{array}\right]$$

$$+ \left[\begin{array}{l} - z_i y_i pr \dfrac{\partial \psi}{\partial q_r} + z_i^2 pr \dfrac{\partial \theta}{\partial q_r} + z_i \dot{q} \dfrac{\partial x_0}{\partial q_r} - y_i z_i \dot{q} \dfrac{\partial \psi}{\partial q_r} + z_i^2 \dot{q} \dfrac{\partial \theta}{\partial q_r} \\ + x_i z_i q_r \dfrac{\partial \psi}{\partial q_r} - z_i^2 q_r \dfrac{\partial \phi}{\partial q_r} - z_i \dot{p} \dfrac{\partial y_0}{\partial q_r} - x_i z_i \dot{p} \dfrac{\partial \psi}{\partial q_r} - z_i^2 \dot{p} \dfrac{\partial \phi}{\partial q_r} \\ + x_i z_i (p^2+q^2) \dfrac{\partial \theta}{\partial q_r} - y_i z_i (p^2+q^2) \dfrac{\partial \phi}{\partial q_r} + y_i \dot{p} \dfrac{\partial z_0}{\partial q_r} - x_i y_i \dot{p} \dfrac{\partial \theta}{\partial q_r} \end{array}\right]$$

$$\left.\left. + \left[\begin{array}{l} - y_i \dot{r} \dfrac{\partial x_0}{\partial q_r} + y_i^2 \dot{r} \dfrac{\partial \psi}{\partial q_r} - z_i y_i \dot{r} \dfrac{\partial \theta}{\partial q_r} \\ + x_i \dot{r} \dfrac{\partial y_0}{\partial q_r} + x_i^2 \dot{r} \dfrac{\partial \psi}{\partial q_r} + x_i z_i \dot{r} \dfrac{\partial \phi}{\partial q_r} \\ + y_i^2 \dot{p} \dfrac{\partial \phi}{\partial q_r} - x_i \dot{q} \dfrac{\partial z_0}{\partial q_r} + x_i^2 \dot{q} \dfrac{\partial \theta}{\partial q_r} - x_i y_i \dot{q} \dfrac{\partial \phi}{\partial q_r} \end{array}\right] \right]\right]_j \qquad (226)$$

Expanding and identifying mass moment and moment of inertia terms:

$$\left[\sum_{i=1}^{N} m_i \begin{Bmatrix} \ddot{x}_i \\ \ddot{y}_i \\ \ddot{z}_i \end{Bmatrix}_{EST} \cdot \frac{\partial}{\partial q_r} \begin{Bmatrix} x_i \\ y_i \\ z_i \end{Bmatrix}\right]_j =$$

$$\begin{bmatrix} M\ddot{x} \dfrac{\partial x_C}{\partial q_r} - M\bar{y}\ddot{x} \dfrac{\partial \psi}{\partial q_r} + M\bar{z}\ddot{x} \dfrac{\partial \theta}{\partial q_r} - M\bar{x}(r^2+q^2) \dfrac{\partial x_0}{\partial q_r} + I_{XY}(r^2+q^2) \dfrac{\partial \psi}{\partial q_r} \\ M\ddot{y} \dfrac{\partial y_0}{\partial q_r} + M\bar{x}\ddot{y} \dfrac{\partial \psi}{\partial q_r} - M\bar{z}\ddot{y} \dfrac{\partial \phi}{\partial q_r} + M\bar{x}pq \dfrac{\partial y_0}{\partial q_r} + I_X pq \dfrac{\partial \psi}{\partial q_r} - I_{XZ} pq \dfrac{\partial \phi}{\partial q_r} \\ M\ddot{z} \dfrac{\partial z_0}{\partial q_r} - M\bar{x}\ddot{z} \dfrac{\partial \theta}{\partial q_r} + M\bar{y}\ddot{z} \dfrac{\partial \phi}{\partial q_r} + M\bar{x}pr \dfrac{\partial z_0}{\partial q_r} - I_X pr \dfrac{\partial \theta}{\partial q_r} + I_{XY} pr \dfrac{\partial \phi}{\partial q_r} \end{bmatrix}$$

$$+ \begin{bmatrix} - I_{XZ}(r^2+q^2) \dfrac{\partial \theta}{\partial q_r} + M\bar{y}pq \dfrac{\partial x_0}{\partial q_r} - I_Y pq \dfrac{\partial \psi}{\partial q_r} + I_{YZ} pq \dfrac{\partial \theta}{\partial q_r} + M\bar{z}pr \dfrac{\partial x_0}{\partial q_r} \\ - M\bar{y}(r^2+p^2) \dfrac{\partial y_0}{\partial q_r} - I_{XY}(r^2+p^2) \dfrac{\partial \psi}{\partial q_r} + I_{YZ}(r^2+p^2) \dfrac{\partial \phi}{\partial q_r} + M\bar{z}qr \dfrac{\partial y_0}{\partial q_r} \\ + M\bar{y}qr \dfrac{\partial z_0}{\partial q_r} - I_{XY} qr \dfrac{\partial \theta}{\partial q_r} + I_Y qr \dfrac{\partial \phi}{\partial q_r} - M\bar{z}(p^2+q^2) \dfrac{\partial z_0}{\partial q_r} + I_{XZ}(p^2+q^2) \dfrac{\partial \theta}{\partial q_r} \end{bmatrix}$$

$$+ \begin{bmatrix} - I_{ZY} pr \dfrac{\partial \psi}{\partial q_r} + I_Z pr \dfrac{\partial \theta}{\partial q_r} + M\bar{z}\dot{q} \dfrac{\partial x_0}{\partial q_r} - I_{YZ}\dot{q} \dfrac{\partial \psi}{\partial q_r} + I_Z\dot{q} \dfrac{\partial \theta}{\partial q_r} - M\bar{y}\dot{r} \dfrac{\partial x_0}{\partial q_r} \\ + I_{XZ} qr \dfrac{\partial \psi}{\partial q_r} - I_Z qr \dfrac{\partial \phi}{\partial q_r} - M\bar{z}\dot{p} \dfrac{\partial y_0}{\partial q_r} - I_{XZ}\dot{p} \dfrac{\partial \psi}{\partial q_r} + I_Z\dot{p} \dfrac{\partial \phi}{\partial q_r} + M\bar{x}\dot{r} \dfrac{\partial y_0}{\partial q_r} \\ - I_{YZ}(p^2+q^2) \dfrac{\partial \phi}{\partial q_r} + M\bar{y}\dot{p} \dfrac{\partial z_0}{\partial q_r} - I_{XY}\dot{p} \dfrac{\partial \theta}{\partial q_r} + I_Y\dot{p} \dfrac{\partial \phi}{\partial q_r} - M\bar{x}\dot{q} \dfrac{\partial z_0}{\partial q_r} + I_X\dot{q} \dfrac{\partial \theta}{\partial q_r} \end{bmatrix}$$

$$+ \begin{bmatrix} + I_Y\dot{r} \dfrac{\partial \psi}{\partial q_r} - I_{YZ}\dot{r} \dfrac{\partial \theta}{\partial q_r} \\ + I_X\dot{r} \dfrac{\partial \psi}{\partial q_r} - I_{XZ}\dot{r} \dfrac{\partial \phi}{\partial q_r} \\ - I_{XY}\dot{q} \dfrac{\partial \phi}{\partial q_r} \end{bmatrix}_j \qquad (227)$$

and finally collecting and grouping terms yields the final and complete definition of the terms of Equation 211 for the estimated elemental accelerations.

$$\left[\sum_{i=1}^{N} m_i \begin{Bmatrix} \ddot{x} \\ \ddot{y} \\ \ddot{z} \end{Bmatrix}_{EST} \cdot \frac{\partial}{\partial q_r} \begin{Bmatrix} x \\ y \\ z \end{Bmatrix}\right]_j =$$

$$\left[M \begin{Bmatrix} \ddot{x} \\ \ddot{y} \\ \ddot{z} \end{Bmatrix} + M\bar{x} \begin{Bmatrix} -(r^2+q^2) \\ pq+\dot{r} \\ pr-\dot{q} \end{Bmatrix} + M\bar{y} \begin{Bmatrix} pq-\dot{r} \\ -(r^2+p^2) \\ qr+\dot{p} \end{Bmatrix} + M\bar{z} \begin{Bmatrix} pr+\dot{q} \\ qr-\dot{p} \\ -(p^2+q^2) \end{Bmatrix} \right] \frac{\partial}{\partial q_r} \begin{Bmatrix} x_0 \\ y_0 \\ z_0 \end{Bmatrix}$$

$$+ M \left[\frac{\partial \phi}{\partial q_r} \begin{Bmatrix} 0 \\ -\bar{z}\ddot{y} \\ \bar{y}\ddot{z} \end{Bmatrix} + \frac{\partial \theta}{\partial q_r} \begin{Bmatrix} \bar{z}\ddot{x} \\ 0 \\ -\bar{x}\ddot{z} \end{Bmatrix} + \frac{\partial \psi}{\partial q_r} \begin{Bmatrix} -\bar{y}\ddot{x} \\ \bar{x}\ddot{y} \\ 0 \end{Bmatrix} \right]$$

$$+ \begin{bmatrix} I_X(0) & +I_Y\left(-\frac{\partial \psi}{\partial q_r}(pq-\dot{r})\right) & +I_Z\left(\frac{\partial \theta}{\partial q_r}(pr+\dot{q})\right) \\ I_X\left(\frac{\partial \psi}{\partial q_r}(pq+\dot{r})\right) & +I_Y(0) & -I_Z\left(\frac{\partial \phi}{\partial q_r}(qr-\dot{p})\right) \\ -I_X\left(\frac{\partial \theta}{\partial q_r}(pr-\dot{q})\right) & +I_Y\left(\frac{\partial \phi}{\partial q_r}(qr+\dot{p})\right) & +I_Z(0) \end{bmatrix}$$

$$+ \begin{bmatrix} I_{XY}(r^2+q^2)\frac{\partial \psi}{\partial q_r} - I_{XZ}(r^2+q^2)\frac{\partial \theta}{\partial q_r} + I_{YZ}\left((pq-\dot{r})\frac{\partial \theta}{\partial q_r} - (pr+\dot{q})\frac{\partial \psi}{\partial q_r}\right) \\ -I_{XY}(r^2+p^2)\frac{\partial \psi}{\partial q_r} + I_{XZ}\left(-(pq+\dot{r})\frac{\partial \phi}{\partial q_r} + (qr-\dot{p})\frac{\partial \psi}{\partial q_r}\right) + I_{YZ}(r^2+p^2)\frac{\partial \phi}{\partial q_r} \\ I_{XY}\left((pr-\dot{q})\frac{\partial \phi}{\partial q_r} - (qr+\dot{p})\frac{\partial \theta}{\partial q_r}\right) + I_{XZ}(p^2+q^2)\frac{\partial \theta}{\partial q_r} - I_{YZ}(p^2+q^2)\frac{\partial \phi}{\partial q_r} \end{bmatrix}_j$$

(225)

where in this case the summation $\sum_{i=1}^{N}$ represents summation over the jth rigid body element. With this in mind, substituting Equations 228 and 2_3 back into Equation 201 yields the complete form of the Lagrange energy equation in constrained coordinates with distributed elemental masses and forces from which the REXOR II equations of motion are all developed. Also including these terms as well as the moment terms of Equation 213 in Equation 211 yields the final form of the equation as used in REXOR II. This form will be presented following the development of the generalized mass damping and stiffness matrices.

From Equation 209 it is easily seen, by examining the coefficients of the corrective accelerations that generalized mass matrix elements, M_{rk}, can be written as

$$M_{rk} = \sum_{i=1}^{N} m_i \left(\frac{\partial x_i}{\partial q_r} \frac{\partial x_i}{\partial q_k} + \frac{\partial y_i}{\partial q_r} \frac{\partial y_i}{\partial q_k} + \frac{\partial z_i}{\partial q_r} \frac{\partial z_i}{\partial q_k} \right) \tag{229}$$

This equation is for point masses. Actually, as discussed earlier, the REXOR II equations model a set of distributed masses characterized by an overall mass, center of gravity, and moment of inertia values. As shown in the previous section, extension to the distributed mass form is made by describing the particle absolute coordinates in terms of the position of a relative coordinate set in inertial space and the particle position in terms of this relative set as developed in Section 4.4. For a rigid body the associated relative set and the particle associated with the body maintain a fixed relationship. The summing over the particles of the system then becomes a sum over products of masses and lengths yielding mass moment and moment of inertia terms.

The mass elements can be developed by substituting the partial derivatives developed in the preceding discussion. These partials describe both the motion of the mass element reference and also the distributed masses within the rigid body elemental masses.

Substituting these partials, Equations 223, 224 and 225 in the generalized mass expression, Equation 229 yields:

$$M_{rk} = \sum_{i=1}^{N} m_i \left(\frac{\partial x_0}{\partial q_r} \frac{\partial x_0}{\partial q_k} - y_i \frac{\partial x_0}{\partial q_r} \frac{\partial x_0}{\partial q_k} + z_i \frac{\partial x_0}{\partial q_r} \frac{\partial \theta}{\partial q_k} - y_i \frac{\partial \psi}{\partial q_r} \frac{\partial x_0}{\partial q_k} \right.$$

$$+ y_i^2 \frac{\partial \psi}{\partial q_r} \frac{\partial \psi}{\partial q_k} - y_i z_i \frac{\partial \psi}{\partial q_r} \frac{\partial \theta}{\partial q_k} + z_i \frac{\partial \theta}{\partial q_r} \frac{\partial x_0}{\partial q_k} + y_i z_i \frac{\partial \theta}{\partial q_r} \frac{\partial \psi}{\partial q_k}$$

$$+ z_i^2 \frac{\partial \theta}{\partial q_r} \frac{\partial \theta}{\partial q_k} + \frac{\partial y_0}{\partial q_r} \frac{\partial y_0}{\partial q_k} + x_i \frac{\partial y_0}{\partial q_r} \frac{\partial \psi}{\partial q_k} - z_i \frac{\partial y_0}{\partial q_r} \frac{\partial \phi}{\partial q_k}$$

$$+ x_i \frac{\partial \psi}{\partial q_r} \frac{\partial y_0}{\partial q_k} + x_i^2 \frac{\partial \psi}{\partial q_r} \frac{\partial \psi}{\partial q_k} - x_i z_i \frac{\partial \psi}{\partial q_r} \frac{\partial \phi}{\partial q_k} - z_i \frac{\partial \phi}{\partial q_r} \frac{\partial y_0}{\partial q_k}$$

$$- z_i x_i \frac{\partial \phi}{\partial q_r} \frac{\partial \psi}{\partial q_k} + z_i^2 \frac{\partial \phi}{\partial q_r} \frac{\partial \phi}{\partial q_k} + \frac{\partial z_0}{\partial q_r} \frac{\partial z_0}{\partial q_k} - x_i \frac{\partial z_0}{\partial q_r} \frac{\partial \phi}{\partial q_k}$$

$$+ y_i \frac{\partial z_0}{\partial q_r} \frac{\partial \phi}{\partial q_k} - x_i \frac{\partial \theta}{\partial q_r} \frac{\partial z_0}{\partial q_k} + x_i^2 \frac{\partial \theta}{\partial q_r} \frac{\partial \theta}{\partial q_k} - x_i y_i \frac{\partial \theta}{\partial q_r} \frac{\partial \phi}{\partial q_k}$$

$$\left. + y_i \frac{\partial \phi}{\partial q_r} \frac{\partial z_0}{\partial q_k} - x_i y_i \frac{\partial \phi}{\partial q_r} \frac{\partial \theta}{\partial q_k} + y_i^2 \frac{\partial \phi}{\partial q_r} \frac{\partial \phi}{\partial q_k} \right) \qquad (230)$$

and using moment of inertia and mass moment definitions:

$$M_{rk} = M\left(\frac{\partial x}{\partial q_r}\frac{\partial x}{\partial q_k} + \frac{\partial y}{\partial q_r}\frac{\partial y}{\partial q_k} + \frac{\partial z}{\partial q_r}\frac{\partial z}{\partial q_k}\right) + I_{ZZ}\left(\frac{\partial \psi}{\partial q_r}\frac{\partial \psi}{\partial q_k}\right)$$

$$+ I_{XX}\left(\frac{\partial \phi}{\partial q_r}\frac{\partial \phi}{\partial q_k}\right) + I_{YY}\left(\frac{\partial \theta}{\partial q_r}\frac{\partial \theta}{\partial q_k}\right) + I_{XZ}\left(-\frac{\partial \psi}{\partial q_r}\frac{\partial \phi}{\partial q_k} - \frac{\partial \phi}{\partial q_r}\frac{\partial \psi}{\partial q_k}\right)$$

$$+ I_{XY}\left(-\frac{\partial \theta}{\partial q_r}\frac{\partial \phi}{\partial q_k} - \frac{\partial \phi}{\partial q_r}\frac{\partial \theta}{\partial q_k}\right) + I_{YZ}\left(-\frac{\partial \psi}{\partial q_r}\frac{\partial \theta}{\partial q_k} - \frac{\partial \theta}{\partial q_r}\frac{\partial \psi}{\partial q_k}\right)$$

$$+ M\bar{x}\left(\frac{\partial y}{\partial q_r}\frac{\partial \psi}{\partial q_k} + \frac{\partial \psi}{\partial q_r}\frac{\partial y}{\partial q_k} - \frac{\partial \theta}{\partial q_r}\frac{\partial z}{\partial q_k} - \frac{\partial z}{\partial q_r}\frac{\partial \theta}{\partial q_k}\right)$$

$$+ M\bar{y}\left(-\frac{\partial x}{\partial q_r}\frac{\partial \psi}{\partial q_k} - \frac{\partial \psi}{\partial q_r}\frac{\partial x}{\partial q_k} + \frac{\partial \phi}{\partial q_r}\frac{\partial z}{\partial q_k} + \frac{\partial z}{\partial q_r}\frac{\partial \phi}{\partial q_k}\right)$$

$$+ M\bar{z}\left(\frac{\partial x}{\partial q_r}\frac{\partial \theta}{\partial q_k} + \frac{\partial \theta}{\partial q_r}\frac{\partial x}{\partial q_k} - \frac{\partial \phi}{\partial q_r}\frac{\partial y}{\partial q_k} - \frac{\partial y}{\partial q_r}\frac{\partial \phi}{\partial q_k}\right) \qquad (231)$$

and is identified as a generalized mass. For orthogonal systems M_{rk} is zero except for $r = k$. The development of REXOR II is mostly nonorthogonal coordinates, therefore, the generalized mass matrix has many off-diagonal terms.

Similarly, terms can be developed for the strain (potential) energy and damping functions.

$$U = \frac{1}{2}\sum_{i=1}^{N}\left[\left(k_{x_i} x_i^2 + k_{y_i} y_i^2 + k_{z_i} z_i^2\right)\right.$$

$$\left. + \left(K_{\phi_i} \phi_i^2 + K_{\theta_i} \theta_i^2 + K_{\psi_i} \psi_i^2\right)\right] \qquad (232)$$

$$\frac{\partial U}{\partial q_r} = \sum_{i=1}^{N} \left(k_{x_i} x_i \frac{\partial x_i}{\partial q_r} + k_{y_i} y_i \frac{\partial y_i}{\partial q_r} + k_{z_i} z_i \frac{\partial z_i}{\partial q_r} \right.$$

$$\left. + K_{\phi_i} \phi_i \frac{\partial \phi_i}{\partial q_r} + K_{\theta_i} \theta_i \frac{\partial \theta_i}{\partial q_r} + K_{\psi_i} \psi_i \frac{\partial \psi_i}{\partial q_r} \right)$$

$$= \sum_{i=1}^{N} \left[k_{x_i} \frac{\partial x_i}{\partial q_r} \sum_{k=1}^{n} \frac{\partial x_i}{\partial q_k} q_k + k_{y_i} \frac{\partial y_i}{\partial q_r} \sum_{k=1}^{n} \frac{\partial y_i}{\partial q_k} q_k \right.$$

$$+ k_{z_i} \frac{\partial z_i}{\partial q_r} \sum_{k=1}^{n} \frac{\partial z_i}{\partial q_k} q_k + k_{\phi_i} \frac{\partial \phi_i}{\partial q_r} \sum_{k=1}^{n} \frac{\partial \phi_i}{\partial q_k} q_k$$

$$\left. + k_{\theta_i} \frac{\partial \theta_i}{\partial q_r} \sum_{k=1}^{n} \frac{\partial \theta_i}{\partial q_k} q_k + k_{\psi_i} \frac{\partial \psi_i}{\partial q_r} \sum_{k=1}^{n} \frac{\partial \psi_i}{\partial q_k} q_k \right] \qquad (233)$$

Define

$$\sum_{i=1}^{N} \left[k_{x_i} \frac{\partial x_i}{\partial q_r} \frac{\partial x_i}{\partial q_k} + k_{y_i} \frac{\partial y_i}{\partial q_r} \frac{\partial y_i}{\partial q_k} + k_{z_i} \frac{\partial z_i}{\partial q_r} \frac{\partial z_i}{\partial q_k} \right.$$

$$\left. + k_{\phi_i} \frac{\partial \phi_i}{\partial q_r} \frac{\partial \phi_i}{\partial q_k} + k_{\theta_i} \frac{\partial \theta_i}{\partial q_r} \frac{\partial \theta_i}{\partial q_k} + k_{\psi_i} \frac{\partial \psi_i}{\partial q_r} \frac{\partial \psi_i}{\partial q_k} \right] = K_{rk} \qquad (234)$$

Similarly for damping:

$$\sum_{i=1}^{N} \left[c_{x_i} \frac{\partial x_i}{\partial q_r} \frac{\partial x_i}{\partial q_k} + c_{y_i} \frac{\partial y_i}{\partial q_r} \frac{\partial y_i}{\partial q_k} + c_{z_i} \frac{\partial z_i}{\partial q_r} \frac{\partial z_i}{\partial q_k} \right.$$

$$\left. + c_{\phi_i} \frac{\partial \phi_i}{\partial q_r} \frac{\partial \phi_i}{\partial q_k} + c_{\theta_i} \frac{\partial \theta_i}{\partial q_r} \frac{\partial \theta_i}{\partial q_k} + c_{\psi_i} \frac{\partial \psi_i}{\partial q_r} \frac{\partial \psi_i}{\partial q_k} \right] = C_{rk} \qquad (235)$$

The stiffness and damping matrix terms in REXOR II are defined with reference to relative coordinates; which parallels the physical configuration. The coordinates used with these terms then should be on a relative basis. This statement at first appears to be contradictory to the premise of the equation development. However, if these matrix terms were defined on an absolute basis the terms other than those associated with a relative motion would be identically zero. The integration of the accelerations produces changes in velocity and position. These changes with the proper starting reference are the relative coordinates and velocities.

Equation 211 is now repeated here in a slightly expanded form to include the effect of applied elemental moments, Equation 213, and distributed elemental masses, Equation 228.

$$\begin{Bmatrix} \ddot{q}_1 \\ \cdot \\ \cdot \\ \cdot \\ \ddot{q}_n \end{Bmatrix}_{CORR} = -\underbrace{\begin{bmatrix} M_{rk} \\ \text{MASS} \\ \text{MATRIX} \end{bmatrix}^{-1}}_{\text{(Equation 231)}} \left\{ \begin{Bmatrix} \sum_{i=1}^{N} \left[\left(m_i \ddot{x}_{i_{EST}} - F_{x_i} \right) \frac{\partial x_i}{\partial q_1} + M_{x_i} \frac{\partial \phi_i}{\partial q_1} + \cdots \right] \\ \cdot \\ \cdot \\ \cdot \\ \sum_{i=1}^{N} \left[\left(m_i \ddot{x}_{i_{EST}} - F_{x_i} \right) \frac{\partial x_i}{\partial q_n} + M_{x_i} \frac{\partial \phi_i}{\partial q_1} + \cdots \right] \end{Bmatrix}}_{\text{(Sum of Equations 213 and 228)}} + \underbrace{\begin{bmatrix} C_{rk} \\ \text{DAMPING} \\ \text{MATRIX} \end{bmatrix}}_{\text{(Equation 235)}} \begin{Bmatrix} \dot{q}_1 \\ \cdot \\ \cdot \\ \cdot \\ \dot{q}_n \end{Bmatrix} + \underbrace{\begin{bmatrix} K_{rk} \\ \text{STIFFNESS} \\ \text{MATRIX} \end{bmatrix}}_{\text{(Equation 234)}} \begin{Bmatrix} q_1 \\ \cdot \\ \cdot \\ \cdot \\ q_n \end{Bmatrix} \right\} \qquad (236)$$

Even though Q_r was defined as the generalized forces of the system, for the purpose of further development and of the application of the above equation in the REXCR II analysis, each line in the large brackets on the right side of Equation 236 will hereafter be referred to as a generalized force or a generalized delta force and will be referred to by the symbol, FR, in the following development.

In REXOR II use is made of matrix notation to produce compact partial derivative, generalized mass and generalized force expressions. The partial derivative set

$$\frac{\partial x}{\partial q_r}, \frac{\partial y}{\partial q_r}, \frac{\partial z}{\partial q_r}, \frac{\partial \phi}{\partial q_r}, \frac{\partial \theta}{\partial q_r}, \frac{\partial \psi}{\partial q_r}$$

is replaced by

$$\left\{\frac{\partial \tau}{\partial q_r}\right\}.$$

Usually the generalized coordinates q are grouped as three linear plus three rotational motions. The full partial derivative for system coordinate A and generalized coordinate set B is:

$$\left[\frac{\partial \tau_{OA}}{\partial \gamma_B}\right]$$

The generalized mass expression (Equation 231) can be rewritten as:

$$M_{rk} = \left\{\frac{\partial \tau}{\partial q_r}\right\}^T \begin{bmatrix} M & 0 & 0 & 0 & M\bar{Z} & -M\bar{Y} \\ 0 & M & 0 & -M\bar{Z} & 0 & M\bar{X} \\ 0 & 0 & M & M\bar{Y} & -M\bar{X} & 0 \\ 0 & -M\bar{Z} & M\bar{Y} & I_{XY} & -I_{XY} & -I_{XZ} \\ M\bar{Z} & 0 & -M\bar{X} & -I_{XY} & I_{YY} & -I_{YZ} \\ -M\bar{Y} & M\bar{X} & 0 & -I_{XZ} & -I_{YZ} & I_{ZZ} \end{bmatrix} \left\{\frac{\partial \tau}{\partial q_k}\right\} \qquad (237)$$

The generalized delta force, ΔQ_B, can be expressed in matrix notation for contribution of coordinate set A as:

$$\left\{\Delta Q_B\right\} = \left[\frac{\partial T_A}{\partial T_B}\right]^T \left\{ \begin{bmatrix} F_X \\ F_Y \\ F_Z \\ F\phi \\ F\theta \\ F\psi \end{bmatrix}_A - \begin{bmatrix} M & & & 0 & M\bar{Z} & -M\bar{Y} \\ & M & & -M\bar{Z} & 0 & M\bar{X} \\ & & M & M\bar{Y} & -M\bar{X} & 0 \\ 0 & -M\bar{Z} & M\bar{Y} & I_{XX} & -I_{XY} & -I_{XZ} \\ M\bar{Z} & 0 & -M\bar{X} & -I_{XY} & I_{YY} & -I_{YZ} \\ -M\bar{Y} & M\bar{X} & 0 & -I_{XZ} & -I_{YZ} & I_{ZZ} \end{bmatrix}_A \begin{Bmatrix} \ddot{X} \\ \ddot{Y} \\ \ddot{Z} \\ \dot{p} \\ \dot{q} \\ \dot{r} \end{Bmatrix}_A \right.$$

$$- \left\{ \begin{bmatrix} 0 & -r & q \\ r & 0 & -p \\ -q & p & 0 \end{bmatrix}_A \begin{bmatrix} 0 & M\bar{Z} & -M\bar{Y} \\ -M\bar{Z} & 0 & M\bar{X} \\ M\bar{Y} & -M\bar{X} & 0 \end{bmatrix}_A \begin{Bmatrix} p \\ q \\ r \end{Bmatrix}_A \right.$$

$$\left. \left. - \begin{bmatrix} 0 & -r & q \\ r & 0 & -p \\ -q & p & 0 \end{bmatrix}_A \begin{bmatrix} I_{XX} & -I_{XY} & -I_{XZ} \\ -I_{XY} & I_{YY} & -I_{YZ} \\ -I_{XZ} & -I_{YZ} & I_{ZZ} \end{bmatrix}_A \begin{Bmatrix} p \\ q \\ r \end{Bmatrix}_A \right\} \right.$$

$$\left. - \left[C_A\right] \begin{Bmatrix} X \\ \dot{Y} \\ \dot{Z} \\ p \\ q \\ r \end{Bmatrix}_A - \left[K_A\right] \begin{Bmatrix} X \\ Y \\ Z \\ \phi \\ \theta \\ \psi \end{Bmatrix}_A \right\} \tag{238}$$

5.4 Overview of Rotor-Blade Model

Many elements of the rotorcraft can be directly modeled following the methods developed in Sections 5 through 5.2 and systematized in Section 5.5. However, there are enough special considerations and concepts involved in modeling the individual blades and combined rotor to justify a separate section to address these topics.

5.4.1 Concept of modes. - The basic textbook principles governing solutions for eigenvalues (natural frequencies) and eigenvectors (mode shapes) for systems of several degrees of freedom can be applied to those of many degrees of freedom. For each independent degree of freedom there is an additional natural frequency and mode shape.

Free vibrations of continuous systems such as beams, or for example the helicopter fuselage, or rotor blades, are generally analyzed mathematically by reducing the system to a system of discrete masses and elastic constraints.

5.4.2 Blade bending - modal variable. - The blade is a twisted rotating beam and its analysis requires considering the coupled flapwise-chordwise-torsional response of the blade. For the REXOR II analysis, coupled flapwise-chordwise mode shapes are used, upon which is superimposed one of a number of torsional response representations of varying complexity (Sections 4.3.4, 5.4.7, 5.6.5, and 5.6.6).

If one applies generalized coordinates, each blade mode in the analysis may be treated as a single degree of freedom. The generalized coordinates are called normal coordinates for the special case when the modes are orthogonal, in which case the generalized mass matrix reduces to a diagonal matrix, as does the generalized stiffness matrix.

The REXOR II analysis uses blade modes calculated for the blade at a fixed rpm, fixed collective, and in an unswept, unconed orientation. Since the program allows for variation of all of these parameters, which is accounted for in the overall REXOR II analysis, the predetermined modes become non-orthogonal as used in the program. Thus, blade motion is effectively described by a set of modal variables, each representing a characteristic frequency, and a set of modal coefficients that describe the relative amplitude of oscillation for each blade segment and each frequency.

Since the modes are nonorthogonal, we will find in REXOR II, as would be expected in such a case, off-diagonal coupling terms in both the generalized mass and stiffness matrices. It can readily be shown in cases

where generalized or normal coordinates are applied, that relatively few modes need be taken to define accurately the time-history of blade deflection. This assumes that the primary frequencies of excitation fall within the range of modes considered.

5.4.3 Blade mode generation. - The blade modes can be determined by any appropriate classical method of analysis for coupled flapwise-inplane bending beams. The only requirements is a cantilever (hinge or hingeless) boundary condition for the modes and that the terms included in the homogenous part of equations 28 and 29 of Reference 5 be accounted for. These equations are repeated here for convenience. Flapwise:

$$\left[(EI_1 \cos^2\beta + EI_2 \sin^2\beta)w'' + (EI_2 - EI_1) \sin\beta \cos\beta \, v''\right]''$$

$$- (Tv')' - \Omega^2 mv + m\ddot{v} = 0 \tag{239}$$

and inplanewise:

$$\left[(EI_2 - EI_1) \sin\beta \cos\beta \, w'' + (EI_1 \sin^2\beta + EI_2 \cos^2\beta)v''\right]''$$

$$- (Tv')' - \Omega^2 mv + m\ddot{v} = 0 \tag{240}$$

5.4.4 Modal coefficients. - Several additional points need to be made regarding modes in order that the equation development be properly understood. First, the same modal coefficients apply to the first and second time derivatives of the function, since

$$\frac{\partial Z_S}{\partial A_i} = f(x) \tag{241}$$

Then

$$\dot{Z}_S = \frac{\partial Z_S}{\partial A_1}\dot{A}_1 + \frac{\partial Z_S}{\partial A_2}\dot{A}_2 + \cdots + \frac{\partial Z_S}{\partial A_n}\dot{A}_n \qquad (241)$$

$$\ddot{Z}_S = \frac{\partial Z_S}{\partial A_1}\ddot{A}_1 + \frac{\partial Z_S}{\partial A_2}\ddot{A}_2 + \cdots + \frac{\partial Z_S}{\partial A_n}\ddot{A}_n \qquad (243)$$

Second, the motion is not necessarily confined to one direction. A given modal frequency may excite or couple with motions in other directions. For example:

$$Y_S = \frac{\partial Y_S}{\partial A_1}A_1 + \frac{\partial Y_S}{\partial A_2}A_2 + \cdots + \frac{\partial Y_S}{\partial A_n}A_n \qquad (244)$$

$$\dot{Y}_S = \frac{\partial Y_S}{\partial A_1}\dot{A}_1 + \frac{\partial Y_S}{\partial A_2}\dot{A}_2 + \cdots + \frac{\partial Y_S}{\partial A_n}\dot{A}_n \qquad (245)$$

$$\ddot{Y}_S = \frac{\partial Y_S}{\partial A_1}\ddot{A}_1 + \frac{\partial Y_S}{\partial A_2}\ddot{A}_2 + \cdots + \frac{\partial Y_S}{\partial A_n}\ddot{A}_n \qquad (246)$$

5.4.5 Independent blades. - In REXOR II the blade motions are computed and tracked individually. One set of equations operates on a blade in BLE coordinates as explained in Section 5.4.11. The result for a time step is stored in BLn coordinates for that blade. The operating set in BLE coordinates then performs the computations for the next blade in turn.

5.4.6 Blade element aerodynamic forces - overview. - The functions F_{X_i}, F_{Y_i}, F_{Z_i}, and moment terms from Section 5.2 are primarily aerodynamic loads for the blade equations. These loads are derived from blade inertial velocity (equivalent to air velocity) and table lookup aerodynamic coefficients as given in Section 6.

5.4.7 Blade torsional response.

5.4.7.1 Pitch horn bending. - Several alternate approaches to modeling blade feathering dynamics exist in REXOR II. One approach is to assume the blade is torsionally rigid, and that the flexibility is in the pitch horn.

5.4.7.2 Quasi-static blade torsion. - The blade pitch horn bending description is improved by the addition of a blade twist dependent on the moment loading. This quasi-static torsion is computed by integrating the blade pitching moment times the torsional flexibility from tip into the root. (Developed in Sections 4.3.4 and 5.6.5.)

5.4.7.3 Dynamic blade torsion. - A third approach to blade torsional response in REXOR is an uncoupled torsional mode which operates as additional blade twist. This material is developed in Section 5.6.

5.4.8 Radial integration. - For each element of a rotor blade the equations of motion are formed per Section 5.2.9. As briefly touched on in Section 5.4.6 these data are formed in BLE axis. These elements are summed to total equations for each blade in BLn coordinate at the blade root. This is explained in Sections 5.6.3 and 5.6.4. These blade root summations are also used in the fuselage axis (Section 5.8).

5.5 Equation System Development

5.5.1 Reference to base operation matrix. - The equation of motion, as developed in Sections 5.2 and 5.3 and as presented in most general form by Equation 236, may be given in abbreviated form as

$$\left\{ \ddot{q}_r \right\}_{CORR} = \left[M_{rk} \right]^{-1} \left\{ F_r \right\}_{EST} \qquad (247)$$

The M_{rk}'s are the generalized mass matrix elements, the F_r's are the generalized forces, and the q_r's the generalized coordinates or degrees of freedom. As explained previously, the F_r's are the complete set of

external forces and internal reactions computed with estimated values of the accelerations, $\ddot{q}_{r_{EST}}$'s, at the next time point. The $\ddot{q}_{r_{CORR}}$'s are then corrections to the estimated values.

The generalized mass, M_{rk}, is developed in Section 5.3. The generalized force may be expanded as (using the point mass form):

$$F_r = -\sum_{i=1}^{N}\left[m_i\left(\ddot{x}_i\frac{\partial X_i}{\partial q_r} + \ddot{Y}_i\frac{\partial Y_i}{\partial q_r} + \ddot{Z}_i\frac{\partial Z_i}{\partial q_r}\right)\right] - \frac{\partial B}{\partial \dot{q}_r} - \frac{\partial U}{\partial q_r}$$

$$+ F_{FR_r} + F_{A_r} + F_{c_r} \qquad (248)$$

The inertia, damping, and elastic terms are developed further in Section 5.3 (see Equation 236). The friction force F_{FR_r}, the aerodynamic external forces F_{A_r}, and the pilot control forces F_{c_r} are described as needed. Note that the potential energy and dissipation terms have been directly included in the force expression. Where the stiffness and damping matrices are simple diagonals, this is done. In the case of the blade equations the distinct stiffness and damping matrix form (Section 5.3) is computed before combining all the applied forces, internal reactions, stiffness and damping terms into an overall force.

5.5.2 Organization by degrees of freedom. - In developing the equations of motion there are three types of ingredients needed:

- Generalized masses
- Generalized forces
- Partial derivatives (used in both of the above items)

The equation development can then proceed with these ingredients along one of two lines of organization.

- For every major rotorcraft piece (fuselage, rotor, etc.), compute all the ingredients and sort according to degree of freedom for equation use.

- For every degree-of-freedom group, sort through the rotorcraft pieces for applicable ingredients. Sorting is minimal because of close association of degrees of freedom and component parts.

The latter development is used here. The degrees of freedom modeled are given in Figure 11.

The following subsections will describe the appropriate partial differentiations, the generalized masses, and the generalized forces in detail. Each generalized mass couples the inertia of one generalized coordinate with another or itself. The algebraic equations for each generalized mass will be given only once. If the reader cannot find a particular mass element under one subsection, he should look into the other subsection relating to the coupled generalized coordinate.

5.5.3 Partial derivatives. - The generalized masses and forces use partial derivatives which describe the variational motion of each physical mass element in rectangular coordinates relative to the motion of each generalized coordinate. The partial derivatives required are determined from the generalized mass and force expressions for distributed masses of Section 5.2. The partial derivatives are easily constructed from the coordinate transformations which have been developed.

In developing the motions of a physical mass element relative to a generalized coordinate, a number of transforms may be used. These can be categorized as either linear or Euler axes transforms which either displace without rotation or rotate without displacement. The overall partial will be the product of partials associated with each of these transforms. The typical form of these partials will now be illustrated.

To obtain the partials, the equations relating the velocities are obtained first. Reviewing Sections 4.4.1 and 4.4.2, the velocity relations of interest are restated. For linear transforms:

$$\begin{Bmatrix} \dot{X} \\ \dot{Y} \\ \dot{Z} \end{Bmatrix}_b = \begin{Bmatrix} \dot{X}_C \\ \dot{Y}_O \\ \dot{Z}_O \end{Bmatrix}_a + \begin{Bmatrix} \dot{X} \\ \dot{Y} \\ \dot{Z} \end{Bmatrix}_a + \begin{bmatrix} 0 & Z_a & -Y_a \\ -Z_a & 0 & X_a \\ Y_a & -X_a & 0 \end{bmatrix} \begin{Bmatrix} p \\ q \\ r \end{Bmatrix}_a \qquad (237)$$

$$\begin{Bmatrix} p \\ q \\ r \end{Bmatrix}_b = \begin{Bmatrix} p \\ q \\ r \end{Bmatrix}_a \tag{238}$$

and for Euler transforms

$$\begin{Bmatrix} \dot{X} \\ \dot{Y} \\ \dot{Z} \end{Bmatrix}_b = \left[T_{a-b}\right] \begin{Bmatrix} \dot{X} \\ \dot{Y} \\ \dot{Z} \end{Bmatrix}_a \tag{239}$$

$$\begin{Bmatrix} p \\ q \\ r \end{Bmatrix}_b = \begin{Bmatrix} 0 \\ 0 \\ \dot{\psi}_b \end{Bmatrix}_a + \left[T_\psi\right] \left\{ \begin{Bmatrix} 0 \\ \dot{\theta}_b \\ 0 \end{Bmatrix}_a + \left[T_\theta\right] \left\{ \begin{Bmatrix} \dot{\phi}_b \\ 0 \\ 0 \end{Bmatrix}_a + \left[T_\phi\right] \begin{Bmatrix} p \\ q \\ r \end{Bmatrix}_a \right\} \right\} \tag{240}$$

The partials of interest are conveniently organized into 3 by 3 matrices. They are for the linear transform:

$$\left[\frac{\partial}{\partial X_{0a}} \begin{Bmatrix} X \\ Y \\ Z \end{Bmatrix}_b \middle| \frac{\partial}{\partial Y_{0a}} \begin{Bmatrix} X \\ Y \\ Z \end{Bmatrix}_b \middle| \frac{\partial}{\partial Z_{0a}} \begin{Bmatrix} X \\ Y \\ Z \end{Bmatrix}_b \right] = \left[I\right] = \begin{bmatrix} 1 & 0 & 0 \\ 0 & 1 & 0 \\ 0 & 0 & 1 \end{bmatrix} \tag{241}$$

$$\left[\frac{\partial}{\partial X_a} \begin{Bmatrix} X \\ Y \\ Z \end{Bmatrix}_b \middle| \frac{\partial}{\partial Y_a} \begin{Bmatrix} X \\ Y \\ Z \end{Bmatrix}_b \middle| \frac{\partial}{\partial Z_a} \begin{Bmatrix} X \\ Y \\ Z \end{Bmatrix}_b \right] = \left[I\right] \tag{242}$$

$$\left[\frac{\partial}{\partial \phi_a} \begin{Bmatrix} X \\ Y \\ Z \end{Bmatrix}_b \middle| \frac{\partial}{\partial \theta_a} \begin{Bmatrix} X \\ Y \\ Z \end{Bmatrix}_b \middle| \frac{\partial}{\partial \psi_a} \begin{Bmatrix} X \\ Y \\ Z \end{Bmatrix}_b \right] = \begin{bmatrix} 0 & Z_a & -Y_a \\ -Z_a & 0 & X_a \\ Y_a & -X_a & 0 \end{bmatrix} \tag{243}$$

$$\left[\frac{\partial}{\partial X_a}\begin{Bmatrix}\phi\\ \theta\\ \psi\end{Bmatrix}_b \;\middle|\; \frac{\partial}{\partial Y_a}\begin{Bmatrix}\phi\\ \theta\\ \psi\end{Bmatrix}_b \;\middle|\; \frac{\partial}{\partial Z_a}\begin{Bmatrix}\phi\\ \theta\\ \psi\end{Bmatrix}_b\right] = [0] \tag{244}$$

$$\left[\frac{\partial}{\partial \phi_a}\begin{Bmatrix}\phi\\ \theta\\ \psi\end{Bmatrix}_b \;\middle|\; \frac{\partial}{\partial \theta_a}\begin{Bmatrix}\phi\\ \theta\\ \psi\end{Bmatrix}_b \;\middle|\; \frac{\partial}{\partial \psi_a}\begin{Bmatrix}\phi\\ \theta\\ \psi\end{Bmatrix}_b\right] = [I] \tag{245}$$

For the Euler angles defined in Section 4.4.2:

$$\left[\frac{\partial}{\partial X_a}\begin{Bmatrix}X\\ Y\\ Z\end{Bmatrix}_b \;\middle|\; \frac{\partial}{\partial Y_a}\begin{Bmatrix}X\\ Y\\ Z\end{Bmatrix}_b \;\middle|\; \frac{\partial}{\partial Z_a}\begin{Bmatrix}X\\ Y\\ Z\end{Bmatrix}_b\right] = [T_{a-b}] \tag{246}$$

$$\left[\frac{\partial}{\partial \phi_a}\begin{Bmatrix}X\\ Y\\ Z\end{Bmatrix}_b \;\middle|\; \frac{\partial}{\partial \theta_a}\begin{Bmatrix}X\\ Y\\ Z\end{Bmatrix}_b \;\middle|\; \frac{\partial}{\partial \psi_a}\begin{Bmatrix}X\\ Y\\ Z\end{Bmatrix}_b\right] = [0] \tag{247}$$

$$\left[\frac{\partial}{\partial X_a}\begin{Bmatrix}\phi\\ \theta\\ \psi\end{Bmatrix}_b \;\middle|\; \frac{\partial}{\partial Y_a}\begin{Bmatrix}\phi\\ \theta\\ \psi\end{Bmatrix}_b \;\middle|\; \frac{\partial}{\partial Z_a}\begin{Bmatrix}\phi\\ \theta\\ \psi\end{Bmatrix}_b\right] = [0] \tag{248}$$

$$\left[\frac{\partial}{\partial \phi_a}\begin{Bmatrix}\phi\\ \theta\\ \psi\end{Bmatrix}_b \;\middle|\; \frac{\partial}{\partial \theta_a}\begin{Bmatrix}\phi\\ \theta\\ \psi\end{Bmatrix}_b \;\middle|\; \frac{\partial}{\partial \psi_a}\begin{Bmatrix}\phi\\ \theta\\ \psi\end{Bmatrix}_b\right] = [T_{a-b}] \tag{249}$$

$$\left[\frac{\partial}{\partial\phi_b}\begin{Bmatrix}\phi\\ \theta\\ \psi\end{Bmatrix}_b \;\middle|\; \frac{\partial}{\partial\theta_b}\begin{Bmatrix}\phi\\ \theta\\ \psi\end{Bmatrix}_b \;\middle|\; \frac{\partial}{\partial\psi_b}\begin{Bmatrix}\phi\\ \theta\\ \psi\end{Bmatrix}_b\right] = \begin{bmatrix}\cos\psi\cos\theta & \sin\psi & 0\\ -\sin\psi\cos\theta & \cos\psi & 0\\ 0 & 0 & 1\end{bmatrix} \quad (250)$$

For Euler angles defined in reversed order or reversed sign the last matrix will differ. Note by inspection that rotary to linear derivatives such as $\frac{\partial\theta}{\partial x}$ are all zero. The derivatives can be strung together to get motion in a third axis c relative to motion in axis a. Abbreviating the matrices:

$$\left[\frac{\partial r_c}{\partial\zeta_a}\right] = \left[\frac{\partial r_c}{\partial r_b}\right]\left[\frac{\partial r_b}{\partial\zeta_a}\right] + \left[\frac{\partial r_c}{\partial\zeta_b}\right]\left[\frac{\partial\zeta_b}{\partial\zeta_a}\right] \quad (251)$$

$$\left[\frac{\partial r_c}{\partial r_a}\right] = \left[\frac{\partial r_c}{\partial r_b}\right]\left[\frac{\partial r_b}{\partial r_a}\right] \quad (252)$$

$$\left[\frac{\partial\zeta_c}{\partial r_a}\right] = 0 \quad (253)$$

$$\left[\frac{\partial\zeta_c}{\partial\zeta_a}\right] = \left[\frac{\partial\zeta_c}{\partial\zeta_b}\right]\left[\frac{\partial\zeta_b}{\partial\zeta_a}\right] \quad (254)$$

assuming in general

$$r_b = r_b(r_a, \zeta_a) \quad (255)$$

and

$$\zeta_c = \zeta_c(r_b, \zeta_b) \quad (256)$$

The abbreviations used are

$$r = \{X, Y, Z\} \tag{257}$$

and

$$\zeta = \{\phi, \theta, \psi\} \tag{258}$$

Transformations may involve linear and rotational operations. Partial derivatives showing the combined operations may be generated using a linear transform from set a to b, followed by a rotation from b to c. This sequence gives:

$$\left[\frac{\partial r_c}{\partial \zeta_a}\right] = \left[T_{a-c}\right] \begin{bmatrix} 0 & Z_a & -Y_a \\ -Z_a & 0 & X_a \\ Y_a & -X_a & 0 \end{bmatrix} \tag{259}$$

$$\left[\frac{\partial r_c}{\partial r_a}\right] = \left[T_{a-c}\right] \tag{260}$$

$$\left[\frac{\partial \zeta_c}{\partial r_a}\right] = 0 \tag{261}$$

$$\left[\frac{\partial \zeta_c}{\partial \zeta_a}\right] = \left[T_{a-c}\right] \tag{262}$$

5.5.4 Generalized masses. - As discussed before, the helicopter is assumed to consist of a finite number of mass elements. They are the

- fuselage
- tail rotor
- engine rotor
- swashplate
- fixed hub (all parts that do not feather)
- k mass elements on each of b blades.

The reader should realize the mass matrix is symmetric from the definition of Equation (209) and interchange of the order of differentiation.

$$M_{kr} = M_{rk} \tag{263}$$

Only the elements in the diagonal and the upper right triangle will be given in the following sections.

Each of these mass elements must be summed for each of the generalized mass matrix elements. Each mass is handled with the distributed mass M_{rk} relation of Section 5.2. Fortunately, only the fuselage requires the full equation. The center-of-gravity terms drop out if the mass motion is determined at the center of gravity. This situation is true for the blade line which passes through the center of gravity of the blade section mass elements. Only the fuselage, the swashplate and the shaft/transmission have reference axis origin off the center of gravity. Another simplification is that cross products of inertia exist only for the fuselage and the shaft/transmission. Each blade mass element is considered to be in the shape of a rod lying along the chord at the blade station in question.

Certain small terms and factors are dropped from the generalized masses. As discussed in Section 5.3, the equations of motion are solved for small incremental corrections to the accelerations. With this formulation the masses can tolerate approximations as contrasted to the generalized forces.

5.5.5 Generalized forces. - The equation formulation, Section 5.3, requires that precision be used in compiling the generalized forces per Equation 247, expanded per Section 5.3, Equation 236, to include rigid body distributed mass elements. This formulation includes for each degree of freedom:

- Summation over all mass elements of the mass times inertial acceleration times partial derivative. (Section 5.3 expression for distributed masses.)
- External (aerodynamic) loadings times a partial derivative.
- Potential energy and damping terms or assembled stiffness and damping terms with partial derivatives (Section 5.3).

For some degrees of freedom the applicable mass elements and the total integration are directly written as final results which can be verified by inspection. Degrees of freedom that properly include summation over the main rotor blades involve some extensive numerical integrations and complicated coordinate transformations.

5.6 Blade Bending and Torsion Equations

5.6.1 Blade radial summation. - The contribution from all the individual blade sections are summed to give the blade generalized masses and forces. These are given for blade root, bending, feathering, and torsion motions. The blade root values are then transformed to the final degree of freedom variables by partial derivatives. The summation is carried out over all elements of the rotorcraft, including the independent blades. Due to the relative isolation of one blade's modes from another, only the 4 by 4 submass matrices along the diagonal of the 4b by 4b rotor matrix are filled, where b is the number of blades.

5.6.2 Partial derivatives. - The generalized masses and forces utilize partials relating the X, Y, Z, ϕ, θ, and ψ linear and rotary motion of each blade element to the blade bending, blade torsion, body, rotor, and swashplate degrees of freedom. Only the blade bending, torsion, and feathering partials are derived in this section; the blade partials for other degrees of freedom are to be found in their respective sections.

As developed in Section 4.3.4, the blade torsion may be modeled either as a pitch horn bending or an uncoupled dynamic torsion mode. For the former case the partial $\frac{\partial \phi_{Fn}}{\partial \beta_{PHn}}$ is a blade spanwise constant multiplier to summations which couple in the feather angle. In the latter case, $\frac{\partial \phi_{BLE}}{\partial \beta_{PHn}}$ is a function of span and blade number.

The first partials to be considered are those relating motions at any point i on the blade to the rigid body motion of the blade root. These partials are:

$$\left[\frac{\partial\left(r_{BLE}\right)_{BLn}}{\partial r_{OBLn}}\right] = \begin{bmatrix} \frac{\partial\left(X_{BLE}\right)_{BLn}}{\partial X_{OBLn}} & \frac{\partial\left(X_{BLE}\right)_{BLn}}{\partial Y_{OBLn}} & \frac{\partial\left(X_{BLE}\right)_{BLn}}{\partial Z_{OBLn}} \\ \frac{\partial\left(Y_{BLE}\right)_{BLn}}{\partial X_{OBLn}} & \frac{\partial\left(Y_{BLE}\right)_{BLn}}{\partial Y_{OBLn}} & \frac{\partial\left(Y_{BLE}\right)_{BLn}}{\partial Z_{OBLn}} \\ \frac{\partial\left(Z_{BLE}\right)_{BLn}}{\partial X_{OBLn}} & \frac{\partial\left(Z_{BLE}\right)_{BLn}}{\partial Y_{OBLn}} & \frac{\partial\left(Z_{BLE}\right)_{BLn}}{\partial Z_{OBLn}} \end{bmatrix} = \left[I \right] \qquad (264)$$

$$\left[\frac{\partial\left(r_{BLE}\right)_{BLn}}{\partial\zeta_{BLn}}\right] = \begin{bmatrix} \frac{\partial\left(X_{BLE}\right)_{BLn}}{\partial\phi_{BLn}} & \frac{\partial\left(X_{BLE}\right)_{BLn}}{\partial\theta_{BLn}} & \frac{\partial\left(X_{BLE}\right)_{BLn}}{\partial\psi_{BLn}} \\ \frac{\partial\left(Y_{BLE}\right)_{BLn}}{\partial\phi_{BLn}} & \frac{\partial\left(Y_{BLE}\right)_{BLn}}{\partial\theta_{BLn}} & \frac{\partial\left(Y_{BLE}\right)_{BLn}}{\partial\psi_{BLn}} \\ \frac{\partial\left(Z_{BLE}\right)_{BLn}}{\partial\phi_{BLn}} & \frac{\partial\left(Z_{BLE}\right)_{BLn}}{\partial\theta_{BLn}} & \frac{\partial\left(Z_{BLE}\right)_{BLn}}{\partial\psi_{BLn}} \end{bmatrix} = \begin{bmatrix} 0 & Z_{BLE} & -Y_{BLE} \\ -Z_{BLE} & 0 & X_{BLE} \\ Y_{BLE} & -X_{BLE} & 0 \end{bmatrix} \tag{265}$$

$$\left[\frac{\partial\zeta_{BLE}}{\partial\zeta_{BLn}}\right] = \begin{bmatrix} \frac{\partial\left(\phi_{BLE}\right)_{BLE}}{\partial\phi_{BLn}} & \frac{\partial\left(\phi_{BLE}\right)_{BLE}}{\partial\theta_{BLn}} & \frac{\partial\left(\phi_{BLE}\right)_{BLE}}{\partial\psi_{BLn}} \\ \frac{\partial\left(\theta_{BLE}\right)_{BLE}}{\partial\phi_{BLn}} & \frac{\partial\left(\theta_{BLE}\right)_{BLE}}{\partial\theta_{BLn}} & \frac{\partial\left(\theta_{BLE}\right)_{BLE}}{\partial\psi_{BLn}} \\ \frac{\partial\left(\psi_{BLE}\right)_{BLE}}{\partial\phi_{BLn}} & \frac{\partial\left(\psi_{BLE}\right)_{BLE}}{\partial\theta_{BLn}} & \frac{\partial\left(\psi_{BLE}\right)_{BLE}}{\partial\psi_{BLn}} \end{bmatrix} = \left[T_{BLn-BLE}\right] \tag{266}$$

Note that X_{BLE}, Y_{BLE} and Z_{BLE} are expressed in blade root coordinates; while ϕ_{BLE}, θ_{BLE} and ψ_{BLE} are in terms of blade element axes aligned with the blade element principal axes.

Next consider the blade Y and Z bending response with respect to the blade bending modes. A number of equations can be used to develop the required expressions. The velocity equations from Section 4.5.5 are selected for ease of analysis. Using cancellation of the dots (Section 5.2):

$$\left(\frac{\partial\dot{Y}(i)_{BLE}}{\partial\dot{A}_{mn}}\right)_{BLn} = \left(\frac{\partial Y(i)_{BLE}}{\partial A_{mn}}\right)_{BLn} \tag{267}$$

$$\left(\frac{\partial \dot{Z}(i)_{BLE}}{\partial \dot{A}_{mn}}\right)_{BLn} = \left(\frac{\partial Z(i)_{BLE}}{\partial A_{mn}}\right)_{BLn} \tag{268}$$

gives:

$$\begin{Bmatrix} 0 \\ \frac{\partial Y_{BLE}}{\partial A_{mn}} \\ \frac{\partial Z_{BLE}}{\partial A_{mn}} \end{Bmatrix}_{BLn} = \left[\frac{\partial Z'_{FA}}{\partial A_m}\left[\left[\dot{T}_{Z'_{FA}}\right]^T \left[T_{Y'_{FA}}\right]^T \left[T_{\Delta\phi_F}\right]^T \left[T_{Y'_{FA}}\right] \left[T_{Z'_{FA}}\right] + \left[T_{Z'_{FA}}\right]^T \left[T_{Y'_{FA}}\right]^T \left[T_{\Delta\phi_f}\right]^T \left[T_{Y'_{FA}}\right] \left[\dot{T}_{Z'_{FA}}\right]\right]\right.$$

$$+ \frac{\partial Y'_{FA}}{\partial A_m}\left[\left[T_{Z'_{FA}}\right]^T \left[\dot{T}_{Y'_{FA}}\right]^T \left[T_{\Delta\phi_F}\right]^T \left[T_{Y'_{FA}}\right] \left[T_{Z'_{FA}}\right] + \left[T_{Z'_{FA}}\right]^T \left[T_{Y'_{FA}}\right]^T \left[T_{\Delta\phi_f}\right]^T \left[\dot{T}_{Y'_{FA}}\right] \left[T_{Z'_{FA}}\right]\right]$$

$$\left. + \frac{\partial \phi_{Fn}}{\partial A_m}\left[\left[T_{Z'_{FA}}\right]^T \left[T_{Y'_{FA}}\right]^T \left[\dot{T}_{\Delta\phi_F}\right]^T \left[T_{Y'_{FA}}\right] \left[T_{Z'_{FA}}\right]\right]\right]$$

$$\cdot \left\{\left[\frac{\partial r_{BLE}}{\partial A_{mn}}\right] \left\{A_{mn}\right\} + \left\{r_{s_{BLE}}\right\}\right\}$$

$$+ \left[T_{Z'_{FA}}\right]^T \left[T_{Y'_{FA}}\right]^T \left[T_{\Delta\phi_F}\right]^T \left[T_{Y'_{FA}}\right] \left[T_{Z'_{FA}}\right] \left\{\left\{\frac{\partial r_{BLE}}{\partial A_{mn}}\right\} - \left\{\frac{\partial r_{IB}}{\partial A_{mn}}\right\}\right\} + \left\{\frac{\partial r_{IB}}{\partial A_{mn}}\right\} \tag{269}$$

where

$$\left\{ r_{S_{BLE}} \right\} = \left[T_{\beta_{FA}} \right]^T \left[T_{\phi_{REF}} \right]^T \left[T_{\beta_{FA}} \right] \left\{ \left[\left[T_{\tau_Q} \right]^T \left[T_\gamma \right]^T \right. \right.$$
$$\cdot \left\{ \left[\left[T_{\beta_Q} \right]^T \left\{ \left[\left[T_{\phi_T} \right]^T \left\{ r_{CG_{BLE}} \right\} - \left[\left[T_{\phi_{TW}} \right]^T - \left[T_{\phi_T} \right]^T \right] \left\{ r_{sc} \right\} \right\} \right. \right. \right.$$
$$\left. \left. - \left[T_{\beta_Q} \right]^T \left\{ r_{SW} \right\} \right\} + \left\{ \left[T_{\beta_Q} \right]^T \left\{ r_{SW} \right\} + \left\{ r_{jog} \right\} \right.$$
$$\left. \left. \left. - \left[T_{\beta_Q} \right]^T \left\{ r_p \right\} \right] \right] + \left\{ \left[T_{\beta_Q} \right]^T \left\{ r_p \right\} - \left\{ r_{IB} \right\} \right\} \qquad (270)$$

$\frac{\partial \phi_F}{\partial A_1}$, $\frac{\partial \phi_F}{\partial A_2}$, and $\frac{\partial \phi_F}{\partial A_3}$ are input data.

The angular derivatives with respect to the blade bending modes are also constructed in the velocity form.

$$\left\{ \begin{matrix} \frac{\partial p}{\partial \dot{A}_{mn}} \\ \frac{\partial q}{\partial \dot{A}_{mn}} \\ \frac{\partial r}{\partial \dot{A}_{mn}} \end{matrix} \right\}_{BLE} = \left\{ \begin{matrix} \frac{\partial \phi_{BLE}}{\partial A_{mn}} \\ \frac{\partial \theta_{BLE}}{\partial A_{mn}} \\ \frac{\partial \psi_{BLE}}{\partial A_{mn}} \end{matrix} \right\}_{BLE} \qquad (271)$$

Note that the angular derivatives, being applied to local segments, are presented in BLE axis. Referring to Equation 132:

$$\left\{\begin{matrix} \frac{\partial \phi_{BLE}}{\partial A_{mn}} \\ \frac{\partial \theta_{BLE}}{\partial A_{mn}} \\ \frac{\partial \psi_{BLE}}{\partial A_{mn}} \end{matrix}\right\}_{BLE} = \left[T_{\phi_T}\right]\left[T_{\beta_0}\right]\left[T_Y\right]\left[T_{\tau_0}\right]\left[T_{\beta_{FA}}\right]^T\left[T_{\phi_{REF}}\right]\left[T_{\beta_{FA}}\right]$$

$$\cdot\left\{\left\{\begin{matrix} 0 \\ 0 \\ \frac{\partial Y'_{BEND}}{\partial A_{mn}} \end{matrix}\right\} + \left[T_{Y'_{BEND}}\right]\left\{\left\{\begin{matrix} 0 \\ \frac{-\partial Z'_{BEND}}{\partial A_{mn}} \\ 0 \end{matrix}\right\} + \left[T_{Z'_{BEND}}\right]\left[T_{Z'_{FA}}\right]\left[T_{Y'_{FA}}\right]\left\{\left\{\begin{matrix} \frac{\partial \phi_{Fn}}{\partial A_{mn}} \\ 0 \\ 0 \end{matrix}\right\}\right\}\right\} \quad (272)$$

From:

$$\left\{\begin{matrix} Y'_{BEND} \\ Z'_{BEND} \end{matrix}\right\} = \left[\begin{matrix} Y'_1 & Y'_2 & Y'_3 \\ Z'_1 & Z'_2 & Z'_3 \end{matrix}\right]\left\{\begin{matrix} A_{1n} \\ A_{2n} \\ A_{3n} \end{matrix}\right\} \quad (273)$$

Gives:

$$\left\{\begin{matrix} \frac{\partial Y'_{BEND}}{\partial A_{mn}} \\ \frac{\partial Z'_{BEND}}{\partial A_{mn}} \end{matrix}\right\} = \left\{\begin{matrix} Y'_m \\ Z'_m \end{matrix}\right\} \quad (274)$$

Also note that in the same context and argument of Section 4.5.5 the feathering axis slopes, Y'_{FA} and Z'_{FA} have been neglected in the above angular partials.

Derivatives with respect to the blade feathering are also constructed using cancellation of the dots.

$$\left\{ \begin{array}{c} \dfrac{\partial Y_{BLE}}{\partial \phi_{Fn}} \\ \\ \dfrac{\partial Z_{BLE}}{\partial \phi_{Fn}} \end{array} \right\} = \left\{ \begin{array}{c} \dfrac{\partial \dot{Y}_{BLE}}{\partial \dot{\phi}_{Fn}} \\ \\ \dfrac{\partial \dot{Z}_{BLE}}{\partial \dot{\phi}_{Fn}} \end{array} \right\} \tag{275}$$

gives:

$$\left\{ \begin{array}{c} 0 \\ \\ \dfrac{\partial Y_{BLE}}{\partial \phi_{Fn}} \\ \\ \dfrac{\partial Z_{BLE}}{\partial \phi_{Fn}} \end{array} \right\}_{BLn} = \left[T_{Z'FA} \right]^T \left[T_{Y'FA} \right]^T \left[\dot{T}_{\Delta\phi_F} \right]^T \left[T_{Y'FA} \right] \left[T_{Z'FA} \right] \cdot \left\{ \left[\frac{\partial r_{BLE}}{\partial A_{mn}} \right] \left\{ A_{mn} \right\} + \left\{ r_{S_{BLE}} \right\} + \left\{ r_{IB} \right\} \right\} \tag{276}$$

Similarly, for angular motion:

$$\begin{Bmatrix} \frac{\partial \phi_{BLE}}{\partial \phi_{Fn}} \\ \frac{\partial \theta_{BLE}}{\partial \phi_{Fn}} \\ \frac{\partial \psi_{BLE}}{\partial \phi_{Fn}} \end{Bmatrix}_{BLE} = \left[T_{\phi_T}\right]\left[T_{\beta_0}\right]\left[T_\gamma\right]\left[T_{\tau_0}\right]\left[T_{\beta_{FA}}\right]^T\left[T_{\phi_{REF}}\right]\left[T_{\beta_{FA}}\right]$$

$$\cdot \left[T_{Y'_{BEND}}\right]\left[T_{Z'_{BEND}}\right]\left[T_{Z'}\right]^T\left[T_{Y'_{FA}}\right]^T \begin{Bmatrix} 1 \\ 0 \\ 0 \end{Bmatrix}$$

$$\cong \begin{Bmatrix} 1 \\ 0 \\ 0 \end{Bmatrix} \text{ (as programmed)} \tag{277}$$

The partials developed with respect to ϕ_{Fn} are used directly in swashplate and rotor summations as well as some of the following mass and force terms. Some terms require a further compounding derivative, $\frac{\partial \phi_{Fn}}{\partial \beta_{PHn}}$, for the case of the pitch horn bending torsion option. Taking the deg ee of freedom to be pitch horn angular deflection about the feather axis, the constant is approximately 1/e. For the dynamic torsion option a different set of mass formulations is used in terms of BLE axis, obviating the need for the compounded derivative. As indicated in Section 4.5.5, expressions inboard of X_{SW} equal expressions outboard of X_{SW} with

$$\left[T_\gamma\right]\left[T_{\tau_0}\right] = \left[I\right] \tag{278}$$

and

$$\left\{r_{SW}\right\} = \left\{r_{jog}\right\} = \left\{ 0 \right\} \tag{279}$$

Blade X motions must now be accounted for. The assumption of the neutral axis as the axis of no stretch is discussed in Section 4.5.5 and the derivation of the X motions shown. The equation for the partials in BLn axis for a point on the neutral axis is taken from the formulation for the X velocities:

$$\left(\frac{\partial X(i)_{NA}}{\partial A_{mn}}\right)_{BLn} = \sum_{i=2}^{k} \left(\frac{-\left(Y(i)_{NA} - Y(i-1)_{NA}\right)\left(\frac{\partial Y(i)_{NA}}{\partial A_{mn}} - \frac{\partial Y(i-1)_{NA}}{\partial A_{mn}}\right)}{X(i)_{NA} - X(i-1)_{NA}} \right.$$

$$\left. \frac{-\left(Z(i)_{NA} - Z(i-1)_{NA}\right)\left(\frac{\partial Z(i)_{NA}}{\partial A_{mn}} - \frac{\partial Z(i-1)_{NA}}{\partial A_{mn}}\right)}{X(i)_{NA} - X(i-1)_{NA}} \right)_{BLn}$$

and

$$\left(\frac{\partial X(i)_{NA}}{\partial A_{mn}}\right)_{Bln} = 0 \qquad (\quad)$$

The program data, however, is at the blade center-of-gravity axis. The transfer is:

$$\begin{Bmatrix} \frac{\Delta\partial X(i)_{NA}}{\partial A_{mn}} \\ \frac{\partial Y(i)_{NA}}{\partial A_{mn}} \\ \frac{\partial Z(i)_{NA}}{\partial A_{mn}} \end{Bmatrix}_{BLn} = \begin{Bmatrix} 0 \\ \frac{\partial Y(i)_{BLE}}{\partial A_{mn}} \\ \frac{\partial Z(i)_{BLE}}{\partial A_{mn}} \end{Bmatrix}_{BLn} + \left[T_{BLn-BLE}\right]^{T} \begin{Bmatrix} \left(-\frac{\partial \psi_{BLE}}{\partial A_{mn}}\right) Y(i)_{ONA} \\ 0 \\ \left(\frac{\partial \phi_{BLE}}{\partial A_{mn}}\right) Y(i)_{ONA} \end{Bmatrix} \qquad (281)$$

where the right-hand side elements are from Section 4.5.5 and the previous development of this section. The distance $Y(i)_{ONA} = Y(i)_{NA} - Y(i)_{CG\ BLE}$ is the distance the neutral axis is from the center-of-gravity axis, positive forward. The partials $\frac{\partial Y(i)_{NA}}{\partial A_{mn}}$ and $\frac{\partial Z(i)_{NA}}{\partial A_{mn}}$ are used in the preceding equation for $\frac{\partial X(i)_{NA}}{\partial A_{mn}}$. $\frac{\Delta\partial X(i)_{NA}}{\partial A_{mn}}$ is then the difference in X motions between the reference and the neutral axis, and is subtracted from the neutral axis motions:

$$\left(\frac{\partial X(i)_{BLE}}{\partial A_{mn}}\right)_{BLn} = \left(\frac{\partial X(i)_{NA}}{\partial A_{mn}}\right)_{BLn} - \left(\Delta\frac{\partial X(i)_{NA}}{\partial A_{mn}}\right)_{BLn} \tag{282}$$

to obtain a center-of-gravity value.

The spanwise variation of X with feathering, $\frac{\partial X(i)_{BLE}}{\partial \phi_{Fn}}$, can be derived in a manner similar to $\frac{\partial X(i)_{BLE}}{\partial A_{mn}}$. The formulations are:

$$\left(\frac{\partial X(i)_{BLE}}{\partial \phi_{Fn}}\right)_{BLn} = \left(\frac{\partial X(i)_{NA}}{\partial \phi_{Fn}}\right)_{BLn} - \left(\Delta\frac{\partial X(i)_{NA}}{\partial \phi_{Fn}}\right)_{BLn} \tag{283}$$

where

$$\begin{Bmatrix} \frac{\Delta\partial X(i)_{NA}}{\partial \phi_{Fn}} \\ \frac{\partial Y(i)_{NA}}{\partial \phi_{Fn}} \\ \frac{\partial Z(i)_{NA}}{\partial \phi_{Fn}} \end{Bmatrix}_{BLn} = \begin{Bmatrix} 0 \\ \frac{\partial Y(i)_{BLE}}{\partial \phi_{Fn}} \\ \frac{\partial Z(i)_{BLE}}{\partial \phi_{Fn}} \end{Bmatrix} + \left[T_{BLn-BLE}\right] \begin{Bmatrix} \left(-\frac{\partial \psi_{BLE}}{\partial \phi_{Fn}}\right) Y(i)_{ONA} \\ 0 \\ \left(\frac{\partial \phi_{BLE}}{\partial \phi_{Fn}}\right) Y(i)_{ONA} \end{Bmatrix} \tag{284}$$

and

$$\left(\frac{\partial X(i)_{NA}}{\partial \phi_{Fn}}\right)_{BLn} = \sum_{i=2}^{k} \left(\frac{-\left(Y(i)_{NA} - Y(i-1)_{NA}\right)\left(\frac{\partial Y(i)_{NA}}{\partial \phi_{Fn}} - \frac{\partial Y(i-1)_{NA}}{\partial \phi_{Fn}}\right)}{X(i)_{NA} - X(i-1)_{NA}} \right.$$

$$\left. \frac{-\left(Z(i)_{NA} - Z(i-1)_{NA}\right)\left(\frac{\partial Z(i)_{NA}}{\partial \phi_{Fn}} - \frac{\partial Z(i-1)_{NA}}{\partial \phi_{Fn}}\right)}{X(i)_{NA} - X(i-1)_{NA}} \right)_{BLn}$$

$$\left(\frac{\partial X(1)_{NA}}{\partial \phi_{Fn}}\right)_{BLn} = 0 \qquad (285)$$

The program assumes $\left(\frac{\partial X_{BLE}}{\partial \phi_{Fn}}\right)_{BLn}$ to be zero for generalized mass calculations. This is done because of the latitude possible in the generalized masses and the second order nature of the term. In contrast, the derivative $\left(\frac{\partial X_{BLE}}{\partial \phi_{Fn}}\right)_{BLn}$ is retained. The partial $\left(\frac{\partial \phi_{BLE}}{\partial \phi_{Fn}}\right)$ is set to unity for the generalized mass terms. The full equations are used for all these terms in determining the generalized forces.

A simple partial derivative is also needed when β_{PHn} is defined as dynamic torsion. Since torsion occurs along the bent and twisted blade line, in blade element axis BLE, only the vertical or normal to chord motion of the shear center is of interest, hence,

$$\left(\frac{\partial Z(i)_{BLE}}{\partial \beta_{PHn}}\right)_{BLn} = \left(\frac{\partial Z(i)_{BLE,BLn}}{\partial Z(i)_{BLE}} \frac{\partial Z(i)_{BLE}}{\partial \phi_{BLE}} \frac{\partial \phi_{BLE}}{\partial \beta_{PHn}}\right) =$$

$$\left[T_{BLE - BLn}\right] \left(Y(i)_{SC} - Y(i)_{CG}\right)_{BLE} \frac{\partial \phi_{BLE}}{\partial \beta_{PHn}} \tag{286}$$

$\frac{\partial \phi_{BLE}}{\partial \beta_{PHn}}$ is program input for the torsion mode shape.

Use is made of a blade mode to blade feathering partial derivative array to produce a compact development. This array is simply by definition:

$$\left\{\frac{\partial \tau_{BL}}{\partial \phi_{Fn}}\right\} = \left[\begin{array}{c:c} [0] & \begin{matrix}0\\0\\0\end{matrix} \\ \hdashline \begin{matrix}0 & 0 & 0\end{matrix} & 1 \end{array}\right] \tag{287}$$

where $\left|\tau_{BL}\right| = \left|A_{1n}, A_{2n}, A_{3n}, \phi_{Fn}\right|$.

Additional partial sets which are used to expedite the mass and force expression development are:

$$\left\{\frac{\partial \tau_{O_{BLn}}}{\partial \tau_R}\right\} = \left[\begin{array}{c:c} \left[T_{R-BLn}\right] & [0] \\ \hdashline [0] & \left[T_{R-BLn}\right] \end{array}\right] \tag{288}$$

$$\left\{\frac{\partial \tau_{O_R}}{\partial \tau_H}\right\} = \left[\begin{array}{c:c} \left[T_{H-R}\right] & [0] \\ \hdashline [0] & \left[T_{H-R}\right] \end{array}\right] \tag{289}$$

5.6.3 Generalized masses. - The blade generalized masses in conjunction with partial derivatives couple blade feathering, blade torsion, blade bending, fuselage motions. All the blade generalized masses that assumed to exist are given in the following table. As mentioned before, $\frac{\partial X_{BLE}}{\partial \phi_{Fn}}$ is assumed zero and $\frac{\partial \phi_{BLE}}{\partial \phi_{Fn}}$ is assumed one in the program, although it is given in the table. The blade has a rotary inertia about the center of gravity axis $I_{XX_{BLE}}$. The blade also has inertia $I_{ZZ_{BLE}}$ about a vertical axis.

Table 1 lists all the terms coupling rotary motion at the blade root, $M_{\phi_{BLn}\ \phi_{BLn}}$ and similar terms. However, not all listed are used, as certain approximations are made in developing the principal axis generalized masses which reduce the number of blade coupling generalized masses needed. Since the mass matrix operates on the acceleration error term rather than the total acceleration, these approximations do not detract from the validity of the results produced.

TABLE I. - BLADE GENERALIZED MASSES

Blade Root Coupling

$$M_{Y_{OBLn}\psi_{BLn}} = -M_{Z_{OBLn}\theta_{BLn}} = m_{BLn}X_{CG_{BLn}} = \sum_{i=1}^{k}\left(X_{BLE}(i)\right)_{BLn}\left(m(i)\right) \tag{290}$$

$$M_{Z_{OBLn}\phi_{BLn}} = -M_{X_{OBLn}\psi_{BLn}} = m_{BLn}Y_{CG_{BLn}} = \sum_{i=1}^{k}\left(Y_{BLE}(i)\right)_{BLn}\left(m(i)\right) \tag{291}$$

$$M_{X_{OBLn}\theta_{BLn}} = -M_{Y_{CBLn}\phi_{BLn}} = m_{BLn}Z_{CG_{BLn}} = \sum_{i=1}^{k}\left(Z_{BLE}(i)\right)_{BLn}\left(m(i)\right) \tag{292}$$

$$M_{X_{OBLn}X_{OBLn}} = M_{Y_{OBLn}Y_{OBLn}} = M_{Z_{OBLn}Z_{OBLn}} = m_{BLn} = \sum_{i=1}^{k} m(i) \tag{293}$$

Feather Coupling

$$M_{X_{OBLn}\phi_{Fn}} = \sum_{i=1}^{k} m(i)\left(\frac{\partial X_{BLE}}{\partial \phi_{Fn}}\right)_{BLn} \tag{294}$$

$$M_{Y_{OBLn}\phi_{Fn}} = \sum_{i=1}^{k} m(i)\left(\frac{\partial Y_{BLE}}{\partial \phi_{Fn}}\right)_{BLn} \tag{295}$$

$$M_{Z_{OBLn}\phi_{Fn}} = \sum_{i=1}^{k} m(i)\left(\frac{\partial Z_{BLE}}{\partial \phi_{Fn}}\right)_{BLn} \tag{296}$$

$$M_{\phi_{BLn}\phi_{Fn}} = \sum_{i=1}^{k}\left[m(i)\left(\frac{\partial Y_{BLE}}{\partial \phi_{BLn}}\frac{\partial Y_{BLE}}{\partial \phi_{Fn}} + \frac{\partial Z_{BLE}}{\partial \phi_{BLn}}\frac{\partial Z_{BLE}}{\partial \phi_{Fn}}\right) + I_{XX_{BLE}}(i)\left(\frac{\partial \phi_{BLE}}{\partial \phi_{BLn}}\frac{\partial \phi_{BLE}}{\partial \phi_{Fn}}\right)\right]_{BLn} \tag{297}$$

TABLE 1. - Continued

Feather Coupling (Continued)

$$M_{\theta_{BLn}\phi_{Fn}} = \sum_{i=1}^{k}\left[m(i)\left(\frac{\partial Y_{BLE}}{\partial\theta_{BLn}}\frac{\partial Y_{BLE}}{\partial\phi_{Fn}} + \frac{\partial Z_{BLE}}{\partial\theta_{BLn}}\frac{\partial Z_{BLE}}{\partial\phi_{Fn}}\right) + I_{XX_{BLE}}^{(i)}\left(\frac{\partial\phi_{BLE}}{\partial\theta_{BLn}}\frac{\partial\phi_{BLE}}{\partial\phi_{Fn}}\right)\right]_{BLn} \quad (298)$$

$$M_{\psi_{BLn}\phi_{Fn}} = \sum_{i=1}^{k}\left[m(i)\left(\frac{\partial Y_{BLE}}{\partial\psi_{BLn}}\frac{\partial Y_{BLE}}{\partial\phi_{Fn}} + \frac{\partial Z_{BLE}}{\partial\psi_{BLn}}\frac{\partial Z_{BLE}}{\partial\phi_{Fn}}\right) + I_{XX_{BLE}}^{(i)}\left(\frac{\partial\phi_{BLE}}{\partial\psi_{BLn}}\frac{\partial\phi_{BLE}}{\partial\phi_{Fn}}\right)\right]_{BLn} \quad (299)$$

$$M_{\phi_{Fn}\phi_{Fn}} = \sum_{i=1}^{k}\left[m(i)\left(\left(\frac{\partial X_{BLE}}{\partial\phi_{Fn}}\right)^2 + \left(\frac{\partial Y_{BLE}}{\partial\phi_{Fn}}\right)^2 + \left(\frac{\partial Z_{BLE}}{\partial\phi_{Fn}}\right)^2\right) + I_{XX_{BLE}}^{(i)}\left(\frac{\partial\phi_{BLE}}{\partial\phi_{Fn}}\frac{\partial\phi_{BLE}}{\partial\phi_{Fn}}\right)\right]_{BLn} \quad (300)$$

$$M_{A_{mn}\phi_{Fn}} = \sum_{i=1}^{k}\left[m(i)\left(\frac{\partial X_{BLE}}{\partial A_{mn}}\frac{\partial X_{BLE}}{\partial\phi_{Fn}} + \frac{\partial Y_{BLE}}{\partial A_{mn}}\frac{\partial Y_{BLE}}{\partial\phi_{Fn}} + \frac{\partial Z_{BLE}}{\partial A_{mn}}\frac{\partial Z_{BLE}}{\partial\phi_{Fn}}\right) + I_{XX_{BLE}}^{(i)}\left(\frac{\partial\phi_{BLE}}{\partial A_{mn}}\frac{\partial\phi_{BLE}}{\partial\phi_{Fn}}\right)\right]_{BLn} \quad (301)$$

TABLE 1. - Continued

Blade Bending Coupling

$$M_{X_{OBLn}A_{mn}} = \sum_{i=1}^{k} m(i)\left(\frac{\partial X_{BLE}}{\partial A_{mn}}\right)_{BLn} \tag{302}$$

$$M_{Y_{OBLn}A_{mn}} = \sum_{i=1}^{k} m(i)\left(\frac{\partial Y_{BLE}}{\partial A_{mn}}\right)_{BLn} \tag{303}$$

$$M_{Z_{OBLn}A_{mn}} = \sum_{i=1}^{k} m(i)\left(\frac{\partial Z_{BLE}}{\partial A_{mn}}\right)_{BLn} \tag{304}$$

$$M_{\psi_{BLn}A_{mn}} = \sum_{i=1}^{k}\left[m(i)\left(\frac{\partial X_{BLE}}{\partial \psi_{BLn}}\frac{\partial X_{BLE}}{\partial A_{mn}} + \frac{\partial Y_{BLE}}{\partial \psi_{BLn}}\frac{\partial Y_{BLE}}{\partial A_{mn}} + \frac{\partial Z_{BLE}}{\partial \psi_{BLn}}\frac{\partial Z_{BLE}}{\partial A_{mn}}\right) + I_{XX_{BLE}}\left(\frac{\partial \phi_{BLE}}{\partial \psi_{BLn}}\frac{\partial \phi_{BLE}}{\partial A_{mn}}\right)\right]_{BLn} \tag{305}$$

$$M_{A_{mn}A_{rn}} = \sum_{i=1}^{k}\left[m(i)\left(\frac{\partial X_{BLE}}{\partial A_{mn}}\frac{\partial X_{BLE}}{\partial A_{mn}} + \frac{\partial Y_{BLE}}{\partial A_{mn}}\frac{\partial Y_{BLE}}{\partial A_{mn}} + \frac{\partial Z_{BLE}}{\partial A_{mn}}\frac{\partial Z_{BLE}}{\partial A_{mn}}\right) + I_{XX_{BLE}}\left(\frac{\partial \phi_{BLE}}{\partial A_{mn}}\frac{\partial \phi_{BLE}}{\partial A_{mn}}\right)\right]_{BLn} \tag{306}$$

β_{PHn} Defined As Dynamic Pitch Horn Bending

$$M_{A_{mn}\beta_{PHn}} = M_{A_{mn}\phi_{Fn}}\frac{\partial \phi_{Fn}}{\partial \beta_{PHn}} \tag{307}$$

TABLE 1. - Concluded

β_{PHn} Defined As Dynamic Pitch Horn Bending (Continued)

$$M_{\beta_{PHn}\beta_{PHn}} = M_{\phi_{Fn}\phi_{Fn}}\left(\frac{\partial\phi_{Fn}}{\partial\beta_{PHn}}\right)^2 \tag{308}$$

$$M_{\beta_{PHn}\phi_{Fn}} = M_{\phi_{Fn}\phi_{Fn}}\left(\frac{\partial\phi_{Fn}}{\partial\beta_{PHn}}\right) \quad \text{(used in swashplate)} \tag{309}$$

β_{PHn} Defined As Dynamic Torsion

$$M_{A_{mn}\beta_{PHn}} \equiv \sum_{i=1}^{k}\left[m(i)\left(\frac{\partial Z_{BLE}}{\partial A_{mn}}\right)\left(\frac{\partial Z_{BLE}}{\partial\phi_{BLE}}\right) + I_{XX_{BLE}}(i)\left(\frac{\partial\phi_{BLE}}{\partial A_{mn}}\right)_{BLn}\right]_{BLn}\left(\frac{\partial\phi_{BLE}}{\partial\beta_{PHn}}\right)_{BLn} \tag{310}$$

$$M_{\beta_{PHn}\beta_{PHn}} \equiv \sum_{i=1}^{k}\left[m(i)\left(\frac{\partial Z_{BLE}}{\partial\phi_{BLE}}\right)^2 + I_{XX_{BLE}}(i)\right]_{BLn}\left(\frac{\partial\phi_{BLE}}{\partial\beta_{PHn}}\right)^2_{BLn} \tag{311}$$

$$M_{\beta_{PHn}\phi_{Fn}} \equiv \sum_{i=1}^{k}\left[m(i)\left(\frac{\partial Z_{BLE}}{\partial\phi_{Fn}}\right)\left(\frac{\partial Z_{BLE}}{\partial\phi_{BLE}}\right) + I_{XX_{BLE}}(i)\frac{\partial\phi_{BLE}}{\partial\phi_{Fn}}\right]_{BLn}\left(\frac{\partial\phi_{BLE}}{\partial\beta_{PHn}}\right)_{BLn}$$

(used in swashplate) (312)

To save computation time some of the masses generated by the blade intergration and summation process in Table 1 are saved as a pseudo mass associated with a fictitious rotor coordinate (R). Thus for any given time step the sum of the rotor blades can be treated as an equivalent mass matrix:

$$\left[M_{OR}\right] = \sum_{n=1}^{N_b} \left\{\frac{\partial \tau_{O_{BLn}}}{\partial \tau_R}\right\} \sum_{i=1}^{\tau k} \left\{\frac{\partial \tau_{BLE}}{\partial \tau_{BLn}}\right\}^T \begin{bmatrix} m(i) & 0 & 0 & & & \\ 0 & m(i) & 0 & & \left[0\right] & \\ 0 & 0 & m(i) & & & \\ & & & I_{XX} & 0 & 0 \\ & \left[0\right] & & 0 & 0 & 0 \\ & & & 0 & 0 & I_{ZZ} \end{bmatrix}_{BLE}$$

$$\bullet \left\{\frac{\partial \tau_{BLE}}{\partial \tau_{BLn}}\right\} \quad \left\{\frac{\partial \tau_{O_{BLn}}}{\partial \tau_R}\right\} \tag{313}$$

The couplings of the pseudo rotor coordinate to blade and hub coordinates are also formed as an intermediate step to save repetitious blade integration.

$$\left[M_{O_{RBL}}\right]_n = \left\{\frac{\partial \tau_{O_{BLn}}}{\partial \tau_R}\right\}^T \left[M_{O_{BLBL}}\right]_n \tag{314}$$

Where the array $\left[M_{O_{BLBL}}\right]_n$ is the feather and bending coupling terms for the n^{th} blade. Ie.,

$$\left[M_{O_{BLBL}}\right]_n = \begin{bmatrix} M_{X_{OBLn}A_1} & M_{X_{OBLn}A_2} & M_{X_{OBLn}A_3} & M_{X_{OBLn}\phi_{Fn}} \\ M_{Y_{OBLn}A_1} & M_{Y_{OBLn}A_2} & M_{Y_{OBLn}A_3} & M_{Y_{OBLn}\phi_{Fn}} \\ M_{Z_{OBLn}A_1} & M_{Z_{OBLn}A_2} & M_{Z_{OBLn}A_3} & M_{Z_{CBLn}\phi_{Fn}} \\ M_{\phi_{OBLn}A_1} & M_{\phi_{OBLn}A_2} & M_{\phi_{OBLn}A_3} & M_{\phi_{OBLn}\phi_{Fn}} \\ M_{\theta_{OBLn}A_1} & M_{\theta_{OBLn}A_2} & M_{\theta_{OBLn}A_3} & M_{\theta_{OBLn}\phi_{Fn}} \\ M_{\psi_{OBLn}A_1} & M_{\psi_{OBLn}A_2} & M_{\psi_{OBLn}A_3} & M_{\psi_{OBLn}\phi_{Fn}} \end{bmatrix} \tag{315}$$

In addition to the rigid body motion blade coupling matrix, $\left[M_{O_{BL-BL}}\right]$, the blade mode coupling matrix, $\left[M_{BL-BL}\right]$, will be used in the subsequent development

$$\left[M_{BLBL}\right]_n = \begin{bmatrix} M_{A_1A_1} & M_{A_1A_2} & M_{A_1A_3} & M_{A_1\phi_f} \\ M_{A_2A_1} & M_{A_2A_2} & M_{A_2A_3} & M_{A_2\phi_f} \\ M_{A_3A_1} & M_{A_3A_2} & M_{A_3A_3} & M_{A_3\phi_f} \\ M_{\phi_fA_1} & M_{\phi_fA_2} & M_{\phi_fA_3} & M_{\phi_f\phi_f} \end{bmatrix}_n \tag{316}$$

5.6.4 Generalized forces. - The development herein proceeds by first deriving the equations for the loads on an individual blade element. The blade element loads are composed of aerodynamic and inertial components conveniently found in either the blade root axes BLn or the blade element axes BLE. The loads will be summed in Bln axes with the appropriate transformation. The desired equations are:

$$\begin{Bmatrix} F_X(i)_{BLE} \\ F_Y(i)_{BLE} \\ F_Z(i)_{BLE} \end{Bmatrix}_{BLn} = - m(i) \begin{Bmatrix} \ddot{X}(i)_{BLE} \\ \ddot{Y}(i)_{BLE} \\ \ddot{Z}(i)_{BLE} \end{Bmatrix}^{I}_{BLn} + \left[T_{BLn-BLE}\right]^T \begin{Bmatrix} F_{XA}(i)_{BLE} \\ F_{YA}(i)_{BLE} \\ F_{ZA}(i)_{BLE} \end{Bmatrix} \tag{317}$$

$$\begin{Bmatrix} M_X(i)_{BLE} \\ M_Y(i)_{BLE} \\ M_Z(i)_{BLE} \end{Bmatrix}_{BLn} = \left[T_{BLn-BLE}\right]^T \left\{ - I_{XX_{BLE}} \begin{Bmatrix} \dot{p}_{BLE} + q_{BLE} r_{BLE} \\ 0 \\ \dot{r}_{BLE} - p_{BLE} q_{BLE} \end{Bmatrix} + \begin{Bmatrix} M_{XA}(i)_{BLE} \\ 0 \\ 0 \end{Bmatrix}_{BLn} + \begin{Bmatrix} -Y_{CG}(i)_{BLE} F_{ZA}(i)_{BLE} \\ 0 \\ 0 \end{Bmatrix}_{BLn} \right\}$$

$$+ \begin{bmatrix} 0 & -Z(i)_{BLE} & Y(i)_{BLE} \\ Z(i)_{BLE} & 0 & -X(i)_{BLE} \\ -Y(i)_{BLE} & X(i)_{BLE} & 0 \end{bmatrix}_{BLn} \begin{Bmatrix} F_X(i)_{BLE} \\ F_Y(i)_{BLE} \\ F_Z(i)_{BLE} \end{Bmatrix}_{BLn} \tag{318}$$

The aerodynamic loads are in BLE axes alignment about the blade reference datum line which is the quarter chord. A transfer through the distance $Y_{CG_{BLE}}$ is made to the aerodynamic moment. To put the data on a common

basis with dynamic terms. The blade aerodynamics is detailed in Section 6. Since only the blade section pitching moment is considered, $M_{YA_{BLE}} = M_{ZA_{BLE}} = 0$. Note the blade element is assumed configured as a chordwise rod for inertia; hence

$$\left(I_{XX_{BLE}} = I_{ZZ_{BLE}} \text{ and } I_{YY_{BLE}} = 0\right) \tag{319}$$

A number of blade summations are desired. All will be made in BLn axes along the center-of-gravity axis. The loads at the principal reference axes and for rotor tilt make use of the blade root shears and moment. These are simply the sum of the k total blade elements,

$$\begin{Bmatrix} F_{X_{OBLn}} \\ F_{Y_{OBLn}} \\ F_{Z_{OBLn}} \end{Bmatrix} = \sum_{i=1}^{k} \begin{Bmatrix} F_X(i)_{BLE} \\ F_Y(i)_{BLE} \\ F_Z(i)_{BLE} \end{Bmatrix}_{BLn} \tag{320}$$

and likewise for root moments.

$$\begin{Bmatrix} M_{X_{BLn}} \\ M_{Y_{BLn}} \\ M_{Z_{BLn}} \end{Bmatrix} = \sum_{i=1}^{k} \begin{Bmatrix} M_X(i)_{BLE} \\ M_Y(i)_{BLE} \\ M_Z(i)_{BLE} \end{Bmatrix}_{BLn} \tag{321}$$

The summations illustrated above are for the total inertial and aerodynamic components. In a similar manner, the blade root aerodynamic loads are derived. The blade root loads are summed over all the blade to give main aerodynamic loads for downwash computations (Section 6.2.2) in the manner the total main rotor loads are found in Section 5.9.

Total main rotor root loads are formed from the blade root shears and moments. Using the pseudo rotor coordinate:

$$\begin{Bmatrix} F_X \\ F_Y \\ F_Z \\ F_\phi \\ F_\Theta \\ F_\psi \end{Bmatrix}_{MR} = \sum_{n=1}^{N_b} \left\{\frac{\partial \tau_{OBLn}}{\partial \tau_R}\right\} \begin{Bmatrix} F_{X_{OBLn}} \\ F_{Y_{OBLn}} \\ F_{Z_{OBLn}} \\ M_{X_{BLn}} \\ M_{Y_{BLn}} \\ M_{Z_{BLn}} \end{Bmatrix} \tag{322}$$

Feathering moments are used by the swashplate equations of motion. These moments are:

$$\begin{Bmatrix} M_{X_{Fn}} \\ - \\ - \end{Bmatrix} = \left[T_{BLn-Fn}\right] \left\{ \begin{Bmatrix} M_{X_{BLn}} \\ M_{Y_{BLn}} \\ M_{Z_{BLn}} \end{Bmatrix} + \begin{bmatrix} 0 & Z_{IB} & -Y_{IB} \\ -Z_{IB} & 0 & X_{IB} \\ Y_{IB} & -X_{IB} & 0 \end{bmatrix}_{BLn} \begin{Bmatrix} F_{X_{OBLn}} \\ F_{Y_{OBLn}} \\ F_{Z_{OBLn}} \end{Bmatrix} \right\} \tag{323}$$

where

$$\left[T_{BLn-Fn}\right] = \begin{bmatrix} \cos Y'_{FA} & \sin Y'_{FA} & 0 \\ -\sin Y'_{FA} & \cos Y'_{FA} & 0 \\ 0 & 0 & 1 \end{bmatrix} \begin{bmatrix} \cos Z'_{FA} & 0 & \sin Z'_{FA} \\ 0 & 1 & 0 \\ -\sin Z'_{FA} & 0 & \cos Z'_{FA} \end{bmatrix} \tag{324}$$

Only the X component is used by the program. The equations above transfer the summed blade loads to the inboard bearing, then transform them to feathering axes. Using the blade root loads is correct when one recalls that the blade is defined as those portions that are feathered; the fixed hub is excluded.

The blade bending generalized forces are now presented. They are:

$$F_{A_{mn}} = \sum_{i=1}^{k} \left[\left(\frac{\partial X(i)_{BLE}}{\partial A_{mn}} F_X(i)_{BLE} + \frac{\partial Y(i)_{BLE}}{\partial A_{mn}} F_Y(i)_{BLE} + \frac{\partial Z(i)_{BLE}}{\partial A_{mn}} F_Z(i)_{BLE} \right)_{BLn} \right.$$

$$\left. + \left(\frac{\partial \phi(i)_{BLE}}{\partial A_{mn}} M_Y(i)_{BLE} + \frac{\partial \psi(i)_{BLE}}{\partial A_{mn}} M_Z(i)_{BLE} \right)_{BLn} \right] - \frac{\partial U}{\partial A_{mn}} - \frac{\partial B}{\partial \dot{A}_{mn}} \tag{325}$$

The potential energy is given as:

$$\frac{\partial U}{\partial A_{mn}} = \sum_{j=1}^{3} K_{m,j} A_{jn} \tag{326}$$

where

$$K_{mj} = \int_{ROOT}^{TIP} \left(\frac{\frac{\partial M_Y}{\partial A_{mn}} \frac{\partial M_Y}{\partial A_{jn}}}{EI_{YY}} + \frac{\frac{\partial M_Z}{\partial A_{mn}} \frac{\partial M_Z}{\partial A_{jn}}}{EI_{ZZ}} \right) dS \tag{327}$$

are inputs calculated external to the program from a bending beam model. EI_{YY} and EI_{ZZ} are the flapping and chord stiffness about axes aligned with the blade element principal axes. The chord and flapping moments, M_{Y_i} and M_{Z_i} reflect the contribution of the bending moment from the i (or j) mode. The integration goes from root to tip. The K's are evaluated for whatever normalized modes are used as program input.

The last equation can be derived from the Bernoulli-Euler law for bending beams:

$$M = \frac{EI}{r} \tag{328}$$

where r is a radius of curvature. The strain energy is

$$U = \int_{ROOT}^{TIP} \frac{1}{2}\left(M_Y \frac{d\theta}{dS} + M_Z \frac{d\psi}{dS}\right) dS \tag{329}$$

Substituting in from the Bernoulli-Euler law and noting that $dS = r_Y d\theta = r_Z d\psi$,

$$U = \int_{ROOT}^{TIP} \frac{1}{2}\left(\frac{M_Y^2}{EI_{YY}} + \frac{M_Z^2}{EI_{ZZ}}\right) dS \tag{330}$$

Partial differentiation gives

$$\frac{\partial U}{\partial A_{mn}} = \int_{ROOT}^{TIP} \left(\frac{M_Y \, \partial M_Y/\partial A_{mn}}{EI_{YY}} + \frac{M_Z \, \partial M_Z/\partial A_{mn}}{EI_{ZZ}}\right) dS \tag{331}$$

Considering the moments as a linear sum of components from each bending mode, one has:

$$M_Y = \frac{\partial M_Y}{\partial A_{1n}} A_{1n} + \frac{\partial M_Y}{\partial A_{2n}} A_{2n} + \frac{\partial M_Y}{\partial A_{3n}} A_{3n} = \sum_{j=1}^{3} \frac{\partial M_Y}{\partial A_{jn}} A_{jn} \tag{332}$$

and likewise for M_Z. Then, by substitution, the desired equation is obtained.

5.6.4.1 Blade motion damping. - The blade motion damping is modeled by structural damping, aerodynamic damping, and a mechanical damper for lead-lag motions. The aerodynamic damping is accounted for in the aerodynamic blade loads developed in Section 6.2.

The structural factor is assumed proportional to the spring rate components of Equation 327. The coefficients K_{mj} can be directly identified with the coefficients K_{rk} developed in Section 5.3, Equations 234 and 236. The required damping coefficients, C_{rk}, are then the product of the proportionality factor, C_S, and K_{mj}. The structural damping component is then:

$$\frac{\partial B}{\partial \dot{A}_{mn}} = C_S \sum_{j=1}^{3} K_{mj} \dot{A}_{jn} \tag{333}$$

A lead-lag mechanical damper is usually a rotary or linear motion device employing elastomeric, dry friction, or viscous energy absorbing mechanism. The device is coupled about the blade lead-lag hinge or point of lead-lag motion slope by a linkage array. REXOR II models a rotary viscous damper mounted about a given blade location for which the inplane slope is specified as a function of the blade modal variables. For an articulated blade, this will simply be the motion of the lead-lag hinge. The damper has a pressure relief valve so that an initial damping rate, C_{LAG1}, is replaced by C_{LAG2} above a set motion rate, $\dot{Y}'_1$.

Given the slope rate data, $\dot{Y}_{n_c}$, for blade n at the damper location, c, the initial damping rate segment is defined by $\left|\dot{Y}'_{n_c}\right| < \dot{Y}'_1$. The damping is

$$\Delta \frac{\partial B}{\partial \dot{A}_{mn}} = - (C_{LAG1}) \left(\dot{Y}'_{n_c}\right) \left(\frac{\partial Y'_c}{\partial A_m}\right) \tag{334}$$

where

$$\dot{Y}'_{n_c} = \sum_{j=1}^{3} \left(\frac{\partial Y'_c}{\partial A_j} \dot{A}_{jn}\right) \tag{335}$$

Beyond the pressure relief opening point the damping contribution is

$$\Delta \frac{\partial B}{\partial \dot{A}_{mn}} = - \left[\left(\dot{Y}'_1\right) \left(\text{SIGN} \left(\dot{Y}'_{n_c}\right)\right) C_{LAG1} + (C_{LAG2}) \left(\dot{Y}'_{n_c} - \left(\dot{Y}'_1\right)\right) \left(\text{SIGN} \left(\dot{Y}'_{n_c}\right)\right) \right] \left(\frac{\partial Y'_c}{\partial A_{mn}}\right) \tag{336}$$

The generalized force is developed for pitch horn bending and dynamic torsion. For pitch horn bending,

$$F_{\beta_{PHn}} = M_{Fn} \frac{\partial \phi_{Fn}}{\partial \beta_{PHn}} - K_{\beta_{PHn}} \beta_{PHn} \tag{337}$$

where M_{Fn} is the total feather moment as derived in Section 5.10. For the uncoupled dynamic torsion option,

$$F_{\beta_{PHn}} = \sum_{i=1}^{k} \left(\frac{\partial Z(i)_{BLE}}{\partial \phi_{BLE}} F_Z(i)_{BLE} + M_X(i)_{BLE} \right)_{BLE} \frac{\partial \phi_{BLE}}{\partial \beta_{PHn}} - K_{\beta_{PHn}} \beta_{PHn} \tag{338}$$

in BLE axes. Since the blade elements loads are derived in BLn axes, the transform

$$\begin{Bmatrix} - \\ - \\ F_Z(i)_{BLE} \end{Bmatrix} = \left[T_{BLn-BLE} \right] \begin{Bmatrix} F_X(i)_{BLE} \\ F_Y(i)_{BLE} \\ F_Z(i)_{BLE} \end{Bmatrix}_{BLn} \tag{339}$$

is needed. The spring constant can be interpreted as

$$K_{\beta_{PHn}} = M_{\beta_{PHn}} \omega_{\beta_{PHn}}^2 \tag{340}$$

where the generalized mass is computed continuously and $\omega_{\beta_{PH}}$ is the nautral frequency of the uncoupled torsion mode, a program input constant.

5.6.5 Quasi-static blade torsion. - To improve the pitch horn bending blade feathering representation a quasi-static blade torsion distribution is introduced. Quasi-static torsion is computed from the structural stiffness, GJ_{SC}, at each station and the torque MX_{SC} at the shear center. The torque is summed from the tip to the blade station in question as shown in Section 4.3.4. The increment of twist produced at a blade station j can be displayed as:

$$\tau_T \dot{\phi}_{Tj} + \phi_{Tj} = \frac{M_{X_{SCj}}}{GJ_{SCj}} \tag{341}$$

assuming a first-order lag represents the torsional dynamics. The time constant τ_T is chosen to be representative of the blade first torsional mode frequency.

To obtain this result, the available computation elements require some further operations. First, REXOR II conducts blade integrations from root to tip, in BLn axes. To obtain tip to root values:

$$\begin{Bmatrix} F_{X_{BLEj}} \\ F_{Y_{BLEj}} \\ F_{Z_{BLEj}} \\ M_{X_{BLEj}} \\ M_{Y_{BLEj}} \\ M_{Z_{BLEj}} \end{Bmatrix}_{BLn} = \begin{Bmatrix} F_{XO} \\ F_{YO} \\ F_{ZO} \\ M_{XO} \\ M_{YO} \\ M_{ZO} \end{Bmatrix}_{BLn} - \sum_{i=1}^{j} \begin{Bmatrix} F_{X_{BLE}}(i) \\ F_{Y_{BLE}}(i) \\ F_{Z_{BLE}}(i) \\ M_{X_{BLE}}(i) \\ M_{Y_{BLE}}(i) \\ M_{Z_{BLE}}(i) \end{Bmatrix}_{BLn} \tag{342}$$

Note the summation is conducted from root to the station j in question. Thus the j represents a summation whereas the i represents a blade station.

Second, these data are used to form the required torque at the shear center.

$$\left\{\begin{matrix} M_{X_{SCj}} \\ - \\ - \end{matrix}\right\}_{PLn} = \left[\begin{matrix} 1 & Y'_{SC} & Z'_{SC} \\ - & - & - \\ - & - & - \end{matrix}\right] \left\{ \left\{\begin{matrix} M_{X_{BLEj}} \\ M_{Y_{BLEj}} \\ M_{Z_{BLEj}} \end{matrix}\right\}_{BLn} + \left[\begin{matrix} 0 & Z_{SC} & -Y_{SC} \\ -Z_{SC} & 0 & X_{SC} \\ Y_{SC} & -X_{SC} & 0 \end{matrix}\right]_{BLn} \left\{\begin{matrix} F_{X_{BLEj}} \\ F_{Y_{BLEj}} \\ F_{Z_{BLEj}} \end{matrix}\right\}_{BLn} \right\} \tag{343}$$

Small angles are assumed. The moments $\left(M_{X_{BLE}}\right)_{BLn}$ etc., act along the BLn axes and hence the matrix of lengths $\left(X_{SC}\right)_{BLn}$ etc., are employed to obtain moments at the shear center which are then transformed into shear center axes, subscripted SC, parallel to blade element center-of-gravity axes, subscripted BLE.

The blade deflections and slope in BLn are also needed for the above expressions.

$$\left\{\begin{matrix} X_{SC} \\ Y_{SC} \\ Z_{SC} \end{matrix}\right\}_{BLn} = \left\{\begin{matrix} X_{BLE} \\ Y_{BLE} \\ Z_{BLE} \end{matrix}\right\}_{BLn} + \left[T_{BLn-BLE}\right]^T \left\{\begin{matrix} 0 \\ Y_{SC}-Y_{CG} \\ 0 \end{matrix}\right\}_{BLE} \tag{344}$$

and

$$\left\{\begin{matrix} 0 \\ Y'_{SC} \\ Z'_{SC} \end{matrix}\right\}_{BLn} = \left\{\begin{matrix} 0 \\ Y'_{BLE} \\ Z'_{BLE} \end{matrix}\right\}_{BLn} \tag{345}$$

5.6.6 Quasi-static pitch horn bending. - To facilitate troubleshooting numerical instability problems as optional quasi-static pitch horn bending degree of freedom is available. The computation elements are the same as developed in Section 5.6.4 except that the solution does not use generalized masses, is therefore an uncoupled mode, and is calculated externally to the main computation flow. The formulation used is:

$$\tau_{PH}\,\dot{\phi}_{FnPH} + \phi_{FnPH} = \frac{M_{Fn}}{K_{\beta_{PH}}} \tag{346}$$

The dynamics are assumed represented by a first-order lag with β_{PH} as the time constant. The variable ϕ_{FnPH} is used to distinguish this formulation from the usual β_{PHn} symbology.

5.7 Shaft Axes Equations

5.7.1 Transmission isolation mount. - The shaft equations couple the spring mounted transmission, swashplate and rotor to the ground side of the mounting springs (fuselage). The fuselage is the reference coordinate set hence derivatives with respect to the rotor, hub, swashplate and transmission masses exist for the shaft axes equations.

5.7.2 Partial derivatives. - By using rotor pseudo coordinate masses only a few operations are required to assemble the coupled mass terms using one derivative vector, $\left|\partial\tau_{O_H}/\partial\tau_S\right|$.

Expanding:

$$\left\{\frac{\partial\tau_{O_H}}{\partial\tau_S}\right\} = \left[\begin{array}{c:c} \left[T_{S-H}\right] & \left[T_{S-H}\right]\left[\begin{matrix} 0 & Z & -Y \\ -Z & 0 & X \\ Y & -X & 0 \end{matrix}\right]_{S-H} \\ \hline [0] & \left[\begin{matrix} \cos\psi_S\cos\theta_S & \sin\psi_S & 0 \\ -\sin\psi_S\cos\theta_S & \cos\psi_S & 0 \\ \sin\theta_S & 0 & 1 \end{matrix}\right] \end{array}\right] \tag{347}$$

This expression is a compact notation form of the development of section 5.5.3. Note that the angle to angle portion of the array is not a full transformation, but rather reflects the relation of a dependent coordinate to an independent Euler angle.

The hub to swashplate partial $\left\{\partial\tau_{O_{SP}}/\partial\tau_H\right\}$ is developed in the next section.

5.7.3 Generalized masses. - The shaft axes matrix elements couple to the blade (A_{mn}, β_{PHn}) and swashplate generalized coordinates as well as to itself. Use is made of matrix notation and the rotor pseudo coordinate to produce a compact notation.

TABLE 2. - GENERALIZED MASSES

$$\left[M_S\right] = \left\{\frac{\partial\tau_{O_H}}{\partial\tau_S}\right\}^T \left\{\frac{\partial\tau_{O_R}}{\partial\tau_H}\right\}^T \left[M_{O_R}\right] \left\{\frac{\partial\tau_{O_R}}{\partial\tau_H}\right\} \left\{\frac{\partial\tau_{O_H}}{\partial\tau_S}\right\} + \left\{\frac{\partial\tau_{O_H}}{\partial\tau_S}\right\}^T \left[\left[M_{O_T}\right] + \left[M_{O_H}\right]\right] \left\{\frac{\partial\tau_{O_H}}{\partial\tau_S}\right\} + \left\{\frac{\partial\tau_{O_H}}{\partial\tau_S}\right\}^T \left\{\frac{\partial\tau_{O_{SP}}}{\partial\tau_H}\right\}^T \left[M_{O_{SP}}\right] \left\{\frac{\partial\tau_{O_{SP}}}{\partial\tau_H}\right\} \left\{\frac{\partial\tau_{O_H}}{\partial\tau_S}\right\} \tag{348}$$

$$\left[M_{S_{BL}}\right] = \left\{\frac{\partial\tau_{O_H}}{\partial\tau_S}\right\}^T \left\{\frac{\partial\tau_{O_R}}{\partial\tau_H}\right\}^T \left[M_{O_{R\ BL}}\right] \tag{349}$$

$$\left[M_{S_{SP}}\right] = \left\{\frac{\partial\tau_{O_H}}{\partial\tau_S}\right\}^T \left\{\frac{\partial\tau_{O_{SP}}}{\partial\tau_H}\right\}^T \left[M_{O_{SP}}\right] \left\{\frac{\partial\tau_{O_{SP}}}{\partial\tau_{SP}}\right\} \tag{350}$$

The element masses are defined as:

$$\left[M_{O_H}\right] = \begin{bmatrix} m_H & & & & & \\ & m_H & & & & \\ & & m_H & & & \\ & & & I_{XX} & & \\ & & & & I_{YY} & \\ & & & & & I_{ZZ} \end{bmatrix} \tag{351}$$

$$\left[M_{O_{SP}}\right] = \begin{bmatrix} m_{SP} & & & & & \\ & m_{SP} & & & & \\ & & m_{SP} & & & \\ & & & I_{XX_{SP}} & & \\ & & & & I_{YY_{SP}} & \\ & & & & & I_{ZZ_{SP}} \end{bmatrix} \tag{352}$$

TABLE 2. - Concluded

$$\left[M_{O_T}\right] = \begin{bmatrix} m & 0 & 0 & mZ & -mY \\ 0 & m & 0 & -mZ & mX \\ 0 & 0 & m & mY & -mX \\ 0 & -mZ & mY & I_{XX} + m(Y^2 + Z^2) & -I_{XY} - mXY & -I_{XZ} - mXZ \\ mZ & 0 & -mX & -I_{XY} - mXY & I_{YY} + m(X^2 + Z^2) & -I_{YZ} - mYZ \\ -mY & mX & 0 & -I_{XZ} - mXZ & -I_{YZ} - mYZ & I_{ZZ} + m(X^2 + Y^2) \end{bmatrix}_T \quad (353)$$

5.7.4 Generalized forces. - The shaft axes exercise the transmission mount springs $[K_S]$ and dampers $[C_S]$. Rotor loads, reflected through the hub coordinates also appear in the shaft generalized forces.

TABLE 3. - GENERALIZED FORCES

$$\begin{Bmatrix} F_X \\ F_Y \\ F_Z \\ F_\phi \\ F_\Theta \\ F_\Psi \end{Bmatrix}_{\mathcal{E}} = \left[\frac{\partial \tau_{O_H}}{\partial \tau_S}\right]^T \left[\frac{\partial \tau_{O_R}}{\partial \tau_H}\right]^T \begin{Bmatrix} F_X \\ F_Y \\ F_Z \\ F_\phi \\ F_\Theta \\ F_\Psi \end{Bmatrix}_{MR} - [C_S] \begin{Bmatrix} \dot{X} \\ \dot{Y} \\ \dot{Z} \\ \dot{\phi} \\ \dot{\Theta} \\ \dot{\Psi} \end{Bmatrix}_S - [K_S] \begin{Bmatrix} X \\ Y \\ Z \\ \phi \\ \Theta \\ \Psi \end{Bmatrix}_S$$

TABLE 3. - Concluded

$$-\left\{\frac{\partial \tau_{O_H}}{\partial \tau_S}\right\}^T \left\{\left[\left[M_{O_H}\right]+\left[M_{O_T}\right]\right]\begin{Bmatrix}\ddot{X}_o\\ \ddot{Y}_o\\ \ddot{Z}_o\\ \dot{p}\\ \dot{q}\\ \dot{r}\end{Bmatrix}_H + \left\{\begin{bmatrix}o & -r & q\\ r & o & p\\ -q & p & o\end{bmatrix}_H \begin{bmatrix}(3\ X\ 3)\\ \text{from}\\ (1,\ 4)\end{bmatrix}\begin{Bmatrix}p\\ q\\ r\end{Bmatrix}_H\right\}\right.$$

$$\left.\left\{\begin{bmatrix}o & -r & q\\ r & o & p\\ -q & p & o\end{bmatrix}_H \begin{bmatrix}(3\ X\ 3)\\ \text{from}\\ (4,\ 4)\end{bmatrix}\begin{Bmatrix}p\\ q\\ r\end{Bmatrix}_H\right\}\right\}$$

of

$$\left[\left[M_{O_H}\right]+\left[M_{O_T}\right]\right]$$

$$-\left\{\frac{\partial \tau_{O_{SP}}}{\partial \tau_H}\right\}^T \left\{\left[M_{O_{SP}}\right]\begin{Bmatrix}\ddot{X}_o\\ \ddot{Y}_o\\ \ddot{Z}_o\\ \dot{p}\\ \dot{q}\\ \dot{r}\end{Bmatrix}_{SP} + \left\{\begin{Bmatrix}o\\ o\\ o\end{Bmatrix}\right.\right.$$

$$\left.\left.\begin{bmatrix}o & -r & q\\ r & o & -p\\ -q & p & o\end{bmatrix}_{SP}\begin{bmatrix}I_{XX} & & \\ & I_{YY} & \\ & & I_{ZZ}\end{bmatrix}_{SP}\begin{Bmatrix}p\\ q\\ r\end{Bmatrix}_{SP}\right\}\right\}$$

(354)

5.8 Principal Reference Axis Equations

5.8.1 Nonzero contributions from most vehicle mass elements. - The principal reference axis equations of motion consider contributions from all of the physical elements of the rotorcraft. The elements involved are:

- Main rotor - defined as all portions that can be feathered
- Rotor hub - includes all portions of the main rotor assembly that cannot be feathered, and is treated as a rigid body
- Swashplate
- Tail rotor

- Fuselage
- Engine

The six rigid degrees of freedom: X, Y, Z, ϕ, θ, ψ are taken with respect to the stationary fuselage axes which are also the principal axes. The other elements considered are then referenced to the fuselage axes. The hub is subject to shaft bending motions relative to the principal axes. The tail rotor is installed on the fuselage and rotates at the main rotor speed times an appropriate gear ratio. Positive rotations are defined as:

- Hub
- Swashplate

} same as main rotor

- Tail rotor - Clockwise looking right
- Engine - Counterclockwise looking forward

The engine is treated as a rigid rotating body but the tail rotor is allowed to flap (teetering hinge, etc.). This flapping is considered secondary and enters only into the aerodynamic computations. The main rotor is allowed feathering, bending and twisting.

5.8.2 Partial derivatives. - Elements used the reference axis masses and forces can by in large be conveniently related to either the fuselage or hub coordinates. Since the reference set is taken to be the fuselage coordinate set, no partials are required in this instance.

Partials relating hub coordinate motion to reference generalized follow the scheme given in section 5.5.3.

$$\left\{\frac{\partial \tau_{O_H}}{\partial \tau_{REF}}\right\} = \left[\frac{\partial \tau_{O_H}}{\partial \tau_F}\right]\left\{\frac{\partial \tau_{O_F}}{\partial \tau_{REF}}\right\}$$

$$= \left[\begin{array}{c|c} \left[T_{F-H}\right] & \left[T_{F-H}\right]\left[\begin{array}{ccc} 0 & Z & -Y \\ -Z & 0 & X \\ Y & -X & 0 \end{array}\right]_{F-H} \\ \hline \left[0\right] & \left[T_{F-H}\right] \end{array}\right] \qquad (355)$$

where

$$\left\{\frac{\partial \tau_{O_F}}{\partial \tau_{REF}}\right\} \equiv [I] \qquad (356)$$

The swashplate system is physically connected with the hub structure, and partial derivatives describing its motion are taken through this intermediate, hub, coordinate. Note due to a parallelogram linkage the swashplate vertical motion is assumed to be unaffected by tilt angle.

$$\left\{\frac{\partial \tau_{O_{SP}}}{\partial \tau_H}\right\} = \left[\begin{array}{ccc:ccc} 1 & 0 & 0 & 0 & Z_{SP} & 0 \\ 0 & 1 & 0 & -Z_{SP} & 0 & 0 \\ 0 & 0 & 1 & 0 & 0 & 0 \\ \hdashline \multicolumn{3}{c:}{[0]} & \multicolumn{3}{c}{\left[T_{H\text{-}SP}\right]} \end{array}\right] \tag{357}$$

5.8.3 Generalized masses. - Use is made of matrix notation and the pseudo rotor coordinate to express the reference generalized masses given in Table 4.

TABLE 4. - REFERENCE AXIS GENERALIZED MASSES

$$\left[M_{REF\text{-}BL}\right] = \left\{\frac{\partial \tau_{O_H}}{\partial \tau_{REF}}\right\}^T \left\{\frac{\partial \tau_{O_R}}{\partial \tau_H}\right\}^T \left[M_{O_{R\text{-}BL}}\right] \tag{358}$$

where $\left[M_{O_{R\text{-}BL}}\right]$ is given in Table 1.

$$\left[M_{REF\text{-}SP}\right] = \left\{\frac{\partial \tau_{O_H}}{\partial \tau_{REF}}\right\}^T \left\{\frac{\partial \tau_{O_{SP}}}{\partial \tau_H}\right\}^T \left[M_{O_{SP}}\right] \left\{\frac{\partial \tau_{O_{SP}}}{\partial \tau_{SP}}\right\} \tag{359}$$

$$\begin{aligned} \left[M_{REF\text{-}S}\right] = {} & \left\{\frac{\partial \tau_{O_H}}{\partial \tau_{REF}}\right\}^T \left\{\frac{\partial \tau_{O_R}}{\partial \tau_H}\right\}^T \left[M_{O_R}\right] \left\{\frac{\partial \tau_{O_R}}{\partial \tau_H}\right\} \left\{\frac{\partial \tau_{O_H}}{\partial \tau_S}\right\} \\ & + \left\{\frac{\partial \tau_{O_H}}{\partial \tau_{REF}}\right\}^T \left[\left[M_{O_H} + M_{O_T}\right]\right] \left\{\frac{\partial \tau_{O_H}}{\partial \tau_S}\right\} \\ & + \left\{\frac{\partial \tau_{O_H}}{\partial \tau_{REF}}\right\}^T \left\{\frac{\partial \tau_{O_{SP}}}{\partial \tau_H}\right\}^T \left[M_{O_{SP}}\right] \left\{\frac{\partial \tau_{O_{SP}}}{\partial \tau_H}\right\} \left\{\frac{\partial \tau_{O_H}}{\partial \tau_S}\right\} \end{aligned} \tag{360}$$

TABLE 4. - Continued

$$\left[M_{REF}\right] = \left\{\frac{\partial \tau_{O_H}}{\partial \tau_{REF}}\right\}^T \left\{\frac{\partial \tau_{O_R}}{\partial \tau_H}\right\}^T \left[M_{O_R}\right] \left\{\frac{\partial \tau_{O_R}}{\partial \tau_H}\right\} \left\{\frac{\partial \tau_{O_H}}{\partial \tau_{REF}}\right\}$$
$$+ \left\{\frac{\partial \tau_{O_H}}{\partial \tau_{REF}}\right\}^T \left[\left[M_{O_T}\right] + \left[M_{C_H}\right]\right] \left\{\frac{\partial \tau_{O_H}}{\partial \tau_{REF}}\right\}$$
$$+ \left\{\frac{\partial \tau_{O_H}}{\partial \tau_{REF}}\right\}^T \left\{\frac{\partial \tau_{O_{SP}}}{\partial \tau_H}\right\}^T \left[M_{O_{SP}}\right] \left\{\frac{\partial \tau_{O_{SP}}}{\partial \tau_H}\right\} \left\{\frac{\partial \tau_{O_H}}{\partial \tau_{REF}}\right\}$$
$$+ \left[\left[M_{O_F}\right] + \left[M_{ENG}\right] + \left[M_{TR}\right]\right] \tag{361}$$

where

$$\left[M_{O_F}\right] = \begin{bmatrix} m & 0 & mZ & -mY \\ & m & -mZ & 0 & mX \\ & & m & mY & -mX & 0 \\ 0 & -mZ & mY & I_{XX} & -I_{XY} & -I_{XZ} \\ & & & +m(Y^2 + Z^2) & -mXY & -mXZ \\ mZ & 0 & -mX & -I_{XY} & I_{YY} & -I_{YZ} \\ & & & -m_{XY} & +m(X^2 + Z^2) & -mYZ \\ -mY & mX & 0 & -I_{XZ} & -I_{YZ} & I_{ZZ} \\ & & & -mXZ & -mYZ & +m(X^2 + Y^2) \end{bmatrix}_F \tag{362}$$

TABLE 4. - Concluded

and

$$\left[M_{ENG}\right] = \begin{bmatrix} 0 & & & & & \\ & 0 & & & & \\ & & 0 & & & \\ & & & I_{XX} & & \\ & & & & I_{XX}/2 & \\ & & & & & I_{XX}/2 \end{bmatrix}_{ENG} \tag{363}$$

$$\left[M_{TR}\right] = \begin{bmatrix} 0 & & & & & \\ & 0 & & & & \\ & & 0 & & & \\ & & & I_{YY}/2 & & \\ & & & & I_{YY} & \\ & & & & & I_{YY}/2 \end{bmatrix}_{TR} \tag{364}$$

The mass of the fuselage is considered to contain the engine and tail rotor masses, although the moment of inertias is treated separately.

5.8.4 Generalized forces. - The loads associated with the six reference axis degrees of freedom are listed in Table 5. The tail rotor and engine are assumed to have shafts parallel to the fuselage axes. The transfer of the aerodynamic loads from tail rotor axes with origin at hub center and parallel to the fuselage reference axes is shown in the table. The fuselage aerodynamic loads include tail rotor and propulsion terms. Further development of the main rotor blade component loads is in Section 5.6.1 and the aerodynamics for all rotors and fixed surfaces is left to Section 6.

TABLE 5. - REFERENCE AXIS GENERALIZED FORCES

$$\left\{\begin{matrix} F_X \\ F_Y \\ F_Z \\ F\phi \\ F\theta \\ F\psi \end{matrix}\right\}_{REF} = \left\{\frac{\partial \tau_{O_H}}{\partial \tau_{REF}}\right\}^T \left\{\frac{\partial \tau_{O_R}}{\partial \tau_R}\right\}^T \left\{\begin{matrix} F_X \\ F_Y \\ F_Z \\ F\phi \\ F\theta \\ F\psi \end{matrix}\right\}_{MR}$$

$$+ \left\{\frac{\partial \tau_{O_F}}{\partial \tau_{REF}}\right\}^T \left\{\left\{\begin{matrix} F_X \\ F_Y \\ F_Z \\ F\phi \\ F\theta \\ F\psi \end{matrix}\right\}_{F_A} - \left[M_{O_F}\right] \left\{\begin{matrix} \ddot{X}_o \\ \ddot{Y}_o \\ \ddot{Z}_o \\ \dot{p} \\ \dot{q} \\ \dot{r} \end{matrix}\right\}_F\right.$$

$$\left. - \left\{\left[\begin{matrix} o & -r & q \\ r & o & -p \\ -q & p & o \end{matrix}\right]_F \left[\begin{matrix} (3 \times 3) \\ \text{from} \\ (1, 4) \end{matrix}\right] \left\{\begin{matrix} p \\ q \\ r \end{matrix}\right\}_F \right\}$$

$$\left. - \left\{\left[\begin{matrix} o & -r & q \\ r & o & -p \\ -q & p & o \end{matrix}\right]_F \left[\begin{matrix} (3 \times 3) \\ \text{from} \\ (4, 4) \end{matrix}\right] \left\{\begin{matrix} p \\ q \\ r \end{matrix}\right\}_F \right\} \right\}$$

of

$$\left[M_{O_F}\right]$$

TABLE 5. - Continued

$$
-\left\{\frac{\partial \tau_{O_H}}{\partial \tau_{REF}}\right\}^T \left\{ \left[\left[M_{O_H}\right] + \left[M_{O_T}\right]\right] \begin{Bmatrix} \ddot{X}_o \\ \ddot{Y}_o \\ \ddot{Z}_o \\ \dot{p} \\ \dot{q} \\ \dot{r} \end{Bmatrix}_H + \left\{ \begin{bmatrix} o & -r & q \\ r & o & p \\ -q & p & o \end{bmatrix}_H \begin{bmatrix} (3 \times 3) \\ \text{from} \\ (1,\ 4) \end{bmatrix} \begin{Bmatrix} p \\ q \\ r \end{Bmatrix}_H \right\} \right.
$$

$$
\left. + \left\{ \begin{bmatrix} o & -r & q \\ r & o & p \\ -q & p & o \end{bmatrix}_H \begin{bmatrix} (3 \times 3) \\ \text{from} \\ (4,\ 4) \end{bmatrix} \begin{Bmatrix} p \\ q \\ r \end{Bmatrix}_H \right\} \right\}
$$

of

$$
\left[\left[M_{O_H}\right] + \left[M_{O_T}\right]\right]
$$

$$
-\left\{\frac{\partial \tau_{O_H}}{\partial \tau_{REF}}\right\}^T \left\{\frac{\partial \tau_{O_{SP}}}{\partial \tau_H}\right\}^T \left\{ \left[M_{O_{SP}}\right] \begin{Bmatrix} \ddot{X}_o \\ \ddot{Y}_o \\ \ddot{Z}_o \\ \dot{p} \\ \dot{q} \\ \dot{r} \end{Bmatrix}_{SP} \right.
$$

$$
\left. + \left\{ \begin{Bmatrix} o \\ o \\ o \end{Bmatrix} \begin{bmatrix} o & -r & q \\ r & o & -p \\ -q & p & o \end{bmatrix}_{SP} \begin{bmatrix} I_{XX} & & \\ & I_{YY} & \\ & & I_{ZZ} \end{bmatrix}_{SP} \begin{Bmatrix} p \\ q \\ r \end{Bmatrix}_{SP} \right\} \right\}
$$

C-3

TABLE 5. - Concluded

$$-\left\{\frac{\partial \tau_{TR}}{\partial \tau_{REF}}\right\}^{T}\left\{\left[M_{TR}\right]\begin{Bmatrix}-\\-\\-\\\dot{p}\\\dot{q}\\\dot{r}\end{Bmatrix}_{TR}+\left\{\begin{bmatrix}0\end{bmatrix}\begin{bmatrix}0 & -r & q\\ r & 0 & -p\\ -q & p & 0\end{bmatrix}_{TR}\begin{bmatrix}(3\times 3)\\ \text{from}\\ (4,4)\\ \text{of}\\ \left[M_{TR}\right]\end{bmatrix}\begin{Bmatrix}p\\q\\r\end{Bmatrix}_{TR}\right\}\right\}$$

$$-\left\{\frac{\partial \tau_{ENG}}{\partial \tau_{REF}}\right\}^{T}\left\{\left[M_{ENG}\right]\begin{Bmatrix}-\\-\\-\\\dot{p}\\\dot{q}\\\dot{r}\end{Bmatrix}_{ENG}+\left\{\begin{bmatrix}0\end{bmatrix}\begin{bmatrix}0 & -r & q\\ r & 0 & -p\\ -q & p & 0\end{bmatrix}_{ENG}\begin{bmatrix}(3\times 3)\\ \text{from}\\ (4,4)\\ \text{of}\\ \left[M_{ENG}\right]\end{bmatrix}\begin{Bmatrix}p\\q\\r\end{Bmatrix}_{ENG}\right\}\right\} \quad (365)$$

The angular velocities and accelerations associated with the engine and tail rotor require special consideration. Here the terms consist of a reference motion plus the turning due to the geared main rotor rate.

Using the rate and acceleration Euler transforms for zero Euler angles (Section 4.4.3):

$$\begin{Bmatrix}p\\q\\r\end{Bmatrix}_{TR-REF}=\begin{Bmatrix}p\\q\\r\end{Bmatrix}_{REF}+G_{TR}\begin{Bmatrix}0\\\dot{\psi}_{R}\\0\end{Bmatrix} \quad (366)$$

$$\begin{Bmatrix} \dot{p} \\ \dot{q} \\ \dot{r} \end{Bmatrix}_{TR-REF} = \begin{Bmatrix} \dot{p} \\ \dot{q} \\ \dot{r} \end{Bmatrix}_{REF} + G_{TR} \begin{bmatrix} -\dot{\psi}_R\, r_{REF} \\ \ddot{\psi}_R \\ \ddot{\psi}_R\, p_{REF} \end{bmatrix} \tag{367}$$

and

$$\begin{Bmatrix} p \\ q \\ r \end{Bmatrix}_{ENG-REF} = \begin{Bmatrix} p \\ q \\ r \end{Bmatrix}_{REF} - G_{ENG} \begin{Bmatrix} \dot{\psi}_R \\ 0 \\ 0 \end{Bmatrix} \tag{368}$$

$$\begin{Bmatrix} \dot{p} \\ \dot{q} \\ \dot{r} \end{Bmatrix}_{ENG-REF} = \begin{Bmatrix} \dot{p} \\ \dot{q} \\ \dot{r} \end{Bmatrix}_{REF} - G_{ENG} \begin{bmatrix} \ddot{\psi}_R \\ \dot{\psi}_R\, r_{REF} \\ \dot{\psi}_R\, q_{REF} \end{bmatrix} \tag{369}$$

5.9 Swashplate Equations

5.9.1 Partial derivatives. - The swashplate partial derivatives are readily obtained from Section 4.3.5. Using matrix notation

$$\begin{Bmatrix} \frac{\partial \tau_{O_{SP}}}{\partial \tau_{SP}} \end{Bmatrix} = \left[\begin{array}{ccc|ccc} 0 & 0 & 0 & & & \\ 0 & 0 & 0 & & \boxed{0} & \\ 0 & 0 & 1 & & & \\ \hline & & & \cos\theta_{SP} & 0 & 0 \\ & \boxed{0} & & 0 & 1 & 0 \\ & & & \sin\theta_{SP} & 0 & 0 \end{array}\right] \tag{370}$$

Since the swashplate axis is directly referenced to the principal (hub) set, the above derivatives are complete. The lack of translation to angular derivatives is explained by the parallelogram linkages used with swashplates to isolate the collective and cyclic inputs. The terms left out of the matrix indicate that the swashplate does not have a yaw degree of freedom.

The reader should be aware that the angular notation ϕ, θ, and Ψ have two meanings, depending on whether they are in the numerator or the denominator of the partial. The numerator is the displacement of the mass element with

respect to the hub axis, whereas the denominator is the degree of freedom incremental variable.

Swashplate motions pick up large inertia loads from the rotor due to blade feathering. Partials relating feathering to swashplate motions are assembled by first relating the feathering motion in the rotating system with feathering in the stationary system:

$$\frac{\partial \phi_{Fn}}{\partial \theta_0} = 1 \tag{371}$$

$$\frac{\partial \phi_{Fn}}{\partial A_{1S}} = -\cos(\psi_{BLn} + \psi_R) \tag{372}$$

$$\frac{\partial \phi_{Fn}}{\partial B_{1S}} = -\sin(\psi_{BLn} + \psi_R) \tag{373}$$

From Section 4.5.8, equations relating swashplate motions to the stationary feather angles give

$$\begin{bmatrix} \frac{\partial A_{1S}}{\partial \phi_{SP}} & \frac{\partial A_{1S}}{\partial \theta_{SP}} \\ \frac{\partial B_{1S}}{\partial \phi_{SP}} & \frac{\partial B_{1S}}{\partial \theta_{SP}} \end{bmatrix} = \frac{d}{e} \left[T_{\psi_{PH}} \right] \tag{374}$$

and

$$\begin{Bmatrix} \frac{\partial A_{1S}}{\partial \theta_0} \\ \frac{\partial B_{1S}}{\partial \theta_0} \end{Bmatrix} = \left(\frac{d}{e}\right)_1 \left[T_{\psi_{PH}} \right] \begin{Bmatrix} \phi_{SP} \\ \theta_{SP} \end{Bmatrix} \tag{375}$$

where

$$\left[T_{\psi_{PH}}\right] = \begin{bmatrix} \sin\psi_{PH} & \cos\psi_{PH} \\ \cos\psi_{PH} & -\sin\psi_{PH} \end{bmatrix} \tag{376}$$

Also

$$\frac{\partial\theta_0}{\partial Z_{SP}} = -\frac{1}{e} \tag{377}$$

The $\left[T_{\psi_{PH}}\right]$ matrix does not follow the conventional Euler angle notation since a desire existed to define ψ_{PH} as the angle the pitch horn to pitch link attachment point leads the blade. The overall derivatives can be put together as:

$$\frac{\partial\phi_{Fn}}{\partial\phi_{SP}} = \frac{\partial\phi_{Fn}}{\partial A_{1S}}\frac{\partial A_{1S}}{\partial\phi_{SP}} + \frac{\partial\phi_{Fn}}{\partial B_{1S}}\frac{\partial B_{1S}}{\partial\phi_{SP}} \tag{378}$$

$$\frac{\partial\phi_{Fn}}{\partial\theta_{SP}} = \frac{\partial\phi_{Fn}}{\partial A_{1S}}\frac{\partial A_{1S}}{\partial\theta_{SP}} + \frac{\partial\phi_{Fn}}{\partial B_{1S}}\frac{\partial B_{1S}}{\partial\theta_{SP}} \tag{379}$$

$$\frac{\partial\phi_{Fn}}{\partial Z_{SP}} = \left(\frac{\partial\phi_{Fn}}{\partial\theta_0} + \frac{\partial\phi_{Fn}}{\partial A_{1S}}\frac{\partial A_{1S}}{\partial\theta_0} + \frac{\partial\phi_{Fn}}{\partial B_{1S}}\frac{\partial B_{1S}}{\partial\theta_0}\right)\frac{\partial\theta_0}{\partial Z_{SP}} \tag{380}$$

These partials are the elements of the $\left\{\frac{\partial\phi_{Fn}}{\partial\tau_{SP}}\right\}$ vector.

5.9.2 Generalized masses. - Table 6 presents the generalized masses which couple the swashplate motions with one and another and with the blade fuselage degrees of freedom. The table uses summations of the blade that are described in detail in Section 5.6.1.

TABLE 6. - SWASHPLATE GENERALIZED MASSES

$$\left[M_{SP-BL}\right] = \sum_{n=1}^{N_b} \left[\frac{\partial \phi_{Fn}}{\partial \tau_{SP}}\right]^T \left[\frac{\partial \tau_{BL}}{\partial \phi_{Fn}}\right]^T \left[M_{BL-BL}\right]_n \tag{381}$$

$$\left[M_{SP}\right] = \sum_{n=1}^{N_b} \left[\frac{\partial \phi_{Fn}}{\partial \tau_{SP}}\right]^T \left[\frac{\partial \tau_{BL}}{\partial \phi_{Fn}}\right]^T \left[M_{BL-BL}\right]_n \left[\frac{\partial \tau_{BL}}{\partial \phi_{Fn}}\right] \left[\frac{\partial \phi_{Fn}}{\partial \tau_{SP}}\right]$$

$$+ \left[\frac{\partial \tau_{oSP}}{\partial \tau_{SP}}\right]^T \left[M_{oSP}\right] \left[\frac{\partial \tau_{oSP}}{\partial \tau_{SP}}\right] \tag{382}$$

5.9.3 Generalized forces. - The generalized forces are: (assuming a constant speed drive)

$$F_{\phi_{SP}} = -\frac{\partial \phi_{oSP}}{\partial \phi_{SP}}\left(\dot{p}_{SP}\, I_{XX_{SP}} + q_{SP}\, r_{SP}\left(I_{ZZ}-I_{XX}\right)_{SP}\right) - \frac{\partial \psi_{oSP}}{\partial \phi_{SP}}\, \dot{r}_{SP}\, I_{ZZ_{SP}}$$

$$+ \sum_{n=1}^{b} M_{Fn} \frac{\partial \phi_{Fn}}{\partial \phi_{SP}} - \frac{\partial U}{\partial \phi_{SP}} - \frac{\partial B}{\partial \dot{\phi}_{SP}} - M_{FR,\phi_{SP}} \tag{383}$$

$$F_{\theta_{SP}} = -\frac{\partial \theta_{oSP}}{\partial \theta_{SP}}\left(\dot{q}_{SP}\, I_{YY_{SP}} - r_{SP}\, p_{SP}\left(I_{ZZ}-I_{XX}\right)_{SP}\right)$$

$$+ \sum_{n=1}^{b} M_{Fn} \frac{\partial \phi_{Fn}}{\partial \theta_{SP}} - \frac{\partial U}{\partial \theta_{SP}} - \frac{\partial B}{\partial \dot{\theta}_{SP}} - M_{FR,\theta_{SP}} \tag{384}$$

Note p, q terms are the same for R and NR systems.

$$F_{Z_{SP}} = -(\ddot{Z}_{SP} + \ddot{Z}_F)\, m_{SP} + \sum_{n=1}^{b} M_{Fn} \frac{\partial \phi_{Fn}}{\partial Z_{SP}} - \frac{\partial U}{\partial Z_{SP}} - \frac{\partial B}{\partial \dot{Z}_{SP}} \tag{385}$$

where

$$\begin{Bmatrix} \dot{p} \\ \dot{q} \\ \dot{r} \end{Bmatrix}_{SP,NR} = \begin{Bmatrix} \dot{p} \\ \dot{q} \\ \dot{r} \end{Bmatrix}_{SP} - \begin{Bmatrix} \dot{\psi} q \\ -\dot{\psi} p \\ \dot{\psi} \end{Bmatrix}_{SP} \tag{386}$$

The moments used in these formulas are developed below.

The feathering moment, M_{Fn}, is taken to be composed of blade and friction loads.

$$M_{Fn} = M_{X_{Fn}} + M_{FR_{Fn}} \tag{387}$$

The detailing of $M_{X_{Fn}}$, feathering moments due to blade loads, is accomplished in Section 5.6.4. The friction load, $M_{FR\ Fn}$, follows the function shown in Figure 30. By reducing $\dot{\phi}_{Fn,BK}$ to near zero, stiction is obtained. Otherwise, if $\dot{\phi}_{Fn,BK}$ is large, the ratio $\frac{M_{FR_{Fn,BK}}}{\dot{\phi}_{Fn,BK}}$ determines the amount of viscous friction.

The remaining portions of the generalized force are the potential energy and dissipation functions. First consider the angular potential energy terms which model the swashplate tilt spring rate. This spring rate has a center dead-band, an operating range spring rate, and a high spring rate to simulate a travel limit stop.

Consider the normal operating range spring rate first. The swashplate springs are defined in control axes (Figure 31) as $K_{\phi_{SP}}$ and $K_{\theta_{SP}}$ (can be unequal in size). To find the elastic spring loads, the swashplate motions are first found in control axes as:

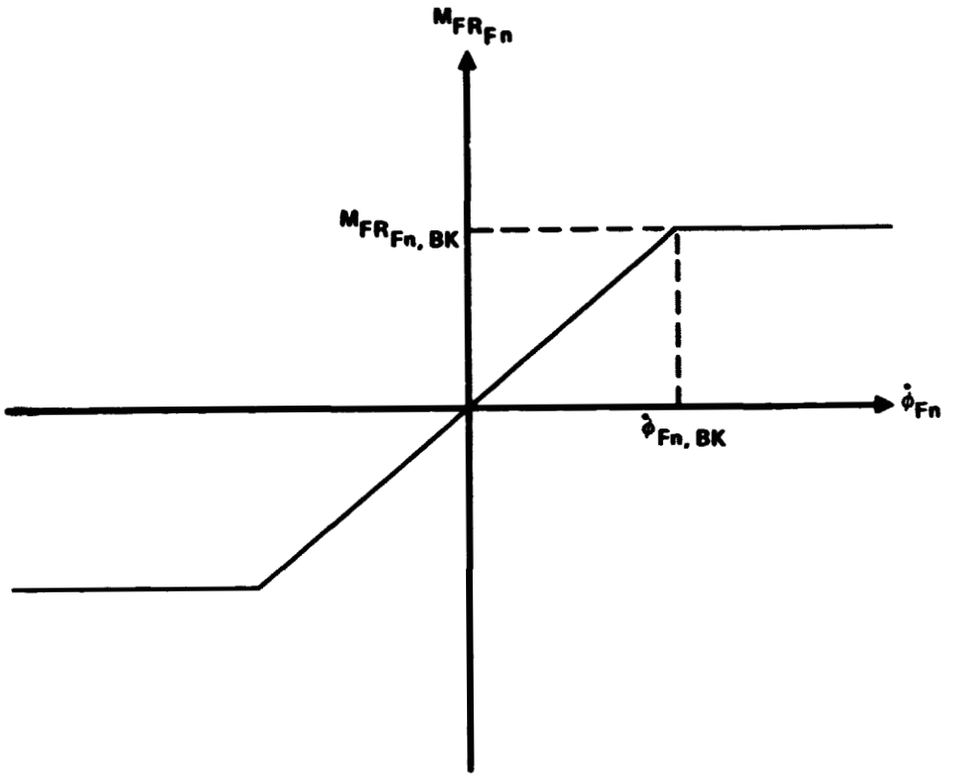

Figure 30. - Swashplate friction.

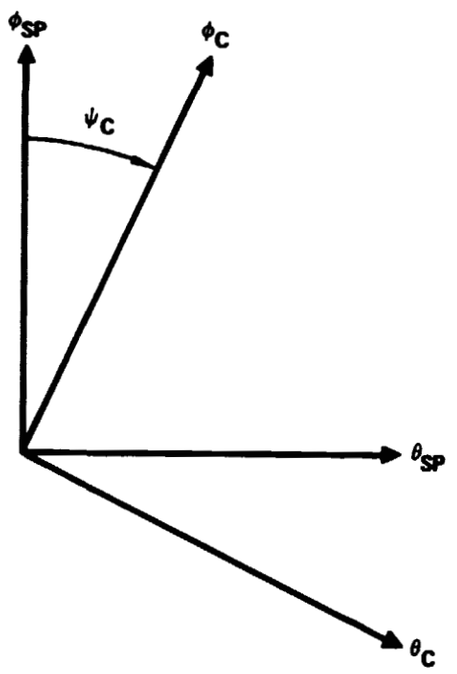

Figure 31. - Control axis.

$$\begin{Bmatrix} \phi_{SP} \\ \theta_{SP} \end{Bmatrix}_C = \begin{bmatrix} \cos\psi_C & \sin\psi_C \\ -\sin\psi_C & \cos\psi_C \end{bmatrix} \begin{Bmatrix} \phi_{SP} \\ \theta_{SP} \end{Bmatrix} \tag{388}$$

The geometric interpretation of ψ_C is shown in Figure 31.

Taking the swashplate deflections in the control axes, subtracting control inputs ϕ_C and θ_C, and using the inverse transform, the swashplate spring terms in swashplate axes become:

$$\begin{Bmatrix} \frac{\partial U}{\partial \phi_{SP}} \\ \frac{\partial U}{\partial \theta_{SP}} \end{Bmatrix}_1 = \begin{bmatrix} \cos\psi_C & -\sin\psi_C \\ \sin\psi_C & \cos\psi_C \end{bmatrix} \begin{Bmatrix} K_{\phi_{SP}} \left(\phi_{SP} - \phi_C\right)_C \\ K_{\theta_{SP}} \left(\theta_{SP} - \theta_C\right)_C \end{Bmatrix} \tag{389}$$

where the subscript (1) is used to distinguish these values (used in subsequent logic calculations) from the final expressions developed below.

Substituting for the swashplate motions in terms of the swashplate axes and rearranging:

$$\begin{Bmatrix} \frac{\partial U}{\partial \phi_{SP}} \\ \frac{\partial U}{\partial \theta_{SP}} \end{Bmatrix}_1 = \left[K_{SP}\right] \begin{Bmatrix} \phi_{SP} \\ \theta_S \end{Bmatrix} - \left[T_{\psi_C}\right]^T \begin{Bmatrix} K_{\phi_{SP}\phi_C} \\ K_{\theta_{SP}\theta_C} \end{Bmatrix} \tag{390}$$

where

$$\left[T_{\psi_C}\right]^T = \begin{bmatrix} \cos\psi_C & -\sin\psi_C \\ \sin\psi_C & \cos\psi_C \end{bmatrix} \tag{391}$$

and

$$\left[K_{SP}\right] = \left[\begin{array}{c|c} K_{\phi_{SP}} \cos^2\psi_C + K_{\theta_{SP}} \sin^2\psi_C & \left(K_{\phi_{SP}} - K_{\theta_{SP}}\right) \sin\psi_C \cos\psi_C \\ \hline \left(K_{\phi_{SP}} - K_{\theta_{SP}}\right) \sin\psi_C \cos\psi_C & K_{\phi_{SP}} \sin^2\psi_C + K_{\theta_{SP}} \cos^2\psi_C \end{array}\right] \tag{392}$$

Note: $\left[K_{SP}\right]$ is a symmetric matrix of constants.

The center dead band is modeled by the following logic.

$$\frac{\partial U}{\partial \phi_{SP}} = 0 \quad \text{if} \quad \left| \left(\frac{\partial U}{\partial \phi_{SP}}\right)_1 \right| \leq K_{SP}(1,1)\ \delta\phi_{SP} \tag{393}$$

otherwise

$$\frac{\partial U}{\partial \phi_{SP}} = \left(\frac{\partial U}{\partial \phi_{SP}}\right)_1 - K_{SP}(1,1)\ \delta\phi_{SP}\ \text{SIGN}\left(\frac{\partial U}{\partial \phi_{SP}}\right)_1 \tag{394}$$

$$\frac{\partial U}{\partial \theta_{SP}} = 0 \quad \text{if} \quad \left| \left(\frac{\partial U}{\partial \theta_{SP}}\right)_1 \right| \leq K_{SP}(2,2)\ \delta\theta_{SP} \tag{395}$$

otherwise

$$\frac{\partial U}{\partial \theta_{SP}} = \left(\frac{\partial U}{\partial \theta_{SP}}\right) - K_{SP}(2,2)\ \delta\theta_{SP}\ \text{SIGN}\left(\frac{\partial U}{\partial \theta_{SP}}\right)_1 \tag{396}$$

$\delta\phi_{SP}$ and $\delta\theta_{SP}$ are input constants giving swashplate angular freeplay.

Swashplate stops are also allowed with spring rate $K_{S,SP}$. A load

$$K_{S,SP}\left(\left(\phi_{SP}^2 + \theta_{SP}^2\right)^{1/2} - \delta_{S,SP}\right) \left\{\begin{matrix} \phi_{SP} \\ \theta_{SP} \end{matrix}\right\} \Big/ \left(\phi_{SP}^2 + \theta_{SP}^2\right)^{1/2} \tag{397}$$

is added to

$$\begin{Bmatrix} \frac{\partial U}{\partial \phi_{SP}} \\ \\ \frac{\partial U}{\partial \theta_{SP}} \end{Bmatrix} \tag{398}$$

to account for a limit travel stop. The limit deflection for the swashplate is

$$\left(\phi_{SP}^{\ 2} + \theta_{SP}^{\ 2}\right)^{1/2} \leq \delta_{S,SP} \tag{399}$$

where $\delta_{S,SP}$ is the circular stop swashplate deflection limit.

The angular damping term is analogous to the spring load:

$$\begin{Bmatrix} \frac{\partial B}{\partial \dot{\phi}_{SP}} \\ \\ \frac{\partial B}{\partial \dot{\theta}_{SP}} \end{Bmatrix} = \left[C_{SP}\right] \begin{Bmatrix} \dot{\phi}_{SP} \\ \\ \dot{\theta}_{SP} \end{Bmatrix} \tag{400}$$

where $\left[C_{SP}\right]$ has the same formulation as $\left[K_{SP}\right]$.

Control friction is treated as having rotating and nonrotating components. The rotating component has already been discussed as part of the feathering moment. The nonrotating component is applied to the swashplate. It has the formulation shown in Figure 31 with a change in labels such that $\dot{\phi}_{Fn}$ is either $\dot{\phi}_{SP}$ or $\dot{\theta}_{SP}$, and $M_{FR_{Fn}}$ is either $M_{FR,\phi_{SP}}$ or $M_{FR,\theta_{SP}}$

The vertical potential energy term is described as:

$$\frac{\partial U}{\partial Z_{SP}} = K_{1Z_{SP}} Z_{SP} + F_C \quad \text{if} \quad \left| Z_{SP} \right| < Z_{1_{SP}} \tag{401}$$

Otherwise

$$\frac{\partial U}{\partial Z_{SP}} = K_{1Z_{SP}} Z_{1_{SP}} + K_{2Z_{SP}}\left(Z_{SP} - Z_{1_{SP}}\right) + F_C \tag{402}$$

F_C is a constant to center the gyro springs.

The spring rate is taken to be $K_{1Z_{SP}}$ out to deflection $Z_{1_{SP}}$ and $K_{2Z_{SP}}$ beyond.

A simple coupling from the rotary dampers gives the vertical dissipation function.

$$\frac{\partial B}{\partial \dot{Z}_{SP}} = C_{Z_{SP}} \dot{Z}_{SP} - R_{Z\phi}\, C_{\phi_{SP}} \dot{\phi}_{SP}\, \phi_{SP} - R_{Z\theta}\, C_{\theta_{SP}} \dot{\theta}_{SP}\, \theta_{SP} \tag{403}$$

where $R_{Z\phi}$, $R_{Z\theta}$ are coupling ratios. Note the effect of vertical motion on the swashplate tilt loads through the rotary dampers is assumed zero.

To correlate with flight test records and/or to force the swashplate vertical response to cross the spring rate changeover a force offset constant is used. Introducing this constant into the swashplate vertical degree of freedom equation line, causes the variables, primarily the swashplate vertical motion, to shift and rebalance the equation.

5.9.4 Control inputs. - The swashplate input is controlled by the pilot's cyclic stick. The input torques are:

$$\begin{Bmatrix} K_{\phi_C}\, \phi_C \\ K_{\theta_C}\, \theta_C \end{Bmatrix} = \begin{Bmatrix} -K_{X_C}\, X_C \\ K_{Y_C}\, Y_C \end{Bmatrix} \tag{404}$$

The inputs are aligned with the control axis (Figure 31).

Note the equivalence of forms in terms of angular commands ϕ_C, θ_C, or longitudinal stick (aft) X_C and lateral stick (right) Y_C.

The controls are frequently linked to the swashplate through actuators which, as a first-order approximation, can be simulated by a first-order lag. See Section 7.2.

5.10 Engine Equations

5.10.1 Rotor azimuth and rotation rate. - The program allows a variation of rotor speed in maneuvers due to variations in the torque required by the various rotors and in the torque supplied by the engine. The dynamic system rotates as a rigid, geared unit. That is, the shafts are not allowed elastic windup. The main rotor speed, $\dot{\psi}_R$ and hence the engine speed, is referenced to the fuselage, and not to inertial space. The displacement ψ_R is the azimuth of the number one blade.

5.10.2 Engine model. - Figure 32 illustrates the engine model used in the program. The figure also plots typical engine torque characteristics. The model represents the first-order lag power response characteristics of the free turbine powerplants commonly used in rotorcraft applications.

Being a perturbation model, the engine is referenced to its trim position. The change in engine torque in a maneuver is

$$M_{XA_{ENG}} - M_{XA_{ENG,TRIM}} = \frac{\partial M_{ENG}}{\partial \dot{\psi}_{GEN}} \dot{\psi}_{GEN} - \frac{\partial M_{ENG}}{\partial \dot{\psi}_{ENC}} \left(\dot{\psi}_{ENG} - \dot{\psi}_{ENG,TRIM} \right) \tag{405}$$

where $0 \le M_{XA_{ENG}} \le M_{XA_{ENG,MAX}}$. The zero limit occurs if the overrunning clutch disconnects the engine in the transition to autorotation. The maximum value corresponds to the engine shaft torque limit.

The gas generator, speed, $\dot{\psi}_{GEN}$, is a degree of freedom. It is considered a secondary degree of freedom in that the coupling through the generalized masses with the primary degrees of freedom can be neglected. An equation for the generation speed can be supplied from its torque characteristics:

$$I_{GEN} \ddot{\psi}_{GEN} + C_{GEN} \dot{\psi}_{GEN} = - K_{ENG1} \ddot{\psi}_{ENG} - K_{ENG2} \left(\dot{\psi}_{ENG} - \dot{\psi}_{ENG,TRIM} \right) \tag{406}$$

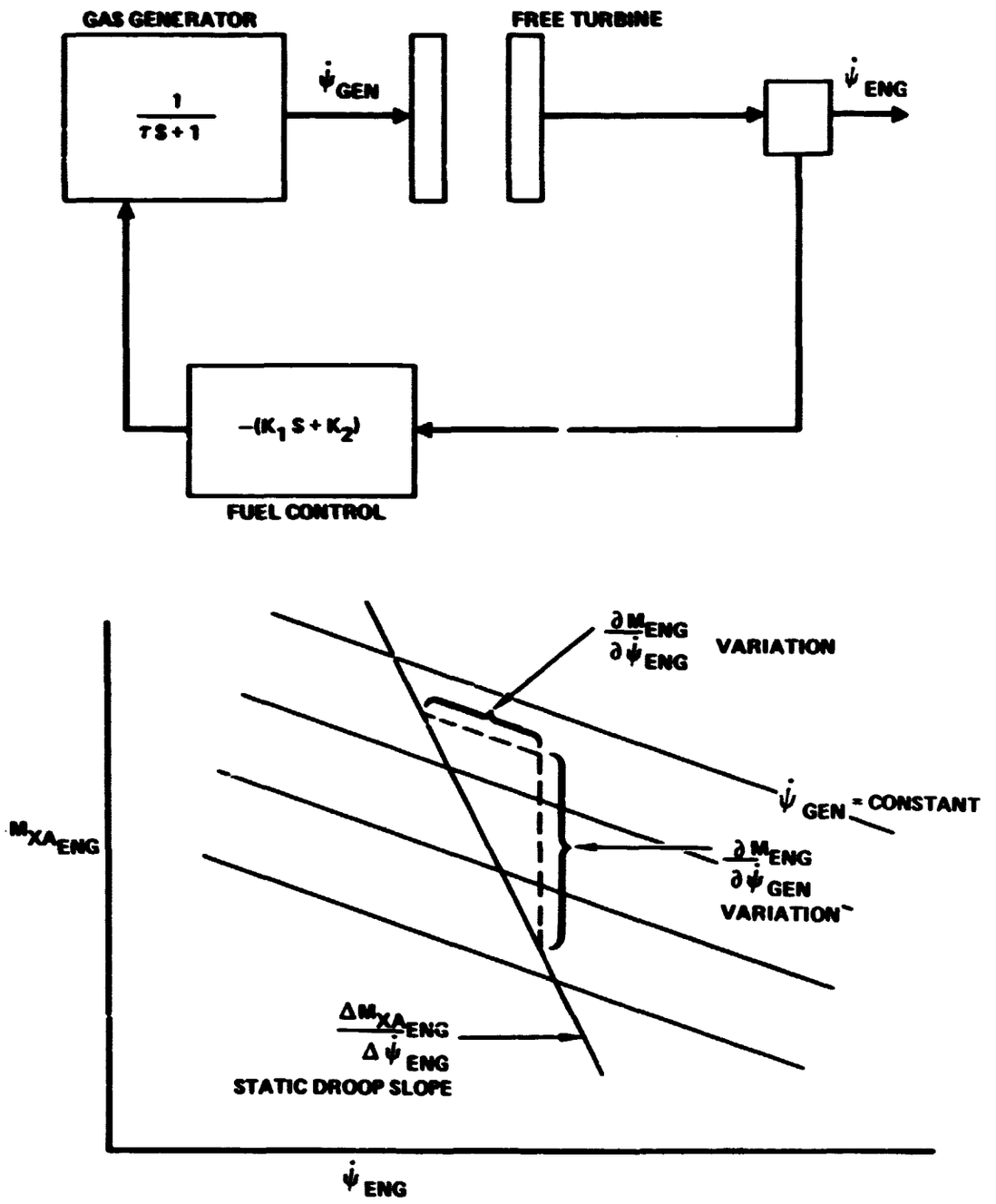

Figure 32. - Engine model and torque-speed characteristics.

The terms on the left represent acceleration inertia torque and steady-state torque. On the right, the fuel control causes torque to be added if the engine speed drops below the trim value. The $\ddot{\psi}_{ENG}$ term exists since the control is modeled with simple lag. Restating this equation, using rotor speed and a generator time constant, gives:

$$\ddot{\psi}_{GEN} = \frac{-\dot{\psi}_{GEN} - K_{R1}\ddot{\psi}_R - K_{R2}(\dot{\psi}_R - \dot{\psi}_{R,TRIM})}{\tau_{GEN}} \tag{407}$$

where $\tau_{GEN} = \frac{I_{GEN}}{C_{GEN}}$ is the order of a second.

The engine droop characteristic can be used to size the engine constants. With $\ddot{\psi}_{GEN} = \ddot{\psi}_R = 0$, substituting the generator equation into the engine equation and rearranging,

$$\frac{\Delta\left(M_{XA_{ENG}}\right)_R}{\Delta\dot{\psi}_R} = \frac{\partial\left(M_{ENG}\right)_R}{\partial\dot{\psi}_{GEN}} K_{R2} - \frac{\partial\left(M_{ENG}\right)_R}{\partial\dot{\psi}_R} \tag{408}$$

Only Δ incremental changes are of interest. The bracket subscripted R indicates the torque is determined at the rotor speed and includes the engine gear ratio. The term on the right is the static droop line shown in Figure 32. This plot also geometrically interprets the partial derivatives on the left.

The generator speed $\dot{\psi}_{GEN}$ is not given a reference. Its value is zero when trim is completed.

5.10.3 Partial derivatives. - Shaft rotation not only involves blade root rotation ψ_R, but also feathering motions. The feathering partial is obtained by differentiating the feather angle equation in Section 4.5.8:

$$\frac{\partial\phi_{Fn}}{\partial\psi_R} = A_{1S}\sin(\psi_{BLn} + \psi_R) - B_{1S}\cos(\psi_{BLn} + \psi_R) \tag{409}$$

A set of partials are defined to relate the various rotating components to the rotor shaft and to the reference set.

$$\left\{\frac{\partial \tau_{OR}}{\partial \psi_R}\right\} = \begin{Bmatrix} 0 \\ 0 \\ 0 \\ 0 \\ 0 \\ 1 \end{Bmatrix} \tag{410}$$

$$\left\{\frac{\partial \tau_{OH}}{\partial \psi_R}\right\} = \begin{Bmatrix} 0 \\ 0 \\ 0 \\ 0 \\ 0 \\ -1 \end{Bmatrix} \tag{411}$$

$$\left\{\frac{\partial \tau_{ENG}}{\partial \psi_R}\right\} = \begin{Bmatrix} 0 \\ 0 \\ 0 \\ -G_{ENG} \\ 0 \\ 0 \end{Bmatrix} \tag{412}$$

$$\left\{\frac{\partial \tau_{TR}}{\partial \psi_R}\right\} = \begin{Bmatrix} 0 \\ 0 \\ 0 \\ 0 \\ G_{TR} \\ 0 \end{Bmatrix} \tag{413}$$

$$\left\{\frac{\partial \tau_{ENG}}{\partial \tau_{REF}}\right\} = [I] \tag{414}$$

$$\left\{\frac{\partial \tau_{TR}}{\partial \tau_{REF}}\right\} = [I] \tag{415}$$

5.10.4 Generalized masses. - The engine degree of freedom couples with every other degree of freedom. Equations for the engine generalized masses are given in Table 7. Matrix notation is again used for compactness. Note the transmission is modeled as a non rotating mass, and therefore does not appear in these masses. The engine degree of freedom contains not only rigid body motion of the rotor blades, but also blade feathering. The feathering contribution is a minor contributor for some of the mass matrices and has been neglected.

TABLE 7. - ENGINE GENERALIZED MASSES

$$\left[M_{R\text{-}BL}\right]_n = \left|\frac{\partial \tau_{OR}}{\partial \psi_R}\right|^T \left[M_{OR\text{-}BL}\right]_n \tag{416}$$

$$\begin{aligned}\left[M_{R\text{-}SP}\right] = &\sum_{n=1}^{Nb} \left|\frac{\partial \tau_{OR}}{\partial \psi_R}\right|^T \left[M_{OR\text{-}BL}\right]_n \left|\frac{\partial \tau_{BL}}{\partial \phi_{Fn}}\right| \left|\frac{\partial \phi_{FN}}{\partial \tau_{SP}}\right| \\ &+ \sum_{n=1}^{Nb} \left|\frac{\partial \phi_{FN}}{\partial \psi_R}\right|^T \left|\frac{\partial \tau_{BL}}{\partial \tau_{FN}}\right|^T \left[M_{BL\text{-}BL}\right]_n \left|\frac{\partial \tau_{BL}}{\partial \phi_{FN}}\right| \left|\frac{\partial \phi_{FN}}{\partial \tau_{SP}}\right| \\ &+ \left|\frac{\partial \tau_{OH}}{\partial \psi_R}\right|^T \left|\frac{\partial \tau_{OSP}}{\partial \tau_H}\right|^T \left[M_{OSP}\right] \left|\frac{\partial \tau_{OSP}}{\partial \tau_{SP}}\right|\end{aligned} \tag{417}$$

$$\begin{aligned}\left[M_{R\text{-}S}\right] = &\left|\frac{\partial \tau_{OR}}{\partial \psi_R}\right|^T \left[M_{OR}\right] \left|\frac{\partial \tau_{OR}}{\partial \tau_H}\right| \left|\frac{\partial \tau_{OH}}{\partial \tau_S}\right| \\ &+ \left|\frac{\partial \tau_{OH}}{\partial \psi_R}\right|^T \left[M_{OH}\right] \left|\frac{\partial \tau_{OH}}{\partial \tau_S}\right| \\ &+ \left|\frac{\partial \tau_{OH}}{\partial \psi_R}\right|^T \left|\frac{\partial \tau_{OSP}}{\partial \tau_H}\right|^T \left[M_{OSP}\right] \left|\frac{\partial \tau_{OSP}}{\partial \tau_H}\right| \left|\frac{\partial \tau_{OH}}{\partial \tau_S}\right|\end{aligned} \tag{418}$$

TABLE 7. - Concluded

$$\left[M_{R-REF}\right] = \left\{\frac{\partial \tau_{OR}}{\partial \psi_R}\right\}^T \left[M_{OR}\right] \left\{\frac{\partial \tau_{OR}}{\partial \tau_H}\right\} \left\{\frac{\partial \tau_{OH}}{\partial \tau_{REF}}\right\}$$

$$+ \left\{\frac{\partial \tau_{OH}}{\partial \psi_R}\right\}^T \left[M_{OH}\right] \left\{\frac{\partial \tau_{OH}}{\partial \tau_{REF}}\right\}$$

$$+ \left\{\frac{\partial \tau_{ENG}}{\partial \psi_R}\right\}^T \left[M_{ENG}\right] \left\{\frac{\partial \tau_{ENG}}{\partial \tau_{REF}}\right\}$$

$$+ \left\{\frac{\partial \tau_{TR}}{\partial \psi_R}\right\}^T \left[M_{TR}\right] \left\{\frac{\partial \tau_{TR}}{\partial \tau_{REF}}\right\} \qquad (419)$$

$$\left[M_R\right] = \left\{\frac{\partial \tau_{OR}}{\partial \tau_R}\right\}^T \left[M_{OR}\right] \left\{\frac{\partial \tau_{OR}}{\partial \psi_R}\right\} + \left\{\frac{\partial \tau_{OH}}{\partial \psi_R}\right\}^T \left[M_{OH}\right] \left\{\frac{\partial \tau_{OH}}{\partial \psi_R}\right\}$$

$$+ \left\{\frac{\partial \tau_{OH}}{\partial \psi_R}\right\}^T \left\{\frac{\partial \tau_{OSP}}{\partial \tau_H}\right\} \left[M_{OSP}\right] \left\{\frac{\partial \tau_{OSP}}{\partial \tau_H}\right\} \left\{\frac{\partial \tau_{OH}}{\partial \tau_R}\right\}$$

$$+ \left\{\frac{\partial \tau_{ENG}}{\partial \psi_R}\right\}^T \left[M_{ENG}\right] \left\{\frac{\partial \tau_{ENG}}{\partial \psi_R}\right\}$$

$$+ \left\{\frac{\partial \tau_{TR}}{\partial \psi_R}\right\}^T \left[M_{TR}\right] \left\{\frac{\partial \tau_{TR}}{\partial \psi_R}\right\} \qquad (420)$$

5.10.5 Generalized forces. - Only one generalized force is needed.

$$F_R = (F_\psi)_{MR} - G_{ENG}\, I_{XX_{ENG}} (\dot{P}_F - G_{ENG}\, \ddot{\psi}_R)$$

$$+ G_{TR} (F_{\phi_{TR_A}} - I_{YY_{TR}} (\dot{q}_F + G_{TR}\, \ddot{\psi}_R))$$

$$- (I_{ZZ_H} + I_{ZZ_{SP}})\, \ddot{\psi}_R + \sum_{n=1}^{Nb} \frac{\partial \phi_{Fn}}{\partial \psi_R} M_{Fn} + G_{ENG} M_{X_{4\ ENG}} \qquad (421)$$

The main rotor contribution (inertial and aerodynamic loads) is given in Section 5.6.4. The tail rotor aerodynamics are described in Section 6.5.

6. AERODYNAMICS

6.1 Introduction

Other than gravity, the external loadings acting on the REXOR II equations of motion can be traced to aerodynamic sources. The following subsections trace the source, nature and use of these aerodynamic loads.

6.1.1 Aerodynamic forces producing surfaces considered. - The aerodynamic loads considered in REXOR II are divided into the categories of (1) associated with the main rotor, or (2) the rest of the rotorcraft (nonrotating surfaces and tail rotor). In view of the stated objectives of REXOR II, the program development emphasis is on the main rotor which is considered in Section 6.2.

The nonrotating components consist of the fuselage, wing, vertical tail, lower horizontal tail, upper horizontal tail, tail rotor, auxiliary thrustors, movable surfaces on the wings and empennage, and dive brakes. Wake effects from the main rotor and wing are addressed in Section 6.3. The nonrotating load elements are mostly developed and assembled in Section 6.4. The tail rotor equations, in integrated form, are developed in Section 6.5, and the auxiliary thrustor formulation is in Section 6.6.

6.1.2 Use of forces generated. - As mentioned, the aerodynamic loads are in essence the external forcing functions of the equations of motion. Generally the developed loads are in the axis of the apparent air velocity of the loaded element. Thus transformations are required to put the loads into the reference axes of the equation of motion considered.

6.2 Main Rotor

6.2.1 Overview. - To generate a main rotor model with sufficient detail to do dynamic investigations, a reasonably good quality aerodynamics presentation is required. To this end a table lookup of blade section properties, multifunction inflow model, quasi-steady aerodynamics, and dynamic stall are used in REXOR II.

6.2.1.1 Blade flow field. - As developed in the following subsections, the instantaneous blade airflow is the inertial velocity of the blade element. This velocity includes the motion of the principal reference set and the motion of the blade element with respect to the principal reference set. The calculation assumes the airmass is at rest, which is reasonable for dynamics investigations.

6.2.1.2 Air pressure and angle of attack. - The dynamic pressure used for these calculations is based on sea level standard density. The loads are ratioed to the actual air density.

The angle of attack is the sum of geometric pitch angle and the instantaneous air velocity. The rate of angle of attack is also calculated and used for the transient blade aero loads, Sections 6.2.3.3 and 6.2.3.4.

6.2.1.3 Forces and moments produced. - The steady blade loads are produced from the air velocity components of Section 6.2.3.1 and the coefficient data (C_L, C_D, C_M) of Section 6.2.4. The transient lift and moment effects are developed in Sections 6.2.3.3 (quasi-steady aerodynamics) and 6.2.3.4 (dynamic stall).

6.2.2 Concept of rotor inflow model. - The main rotor inflow model used in REXOR II is based on the air flow incident upon the rotor disc plus the air velocity imparted due to momentum exchange due to integrated blade span loading. This is to be contrasted with a formulation which tracks the rotor blade positions and the attendant trailing vorticies.

The incident air flow is the inertial velocity of the rotor coordinates, and is directly available from the preceding mechanical development. However a number of assumptions need to be stated and utilized to arrive at the induced velocity component of the inflow model.

6.2.2.1 Induced velocity assumptions. -

1. Only the vertical downwash and its variations radially and azimuthally over the rotor disk are considered. Induced swirl and lateral downwash components are neglected.

2. Downwash effects due to unsteady aerodynamics are not treated here as an overall effect, but as a blade segment condition in Section 6.2.3.3.

3. Rotor-induced flow distribution in hover and forward flight is patterned after Reference 6. This reference assumes a uniform loading in hover. Figure 33, from Reference 7, shows this distribution compared with typical loading and a triangular loading model. Figure 34 from Reference 6 shows the theoretical induced velocity distribution in forward flight as a consequence of a uniform hover distribution. This data is fitted to slopes or a longitudinal skew as a function of speed in REXOR II. Lateral distribution remains uniform in accord with Reference 8, which corrects the lateral distribution work of Reference 6.

4. A variation in lateral and longitudinal induced velocity is included to account for roll and pitch aerodynamic shaft moments.

5. Lifting line theory correction is accounted for by an effective rotor radius, BR.

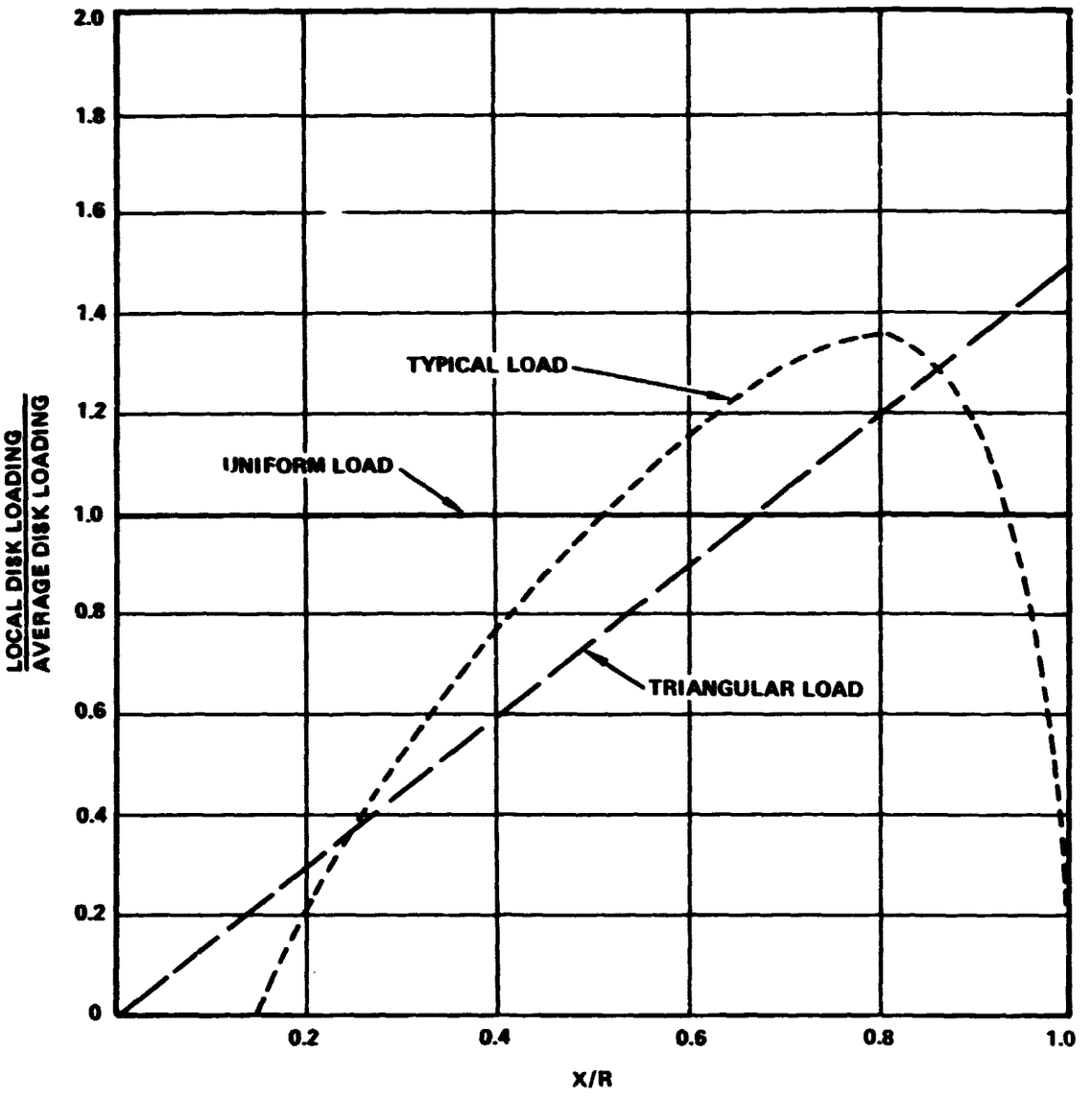

Figure 33. - Blade loading distributions in hover.

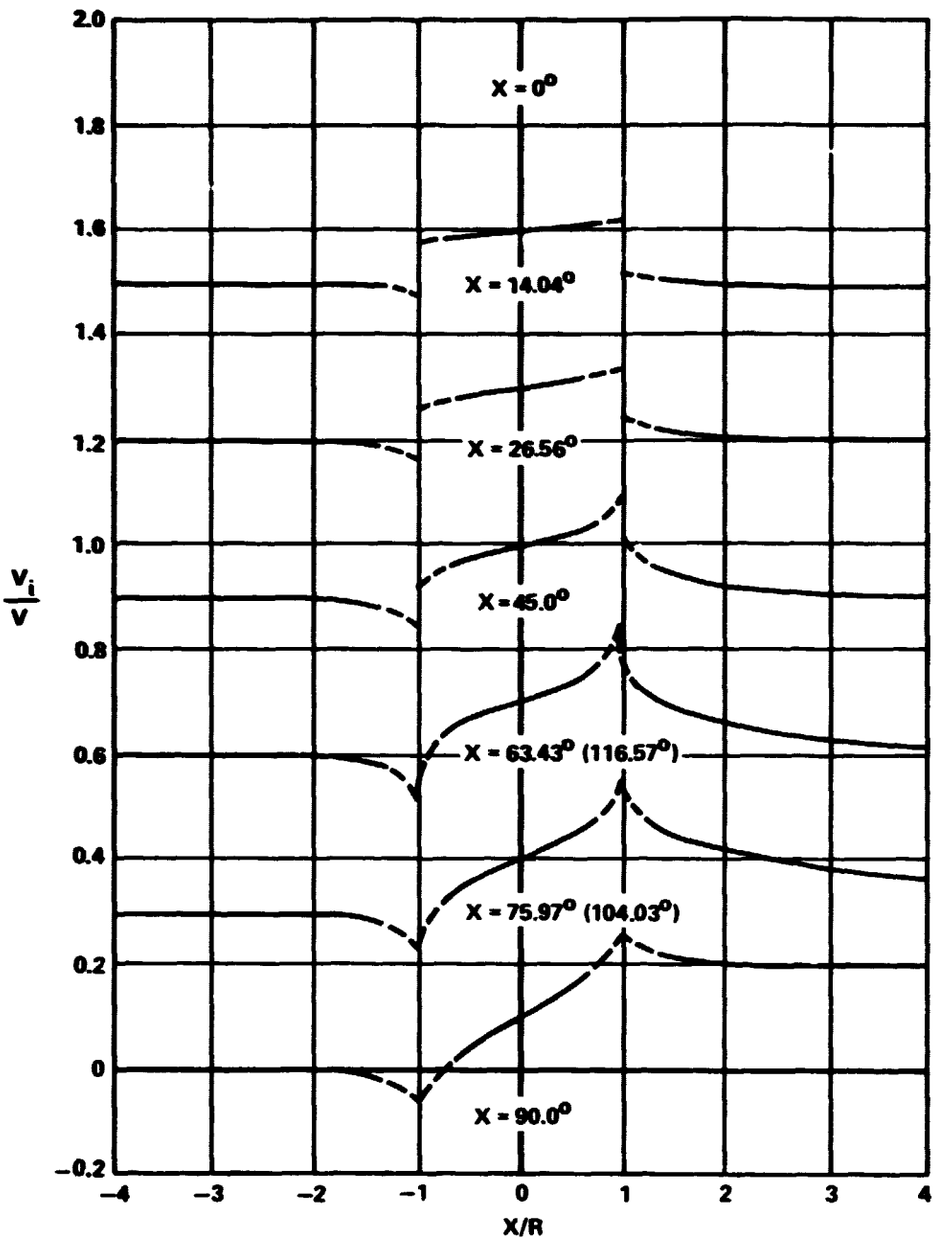

Figure 34. - Induced velocity distribution as a function of wake angle (forward flight).

6. Root cut out effects are ignored.

7. Transient effects are simulated by a single time lag.

6.2.2.2 Steady state values. - The starting point for determining the downwash is momentum theory as applied to an elementary dA:

$$dT = \left(\frac{dm}{dt}\right) 2W_i = \left(\rho V_{iMR}\, dA\right) 2w_i$$

$$= \rho \sqrt{u_H^2 + v_H^2 + (w_H - w_i)^2}\, dA\, 2w_i \qquad (422)$$

The thrust increment is dT, dm/dt is the flow of air through the rotor disk with resultant velocity V_{iMR}, ρ is the air density and w_i the downwash velocity. The velocities are taken in hub coordinates and no effort is made to account for rotor tilt.

The thrust expression above is used to define the following induced velocity components.

Average component, w_i

Longitudinal variation with pitching aerodynamic moment, q_{iMR}

Lateral variation with roll aerodynamic moment, p_{iMR}

The downwash velocity becomes

$$w_i = w_{iMR} + r\, q_{iMR} \cos \psi_R + r\, p_{iMR} \sin \psi_R \qquad (423)$$

The coefficients can be evaluated by equating the thrust and moment values for the main rotor equations to the integrals of the momentum expressions at hand. First consider the thrust expression. The evaluating task can be reduced by employing some boundary conditions. For rotor thrust only (no moment), q_{iMR} and $p_{iMR} = 0$. A convenient expression for the elementary area, dA, is shown in Figure 35. While radial anulii would serve for thrust integration, the form selected is particularly suited for the moment expressions.

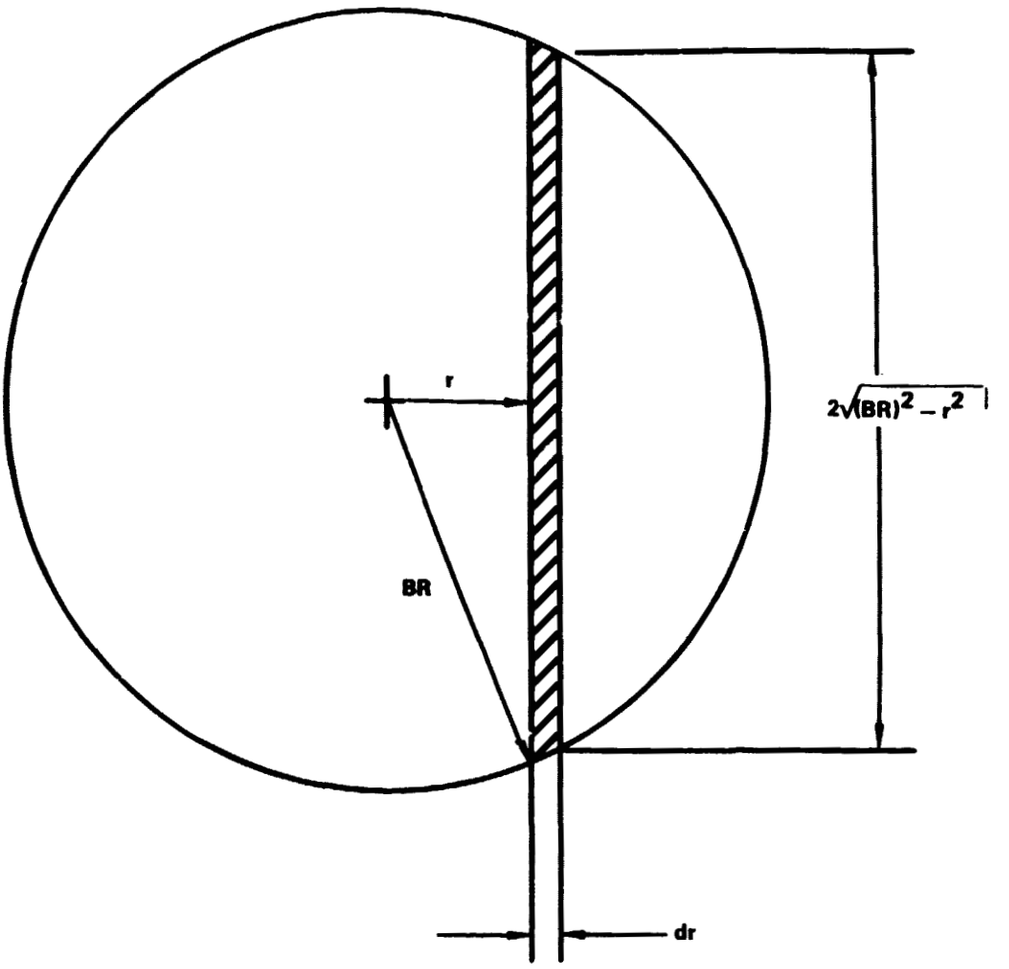

Figure 35. - Incremental area for shaft moment integration.

For the average rotor thrust,

$$-F_{ZA_{MR,H}} = T = \int_{-BR}^{BR} \rho \sqrt{u_H^2 + v_H^2 + \left(w_H - w_{iMR}\right)^2} \left(2\sqrt{(BR)^2 - r^2}\, dr\right) 2\, w_{iMR} \tag{424}$$

A further assumption is required to solve the square root of this expression and the corollary momentum equations.

For forward flight

$$w_i \ll V_{iMR} = \sqrt{u_H^2 + v_H^2 + (w_H - w_{iMR})} = (\text{constant}) \tag{425}$$

Completing the integration gives

$$-F_{ZA_{MR,H}} = \rho\pi (BR)^2 V_{iMR}\, 2\, w_{iMR} \tag{426}$$

Next consider the case of no rolling moment; i.e., only thrust and pitching moment. Figure 35 is used with the incremental strip considered to be right-left oriented so that all equal values of q_{iMR} are integrated at once.

Then,

$$M_{YA_{MR,H}} = \int_{-BR}^{BR} r\, dT$$

$$= \int_{-BR}^{BR} r\rho \sqrt{u_H^2 + v_H^2 + \left(w_H - W_{iMR} - r\, q_{iMR}\right)^2} \tag{427}$$

$$\left(2\sqrt{(BR)^2 - r^2}\, dr\right)\ 2\ \left(w_{iMR} + r\, q_{iMR}\right)$$

or

$$M_{YA_{MR,H}} = \rho \frac{\pi(BR)^4}{4} V_{iMR}\, 2\, q_{iMR} \tag{428}$$

Likewise for rolling moment, and using fore-aft increment strips gives

$$M_{YA_{MR,H}} = \rho \frac{\pi(BR)^4}{4} V_{iMR}\, 2\, p_{iMR} \tag{429}$$

Note the subscript A on $F_{ZA_{MR,H}}$, $M_{XA_{MR,H}}$, and $M_{YA_{MR,H}}$ denotes the aerodynamic component only of main rotor loads in hub axes.

The foregoing expressions are now developed for hovering and low-speed flight. In this condition,

$$u_H^2 + v_H^2 << \left(w_H - w_{iMR}\right)^2 \tag{430}$$

Integrating gives

$$-F_{ZA_{MR,H}} = \rho\pi (BR)^2 \left(w_H - w_{iMR}\right) \; 2\, w_{iMR} \tag{431}$$

and

$$M_{YA_{MR,H}} = \left(\frac{\rho\pi(BR)^4}{4} \left(w_H - w_{iMR}\right)\right) \; 2\, q_{iMR} \left(1 - \frac{w_{iMR}\left(w_H - w_{iMR}\right)}{\left(w_H - w_{iMR}\right)^2}\right) \tag{432}$$

$$M_{XA_{MR,H}} = \left(\frac{\rho\pi(BR)^4}{4} \left(w_H - w_{iMR}\right)\right) \; 2\, p_{iMR} \left(1 - \frac{w_{iMR}\left(w_H - w_{iMR}\right)}{\left(w_H - w_{iMR}\right)^2}\right) \tag{433}$$

The consequence of cyclic, first-harmonic downwash was explored in Reference 9. Their conclusion, which parallels Lockheed's experience, is that the phase and magnitude of the flap response of a hingeless blade to cyclic feathering is markedly affected by cyclic downwash. The shaft moments variation with feathering angle and the phase angle between flap and feathering are both reduced with cyclic downwash, the effect being greater in hover than in forward flight.

A physical interpretation can be rationalized for the formula above, at least in hover, in that the aerodynamic thrust and moment produces a flow of linear and angular momentum. Imagine the flow as a continuous stack of disks having mass per unit thickness $\rho\pi(BR)^2$ and dimetral inertia per unit thickness $\rho(\pi(BR)^4/4)$. $2\,w_{iMR}$, $2\,p_{iMR}$ and $2\,q_{iMR}$ are the final, far downstream position, values of induced velocities obtain by these disks oriented with the flow. The terms $\rho\pi(BR)^2 V_i$ and $\rho\pi(BR)^4/4\ V_i$ are the mass flow per unit time, and the moment of inertia flow per unit time through the actuator disk, which times $2w_{iMR}$, $2p_{iMR}$ or $2q_{iMR}$ is the gain of momentum.

For programming purposes, an empirical blend of the forward flight and hovering sets of expressions is used. The limiting cases of the empirical set give the derived cases. The expressions used are:

$$-F_{ZA_{MR,H}} = \rho\pi(BR)^2\, V_{iMR}\, 2\, w_{iMR} \tag{434}$$

$$-M_{YA_{MR,H}} = \frac{\rho\pi(BR)^4}{4}\, V_{iMR}\, 2\, q_{iMR} \left[1 - \frac{w_{iMR}\,(w_H - w_{iMR})}{V_{iMR}^2}\right] \tag{435}$$

$$-M_{XA_{MR,H}} = \frac{\rho\pi(BR)^4}{4}\, V_{iMR}^2\, p_{iMR} \left[1 - \frac{w_{iMR}\,(w_H - w_{iMR})}{V_{iMR}^2}\right] \tag{436}$$

6.2.2.3 Variations in forward flight and in ground effects. - The previous development can be assembled and combined with linearized forward flight distribution and ground effect factors.

$$(w_{BLE})_{DW,BLn} = w_{iMR}\, f_{iMR} \left[1 + K_{iMR} \frac{r}{R} \cos(\psi_R + \psi_{BLn} + \psi_W)\right]$$

$$+ r p_{iMR} \sin(\psi_R + \psi_{BLn}) + r q_{iMR} \cos(\psi_R + \psi_{BLn}) \tag{437}$$

The ground effect factor, f_{iMR}, and the longitudinal linear gradient factor, K_{iMR}, accounts for forward flight.

Note this formula is in rotating coordinates, and that the forward flight distribution actually is applied along the line of the apparent airflow, ψ_W. In doing this the distribution is valid for forward flight, sideward flight and sideslip conditions. The angle ψ_W is

$$\psi_W = \text{Tan}^{-1}\left(\frac{v_H}{u_H}\right) \tag{438}$$

as shown in Figure 45.

The aerodynamic moment factors, q_{iMR} and p_{iMR}, remain attached to the hub axis.

The downwash factor K_{iMR}, as explained in assumption 3, is given as a function of the wake angle defined as

$$\chi_{iMR} = \text{Tan}^{-1}\frac{\sqrt{u_H^2 + v_H^2}}{w_{iMR} - w_H} \tag{439}$$

which is zero in hover and near 90 degrees in high-speed flight. The function can be constrained by a number of factors. In hover, the value is zero. A 90-degree value of about 1.6 can be read from Figure 34. Also from this figure a set of linearized distributions is read, and plotted as Figure 36.

The ground effect factor,

$$f_{iMR} = 1 - \frac{1}{16}\left(\frac{R}{h}\right)^2 \frac{1}{1 + \frac{u_H^2 + v_H^2}{w_{iMR}^2}} \tag{440}$$

is taken from Reference 10, where $h = -(ZO_H)_E$ is from Section 4.5.1.

6.2.2.4 Downwash transients. - Downwash transients exist due to an apparent mass associated with the induced flow field. Work by Peters, et al. derive

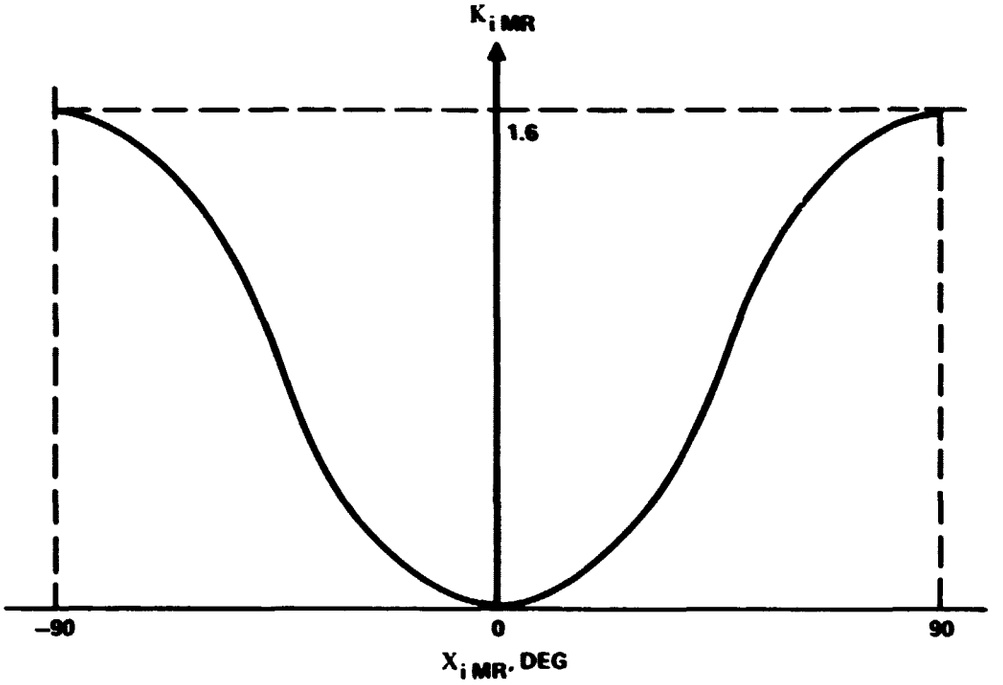

Figure 36. - Typical shape of longitudinal factor curve.

the expressions for collective and cyclic downwash including unsteady components. A good summary of this work is Reference 11.

Converting the referenced work to dimensional form gives equations comparable to (434, 435, 436).

$$w_{iMR} + \frac{4BR}{3\pi} w_{iMR} = -\frac{F_{ZA_{MR,H}}}{2\rho V_{iMR} \pi (BR)^2} \tag{441}$$

$$p_{iMR} + \frac{32}{45\pi} \frac{BR}{V_{iMR}} \frac{\dot{p}_{iMR}}{1 - w_{iMR} (w_H - w_{iMR}) / V_{iMR}}$$

$$= \frac{-2M_{XA_{MR,H}}}{\rho V_{iMR} \pi (BR)^4 \left[1 - w_{iMR} (w_H - w_{iMR}) / V^2_{iMR}\right]} \tag{442}$$

$$q_{iMR} + \frac{32}{45\pi} \frac{BR}{V_{iMR}} \frac{\dot{q}_{iMR}}{\left[1 - w_{iMR} (w_H - w_{iMR}) / V_{iMR}\right]}$$

$$= \frac{-2M_{YA_{MR,H}}}{\rho V_{iMR} \pi (BR)^4 \left[1 - w_{iMR} (w_H - w_{iMR}) / V_{iMR}\right]} \tag{443}$$

These differential equations are solved for w_{iMR}, P_{iMR} and q_{iMR} using numerical (Euler) integration.

6.2.2.5 Iteration of downwash solution. - As is the case with any rotary-wing loading calculation, there is an interplay between the downwash variance from calculating the loading and a variance in the loading from recomputing the downwash. A common practice is to solve an iterative loop to satisfy both equations (i.e., lift and momentum). In REXOR II the iteration does not take place independently, but proceeds stepwise with the rotor azimuthal advance. With the normal, rapid convergence of the iteration the solution will essentially be complete with the step advance. However, large step sizes will incur an additional downwash time lag.

6.2.3 Blade element velocity components. - In the following subsections the blade aerodynamic loading is categorized and developed along two lines. They are:

- Steady-state aerodynamics
- Transient phenomena consisting of quasi-steady aerodynamics and dynamic stall.

6.2.3.1 Sources and resolution from blade motion. - The steady aerodynamics are based on the air velocities while the quasi-steady aerodynamics (from flutter theory) and dynamic stall depend on accelerations.

The air velocity is the blade mechanical velocities summed with a component due to downwash. In a similar manner, the air acceleration is taken to be the mechanical blade accelerations minus the downwash accelerations. The downwash formulation as developed in Section 6.2.2 allows for lags, and it is these lags that result in downwash acceleration terms.

6.2.3.2 Steady aerodynamics. - The air velocities relative to a blade section are desired for an axis system with origin at the quarter chord to match the airfoil table data. From Section 4.5.5, the mechanical blade velocities relative to the free stream or earth axes are available as $\{\dot{X}_{BLE}, \dot{Y}_{BLE}, \dot{Z}_{BLE}\}^I$. The desired relative air velocities at the quarter chord (or blade BLn reference axis) are:

$$\begin{Bmatrix} \dot{X}_{1/4\ c} \\ \dot{Y}_{1/4\ c} \\ \dot{Z}_{1/4\ c} \end{Bmatrix}_{BLE} = \left[T_{BLn - BLE}\right] \left\{ \begin{Bmatrix} \dot{X}_{BLE} \\ \dot{Y}_{BLE} \\ \dot{Z}_{BLE} \end{Bmatrix}_{BLn}^{I} + \begin{Bmatrix} 0 \\ 0 \\ w_{BLE} \end{Bmatrix}_{DW,BLn} \right\} + \begin{Bmatrix} r\ Y_{CG} \\ 0 \\ -p\ Y_{CG} \end{Bmatrix}_{BLE} \tag{444}$$

Where the second vector on the right is the downwash velocity developed in Section 6.2.2, and the third transfers the velocity from the BLE reference point at the blade center of gravity back to the quarter chord. The distance Y_{CG} is positive with the center of gravity ahead of the quarter chord. For notational convenience,

$$\begin{Bmatrix} U_S \\ U_C \\ U_N \end{Bmatrix} = \begin{Bmatrix} -\dot{X}_{1/4\ c} \\ \dot{Y}_{1/4\ c} \\ -\dot{Z}_{1/4\ c} \end{Bmatrix} \tag{445}$$

The angle of attack is defined as

$$\alpha_{1/4\ c} = \sin^{-1}\left(U_N \Big/ \sqrt{U_C^2 + U_N^2}\right) \qquad (446)$$

Airflow aspects of quasi-steady aerodynamic formulation are developed at this point for convenience. The quasi-steady aerodynamic contribution is conceived as composed of circulatory and noncirculatory components. The circulatory components are taken to be equivalent to finding the aerodynamic force, and moment coefficients are based on an angle of attack at the three-quarter chord:

$$\alpha_{3/4\ c} = \alpha_{1/4\ c} + \frac{p_{BLE}\frac{c}{2}}{\sqrt{U_N^2 + U_C^2}} \qquad (447)$$

As such, the effect of angular rates is included in deriving the steady aerodynamic coefficients. The formulation above does not attempt to account for local downwash rotation or curvature and its chordwise variation. The net result is that aerodynamic coefficients determined in Section 6.2.4 are computed with $\alpha_{3/4\ c}$.

A number of quantities used in the dynamic stall computations, Section 6.2.3.4, are also available from the previous mechanical development. They are also defined here for convenience. First, the angle of sideslip appears only in the dynamic stall formulation. For this purpose it is defined as

$$\Lambda = \mathrm{Tan}^{-1}\left(\frac{U_S}{U_C}\right) \qquad (448)$$

Also, dynamic stall is based on the time derivative of the angle of attack at the three-quarter chord:

$$\dot{\alpha}_{3/4\ c} = \frac{1}{1 + (U_N/U_C)^2}\left[\frac{\dot{U}_N}{U_C} - \frac{U_N}{U_C}\frac{\dot{U}_C}{U_C}\right] + \frac{c}{2}\left[\frac{\dot{p}_{BLE}}{\sqrt{U_C^2 + U_N^2}} - p_{BLE}\left(\frac{U_C\,\dot{U}_C + U_N\,\dot{U}_N}{(U_C^2 + U_N^2)^{\frac{3}{2}}}\right)\right] \qquad (449)$$

The above equation requires $\dot{U}_C$ and $\dot{U}_H$.

$$\begin{Bmatrix} \dot{U}_S \\ \dot{U}_C \\ \dot{U}_H \end{Bmatrix} = \begin{bmatrix} -1 & 0 & 0 \\ 0 & 1 & 0 \\ 0 & 0 & -1 \end{bmatrix} \left[T_{BLn} - BLE \right] \left\{ \begin{Bmatrix} \ddot{X}_{BLE} \\ \ddot{Y}_{BLE} \\ \ddot{Z}_{BLE} \end{Bmatrix}^{EI}_{BLn} + \begin{Bmatrix} g_X \\ g_Y \\ g_Z \end{Bmatrix}_{BLn} \right.$$

$$+ \begin{Bmatrix} 0 \\ 0 \\ \dot{w}_{BLE} \end{Bmatrix}_{DW,BLn} + \begin{bmatrix} 0 & r_{BLE} & q_{BLE} \\ -r_{BLE} & 0 & p_{BLE} \\ q_{BLE} & -p_{BLE} & 0 \end{bmatrix}_{BLn} \left. \begin{Bmatrix} \dot{X}_{BLE} \\ \dot{Y}_{BLE} \\ \dot{Z}_{BLE} \end{Bmatrix}^{I}_{BLN} \right\}$$

$$+ \begin{Bmatrix} -(\dot{r}-pq)Y_{CG} \\ 0 \\ (\dot{p}+qr)Y_{CG} \end{Bmatrix}_{BLn} \qquad (450)$$

The inclusion of the gravity term places these accelerations in a true inertial axis system, not earth inertial axes, as appropriate for aerodynamic calculations. See Section 4.5.1. Gravity does cause buoyancy forces, but these can be ignored. The turning acceleration components are also subtracted to produce linear accelerations which correctly model the blade element incident airflow. The gravity vector can be obtained from hub values as:

$$\begin{Bmatrix} g_X \\ g_Y \\ g_Z \end{Bmatrix}_{BLE} = \left[\frac{\partial \zeta_{BLn}}{\partial \zeta_R} \right] \left[\frac{\partial \zeta_R}{\partial \zeta_H} \right] \begin{Bmatrix} g_X \\ g_Y \\ g_Z \end{Bmatrix}_H \qquad (451)$$

By differentiating the downwash velocities, the downwash acceleration is obtained:

$$\left(\dot{w}_{BLE}\right)_{DW,BLn} = \dot{w}_{iMR} \frac{\left(w_{BLE}\right)_{DW,BLn}}{w_{iMR}}$$

$$- w_{iMR} f_{iMR} K_{iMR} \frac{X_{BLn}}{R} \sin(\psi_R + \psi_{BLn} + \psi_w)\dot{\psi}_R$$

$$+ r\dot{p}_{iMR} \sin(\psi_R + \psi_{BLn}) + r\dot{q}_{iMR} \cos(\psi_R + \psi_{BLn})$$

$$+ r\left[p_{iMR} \cos(\psi_R + \psi_{BLn}) - q_{iMR} \sin(\psi_R + \psi_{BLn})\right]\dot{\psi}_R \qquad (452)$$

6.2.3.3 Quasi-steady aerodynamics. - Quasi-steady aerodynamics is accounted for in REXOR II by incorporating the terms from the two-dimensional flutter theory of Theodorsen (reference 12). In the REXOR II analysis, Theodorsen's lift deficiency function C(k) is taken as unity. This means that the flutter theory presently incorporated neglects shed wake effects, or in physical terms does not account for the phase change between blade element lift (or pitching moment) and angle of attack, due to shed vorticity, or the assumption of quasi-steady aerodynamics is expressed by C(k) = 1.

Referring to a classic text on aeroelasticity by Bisplinghoff, Ashley, and Hoffman (Reference 13), the expressions for lift and pitching moment are given as:

$$L = \pi\rho b^2\left[\ddot{h} + U\dot{\alpha} - ba\ddot{\alpha}\right] + 2\pi\rho U\, bC(k)\left[\dot{h} + U\alpha + b\left(\frac{1}{2} - a\right)\dot{\alpha}\right] \qquad (453)$$

and

$$M = \pi\rho b^2\left[ba\ddot{h} - Ub\left(\frac{1}{2} - a\right)\dot{\alpha} - b^2\left(\frac{1}{8} + a^2\right)\ddot{\alpha}\right]$$

$$+ 2\pi\rho U\, b^2\left(a + \frac{1}{2}\right) C(k)\left[\dot{h} + U\alpha + b\left(\frac{1}{2} - a\right)\dot{\alpha}\right] \qquad (454)$$

In REXOR II, the blade aerodynamics and quasi-steady aerodynamics are referenced to the local section quarter-chord properties. This is done because the majority of available airfoil data uses this reference. Note that the final aerodynamic loads are translated to the local BLE axis (c.g. location) for use in the equations of motion.

Reviewing the above expressions, and referencing the rotation point to the quarter chord gives a = -1/2. If we take C(k) as unity, replace 2π for circulatory lift by $(dC_{LR}/d\alpha)$, and substitute c/2 for the semichord b, these equations become

$$L = \frac{\pi\rho c^2}{4}\left[\ddot{h} + U\dot{\alpha} + \frac{c}{4}\ddot{\alpha}\right] + \left(\frac{d\,C_{LR}}{d\,\alpha}\right)\frac{\rho cU}{2}\left[\dot{h} + U\alpha + \frac{c\dot{\alpha}}{2}\right] \tag{455}$$

and:

$$M = \frac{\pi\rho c^2}{4}\left[-\frac{c}{4}\ddot{h} - \frac{Uc}{2}\dot{\alpha} - \frac{c^2}{4}\left(\frac{3}{8}\ddot{\alpha}\right)\right] \tag{456}$$

Note that the entire last term in the moment equation vanishes with a = -1/2. Referring to the lift expression, noncirculatory aerodynamic lift is accounted for in REXOR II by the first term in which $\ddot{h} + U\dot{\alpha}$ are combined into $\dot{U}_N$ in blade element coordinates. The second term results from table lookup where

$$\Delta L = \frac{1}{2}\rho U^2\, c\left(\frac{dC_{LR}}{d\alpha}\right)\alpha = \frac{1}{2}\rho U^2\, c\, C_{LR} \tag{457}$$

in which the angle of attack is previously computed from

$$\alpha_{3/4c} = \left[\frac{\dot{h}}{U} + \alpha + \frac{c\dot{\alpha}}{2U}\right] . \tag{458}$$

The α within the brackets is identified as θ, the actual physical angle of the blade with respect to the freestream direction. The α on the left hand is that due to the air velocities which include the plunging velocity $\dot{h}$ and rotation component $c/2\dot{\alpha}$. Hence $p_{BLE} = \dot{\alpha}$ and $\dot{p}_{BLE} = \ddot{\alpha}$.

The total aerodynamic pitching moment is the sum of the quasi-steady loads computed above and the table lookup blade section properties (Section 6.2.4).

6.2.3.4 Dynamic stall. - Dynamic stall is included in REXOR II based upon the Boeing-Vertol formulation set forth in References 14, 15, and 16. It is similar to the treatment of dynamic stall in the Bell C-81 program. A comparison of REXOR II with the C-81 program is given in Appendix IV, pages 393-404, of Reference 3. Dynamic stall is specifically addressed with respect to the two programs beginning on page 395 of that report. A significant point of difference between the treatment of dynamic stall in the two programs is that C-81 puts a 20-percent limit on the angle-of-attack overshoot in obtaining the dynamic maximum lift coefficient, whereas REXOR II has no limit. The correctness of the treatment of dynamic stall in either program is difficult to assess since the concensus of researchers in this area is that current methods are empirical at best, and much research still remains to be done in this area.

Reference 14 notes that, "The trends show that compressibility effects reduce dynamic-stall delay, and at about M = 0.6 no dynamic-stall delay is evident." For this reason an upper Mach number limit of 0.6 was implemented in the dynamic stall calculations for REXOR II. The test data obtained by Boeing Vertol and given in the references cited was for the Mach number range 0.2 to 0.6. As implemented in REXOR II if $M < 0.25$, the value $M = 0.25$ is used in the analytic expression for developing the stall hysteresis loop.

Reference 15 notes that it was found that, "airfoils used currently by the helicopter industry had stalling dominated by leading edge stall. For this type of stalling process, the dynamic C_L extension was proportional to the time rate of change of the angle of attack."

In that reference, so as to use static airfoil data as much as possible, static stall and dynamic stall are empirically related by developing a reference angle of attack given by

$$\alpha_{REF} = \alpha - \left(\gamma\sqrt{\left|\frac{\alpha c\dot{\alpha}}{2V}\right|}\ \text{sign}(\dot{\alpha})\right) \tag{459}$$

in which,

$$\gamma = \log_e \frac{0.601}{M} \tag{460}$$

and is physically related to dynamic stall delay. α is identified as $\alpha_{3/4c}$ and

$$M = \alpha_s \Big/ \sqrt{U_N^2 + U_C^2} \tag{461}$$

As noted in Reference 16 in regard to dynamic stall..." as a blade element reaches and exceeds the static angle of attack, stall does not occur as long as a sufficient, positive time rate of change of the airfoil angle of attack, $\dot{\alpha}$, is present." The experimentally derived equation for dynamic stall delay is given in the reference as

$$\text{dynamic stall delay} = \gamma \sqrt{\frac{c\dot{\alpha}}{2V}} \tag{462}$$

where

$$\frac{c\dot{\alpha}}{2V} = k \tag{463}$$

the blade element reduced frequency.

Referring to the gamma expression, we note that $\gamma \to 0$ as $M \to 0.601$, which is the upper limit for Mach number values for dynamic stall calculations. Also, note that $\gamma \to 1$ as $M \to 0.2211$, which is approximated by the value of $M = 0.25$, the lower limit in REXOR II for dynamic stall simulation.

The term α_{REF} given above is also called the dynamic angle of attack (Reference 15) and given by the notation α_{DYN}.

6.2.3.4.1 Lift accounting for dynamic stall. - Using the reference or dynamic angle of attack computed from α_{REF}, the REXOR II program implements the "Fast Aerodynamic Table", Section 6.2.4, subroutine and determines the lift coefficient, C_L, corresponding to α_{REF} and the freestream Mach number for the specified blade element and blade azimuth position. Also computed at the given Mach number are the C_L for zero angle of attack and the C_L for a small increment $\Delta\alpha$ with respect to zero. Yawed or radial flow is accounted for by computing the yaw angle of the flow given by:

$$\Lambda = \text{Tan}^{-1}\left(\frac{U_S}{U_C}\right) \tag{464}$$

where U_S and U_C represent blade spanwise and chordwise components of flow respectively.

The slope of the lift curve is then found from:

$$\left(\frac{\partial C_L}{\partial \alpha}\right)_{DYN} = \frac{C_L(\alpha_{REF}, M) - C_L(0,M)}{\alpha_{REF} \cos \Lambda} \tag{465}$$

It can be argued from physical reasonings that the dynamic lift-curve slope cannot exceed the static life-curve slope. As a check, REXOR II also calculates:

$$\left(\frac{\partial C_L}{\partial \alpha}\right)_{0,M} = \frac{C_L(\Delta\alpha, M) - C_L(0,M)}{\Delta\alpha} \tag{466}$$

Only in the event $(\partial C_L/\partial\alpha)_{DYN}$ is greater than $(\partial C_L/\partial\alpha)_{0,M}$ is the latter value used to calculate C_L. Otherwise C_L is calculated by

$$C_L = \left(\frac{\partial C_L}{\partial \alpha}\right)_{DYN} \alpha + C_L(0,M) \tag{467}$$

The ability of this approximation to describe mathematically the lift hysteresis characterized by dynamic stall is shown in Figure 37, which compares analytical results with experimental two-dimensional airfoil data. (From Reference 16.)

The component of the lift force per unit span acting normal to the blade chord axis and including dynamic stall effects is then calculated from

$$\Delta F_{NO} = C_L \, c \, \frac{\rho V^2}{2} \cos \alpha \tag{468}$$

The total normal force is determined by adding to this term the drag component, $C_D \, c \, \rho V^2/2 \sin \alpha$, and the unsteady aerodynamic terms discussed in the previous section. To account for dynamic stall effects on drag, two-dimensional drag coefficient data are used, but as determined at α_{REF}, not α. This is consistent with Reference 15.

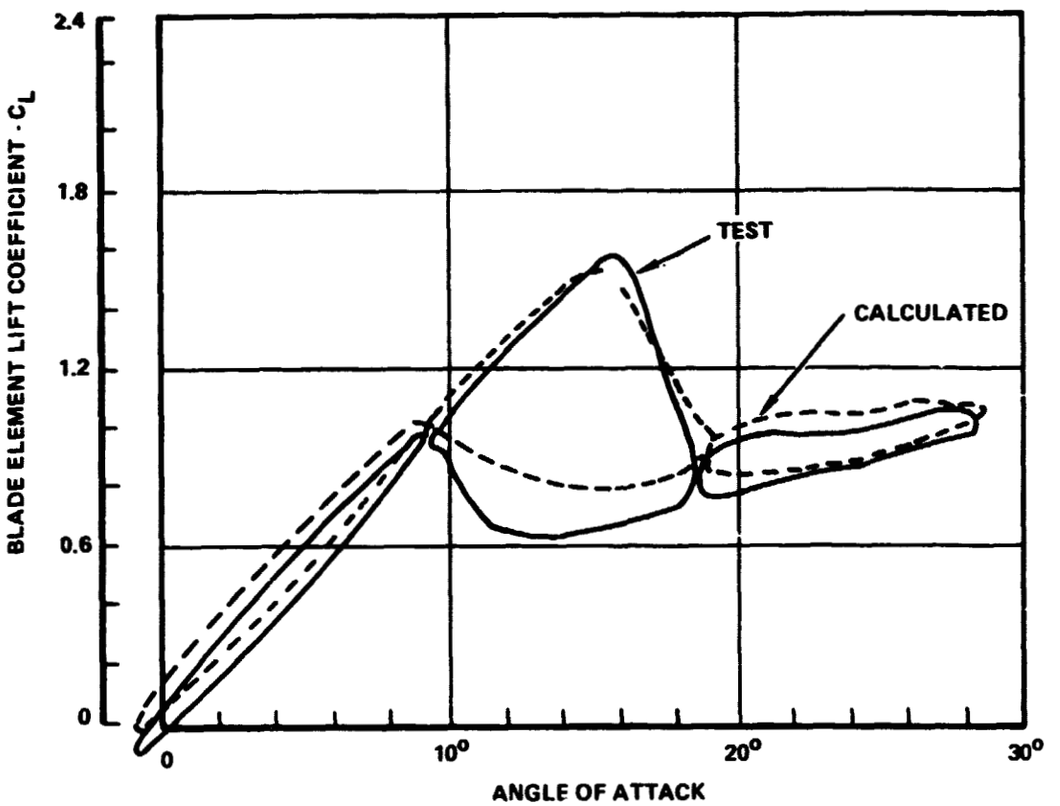

Figure 37. - Dynamic stall-lift coefficient vs angle-of-attack hysteresis loop.

The component of the lift force per unit span parallel to the blade chord axis is found correspondingly from:

$$\Delta F_C = \frac{C_L \, c \, \rho V^2}{2} \sin \alpha \tag{469}$$

The total chordwise force is then obtained by adding the corresponding drag coefficient term multiplied by $\cos \alpha$.

6.2.3.4.2 Pitching moment accounting for dynamic stall. - For determining pitching moments due to dynamic stall (see Reference 13), the reference or dynamic angle of attack given by α_{REF} must be modified. In REXOR II, this is accomplished by multiplying the second term by an empirical constant, K. Hence,

$$\alpha'_{REF} = \alpha'_{DYN} = \alpha - K \left(\gamma \sqrt{\left| \frac{c\dot{\alpha}}{2V} \right|} \; \text{sign}(\alpha) \right) \tag{470}$$

K is selected based upon the dynamic stall characteristics of the airfoil. In general it has been found for conventional rotor blade airfoils that K should be selected so that

$$\alpha'_{REF} = \alpha_{REF} + \Delta\alpha \tag{471}$$

where $\Delta\alpha$ is of the order of 2.5 degrees. With α'_{REF} calculated from the above equation, the moment coefficient is determined from tables such that,

$$C_M = C_M(\alpha'_{REF}, M) \tag{472}$$

A comparison of test and theoretical dynamic C_M from Reference 15 is shown in Figure 38.

The total pitching moment acting per unit span on a blade element is then given by:

$$T(i) = - C_M \, c^2 \frac{\rho V^2}{2} - F_{NO} \, S_Y(i) + \begin{bmatrix} \text{quasi-steady} \\ \text{aero} \\ \text{terms} \end{bmatrix} \tag{473}$$

(Section 6.2.3.3)

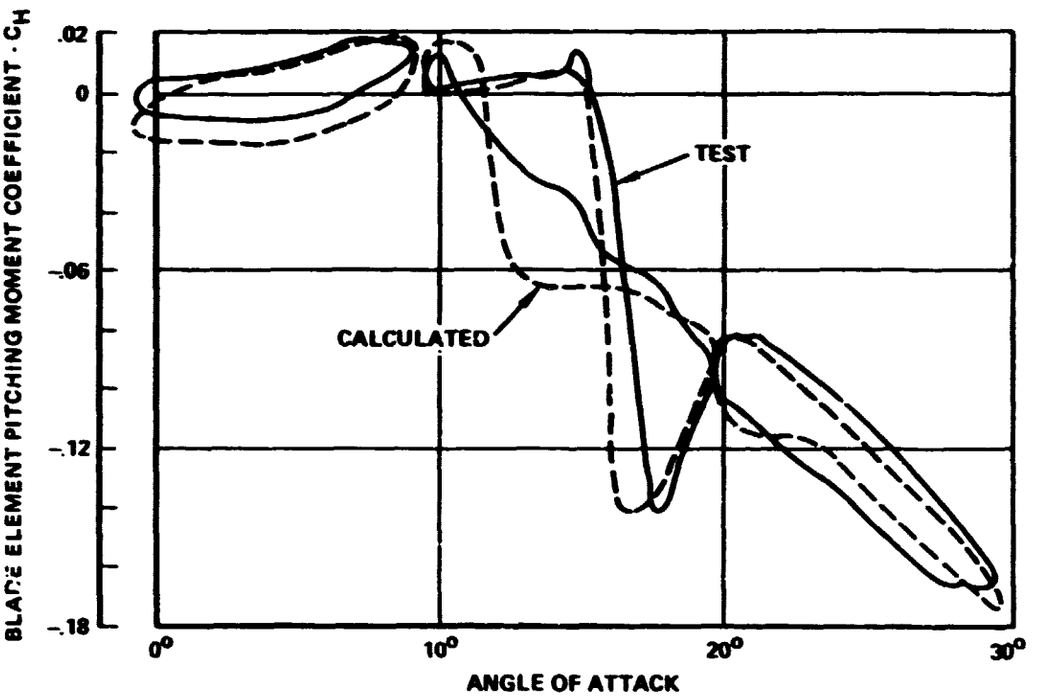

Figure 38. - Dynamic stall - moment coefficient vs angle-of-attack hysteresis loop.

where $S_Y(x)$ represents the distance from the aerodynamic center to the blade elastic axis, and the quasi-steady aerodynamic terms are included as described in Section 6.2.3.3.

6.2.4 Coefficient table lookup - overview. - In cataloging blade section aerodynamic data, C_l, C_D and C_M, there are two procedures available.

- Curve fit the aerodynamic data to the specific airfoil geometry being investigated for the range of Mach number and angle of attack to be considered.
- Tabulate the data as a function of performance and geometric parameters, and interpolate to the exact conditions at hand.

REXOR II uses the second procedure. The data consists of C_L, C_D and C_M tables. Each table is tabulated as a function of angle of attack and Mach number. The table format is organized identically to the Army C-81 program. Thus C-81 airfoil decks may be directly used in REXOR II.

A table set of NACA 0012 section characteristics is included as part of REXOR II. Two external tables may be used; the first of which overrides the resident 0012 data. Changeover of external tables occurs at a preselected blade radial station.

6.2.4.1 Inputs and outputs. - Each table (C_L, C_D, C_M) has a separate angle of attack entry and a common Mach entry. The separate entries are used for dynamic stall calculations. The outputs in addition to C_L, C_D and C_M are the zero angle-of-attack C_L and C_L vs angle of attack slope.

6.2.5 Blade element and rotor aerodynamic loads summary. - The required loads for use in the equations of motion are in BLn axis. Development to this form from BLE axis about this quarter chord point is covered in Section 5.6.4. The BLE axis form is:

$$\begin{Bmatrix} F_{X_A}(i) \\ F_{Y_A}(i) \\ F_{Z_A}(i) \\ M_{X_A}(i) \\ M_{Y_A}(i) \\ M_{Z_A}(i) \end{Bmatrix}_{BLE} = \left[\begin{array}{c|c} [T_{\alpha\text{-BLE}}] & [0] \\ \hline [0] & [T_{\alpha\text{-BLE}}] \end{array}\right] \begin{Bmatrix} 0 \\ -\frac{1}{2}\rho(U_C^2 + U_N^2)\, C_D(i) \\ \frac{1}{2}\rho(U_C^2 + U_N^2)\, C_L(i) \\ \frac{1}{2}\rho c(U_C^2 + U_N^2)\, C_M(i) \\ 0 \\ 0 \end{Bmatrix} +$$

$$+ \begin{Bmatrix} 0 \\ 0 \\ F_{Z_A}(i) \\ M_{X_A}(i) \\ 0 \\ 0 \end{Bmatrix}_{Unsteady,BLE} \tag{474}$$

where,

$$[T_{\alpha\text{-BLE}}] = \begin{bmatrix} 1 & 0 & 0 \\ 0 & \cos(\alpha_{3/4}\, c) & -\sin(\alpha_{3/4}\, c) \\ 0 & \sin(\alpha_{3/4}\, c) & \cos(\alpha_{3/4}\, c) \end{bmatrix} \tag{475}$$

6.3 Interference Terms

6.3.1 Nature of the Phenomenon. - In the process of producing lift, the various parts of the rotorcraft impart a net momentum change to the air mass opposite to the direction of the force produced. This induced air velocity from the momentum change impinges upon other elements of the rotorcraft changing their aerodynamic behavior.

The sources of interest are the main rotor and wing (or lifting body characteristics of the fuselage). The surfaces being affected are the wing plus fuselage and the empennage. The impinging velocity is expressed in Z_F (fuselage vertical) axis as a percentage of the source flow and a function of the wake angle of this flow.

A second interference velocity source is to consider the circulation part of the Theodorsen function. Here the wing or wing equivalent of the fuselage is producing lift at the quarter-chord point according to the air velocity at the 3/4-chord location. Accordingly, the vertical component of air velocity at the wing includes a component,

$$\frac{1}{2} C_{wing} \dot{q}_F \tag{476}$$

Here the wing quarter chord is assumed to lie on the Y_F axis. This component is also effective at the horizontal tail via the wing to horizontal tail downwash factor.

6.3.2 Rotor to wing/fuselage. - The downwash function (percentage of source flow) used in REXOR II is a lookup table of downwash factor, $F(\chi)_{MR-W}$, and idealized main rotor wake angle χ_{MR}

where,

$$\chi_{MR} = \tan^{-1}\left(\frac{u_H}{w_H - w_{iMR}}\right) \tag{477}$$

The table data is linearly interpolated to the required wake angle value.

The fuselage reference downwash velocity at the wing (or equivalent) then is

$$w_{WING} = w_F - w_{iMR} F(\chi)_{MR-W} + \frac{1}{2} C_{WING} q_F \tag{478}$$

and taking time derivatives,

$$\dot{w}_{WING} = \dot{w}_F - \dot{w}_{iMR} F(\chi)_{MR-W} + \frac{1}{2} C_{WING} \dot{q}_F \tag{479}$$

The total air velocity to the wing/fuselage is

$$V_{T_{WING}} = \left(u_F^2 + v_F^2 + w_{WING}^2\right)^{1/2} \tag{480}$$

and the angle of attack is

$$\alpha_{WING} = \tan^{-1}\left(\frac{w_{WING}}{u_F}\right) \tag{481}$$

The total velocity in the fuselage XZ plane is used in the empennage computations:

$$V_{X_Z} = \left(u_F^2 + w_{WING}^2\right)^{1/2} \tag{482}$$

6.3.3 Rotor to horizontal tail. - A downwash factor $F(X)_{MR-HT}$ between the main rotor and horizontal tail is computed in the same manner as $F(X)_{MR-W}$ from the main rotor wake angle χ_{MR}. This data in conjunction with the wing to horizontal tail downwash factor is used to compute incremental air velocities at the horizontal tail.

Evaluating the main rotor increment,

$$w_{iMR_I} = w_{iMR}\left(F(X)_{MR-HT} - F(X)_{MR-W}\right) \tag{483}$$

A increment for an upper horizontal tail is likewise generated:

$$w_{iMR_{IU}} = w_{iMR}\left(F(X)_{MR-HTU} - F(X)_{MR-W}\right) \tag{484}$$

6.3.4 Data sources. - The theoretical downwash factor ranges from 0 at $\chi = 0$ and 180 degrees to 2 at $\chi = 90$ in the fully contracted rotor wake. Several sources of measured data are available to construct a distribution for a given configuration. Reference 12 gives isolated rotor data for field distances and

wake angle ranges suitable for $F(X)_{MR-W}$ and $F(X)_{MR-HT}$. Reference 16 gives a good data set for typical wing locations.

6.3.5 Empennage velocity components. - REXOR II models the empennage assembly as either part of the fuselage-wing aerodynamic table (tail on) or as a separate set of aerodynamic loads (tail off). In either case a set of perturbation velocities is used.

The wing to horizontal tail downwash factor appears explicitly as a quasi-unsteady aerodynamic term. An airflow time delay from the wing to horizontal tail is computed as

$$\Delta t = \frac{\ell_{HT}}{V_{X_Z}} \tag{485}$$

Using the downwash factor $\partial\varepsilon/\partial\alpha$ the vertical airflow component at the horizontal tail is

$$\Delta t\ \dot{w}_{WING}\ \frac{\partial\varepsilon}{\partial\alpha} = \frac{\ell_{HT}}{V_{X_Z}}\ \dot{w}_{WING}\ \frac{\partial\varepsilon}{\partial\alpha} \tag{486}$$

In a like manner the delay in sidewash gives rise to the term $\ell_{VT}/V_{X_Z}\ \dot{r}_F\ \partial\sigma_{VT}/\partial\beta$ on the vertical tail.

The vertical incremental horizontal tail velocity is then:

$$\begin{aligned}\Delta w_{HT} = &-w_{iMR_I} + \ell_{HT}\left(q_F + \frac{\partial\varepsilon}{\partial\alpha}\ \dot{w}_{WING}\Big/ V_{X_Z}\right)\\ &+ \left(\tau_{EL}\ \delta_{EL} + \tau_{HT}\ \delta_{i_{HT}}\right)u_{HT}\end{aligned} \tag{487}$$

The terms τ_{EL} and τ_{HT} introduce equivalent velocities due to elevator and horizontal tail incidence deflections respectively.

Similarly for the upper horizontal tail:

$$\Delta w_{HTU} = -w_{iMR_{IU}} + \ell_{HTU}\left(q_F + \frac{\partial\varepsilon}{\partial\alpha}\dot{w}_{WING}\Big/ V_{X_Z}\right) \tag{488}$$

Assembling the vertical tail lateral incremental velocity:

$$\Delta v_{VT} = -\ell_{VT}\left(r_F - \frac{\partial \sigma_{VT}}{\partial \beta}\frac{\dot{\gamma}_F}{V_{T_{WING}}}\right) + h_{VT}\, p_F + \tau_{RVD}\,\delta_{RVD}\, u_{VT} \qquad (489)$$

Where τ_{RUD} is used to introduce an equivalent velocity due to rudder deflection.

A horizontal and vertical tail longitudinal total velocities are simply developed from a wake deficiency factor

$$u_{HT} = u_F\,\eta_{HT}\,, \qquad (490)$$

$$u_{HTU} = u_F\,\eta_{HTU} \qquad (491)$$

and

$$u_{VT} = u_F\,\eta_{VT} \qquad (492)$$

Then the total vertical velocity at the horizontal tail is:

$$w_{HT} = w_F - w_{iMR}\,F(\chi)_{MR-W} - u_F\,\epsilon_{FT} + \Delta w_{HT} \qquad (493)$$

and

$$w_{HTU} = w_F - w_{iMR}\,F(\chi)_{MR-W} - u_F\,\epsilon_{HTU} + \Delta w_{HTU} \qquad (494)$$

The induced flow field angles ϵ_{HT} and ϵ_{HTU} are a function of wing angle of attack, flap deflection and wing incidence change.

$$\epsilon_{HT} = \epsilon_{o_{HT}} + \frac{\partial \epsilon}{\partial \alpha}\sin\alpha_w + \frac{\partial \epsilon_{HT}}{\partial \alpha_{FL}}\,\delta_{FL} + \frac{\partial \epsilon_{HT}}{\partial i_w}\,\delta_{i_w} \qquad (495)$$

$$\epsilon_{HTU} = \epsilon_{o_{HTU}} + \frac{\partial \epsilon_{HTU}}{\partial \alpha}\sin\alpha_w + \frac{\partial \epsilon_{HTU}}{\partial \delta_{FL}}\,\delta_{FL} + \frac{\partial \epsilon_{HTU}}{\partial i_w}\,\delta_{i_w} \qquad (496)$$

The total lateral velocity at the vertical tail is

$$v_{VT} = v_F - u_F \sigma_{VT} + \Delta v_{VT} \tag{497}$$

Where σ_{VT} is a sidewash coefficient from the fuselage.

$$\sigma_{VT} = \frac{\partial \sigma_{VT}}{\partial \beta} \sin \beta_W \tag{498}$$

6.4 Body Loads

In this section the aerodynamic contributions from the fuselage, wing and empennage are developed. These components are added together with the tail rotor loads, Section 6.5, and auxiliary thrustors, Section 6.6. A transformation to fuselage axes is made from wind axes.

The fuselage, wing and empennage data is composed of STATIC, DERIV, and CONTROL elements. The STATIC data are the steady state load components as would be measured in a wind tunnel. These data may be tail on or off. The DERIV data give additional loads due to velocity component variations from trim for tail on STATIC data as well as steady offsets (unequal wing twist, etc.). Tail off DERIV loads use full tail velocity components rather than variations to generate the empennage forces and moments.

The CONTROL loads account for flap, dive brake, wing incidence, aileron deflection inputs via the control system. The rudder, upper and lower horizontal tail incidence, lower horizontal tail elevator inputs affect the empennage air velocity components, and are developed in Section 6.3.5.

6.4.1 Nonrotating airframe airloads. - The required loads are computed in REXOR II as the sum of steady-state forces and moments plus loads arising from stability derivative type terms and control surface inputs. The steady-state data are formed in terms of overall C_L, C_D, and C_M for the fuselage, wing, and empennage assembly.

The static body loads are:

$$\begin{Bmatrix} F_{X_B} \\ F_{Y_B} \\ F_{Z_B} \\ M_{X_B} \\ M_{Y_B} \\ M_{Z_B} \end{Bmatrix}_{W,STATIC} = \frac{\rho}{\rho_o} \begin{Bmatrix} -C_{D_I} Q_A \\ 0 \\ -C_{L_I} Q_A \\ 0 \\ C_{M_I} Q_A C_{WING} \\ 0 \end{Bmatrix} \tag{499}$$

where:

$$Q_A = \frac{1}{2} \rho S_{WING} V_{X_Z}^2 \tag{500}$$

The wing area, S_{WING}, and chord, C_{WING}, are actual or the equivalent of the lifting fuselage. Alternately, they may be the reference length and area used for the available wind tunnel data. C_{D_I}, C_{L_I} and C_{M_I} are linearly interpolated from input data tables of C_L, C_D, C_M, versus angle of attack, α_W. The data are interpolated on α_{WING} from Section 6.3.2. The loads developed are in wind axis.

The stability derivative load contributions are computed as a 6 by 7 derivative matrix postmultiplied by a velocity component vector. For tail on fuselage aerodynamic data:

$$\left\{\begin{matrix} F_{X_B} \\ F_{Y_B} \\ F_{Z_B} \\ M_{X_B} \\ M_{Y_B} \\ M_{Z_B} \end{matrix}\right\}_{W,DERIV} = \frac{\rho}{\rho_c} \left[F_{MN} \right] \left\{\begin{matrix} u_F^2 \\ v_F^2 \\ |u_F| v_F \\ |u_F| p_F \\ |u_F| \Delta w_{HT} \\ |u_F| \Delta v_{VT} \\ |u_{HTU}| \Delta w_{HTU} \end{matrix}\right\} \tag{501}$$

The components of the $[F_{MN}]$ matrix are discussed in Volume III. Two horizontal tails and one vertical are assumed. The upper tail is considered optional. The matrix also provides for asymmetric effects of wing incidence differential, for linear and quadratic sideslip variations and for wing roll damping.

For tail off data the velocity vector is replaced by

$$\left\{\begin{matrix} u_F^2 \\ v_F^2 \\ |u_F| v_F \\ |u_F| p_F \\ |u_{HT}| w_{HT} \\ |u_{VT}| v_{VT} \\ |u_{HTU}| w_{HTU} \end{matrix}\right\} \tag{502}$$

These terms also produce forces and moments in wind axes.

REXOR II includes the effects of flaps, ailerons and dive brakes in the non-rotating aerodynamic loads. The flap deflections are modeled as linear stability derivatives of C_L, C_D and C_M. The aileron load is the variation of aileron moment volume (rolling moment coefficient times wing area times wing span) with aileron deflection. The input is for one aileron. Dive brakes are represented as a variation of drag area with brake extension. The brake panels are assumed to be on the fuselage vertical axis and a distance - h_{DB} below the fuselage reference.

The desired loads are:

$$\begin{Bmatrix} F_{X_B} \\ F_{Y_B} \\ F_{Z_B} \\ M_{X_B} \\ M_{Y_B} \\ M_{Z_B} \end{Bmatrix}_{W,CONTROL} = \frac{\rho}{\rho_o} \begin{Bmatrix} -\left(\frac{\partial C_D}{\partial \delta_{FL}} \delta_{FL} + \frac{\partial C_D}{\partial \delta_{DB}} \delta_{DB} + \frac{\partial C_D}{\partial \alpha_w} \delta i_w\right) Q_A \\ 0 \\ -\left(\frac{\partial C_L}{\alpha \delta_{FL}} \delta_{FL} + \frac{\partial C_L}{\partial \alpha_w} \delta i_w\right) Q_A \\ 2 \frac{\partial Y_{AIL}}{\partial \delta AIL} \delta_{AIL} Q_A \\ \left(\frac{\partial CM}{\partial \delta FL} C_w \delta_{FL} + h_{DB} \frac{\partial C_D}{\partial \delta DB} + \frac{\partial C_M}{\partial i_w} C_w \delta i_w\right) Q_A \\ 0 \end{Bmatrix} \quad (503)$$

The static and derivative terms are added to form the total body loads and transformed into fuselage axes.

$$\begin{Bmatrix} F_{X_B} \\ F_{Y_B} \\ F_{Z_B} \\ M_{X_B} \\ M_{Y_B} \\ M_{Z_B} \end{Bmatrix}_F = \left[\begin{array}{cc:cc} [T_{\alpha_W}] & [T_{\beta_W}] & [0] & \\ & & & \\ \hdashline & & & \\ [0] & & [T_{\alpha_W}] & [T_{\beta_W}] \end{array}\right] \left\{ \begin{Bmatrix} F_{X_B} \\ F_{Y_B} \\ F_{Z_B} \\ M_{X_B} \\ M_{Y_B} \\ M_{Z_B} \end{Bmatrix}_{W,STATIC} + \begin{Bmatrix} F_{X_B} \\ F_{Y_B} \\ F_{Z_B} \\ M_{X_B} \\ M_{Y_B} \\ M_{Z_B} \end{Bmatrix}_{W,DERIV} + \begin{Bmatrix} F_{X_B} \\ F_{Y_B} \\ F_{Z_B} \\ M_{X_B} \\ M_{Y_B} \\ M_{Z_B} \end{Bmatrix}_{W,CONTROL} \right\} \tag{504}$$

where,

$$[T_{\alpha_W}] = \begin{bmatrix} \cos(\alpha_W) & 0 & -\sin(\alpha_W) \\ 0 & 1 & 0 \\ \sin(\alpha_W) & 0 & \cos(\alpha_W) \end{bmatrix} \tag{505}$$

$$\left[T_{\beta_W}\right] = \begin{bmatrix} \cos(\beta_W) & -\sin(\beta_W) & 0 \\ \sin(\beta_W) & \cos(\beta_W) & 0 \\ 0 & 0 & 1 \end{bmatrix} \tag{506}$$

and

$$\cos(\alpha_W) = u_F/V_{X_Z} \tag{507}$$

$$\sin(\alpha_W) = w_{WING}/V_{X_Z} \tag{508}$$

$$\cos(\beta_W) = V_{X_Z}/V_{T_{WING}} \tag{509}$$

$$\sin(\beta_W) = v_F/V_{T_{WING}} \tag{510}$$

The air velocities w_{WING}, V_{X_Y}, $V_{T_{WING}}$, are defined in Section 6.3.2.

6.4.2 Component additional airloads. - A total array, {QLOADS}, of non main rotor air loads is computed in fuselage axes.

$$\begin{Bmatrix} F_X \\ F_Y \\ F_Z \\ F_\phi \\ F_\theta \\ F_\psi \end{Bmatrix}_{F_A} = \left\{QLOADS\right\}_F = \begin{Bmatrix} F_{X_B} \\ F_{Y_B} \\ F_{Z_B} \\ M_{X_B} \\ M_{Y_B} \\ M_{Z_B} \end{Bmatrix}_F + \begin{Bmatrix} F_{X_{TR}} \\ F_{Y_{TR}} \\ F_{Z_{TR}} \\ M_{X_{TR}} \\ M_{Y_{TR}} \\ M_{Z_{TR}} \end{Bmatrix}_F + \begin{Bmatrix} F_{X_P} \\ F_{Y_P} \\ F_{Z_P} \\ M_{X_P} \\ M_{Y_P} \\ M_{Z_P} \end{Bmatrix}_F \tag{511}$$

The first component is described above. The tail rotor load vector auxiliary thrustor load vector are developed in the following sections.

6.5 Tail Rotor

A number of different levels of aerodynamic presentation accuracy and axis of representation may be used for tail rotor computations. In line with the stated objectives of REXOR II, a linear aerodynamic approach is used. A shaft axis reference is used for the analysis. In this system, the air velocity quantities involved are easy to visualize. Also, the flapping and feathering motions are the true, measureable quantities.

6.5.1 Formulations. - First, consider the airflow quantities available in fuselage axis, Figure 39. Note the tail rotor axes alignment with respect to the fuselage axis system. Formulating the components with respect to the fuselage axes gives:

$$\begin{Bmatrix} u_{TR} \\ v_{TR} \\ w_{TR} \end{Bmatrix}_F = \begin{Bmatrix} u_F \ \eta_{TR} \\ v_F - u_F \ \sigma_{TR} - \ell_{TR} \left(r_F - \frac{\partial \sigma_{TR}}{\partial \beta} \frac{\dot{v}_F}{\omega_w} \right) + h_{TR} \ P_F \\ \omega_{HT} \end{Bmatrix} \qquad (512)$$

where

$$\sigma_{TR} = \frac{\partial \sigma_{TR}}{\partial \beta} \ \text{Sin} \ \beta_w \qquad (513)$$

The vertical component is approximated by the horizontal tail value. Terms subscripted w refer to velocity, w, and sideslip angle, β, at the wing. The flow effects induced by the wing-fuselage bombination are described by the wake velocity deficiency fact or η_{TR}, the side wash angle, τ_{TR}, and its variation with angle of sideslip.

The velocity vector is then rotated through the tail rotor shaft lateral tilt, $\phi_{o_{TR}}$.

$$\begin{Bmatrix} u \\ v \\ w \end{Bmatrix}_{TR} = \begin{bmatrix} 1 & 0 & 0 \\ 0 & \cos\phi_o & \sin\phi_o \\ 0 & -\sin\phi_o & \cos\phi_o \end{bmatrix}_{TR} \begin{Bmatrix} u_{TR} \\ v_{TR} \\ w_{TR} \end{Bmatrix}_F \qquad (514)$$

Constructing the blade element tangential (U_T) and perpendicular (U_P) components, as shown in Figure 40 gives:

$$U_T = (r\,\Omega)_{TR} + u_{TR} \sin \psi_{TR} \tag{515}$$

$$U_P = - v_{TR} - w_{iTR} - r\dot{\beta} - u_{TR}\,\beta \cos \psi_{TR} \tag{516}$$

where,

w_{iTR} is the tail rotor induced velocity

and

$$V_{TR} = - v_{TR} - w_{iTR} \tag{517}$$

Expressing the blade element angle of attack as a small angle of approximation,

$$\alpha_{TR} = \theta + \frac{U_P}{U_T} \tag{518}$$

where,

$$\theta = \theta_{TR} - A_1 \cos \psi_{TR} - B_1 \sin \psi_{TR} \tag{519}$$

A $\delta_{3_{TR}}$ coupling is used to minimize tail rotor flapping. Defining $+\delta_{3_{TR}}$ as a reduction in feathering for positive flapping gives

$$\theta = \theta_{TR} + \delta_{3TR}\, a_{1_{TR}} \cos \psi_{TR} + \delta_{3TR}\, b_{1_{TR}} \sin \psi_{TR} \tag{520}$$

The tail rotor analysis assumes no coning.

The blade flapping, β, is then

$$\beta = - a_{1_{TR}} \cos \psi_{TR} - b_{1_{TR}} \sin \psi_{TR} \tag{521}$$

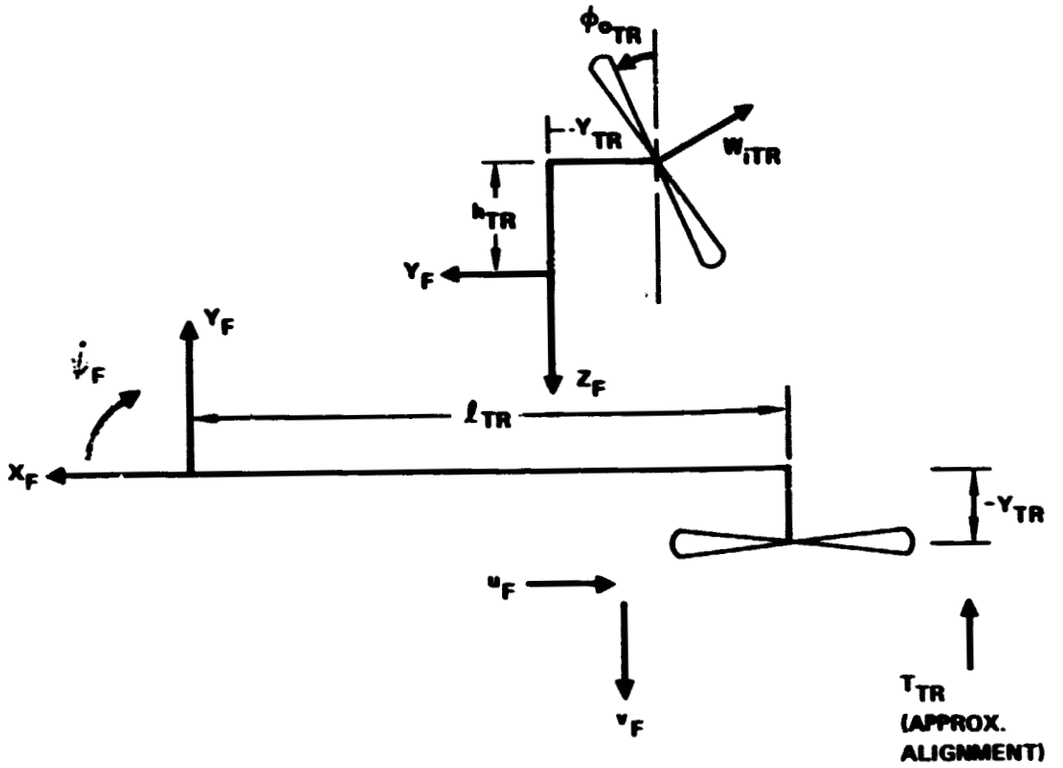

Figure 39. - Overall tail rotor geometry.

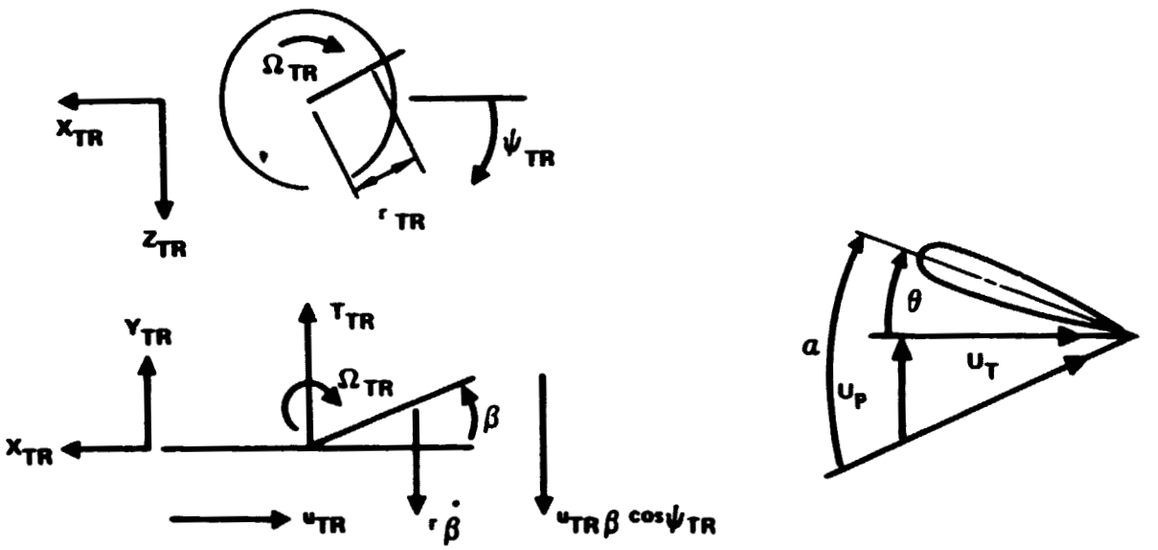

Figure 40. - Tail rotor blade element detail.

The tail rotor expressions of interest are the prime forces added to the fuselage system. First looking at the tail rotor thrust. For a blade element we have

$$d\,T_{TR} = \left[\frac{1}{2}\,\rho a\,b\,c\,\alpha\,U_T^{\,2}\,dr\right]_{TR} \tag{522}$$

where a is the lift curve slope, b is the number of tail rotor blades, and c is the blade chord (assumed constant).

Substituting,

$$d\,T_{TR} = \left[\frac{1}{2}\,\rho a\,b\,c\,(\theta U_T^{\,2} + U_P\,U_T)dr\right]_{TR} \tag{523}$$

Integrating for the entire rotor,

$$T_{TR} = \left[\frac{1}{2\pi}\,\frac{1}{2}\,\rho a\,b\,c\int_0^{2\pi}\int_0^{BR}(\theta U_T^{\,2} + U_P\,U_T)dr\,d\psi\right]_{TR} \tag{524}$$

where B is the finite airfoil lift factor expressed as a so-called tip loss factor.

Noting only even functions contribute to the integrand.

$$T_{TR} = \frac{1}{2}\,\rho a(b\,c\,R)_{TR}\left(\theta_{TR}\,\frac{B^3}{3}\,(\Omega R)^2_{TR} + \theta_{TR}\,\frac{B}{2}\,u_{TR}^{\,2}\right.$$

$$\left. + \frac{B^2}{2}\,(\Omega R)_{TR}\,v_{TR} + (\Omega R)_{TR}\,u_{TR}\,b_{1_{TR}}\,\frac{B^2}{2}\,\delta_{3TR}\right) \tag{525}$$

Note the thrust is independent of the longitudinal flapping, but is a function of lateral cyclic shown as lateral flapping times delta 3.

The required lateral flapping angle is obtained by equating the lateral flapping moment equal to zero.

$$0 = \left[\frac{1}{2\pi} \frac{1}{2} \rho a b c \int_0^{2\pi} \int_0^{BR} (\theta U_T^2 + U_P U_T) \cos \psi \, r \, dr \, d\psi \right]_{TR} \tag{526}$$

gives

$$b_{1_{TR}} = - a_{1_{TR}} \delta_{3TR} \tag{527}$$

To obtain the longitudinal flapping angle, the longitudinal rotor moment is formed and set equal to zero.

$$0 = \left[\frac{1}{2\pi} \frac{1}{2} \rho a b c \int_0^{2\pi} \int_0^{BR} (\theta U_T^2 + U_P U_T) \sin \psi \, r \, dr \, d\psi \right]_{TR} \tag{528}$$

gives

$$a_{1_{TR}} = \frac{u_{TR}\left(\theta_{TR}(\Omega R)_{TR} \frac{8B}{3} + 2V_{TR}\right)}{\delta_{3TR}\left(B^2(\Omega R)_{TR}^2 + \frac{3}{2} u_{TR}^2\right) + B^2(\Omega R)_{TR}^2 - \frac{1}{2} u_{TR}^2} \tag{529}$$

In formulating the tail rotor drive torque, the blade profile drag is expressed as

$$\bar{C}_D = C_{D_0} + k \bar{C}_L^4 \tag{530}$$

where $\bar{C}_L$ is the average lift coefficient. Reviewing the thrust equation with a constant (average) lift coefficient gives

$$T_{TR} = \left[\frac{1}{2\pi} \frac{1}{2} \rho b c \bar{C}_L \int_0^{2\pi} \int_0^{BR} U_T^2 \, dr \, d\psi \right]_{TR} \tag{531}$$

gives

$$C_L = 6 T_{TR} \Big/ \left(\rho \sigma_{TR} A_{TR} \left(B^3 (\Omega R)^2_{TR} + \frac{3}{2} B u_F^2 \right) \right) \tag{532}$$

The drive torque is expressed as the reaction to turning the tail rotor shaft. The plus sign is associated with a clockwise sense of rotation when facing a left-hand mounted tail rotor.

$$d Q_{TR} = \pm \left[-\frac{1}{2} \rho c b r U_T^2 \bar{C}_D + \frac{1}{2} \rho a b c \alpha \phi r U_T^2 \right]_{TR} dr \tag{533}$$

where

$$\phi = \frac{U_P}{U_T} \tag{534}$$

integrating

$$Q_{TR} = \pm \left[\frac{1}{2\pi} \frac{1}{2} \rho b c \int_0^{2\pi} \left(\int_0^{R} - U_T^2 \bar{C}_D \, r \, dr + \int_0^{BR} (a U_T U_P \theta - a U_P^2) r dr \right) d\psi \right]$$

$$= \pm \frac{1}{2} \rho (b c R)_{TR} R_{TR} \left(-\frac{\bar{C}_D}{4} (\Omega R)^2 - \frac{\bar{C}_D}{4} u_{TR}^2 \right.$$

(continued on next page)

$$+ a\,(\Omega R)_{TR}\,\frac{B^3}{3}\,V\,\theta + a\,V_{TR}^2\,\frac{B^2}{2}$$

$$+ a\,a_{1TR}\left(1 - \delta_{3TR}^2\right)V_{TR}\,u_{TR}\,\frac{B^2}{2} + (\Omega R)_{TR}^2\,\frac{B^2}{8}\,a_{1TR}^2\left(1 + \delta_{3TR}^2\right)$$

$$+ a\,a_{1TR}^2\,u_{TR}^2\,\frac{B^2}{8}\left(3 - \delta\frac{2}{3TR}\right)\Bigg) \tag{535}$$

The remaining load term in X_{TR}. Using the same formulation methodology,

$$d\,X_{TR} = -\left[\frac{1}{2}\,\rho\,b\,c\,\bar{C}_D\,U_T^2\,\sin\psi\right.$$

$$\left. - \frac{1}{2}\,\rho\,a\,b\,c\,\alpha\,U_T^2\,(\sin\phi\,\sin\psi + \sin\beta\,\cos\psi)\right]_{TR} dr \tag{536}$$

Making small angle approximations,

$$d\,X_{TR} = \frac{1}{2}\rho(b\,c)_{TR}\left[-\bar{C}_D\,U_T^2\,\sin\psi\right.$$

$$+ a(\theta U_T\,U_P + U_P^2)\,\sin\psi$$

$$\left. - a(\theta\,U_T^2 + U_P\,U_T)\,(a_1\cos^2\psi + b_1\,\sin\psi\,\cos\psi)\right]_{TR} dr \tag{537}$$

integrating

$$X_{TR} = \frac{1}{2\pi}\frac{1}{2}\rho(b\,c)_{TR}\Bigg[\int_0^{2\pi}\Bigg(\int_0^{R} -\bar{C}_D\,U_T^2\sin\psi\;dr + \int_0^{BR}\Bigg(a(\theta U_T U_P + U_P^2)\sin\psi - a(\theta U_T^2 + U_P U_T)(a_1\cos^2\psi + b_1\sin\psi\cos\psi)\Bigg)dr\Bigg)d\psi\Bigg]_{TR}$$

$$= \frac{1}{2}\rho a(b\,c\,R)_{TR}\left(-a_1\theta(\Omega R)^2\frac{B^3}{3} - a_1\frac{B^2}{2}V_{TR}(\Omega R)_{TR} + V_{TR}u_{TR}\theta\frac{B}{2} - a_1^2\left(1+3\delta_{3TR}^2\right)u_{TR}\frac{B^2}{4}(\Omega R)_{TR} - a_1\left(1+\delta_{3TR}^2\right)(\Omega R)_{TR}V_{TR}\frac{B^2}{4} - \frac{C_D}{2a}(\Omega R)_{TR}u_{TR}\right) \qquad (538)$$

The induced velocity is calculated from simplified momentum balance.

$$v_{iTR} = T_{TR}\Big/\left((2\rho\pi R^2 B^2)_{TR}\left(u_{TR}^2 + v_{TR}^2 + u_{TR}^2\right)^{1/2}\right) \qquad (539)$$

Normally, the thrust, flapping, and induced velocity equations are solved as an iterative set. In REXOR II, these equations are solved for every pass (azimuth step) of the main rotor, and the tail rotor set convergence is assumed a priori.

Note that the pitch-flap coupling does not appear in the expressions developed. This is due to the equivalence of flapping and feathering, coupled with the absence of lateral flapping.

6.5.2 Airloads - Control settings. - The force and moment terms are assembled for use in the overall fuselage loads, Section 6.4 The pilot control is the rudder pedals θ_{TR}.

$$\begin{Bmatrix} F_{X_{ATR}} \\ F_{Y_{ATR}} \\ F_{Z_{ATR}} \end{Bmatrix}_F = \frac{\rho}{\rho_o} \begin{bmatrix} 1 & 0 & 0 \\ 0 & \cos\phi_o & -\sin\phi_o \\ 0 & \sin\phi_o & \cos\phi_o \end{bmatrix}_{TR} \begin{Bmatrix} X_{TR} \\ T_{TR}\ S_{TR} \\ 0 \end{Bmatrix} \tag{540}$$

$$\begin{Bmatrix} M_{X_{ATR}} \\ M_{Y_{ATR}} \\ M_{Z_{ATR}} \end{Bmatrix}_F = \frac{\rho}{\rho_o} \begin{bmatrix} 1 & 0 & 0 \\ 0 & \cos\phi_o & -\sin\phi_o \\ 0 & \sin\phi_o & \cos\phi_o \end{bmatrix}_{TR} \begin{Bmatrix} 0 \\ -Q_{TR} \ *\text{Sign}\ (G_{TR}) \\ 0 \end{Bmatrix}$$

$$+ \begin{bmatrix} o & h & \bar{y} \\ -h & 0 & \ell \\ -y & -\ell & 0 \end{bmatrix}_{TR} \begin{Bmatrix} F_{X_{ATR}} \\ F_{Y_{ATR}} \\ F_{Z_{ATR}} \end{Bmatrix}_F \tag{541}$$

S_{TR} is a factor to account for in blockage on the tail rotor thrust. The equations for X_{TR}, T_{TR} and Q_{TR} are based on ρ_o, the sea level density. The sign of G_{TR} allows for a tail rotating in a negative direction; i.e., upper top moving forward.

6.6 Auxiliary Thrustors

REXOR II models the compound helicopter configuration by the inclusion of an auxiliary source of forward thrust. A perturbation bypass jet math model is used. It is assumed that all the thrust units are at the same setting. Furthermore the dynamics of the engine rotating mass are ignored.

6.6.1 Formulations and airloads. - Based on a perturbation model the thrust for all units installed is:

$$T_P = \left(\frac{\partial T}{\partial \delta_p^2} \delta_p^2 + \frac{\partial T}{\partial M_p} M_p + \frac{\partial T}{\partial (M_p \delta_p)} M_p \delta_p \right) \frac{\rho}{\rho_o} \tag{542}$$

where M_p is the freestream Mach number and δ_p represents the total engine control parameter.

The engines are located at height h_p and distance ℓ_p aft of the fuselage axes. A thrust angle θ_o is also assumed. The engine contributions to the fuselage aerodynamic loads are then:

$$\begin{Bmatrix} F_{X_{AP}} \\ F_{Y_{AP}} \\ F_{Z_{AP}} \end{Bmatrix}_F = \begin{bmatrix} \cos\theta_o & 0 & \sin\theta_o \\ 0 & 1 & 0 \\ -\sin\theta_o & 0 & \cos\theta_o \end{bmatrix}_P \begin{Bmatrix} T_p \\ 0 \\ 0 \end{Bmatrix} \tag{543}$$

$$\begin{Bmatrix} M_{X_{AP}} \\ M_{Y_{AP}} \\ M_{Z_{AP}} \end{Bmatrix}_F = \begin{bmatrix} 0 & h_p & 0 \\ -h_p & 0 & \ell_p \\ 0 & -\ell_p & 0 \end{bmatrix} \begin{Bmatrix} F_{X_{AP}} \\ F_{Y_{AP}} \\ F_{Z_{AP}} \end{Bmatrix}_F \tag{544}$$

7. CONTROL SYSTEM

7.1 Overview

REXOR II models vehicles ranging from pure helicopters to winged helicopters to compound helicopters with conventional airplane control surfaces. The control system is modeled as a set of pilot controls (stick, rudder pedals, collective, etc.) which are coupled to the helicopter and airplane aerodynamic surfaces through a set of overall linkage factors (gains). These gains are slaved to a master control (phasing unit) which can be varied from the extremes of pure helicopter to pure airplane type of controls.

7.2 Pilot Controls

To simplify the operation of REXOR II the control inputs are mostly expressed as a percent of full scale (maximum input). The pilot inputs are:

$\% X_{c,p}$	Longitudinal stick
$\% Y_{c,p}$	Lateral stick
$\% r_{c,p}$	Rudder pedals
$\% \delta_{p,p}$	Propulsion setting
$\% \theta_{o,p}$	Collective blade angle
$\Psi_{R,p}$	Rotor speed setting
$\% \delta_{DB,p}$	Dive brake extension angle
$\% \delta_{FL,p}$	Flap extension angle
$\% \delta_{iw,p}$	Command wing incidence change
$\% \delta_{iHT,p}$	Command horizontal tail incidence change.

Pilot controls are combined with trim (T), initial condition (IC), rigging offset (subscript 0), and stability augmentation inputs (SAS). These combined inputs then operate the rotor and fixed aerodynamic surfaces. Scaling factors (K) convert the percentage inputs into angular and linear deflections.

$$X'_c = K_{XCFS}\, G_c(\%X_{c,T} + \%X_{c,p}) + X_{c,SAS} + \frac{\partial X_c}{\partial \theta_0}\,\theta_0 \qquad (545)$$

$$\delta_{EL} = K_{ELFS}\, G_{EL}(\%X_{c,T} + \%X_{c,p}) + \delta_{EL,0} + \delta_{EL,SAS} \qquad (546)$$

$$Y'_c = K_{YCFS}\, G_c(\%Y_{c,T} + \%Y_{c,p}) + Y_{c,SAS} + \frac{\partial Y_c}{\partial \theta_0}\theta_0 \qquad (547)$$

$$\delta_{AIL} = K_{AILFS}\, G_{AIL}(\%Y_{c,T} + \%Y_{c,p}) + \delta_{AIL,0} + \delta_{AIL,SAS} \qquad (548)$$

$$\theta_{OTR} = K_{TRFS}\, G_{TR}(\%r_{c,T} + \%r_{c,p}) + \theta_{oTR,0} + \theta_{OTR,SAS} + \frac{\partial \theta_{oTR}}{\partial \theta_0}\theta_0 \qquad (549)$$

$$\delta_{RUD} = K_{RUDFS}\, G_{RUD}(\%r_{c,T} + \%r_{c,p}) + \delta_{RUD,0} + \delta_{RUD,SAS} \qquad (550)$$

$$\theta_o = K_{\theta_{FS}}\, (\%\theta_{o,p} + \%\theta_{o,T}) - (Z_{sp} - Z_{sp,T})/e \qquad (551)$$

$$\text{where } Z_{sp} = Z_{sp,T}\Big|_{t = t_{TRIM} = t_{FLY}} \qquad (552)$$

$$\delta_p = K_{PFS}\, (\%\delta_{p,T} + \%\delta_{p,p}) \qquad (553)$$

$$\delta_{DB} = K_{DBFS}\, (\%\delta_{DB,p} + \%\delta_{DB,IC}) \qquad (554)$$

$$\delta_{FL} = K_{FLFS}\, (\%\delta_{FL,p} + \%\delta_{FL,IC}) \qquad (555)$$

$$\delta_{iw} = K_{iwFS}\, (\%\delta_{iw,p} + \%\delta_{iw,IC}) \qquad (556)$$

$$\delta_{iHT} = K_{iHTFS}\, (\%\delta_{iHT,p} + \%\delta_{iHT,IC}) \qquad (557)$$

$$\delta_{iHTU} = K_{iHTFS}\, (\%\delta_{iHTU,IC}) \qquad (558)$$

The factors G_c, G_{EL}, G_{AIL}, G_{TR}, G_{RUD} are the slaved gains controlled by the phasing unit.

The quantities X'_c, Y'_c are processed through a first order lag and rate limiting prior to being applied as swashplate input commands, X_c and Y_c.

$$\begin{Bmatrix} X_c \\ Y_c \end{Bmatrix} = \left(\frac{1}{\tau_A S + 1} \right) \begin{Bmatrix} X_c' \\ Y_c' \end{Bmatrix} \tag{559}$$

$$\left\| \begin{Bmatrix} \dot{X}_c \\ \dot{Y}_c \end{Bmatrix} \right\| \leq \dot{\delta}_{MAX} \tag{560}$$

The fixed aerodynamic surface motions are shown in Figure 41. The pilot inputs are depicted in Figure 42.

7.3 Stability Augmentation Systems

REXOR II incorporates stability augmentation inputs to the lateral and longitudinal cyclic inputs, elevator, aileron, tail rotor collective, and rudder. These SAS inputs are all derived from fuselage axis angular rate information. Signal processing consists of a low frequency washout and limiter applied to all throughput. A first order lag is also used on some signals.

The SAS coefficients are also computed on the basis of percentage of full scale deflection of the pilot control they are connected to. The same scaling conversion factors as used for the pilot inputs are applied to the SAS outputs.

The six SAS channels are shown below, Figures 43 through 48.

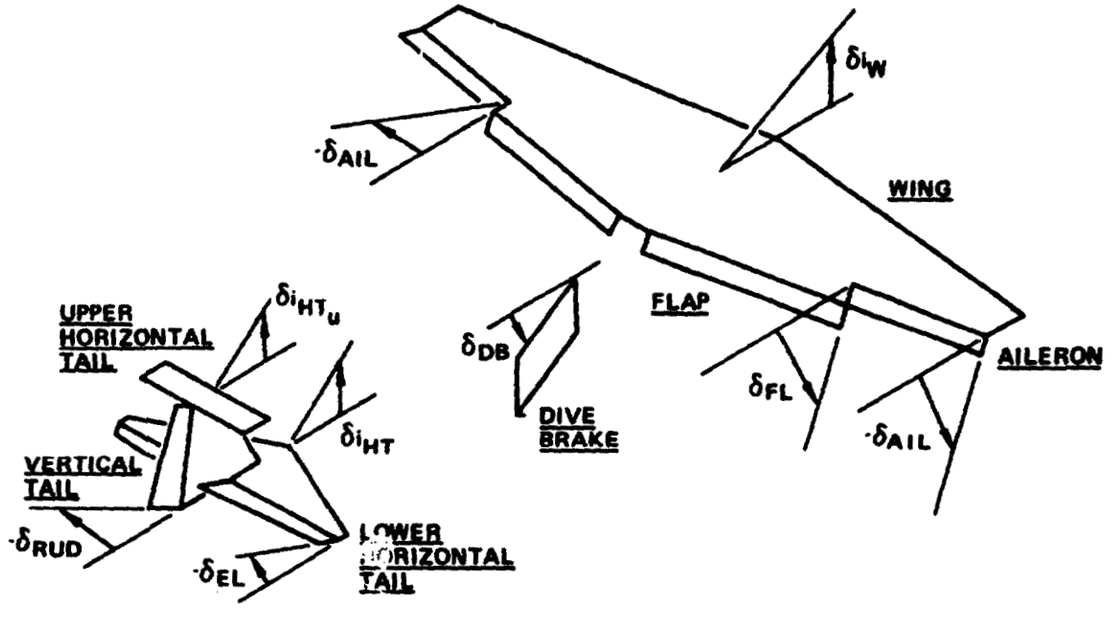

Figure 41. - Fixed aerodynamic surfaces.

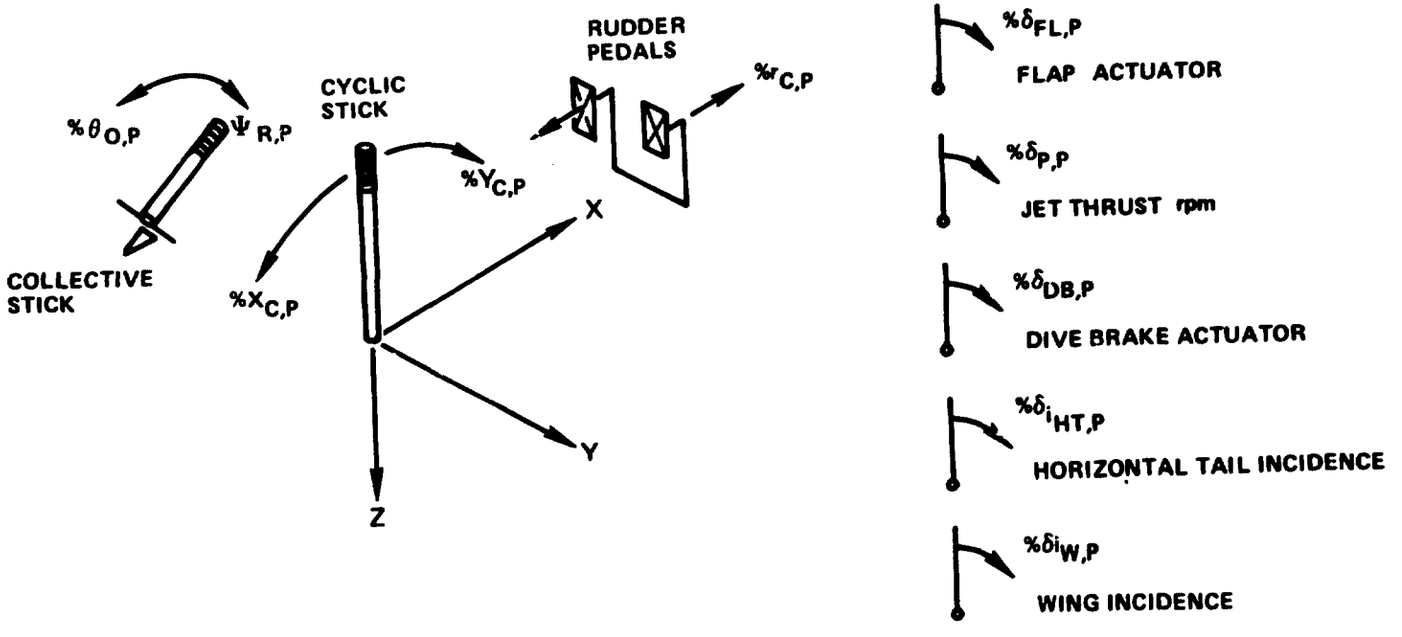

Figure 42. - Pilot controls.

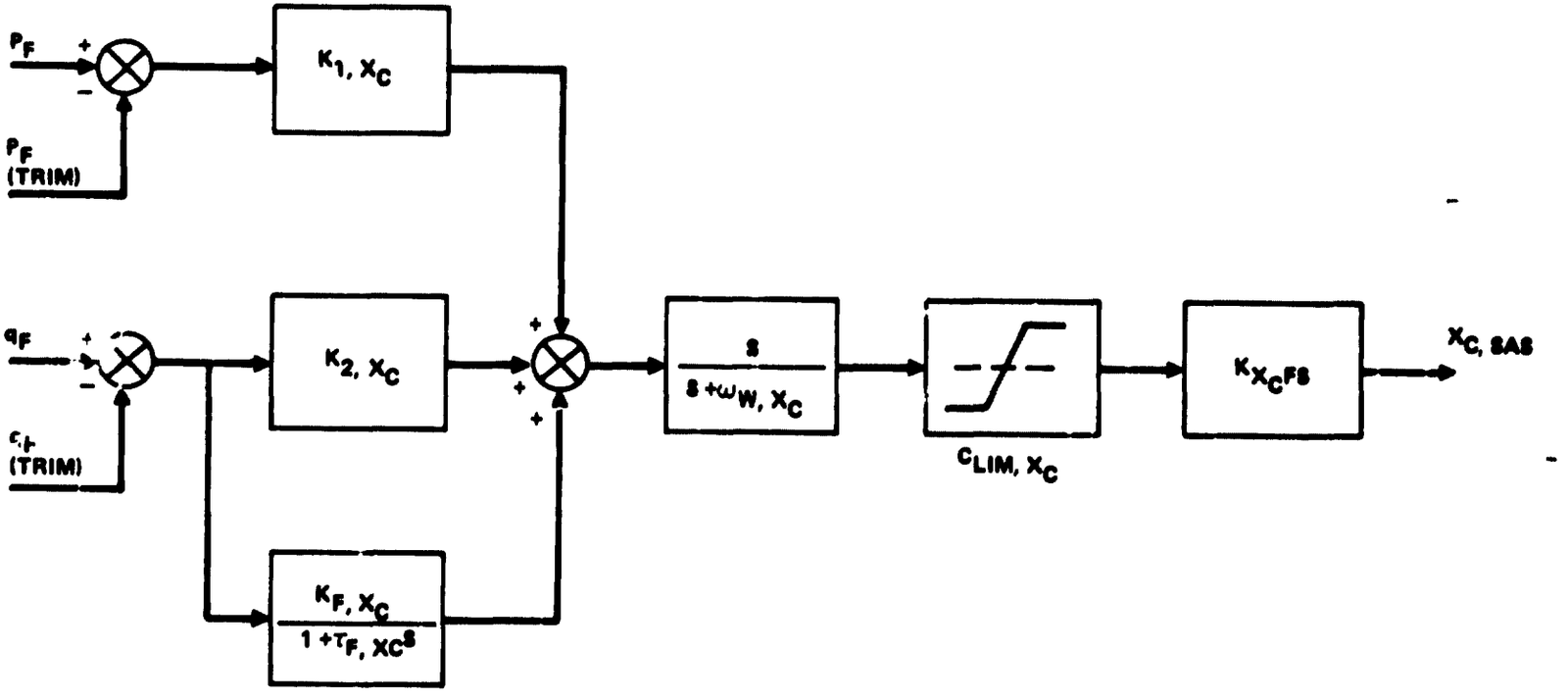

Figure 43. - Longitudinal cyclic stability augmentation.

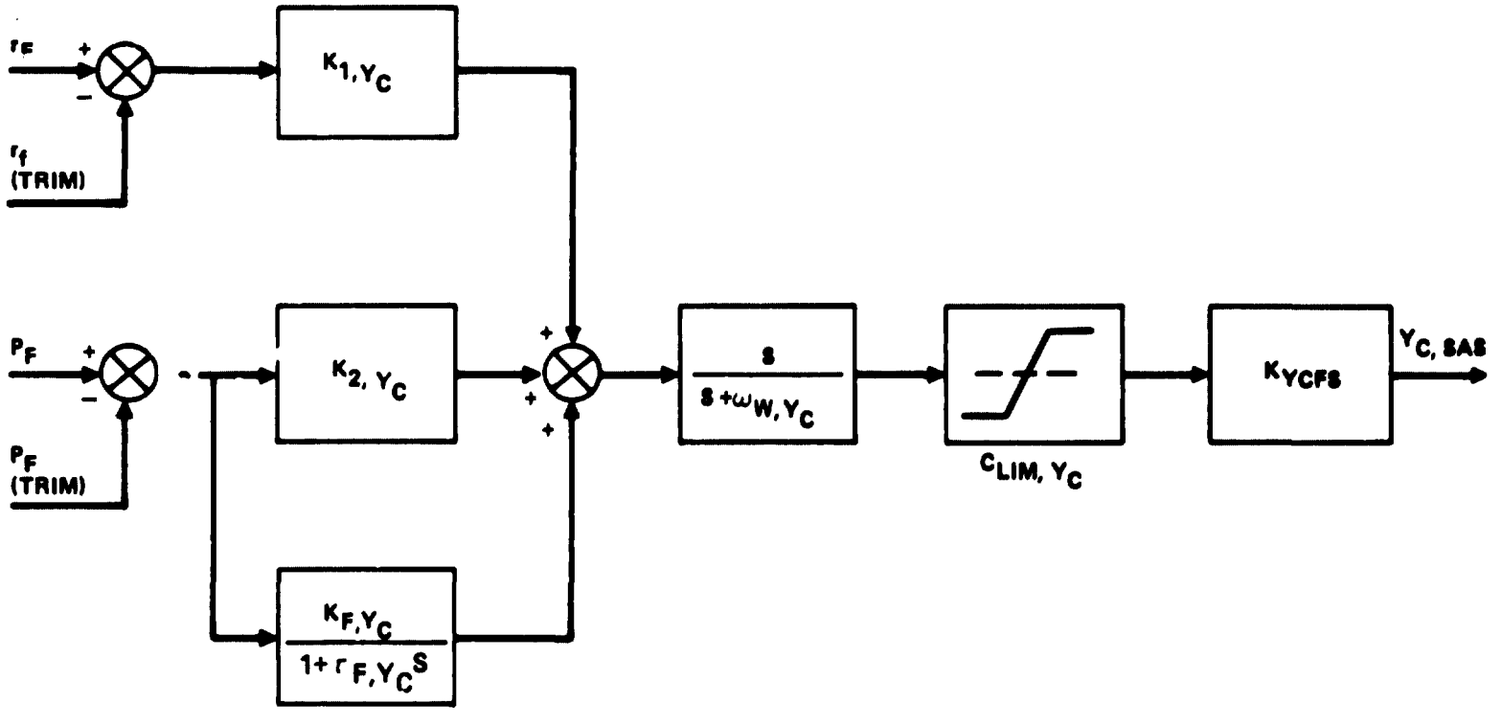

Figure 44. - Lateral cyclic stability augmentation.

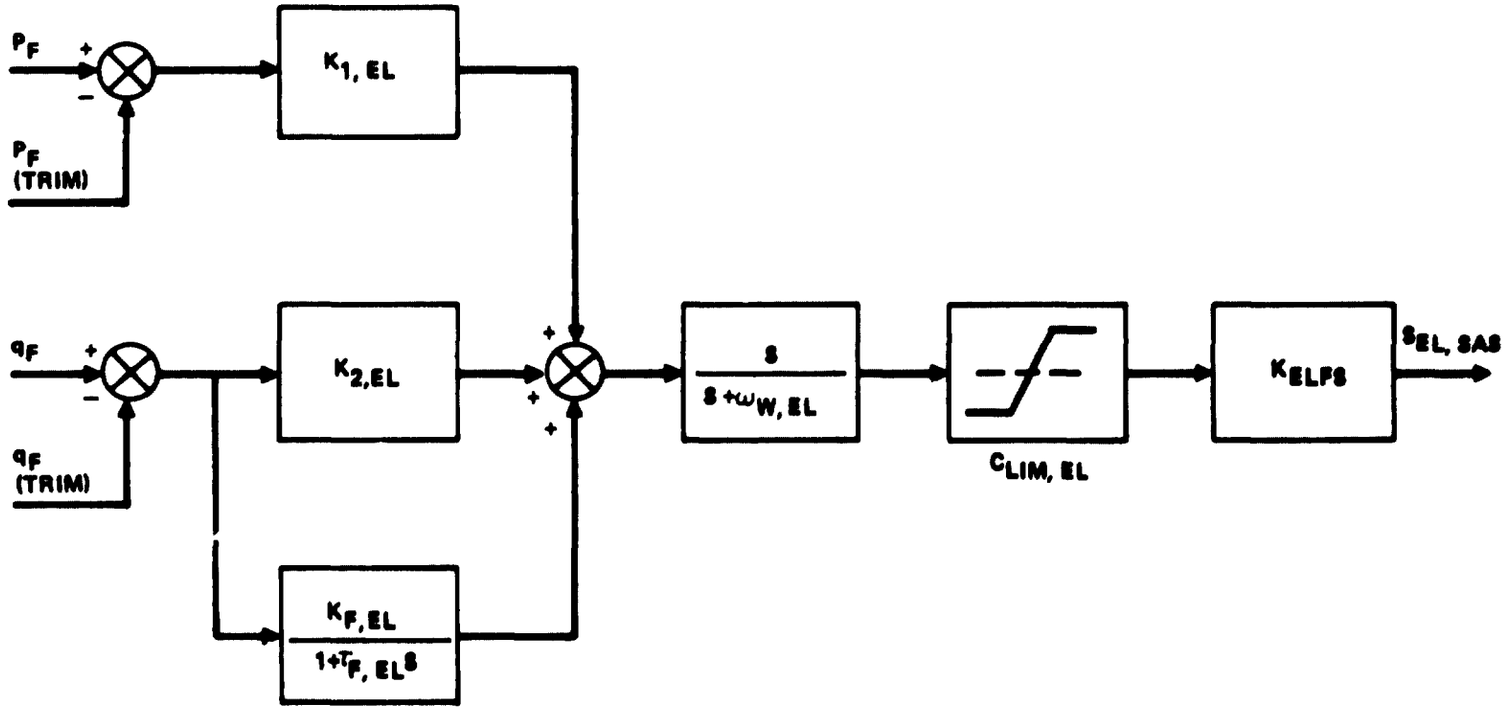

Figure 45. - Elevator stability augmentation.

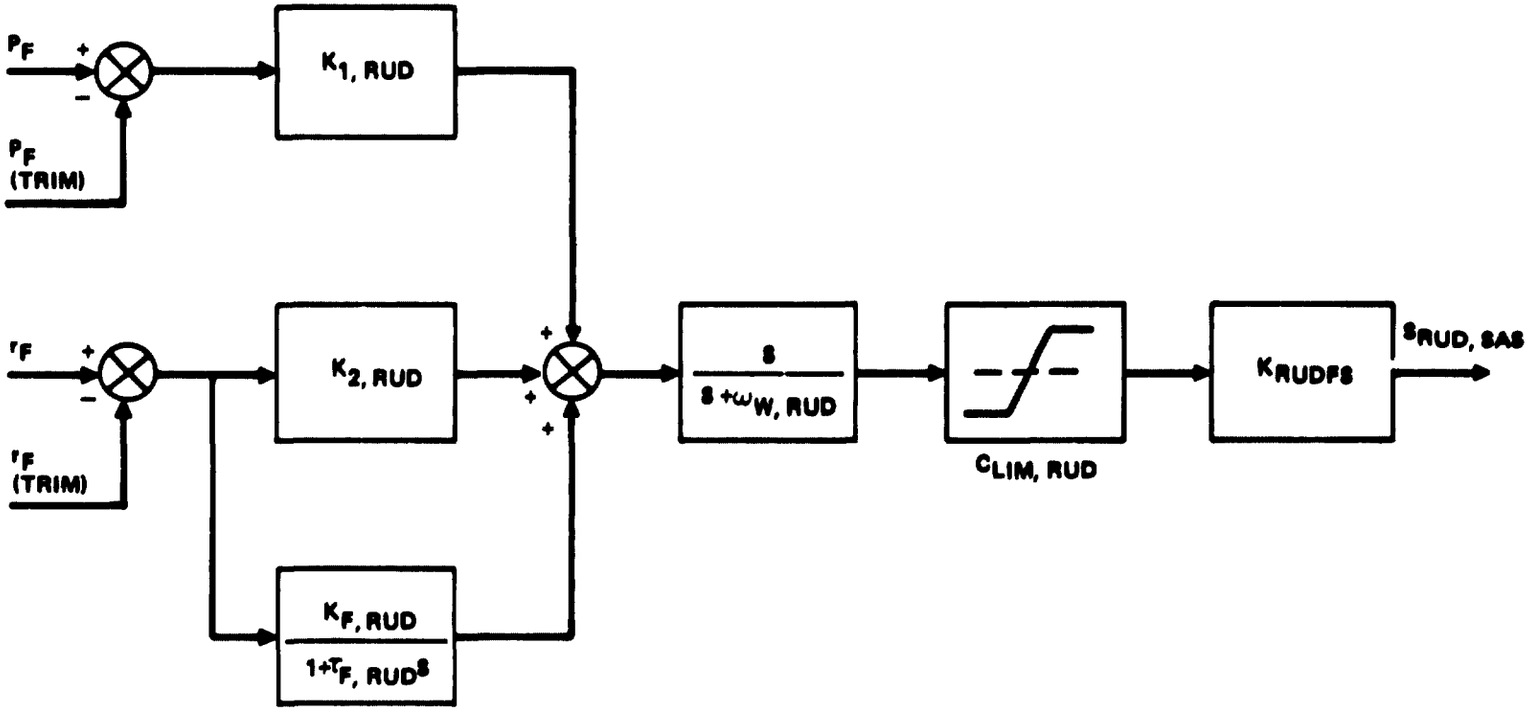

Figure 46. - Rudder stability augmentation.

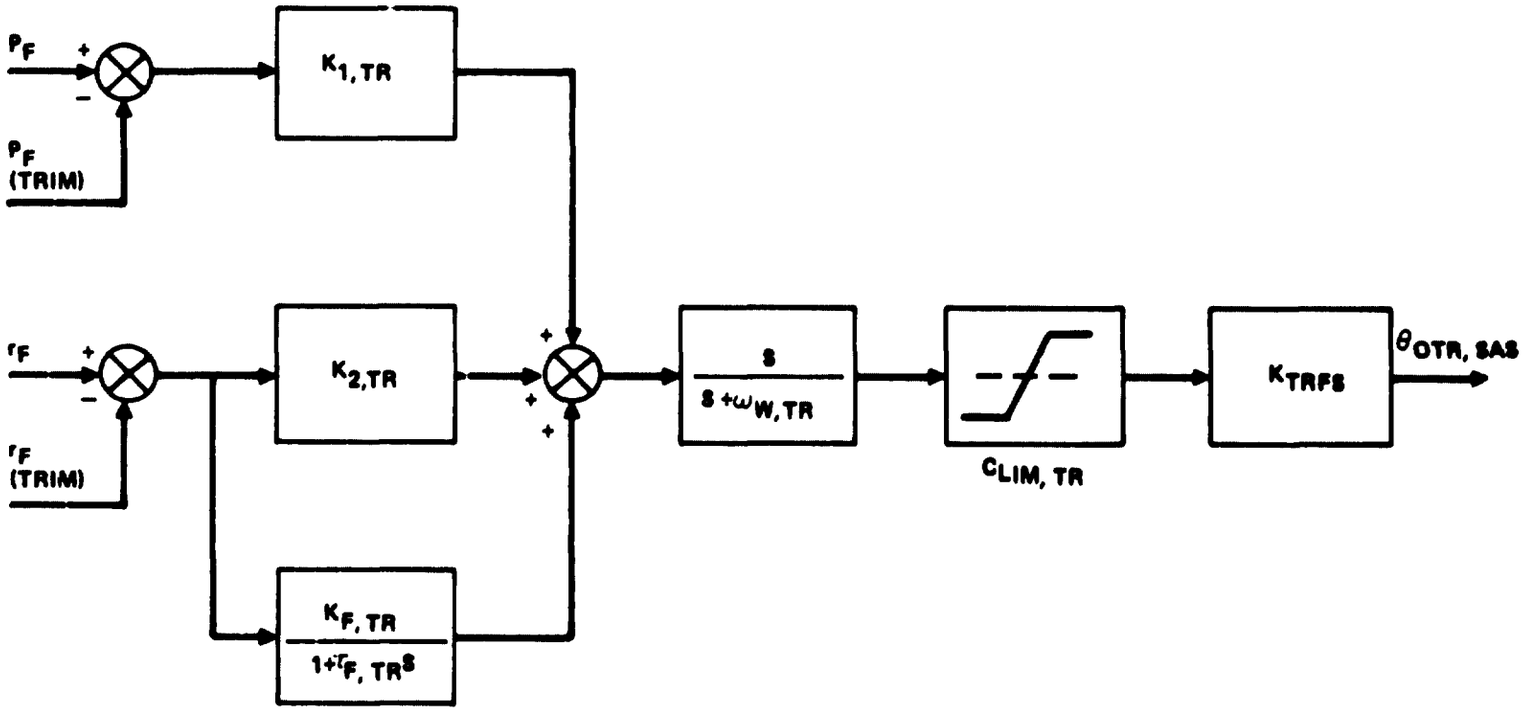

Figure 47. - Tail rotor stability augmentation.

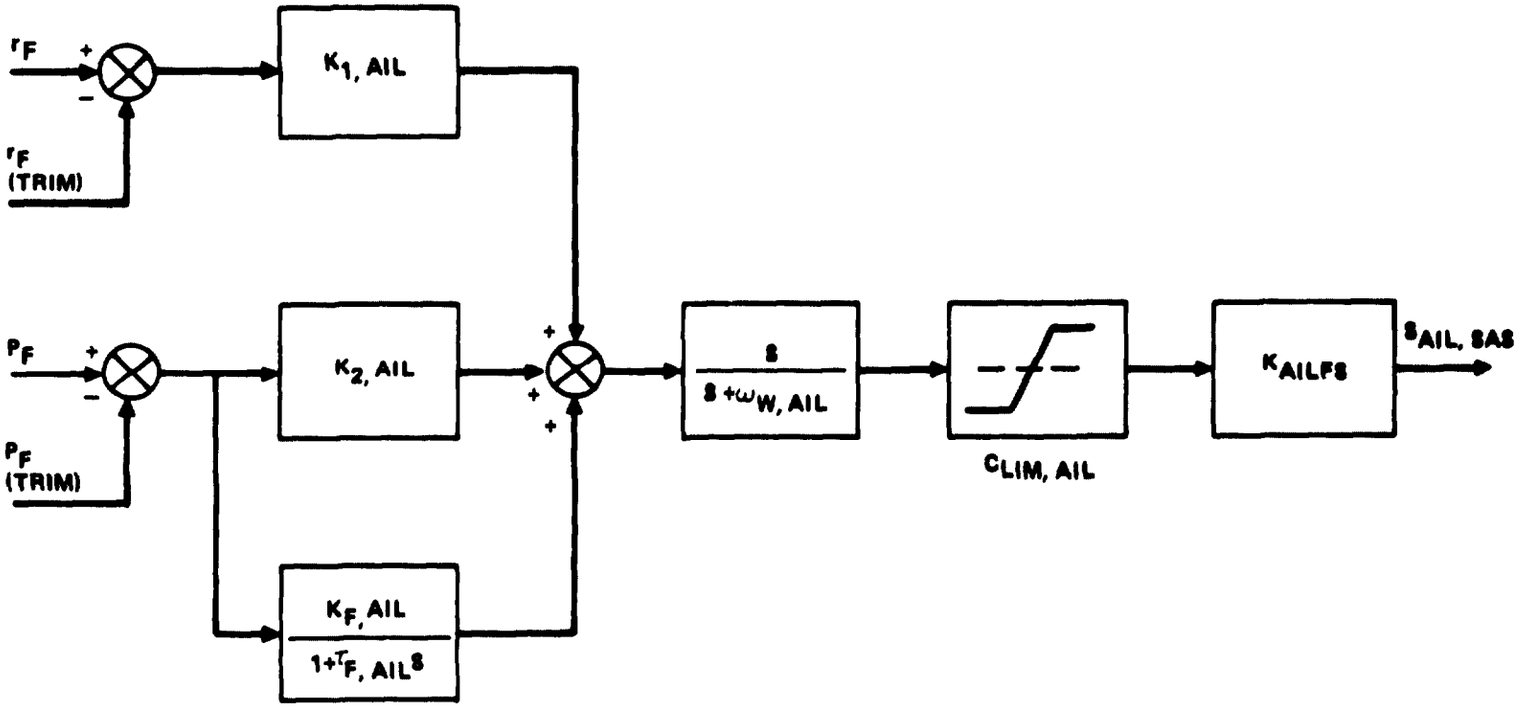

Figure 48. - Aileron stability augmentation.